

**Regioselective Synthesis of C₆₀-Tris- and
Hexakisadducts with C_{3v}-Symmetrical Phosphate
Trismalonate Addends**

**Regioselektive Synthese von C₆₀-Tris- und
Hexakisaddukten mit C_{3v}-symmetrischen
Phosphattrismalonataddenden**

Der Naturwissenschaftlichen Fakultät
der Friedrich-Alexander-Universität
Erlangen-Nürnberg

zur

Erlangung des Doktorgrades Dr. rer. nat.

vorgelegt von

Alexander Gmehling

aus Pegnitz



FRIEDRICH-ALEXANDER
UNIVERSITÄT
ERLANGEN-NÜRNBERG

NATURWISSENSCHAFTLICHE
FAKULTÄT

Als Dissertation genehmigt von der Naturwissenschaftlichen Fakultät der Friedrich-Alexander-Universität Erlangen-Nürnberg

Tag der mündlichen Prüfung: 21.03.2013

Vorsitzender des Promotionsausschusses: Prof. Dr. Johannes Barth

Gutachter: Prof. Dr. Andreas Hirsch
Prof. Dr. Rik Tykwinski

Mein besonderer Dank gilt meinem Doktorvater Prof. Dr. Andreas Hirsch für die Bereitstellung des interessanten und herausfordernden Themas, seine Förderung und die jederzeit willkommenen Diskussionen und Ratschläge.

Die vorliegende Arbeit entstand in der Zeit von Juli 2008 bis Juni 2012 am Lehrstuhl für Organische Chemie II der Friedrich-Alexander-Universität Erlangen-Nürnberg.

Abbreviations

ACN	acetonitrile
Bn	benzyl
calc.	calculated
CD	circular dichroism
COSY	correlation spectroscopy
CuAAC	copper catalyzed azide alkyne cycloaddition
CV	cyclic voltammetry
DABCO	diazabicyclooctane
DBU	1,8-diaza-bicyclo[5.4.0]undec-7-ene
DCM	dichloromethane
DCTB	<i>t</i> -2-(3-(4- <i>t</i> -Butyl-phenyl)-2-methyl-2-propenylidene)malononitrile
DHB	2,5-dihydroxybenzoic acid
DHP	3,4-dihydro-2 <i>H</i> -pyran
DITH	dithranol
DMA	9,10-dimethylantracene
DMF	<i>N,N</i> -dimethyl formamide
EI	electron impact
E_{pa}	electrochemical potential at anodic scan
E_{pc}	electrochemical potential at cathodic scan
EPR	electron paramagnetic resonance
ESI	electrospray ionization
Et	ethyl
EtOH	ethanol
eq.	equivalents
FAB	fast atom bombardment
Fc	ferrocene
HETCOR	heteronuclear correlated spectroscopy

HiRes	high resolution
HPLC	high performance liquid chromatography
IPR	isolated pentagon rule
IR	infrared (spectroscopy)
LAH	lithium aluminium hydride
LUMO	lowest unoccupied molecular orbital
MALDI	matrix assisted laser desorption ionization
Me	methyl
MeOH	methanol
MEM	methoxyethoxymethyl
MS	mass spectrometry
NBA	3-nitrobenzylalcohol
NMR	nuclear magnetic resonance
ODCB	<i>ortho</i> -dichlorobenzene
PPTS	pyridinium <i>para</i> -toluenesulfonate
<i>p</i> -TsOH	<i>para</i> -toluenesulfonic acid
pyr	pyridine
r.t.	room temperature
SIN	sinapic acid
TBABF ₄	tetrabutylammonium tetrafluoroborate
TBAF	tetrabutylammonium fluoride
TBDMS	<i>tert.</i> -butyldimethylsilyl
TBDPS	<i>tert.</i> -butyldiphenylsilyl
TFA	trifluoroacetic acid
THF	tetrahydrofuran
THP	tetrahydropyranyl
TIPS	triisopropylsilyl
TIPSCI	triisopropylsilylchloride
TLC	thin layer chromatography
TMS	trimethylsilyl
TMSBr	trimethylsilyl bromide
TMSCI	trimethylsilyl chloride
TOF	time of flight
UV/Vis	ultraviolet/visible (spectroscopy)

δ	chemical shift
J	coupling constant
λ	wavelength
m/z	mass to charge ratio
$\bar{\nu}$	wavenumber

Contents

1	Introduction	1
1.1	Polyhedra in Organic Chemistry	1
1.2	Structure of Fullerenes	4
1.3	Production and Isolation of Fullerenes	6
1.4	Physical Properties of C ₆₀	7
1.4.1	Solubility	7
1.4.2	UV/Vis- and IR-Spectroscopy	8
1.4.3	Mass-Spectrometry	9
1.4.4	Electrochemical Properties	10
1.4.5	¹ H-NMR Spectroscopy	11
1.4.6	¹³ C-NMR Spectroscopy	11
1.5	Functionalization and Reactivity of C ₆₀	12
1.5.1	General Possibilities	12
1.5.2	Fullerides and Endohedrals	13
1.5.3	Cage Modifications	14
1.5.4	Exohedral Functionalization	20
1.6	Stereochemistry of C ₆₀ Multiple Adducts	24
1.6.1	Stereochemical Nomenclature	24
1.6.2	Synthesis of Defined Multiadducts	26
2	Proposal	31
3	Results & Discussion	33
3.1	Investigations on C ₅₈ N ₂	33
3.1.1	Repetition of the Synthesis	33
3.1.2	Stability of C ₅₈ N ₂	35
3.1.3	Electrochemical & EPR Investigations	36

3.2	Screening for a Novel Template for <i>e,e,e</i> -Trisadducts	40
3.2.1	Concept	40
3.2.2	Iron-Complexes	40
3.2.3	Boron-Templates	42
3.2.4	Silicon Templates	44
3.2.5	Phosphorus-Templates	45
3.3	Development of a New Trismalonate System for the Formation of C_{60} - <i>e,e,e</i> - Trisadducts	50
3.3.1	Proof of Concept	50
3.3.2	Synthesis of Novel Trismalonates	53
3.3.2.1	Synthesis of Malonate Alkanols	53
3.3.2.2	Phosphate Trismalonates	55
3.3.3	Fullerenophosphate- <i>e,e,e</i> -Trisadducts	57
3.3.3.1	Synthesis of Novel <i>e,e,e</i> -Trisadducts	57
3.3.3.2	Fullerenophosphate- <i>e,e,e</i> -Trisadducts with <i>n</i> -Propylspacer	57
3.3.3.3	X-Ray-Crystal Structures of Inverted Fullerenophosphate- <i>e,e,e</i> - Trisadducts	62
3.3.3.4	Fullerenophosphate- <i>e,e,e</i> -Trisadducts with <i>n</i> -Butylspacer	66
3.3.3.5	Fullerenophosphate- <i>e,e,e</i> -Trisadducts with <i>n</i> -Pentyl- and <i>n</i> - Hexylspacer	69
3.3.3.6	Electrochemical Properties	71
3.3.3.7	Attempts for the Synthesis of Chiral Phosphate Trismalonates	73
3.4	Development of C_{60} - <i>e,e,e</i> -Building Blocks	79
3.4.1	Search for a Proper Deprotection Strategy	79
3.4.2	Synthesis of a Homologous Series of <i>e,e,e</i> -Trisbromides	81
3.5	Extension Towards Hexakisadducts	87
3.5.1	Hexakisadducts with Mixed Templates	87
3.5.2	Hexakisadduct Building Blocks	93
3.6	Further Functionalization of C_{60} - <i>e,e,e</i> -Trisbromides	98
3.6.1	Transformation to Azides	98
3.6.2	CLICK-Reaction with Phenylacetylene	100
3.6.3	Complexation Attempts with Zn(II)	102
3.6.4	Synthesis of a Fullerene-Trisporphyrin Tetrad	105
3.6.5	UV/Vis- and Fluorescence-Studies of the C_{60} -Trisporphyrin-Tetrad	109

3.6.6	Complexation-Studies of <i>s</i> -Triazine with the Fullerene-Trisporphyrin-Tetrad	111
4	Summary	117
5	Zusammenfassung	121
6	Experimental Section	125
6.1	Materials and Chemicals	125
6.2	Technical Equipment	125
6.3	General Procedures	128
6.4	General Remarks	131
6.5	Synthetic Procedures & Analytical Data	132
	References	179
7	Appendix	193

1 Introduction

1.1 Polyhedra in Organic Chemistry

Symmetrical objects have always been appealing to people, because they are associated with order, simplicity and beauty. Some of the most symmetrical three-dimensional objects are the five platonic solids (Figure 1.1). Objects crafted in these forms are dated back up to 4000 years in the past.^[1] The ancient Greek were the first to describe these solids mathematically. They are named after the philosopher Plato. He was a polymath and naturally interested in all kinds of science. He connected the platonic solids to alchemy by assigning all four elements to one of the solids, whose structure resembled the macroscopic properties of the element best. The highly symmetric structures have inspired artists and craftsmen and many structures in nature, like viruses, also resemble these solids.^[2, 3]

The platonic solids are regular, convex polyhedra and each is constructed of one type of identical, regular polygons. All edges have the same length, the same number of polygons meet at each vertex and all vertices are equal. The resulting structures are highly symmetric

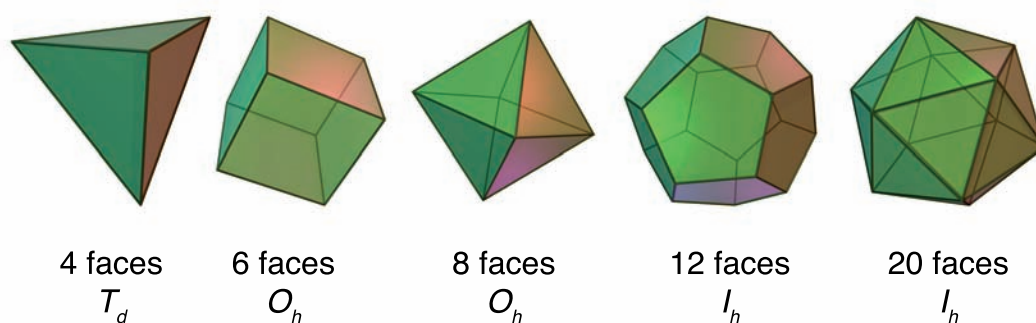


Figure 1.1: The five platonic solids are (from left to right): tetrahedron, hexahedron (cube), octahedron, dodecahedron and icosahedron.^[4] The names are derived from the number of faces. The symmetry group is stated below.

and the vertices, edges and faces cannot be distinguished. Consequently, the description of a platonic solid is very simple, because only the kind of solid and one property, like the length of the edges is sufficient. Already Euclid showed, that there are only five platonic solids, meeting these criteria.^[5] The five platonic solids are the tetrahedron, the hexahedron or cube, the octahedron, the dodecahedron and the icosahedron. The names are derived from the Greek word for the number of faces that each polyhedron has.

There are pairs of platonic solids, which can be constructed from each other by connecting the centers of two adjacent faces. Such two solids are dual to each other. The octahedron and the hexahedron are dual, the dodecahedron and the icosahedron are dual and the tetrahedron is self-dual. In terms of symmetry, the dual solids belong to the same point group and the number of vertices and faces are exchanged. By appropriate centrosymmetric magnification, the dual solid can be used to cut off the vertices of the parent solid in such a way, that the lengths of the old and the new edges are still the same. The resulting solids are only slightly less symmetric and part of the 15 archimedean solids (examples are given in figure 1.2). They can contain now two or three different types of regular polygons but the vertices and edge lengths are still equal. Prisms and antiprisms meet this definition as well as the platonic solids, but they are not considered as archimedean solids.



Figure 1.2: Three out of the 15 archimedean solids (from left to right): truncated hexahedron, truncated icosahedron, truncated icosidodecahedron.^[4] The number and types of regular polygons that they are built from is stated below.

These highly symmetric structures can be found in the crystal structures of minerals and have also roused the attention of organic chemists. Not only simplicity, symmetry and beauty of these compounds is responsible for the attention, but also the synthetic challenge. The challenge to realize these structures as organic compounds, lies in their spherically closed structure, the strain inherent to them and the absence of any functional group, in case of the

parent hydrocarbon. In 1964, cubane **1** (Figure 1.3) was the first platonic hydrocarbon to be synthesized by Eaton and it turned out to be a stable molecule, despite its strain.^[6, 7] The even more strained tetrahedrane wasn't isolated as the parent hydrocarbon until today, but the stable tetra-*tert*-butyl-derivative **2** is known since 1978.^[8] Dodecahedrane **3** is the last of the platonic hydrocarbons that is feasible to prepare, which was accomplished in 1982 by the group of Paquette.^[9] Octahedrane is unlikely to be stable, because all four connections at a corner point to the same direction, which would result in highly distorted carbon atoms. Icosahedrane is even impossible to realize, because every vertex is connected to five other vertices.

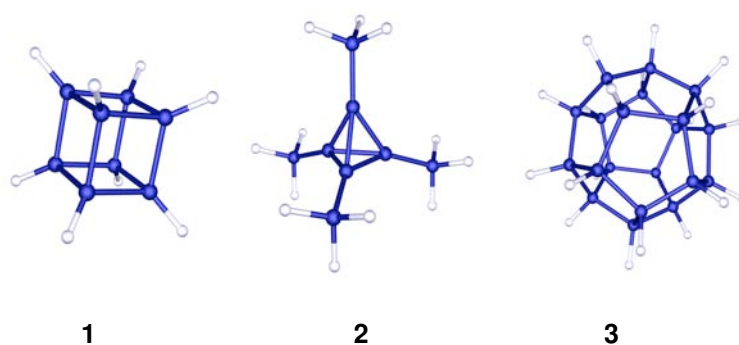


Figure 1.3: The platonic hydrocarbons cubane **1** and dodecahedrane **3** were synthesized as parent compounds. The more strained tetrahedrane was synthesized as *tert*-butyl-derivative **2**.

The most complex organic polyhedron that is available until now is I_h -[60]-fullerene.^[10] It has the structure of a truncated icosahedron, although it does not fit into the definition of an archimedean solid, because it contains two types of bond lengths. Although it can be readily obtained from a chaotic carbon plasma, the defined chemical synthesis is pursued with equal ambition than the synthesis of the platonic hydrocarbons. The synthesis of the bowl-shaped corannulene in 1971 predated even the discovery of C_{60} and probably inspired others to think about such large carbon cages.^[11, 12] Pentaindenocorannulene ($C_{50}H_{20}$) resembles already a very large part of the spherical framework of C_{60} and was prepared in 2007 by a wet-chemical synthesis.^[13] The discovery of a mild cyclization method for aromatic hydrocarbons by HF-elimination through $\gamma-Al_2O_3$ in 2012 was an important step towards the controlled synthesis of fullerenes. C_{60} , higher fullerenes and related structures might become accessible by controlled synthetic methods in the near future.^[14]

1.2 Structure of Fullerenes

Fullerenes are spherically closed all-carbon cages and the third and youngest allotrope of carbon. Diamond and graphite, the other two carbon allotropes, are already known for a very long time, but fullerenes were only discovered in 1985.^[10] Unlike the "older" forms, which are extended, more or less infinite solids on an atomic scale, fullerenes are well-defined molecules. They are built up from an even number of n ($n \geq 20$, except for $n = 22$) three valent, sp^2 hybridized carbon atoms that are arranged in $(n - 20)/2$ hexagons and twelve pentagons. The pentagons introduce curvature, as hexagons yield only flat structures. Exactly twelve pentagons are necessary to obtain a closed network, according to EULER's theorem.^[15] As the carbon atoms are sp^2 hybridized, double bonds have to be involved in bonding. The entire carbon network can be considered as a system of alternating double bonds like in benzene. However it is not aromatic as the two-dimensional analogue because the bond lengths are different.

Stable fullerenes have to obey the isolated pentagon rule (IPR), which means, that each pentagon is completely surrounded by hexagons.^[16] This arrangement avoids double bonds in pentagons, which would lead to increased strain in the carbon network. In IPR-obeying structures the curvature is more uniformly distributed, *i.e.* the sphere has a more relaxed geometry, and the π -electron overlap is maximized, which stabilizes the cluster as well.^[17] In a recent publication, the IPR is explained on basis of geometric constraints and a head-to-tail exclusion rule was suggested for the structure of larger fullerenes with $n \geq 60$.^[18] Another electronic reason, that destabilizes structures with fused pentagons are the formed pentalene-type 8π -electron antiaromatic substructures.^[19, 20] Until today, all isolated parent fullerenes obey the IPR. The smallest stable representatives and the most abundant, are the football shaped C_{60} **4** and the rugby ball shaped C_{70} **5** (Figure 1.4).^[10] I_h - C_{60} is the only

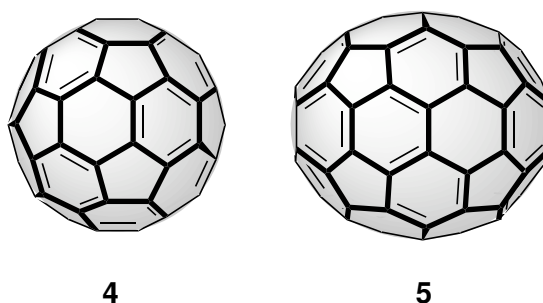


Figure 1.4: Molecular structure of the two most abundant fullerenes C_{60} **4** and C_{70} **5**.

isomer out of the 1812 possible ones, that is formed for 60 carbon atoms. For the next bigger fullerene that was isolated, C_{70} , there exists also only one IPR-obeying structure. From C_{76} on, however, there exist more IPR satisfying structures and their numbers increase with increasing fullerene size.^[21]

Although all isolated parent fullerenes obey the IPR, there are also fullerene structures reported with two or three directly fused pentagons or even fullerenes with four- or seven-membered rings. However, the additional strain has to be compensated somehow and this is usually done either by endohedral encapsulation of metal atoms or clusters or by exohedral functionalization, in most cases chlorination.^[22, 23] Many new fullerene structures have been discovered in the past years and they are topic of intense research. Even derivatives of a non-IPR isomer of C_{60} were recently reported.^[24, 25] A derivative of the smallest member, dodecahedrane $C_{20}H_{20}$, was completely synthesized by chemical methods even three years before the discovery of C_{60} and it consists only of pentagons.^[9] It is to date, the only fullerene-like structure that was synthesized by wet chemical methods. Although IPR-violating structures can be produced and stabilized there are usually no more than two or three pentagons fused in a carbon cage. In $C_{50}Cl_{10}$ *e.g.*, only two pentagons are fused, and only in bigger fullerenes, there were also triplets of pentagons found.^[26, 27, 28]

C_{60} itself resembles a nanosoccerball. All pentagons are separated from each other and hence, it is perfectly stable. Due to the I_h -symmetry and the spherical shape the strain can be distributed over the entire sphere. It has a diameter of 0.7 nm and all 60 carbon atoms can be translated into each other by proper symmetry operations.^[29, 30] There are two types of bond lengths in C_{60} , which demonstrates that it is not aromatic in the classical sense.

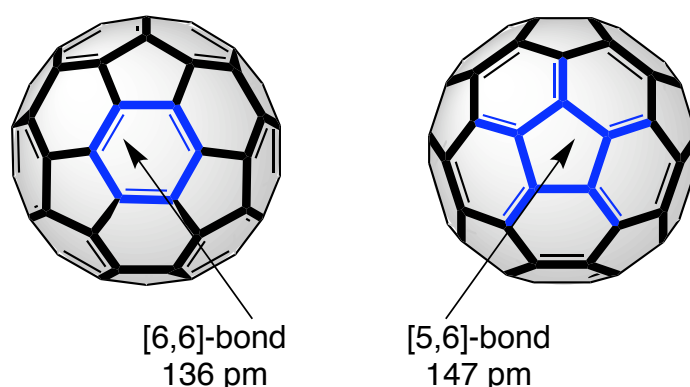


Figure 1.5: The C_{60} framework can be considered to contain 1,3,5-cyclohexatriene- and [5]-radialene-substructures and two different bond lengths.

The localization of double bonds in hexagons is evident from the different bond lengths (Figure 1.5). Those connecting two six-membered rings, the [6,6]-bonds are 136 pm long, whereas the [5,6]-bonds, connecting five- and six-membered rings, are 147 pm long.^[31, 32] Consequently, the [6,6]-bonds are double bonds and the C₆₀ framework can be considered to contain 1,3,5-cyclohexatriene and [5]-radialene substructures.

1.3 Production and Isolation of Fullerenes

Since their first discovery in 1985, many methods were developed to produce fullerenes. The initial process was laser vaporization of a graphite target, but it was only suitable to detect fullerenes in the gas phase by MS.^[10] The first method to produce fullerenes in quantitative amounts was an arc discharge reactor, developed by Krätschmer and Huffman in 1990.^[29] Two graphite electrodes were evaporated in a helium atmosphere of 140 mbar by resistive heating. In the first place a carbon plasma is formed that nucleates upon cooling in the inert gas atmosphere and forms in the end soot that contains 10-15 % fullerenes. The nucleation starts from carbon atoms, that form linear chains or rings of carbon atoms. Upon growth, they wrap up and thereby reduce dangling bonds at the rims.^[33] If this process happens under the right conditions, *i.e.* the right inert gas pressure, adjacent pentagon structures are annealed to IPR allowed structures by the STONE-WALES rearrangement.^[34] As C₆₀ is the smallest stable fullerene to obey the IPR, and as it is extraordinary stable in comparison to fullerenes of similar size (C₅₈ or C₆₂; both have no IPR isomers), it is a kinetic trap and hence, the most abundant fullerene in all production methods. The next most common fullerene, C₇₀ is usually only formed in a ratio of 85 % : 15 % (C₆₀ : C₇₀), which underlines the extraordinary stability of the sixty carbon atom cluster.^[35] Higher fullerenes are also produced but in ever decreasing ratios. There is often more than one IPR-isomer for a given number of carbon atoms, which reduces the yield of a certain compound even more.^[36]

For the production of endohedral metallofullerenes, graphite rods are impregnated with the corresponding metal or metal salt prior to evaporation. For incorporation of metal clusters or for the formation of exohedral derivatives, additional reactive agents are added during the vaporization process. Pure metal clusters, metal nitrides, metal oxides or metal carbides are often encapsulated inside fullerenes.^[37] By electron transfer from the encapsulated cluster to the fullerene cage, otherwise unknown geometries for empty cages are stabilized.^[22, 23] The most prominent example is probably the trimetallic nitride fullerene Sc₃N@I_h-C₈₀.^[38] None of

the two components exists alone, but joined together, it is the third most abundant fullerene after C_{60} and C_{70} .^[37]

Other methods are also applicable to the production of fullerenes. Flame combustion of carbon sources is probably the most important one and is applied on an industrial scale by Mitsubishi Frontier Carbon Corporation.^[39] Due to these developments, C_{60} and C_{70} are today commercially available and affordable.

After fullerene production, the soot is collected and extracted with benzene or toluene to obtain the soluble fullerenes. They are separated by repeated chromatographic procedures, which is rather easy for C_{60} and C_{70} . The higher fullerenes, as well as metallofullerenes or exohedral derivatives are usually formed in very low quantities and they behave so little different that multistage or recycling HPLC separations have to be applied.^[23, 40]

1.4 Physical Properties of C_{60}

1.4.1 Solubility

C_{60} is not only the first fullerene that was detected but also the most abundant fullerene and next to C_{70} the only one that is available in sufficient amounts to allow in depth research. Therefore the following sections on the properties of fullerenes will focus mainly on C_{60} .

For chemical functionalization as well as for most characterization methods, the solubility of a compound is a very important property. In general, C_{60} dissolves best in halogenated aromatic hydrocarbons like ODCB or 1-chloronaphthalene (Table 1.1).^[41] Similar good solubilities are obtained in unsymmetrically substituted polymethylbenzenes, like 1,2,4-trimethylbenzene or 1,2,3,5-tetramethylbenzene. C_{60} is almost insoluble in polar solvents like alcohols or water. Hydrocarbons or halogenated hydrocarbons are slightly better solvents for C_{60} , with tetralin and 1,1,2,2-tetrachloroethane, reaching the same values as aromatic solvents. The latter one is often used in its deuterated form to conduct high-temperature NMR-measurements. CS_2 is another unusual but very useful solvent. It dissolves C_{60} and otherwise hard to solubilize adducts very well and is often used in mixture with $CDCl_3$ for NMR-measurements. For practical reasons, toluene is the solvent of choice for chemical reactions because of its relative intoxicity and because of its rather high volatility in comparison to the other solvents.

For physicochemical measurements, standard organic solvents like THF or DCM might also be sufficient, because only very low concentrations are necessary. C_{60} -derivatives are usu-

ally readily soluble in standard organic solvents, which makes handling much easier. For higher fullerenes the above mentioned "good" solvents have to be used, as the fullerenes become more and more insoluble with increasing size.^[36]

Table 1.1: Solubility of C₆₀ in selected organic solvents.^[41]

solvent	solubility [mg/mL]
water	1.3×10^{-11}
ethanol	0.001
<i>n</i> -pentane	0.005
dichloromethane	0.26
chloroform	0.16
1,1,2,2-tetrachloroethane	5.30
tetralin	16.00
toluene	2.80
chlorobenzene	7.00
1,2,4-trimethylbenzene	17.90
1,2,3,5-tetramethylbenzene	20.80
1,2-dichlorobenzene	27.00
1-chloronaphthalene	51.00
carbon disulfide	7.90

1.4.2 UV/Vis- and IR-Spectroscopy

The UV/Vis-absorption spectrum of C₆₀ shows the most prominent absorptions in the UV-region at 205 nm, 253 nm and 326 nm (Figure 1.6). Responsible for the very characteristic purple color in solution are weak, spin forbidden transitions in the visible region with an onset at 635 nm.^[35] C₇₀ is burgundy red in solution and its absorption onset is red-shifted to 650 nm. For higher fullerenes, the absorption is further shifted to longer wavelengths.^[36] Addends at the fullerene framework alter the absorption spectra as well (Figure 1.6). Additions usually occur at double bonds, remove electrons from the conjugated system and hence disturb the π -system. In case of multiple adducts of C₆₀ the absorption spectrum is characteristic for a certain addition pattern. The spectrum of each of the eight isomeric malonate-bisadducts, *e.g.* has a different and characteristic shape in the region between 400 nm and 800 nm.^[42]

The C_{60} -trisadducts can also be distinguished by their UV/Vis-spectra.^[43] The red *e,e,e*-trisadduct in particular has a characteristic spectrum with absorptions at 252 nm, 282 nm, 380 nm and 484 nm and two shoulders at 302 nm and 564 nm.^[44, 45, 46] If even more addends are attached to the C_{60} -sphere, the color of the corresponding adducts fades until it is only a light yellow in case of T_h -symmetrical hexakisadducts. In that case, the π -system has been reduced to eight separated benzenoid rings, which explains the absence of significant absorptions in the visible region.^[47]

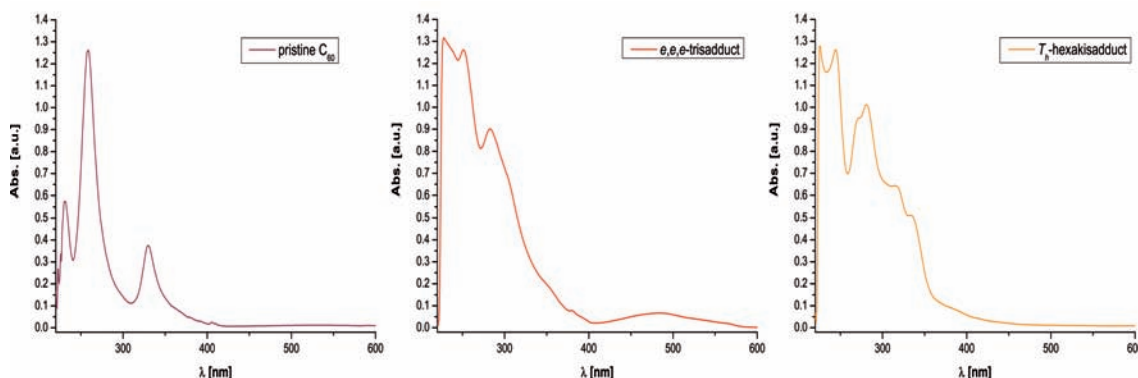


Figure 1.6: The UV/Vis-absorption spectrum of fullerene-adducts is determined by the number of addends and the specific addition pattern. Spectra were recorded in DCM at r.t. and normalized to the corresponding absorption at around 250 nm.

The IR-spectrum of C_{60} is rather simple, due to the high symmetry of the molecule. Two stretching modes appear at 1429 cm^{-1} and 1183 cm^{-1} and two deformation modes appear at 577 cm^{-1} and 529 cm^{-1} .^[35]

1.4.3 Mass-Spectrometry

C_{60} was first detected by mass spectrometry in an ion beam and mass spectrometry is still a very powerful tool to characterize fullerenes and their adducts.^[10] Although it allows no assignment of a special geometry, especially important for higher fullerenes or adducts of C_{60} , it is nevertheless the first proof for the composition of the molecule. In case of hard ionisation, a characteristic process called shrink-wrapping is observed for the fullerene peak. The carbon cluster ejects regularly C_2 -fragments, which is a process, that probably also happens during fullerene formation and which transforms higher fullerenes to more stable ones like C_{60} .^[48] In case of softer ionization techniques like MALDI-TOF-MS, no shrink-wrapping is observed. These techniques are very powerful to detect the unfragmented molecular ion peak. DCTB

is usually the best matrix for MALDI-TOF-MS to ionize fullerenes, but in some cases other matrices (DITH, SIN, DHB) work also well.

1.4.4 Electrochemical Properties

One of the most unique properties of C_{60} is its ability to accept up to six electrons reversibly. This was derived from the calculated HÜCKEL molecular orbital scheme (Figure 1.7).^[49, 50] The LUMO is low in energy and threefold degenerate, which explains the high electron affinity of C_{60} and its smooth reaction with nucleophiles and radicals. It took some time until all six reduction steps were detected by cyclovoltammetry (CV), although the existence of the hexaanion was deduced from intercalation compounds like K_6C_{60} .^[51] C_{60}^{6-} and C_{70}^{6-} were finally detected by CV by the use of ACN/toluene as solvent and a temperature of $-10\text{ }^\circ\text{C}$. All six reduction steps were found to be reversible.^[52] After some optimization the oxidation process to C_{60}^+ was also found to be reversible.^[53] In case of C_{60} -derivatives, the reduction potentials become more cathodically, with increasing number of substituents.^[54] Furthermore, the reversibility is reduced, because isomerizations or retro-BINGEL-reactions occur in case of malonate derivatives (the BINGEL-reaction is explained on page 23).^[55]

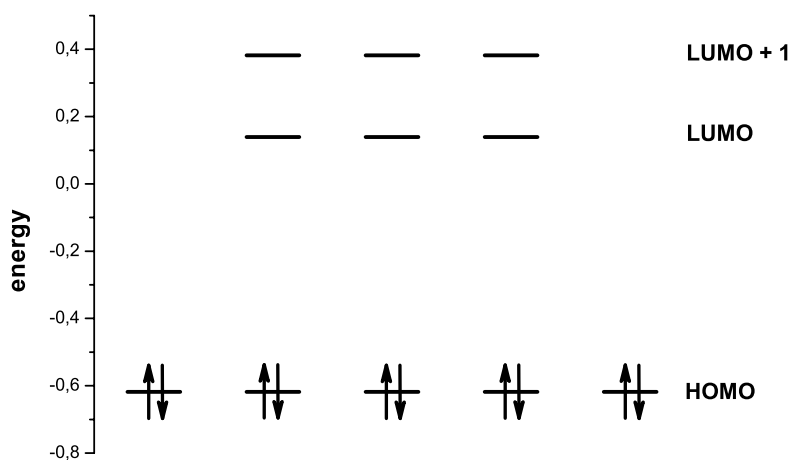


Figure 1.7: The calculated HÜCKEL molecular orbital scheme for the frontier orbitals of C_{60} .^[49]

1.4.5 ^1H -NMR Spectroscopy

^1H -NMR spectroscopy is a valuable tool for structure elucidation of organic compounds and is also very useful for the characterization of fullerene derivatives. It is used to control the formation of adducts but also to monitor reactions on fullerene derivatives. Some unique phenomena are observed when protons are close above the fullerene surface. These helped to elucidate some of C_{60} 's fundamental properties. Calculations of the magnetic properties of C_{60} have shown, that there are paramagnetic ring currents in pentagons and diamagnetic ring currents in hexagons, which almost cancel each other in total.^[56] Nevertheless, nuclei above the surface experience these differences. Protons above a pentagon are shifted to lower field and protons above hexagons are shifted to higher field. This phenomenon is demonstrated with the homologues structures **6**, **7** and **8** (Figure 1.8).^[57] The methine protons resonate at 4.31 ppm, 3.32 ppm and 6.79 ppm, respectively, reflecting the different chemical environment.

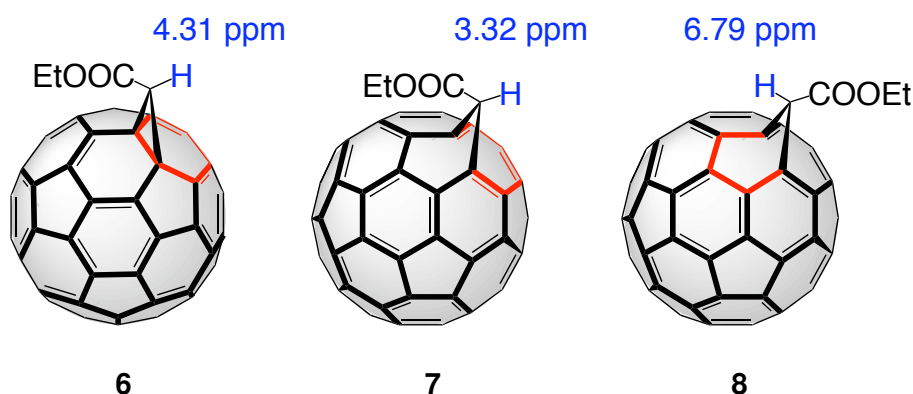


Figure 1.8: The chemical shift of protons above the fullerene surface is influenced by the ring-currents in the underlying polygons.^[57]

1.4.6 ^{13}C -NMR Spectroscopy

In addition to mass spectrometry, ^{13}C -NMR spectroscopy plays another very important role in determining the structure of fullerenes and their adducts. The carbon atoms in fullerenes resonate between 140 ppm and 150 ppm. The exact signal pattern depends on the symmetry of the carbon cluster. As all carbon atoms are equal in C_{60} , the ^{13}C -NMR-spectrum displays only one resonance at 143.2 ppm.^[35] In case of the D_{5h} -symmetrical C_{70} , five resonances are observed, which reflect the five different kinds of carbon atoms in the structure

of the rugby ball.^[35] For higher fullerenes, an interplay between theoretical calculations and observed ^{13}C -NMR-spectra is often necessary to elucidate the structure, if no X-ray crystal structure is available. For C_{60} -addition products the symmetry of the fullerene-core is reduced and a characteristic number of resonances is observed in the region between 140 ppm and 150 ppm for the sp^2 -carbon atoms. The carbon atoms bearing the substituent are now sp^3 -hybridized and their signals are shifted to around 70 ppm. The number of resonances is again determined by the symmetry of the adduct. In case of *e.g.* *e,e,e*-trisadducts with three equal addends the spectrum displays 18 resonances in the sp^2 -region and two resonances in the sp^3 -region, due to the C_3 -symmetry.^[44]

1.5 Functionalization and Reactivity of C_{60}

1.5.1 General Possibilities

Most work on functionalization of fullerenes deals with C_{60} , as it is the only member of the family that is available in reasonable amounts.^[58] Some reports exist also on C_{70} and the higher fullerenes but research on them is limited by the little amounts that are available. This drawback is further complicated by the increasing number of isomers that are formed, even from a monoaddition, if a less symmetrical starting structure is used as it is the case

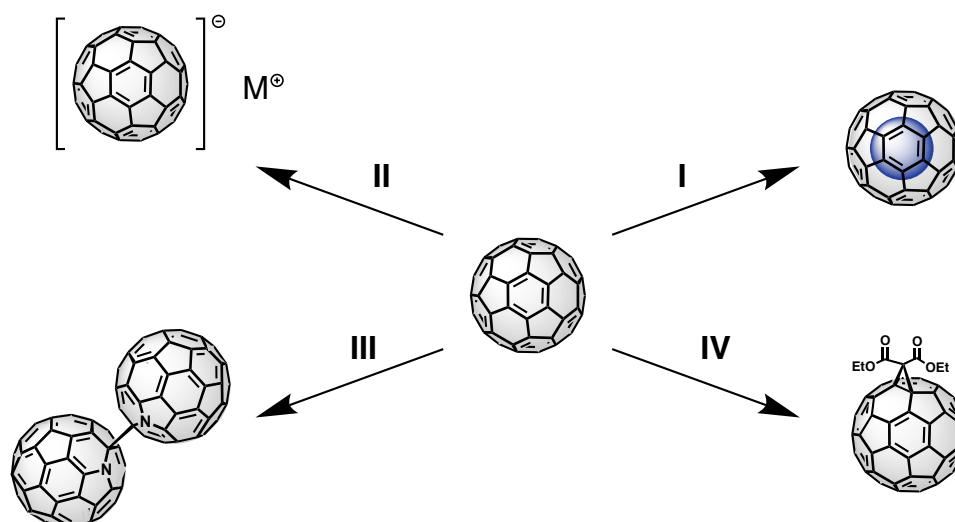


Figure 1.9: There are four different ways to functionalize fullerenes: **I:** endohedral functionalization; **II:** fulleride formation; **III:** cage modification; **IV:** exohedral functionalization.

for C_{70} and the larger fullerenes. Therefore this section deals only with selected aspects of C_{60} -functionalization.

There are in general four substantially different ways to functionalize fullerenes and alter their properties (Figure 1.9). Salt formations (II), cage modifications (III) and exohedral functionalizations (IV) usually start from already formed fullerenes, whereas endohedral fullerenes (I) are prepared during production in most cases.

1.5.2 Fullerides and Endohedrals

Calculations have shown that C_{60} should be a fairly good electron acceptor due to the features of its orbital diagram.^[49] In the first place, electrochemical measurements were conducted, but soon, fullerene salts, called fullerides, were prepared.^[59] Especially the discovery of superconductivity in alkali metal salts of C_{60} accelerated research on these intercalation compounds.^[60] Fullerides with alkali and earth alkali metals as well as mixed compounds of these have been prepared and investigated.^[61] The best superconducting phases contain C_{60}^{3-} . The highest temperature for superconductivity at ambient pressures was found for Cs_2RbC_{60} at 33 K.^[62, 63]

Endohedral functionalization of fullerenes is generally accomplished directly during production, resulting in metallofullerenes with cages usually bigger than C_{60} (page 6). The encapsulated metal or cluster determines the size and structure of the cage and also enables the formation of otherwise unstable cages.^[23, 37] In that manner, especially IPR-forbidden cages are increasingly isolated. Stabilization is usually due to charge transfer from the encapsulated species to the carbon cage and this influences also the chemical reactivity of the metallofullerene.^[37]

Next to metals and their clusters, other small molecules or atoms have been incorporated inside fullerenes. Noble gases were placed inside C_{60} or C_{70} by applying high temperatures and elevated pressures and this was achieved for He, Ne, Ar, Kr and Xe.^[64, 65]

Due to the curvature of C_{60} , the largest part of the p-orbitals points outside and the inner surface of C_{60} is completely inert.^[66] Therefore, highly reactive compounds, like single nitrogen atoms can be trapped within C_{60} , making $N@C_{60}$ a stable compound, despite its radical character. Due to its peculiar spin state, this compound or its derivatives might find use in future quantum computers.^[67] For its preparation, a film of C_{60} was sputtered with nitrogen-ions that subsequently intruded into the carbon cage.^[68]

More stable species were trapped inside C_{60} by a more intuitive method, adapted from the macroscopic world. In a process called molecular surgery, C_{60} was zipped up, filled with an appropriate guest and resealed again to yield the desired endohedral compound. This was elegantly demonstrated for $H_2@C_{60}$.^[69]

1.5.3 Cage Modifications

The most fundamental modification of fullerenes is at the carbon framework itself. Apart from changing the number of carbon atoms or their arrangement, the replacement of carbon atoms by other elements can also be envisaged. The resulting compounds are hence called heterofullerenes.^[70] The first heterofullerenes were detected by mass spectrometry shortly after the discovery of C_{60} . Laser vaporisation of graphite/boron composites with the same setup used to detect C_{60} yielded mass-spectrometric traces of borafullerenes of the composition $C_{60-n}B_n$.^[71] Recently, the borafullerene anion $C_{59}B^-$ was prepared in the gas phase from C_{60} and boron vapor.^[72] Various other heterofullerenes (containing N,^[73, 74] O,^[75, 76] P,^[77] Si,^[78, 79] Ge,^[80] As^[80] or transition metals^[81, 82]) were detected mass spectrometrically, mostly under similar conditions, but none of these compounds were isolated in macroscopic quan-

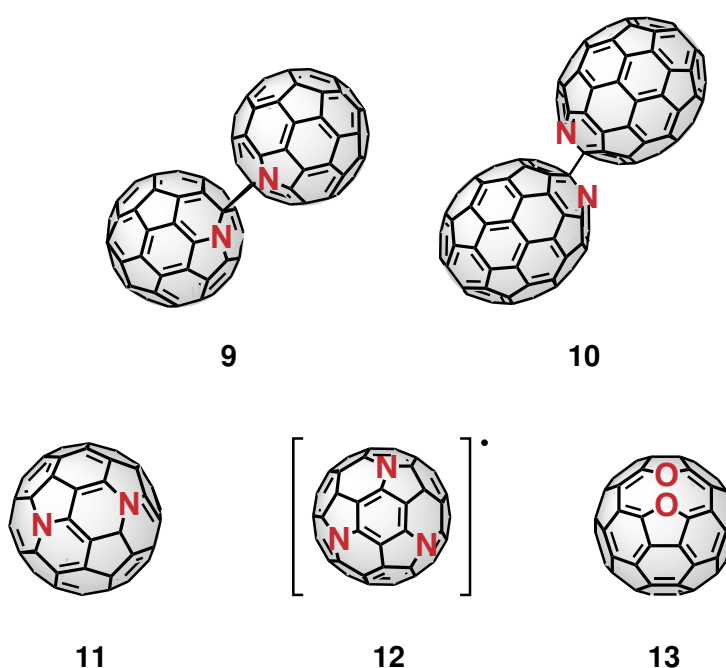


Figure 1.10: The heterofullerenes **9** and **10** are available in bulk quantities. For the heterofullerenes **11**, **12**, and **13** first evidence and synthetic strategies were presented in literature.

ties. The only heterofullerenes available to the chemist to date are $(C_{59}N)_2$ **9** and $(C_{69}N)_2$ **10**.^[83, 84] Various efforts were made in our own group to prepare $C_{58}N_2$ **11**,^[85, 86] most recently in the own master's thesis.^[87] Although many different strategies were employed, only mass spectrometric proof was obtained for $C_{58}N_2$ so far. In recent publications strategies were suggested to prepare $C_{57}N_3$ **12** or $C_{58}O_2$ **13** (Figure 1.10) from appropriate precursors, but to date none of these substances were obtained in macroscopic quantities.^[88, 89]

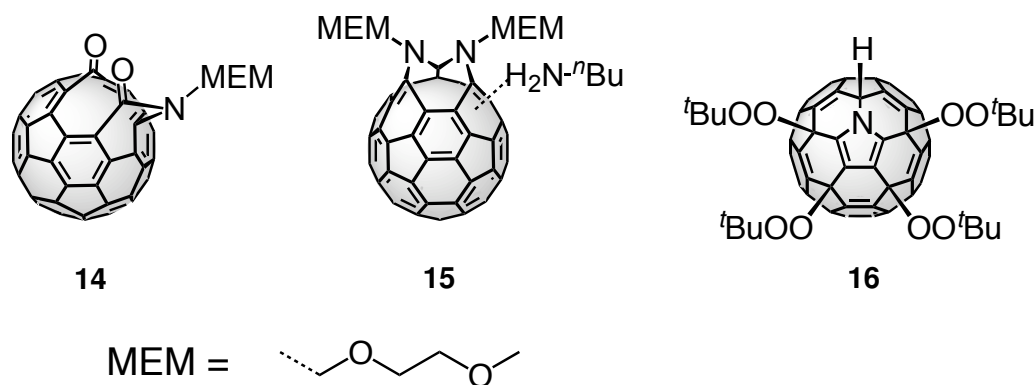
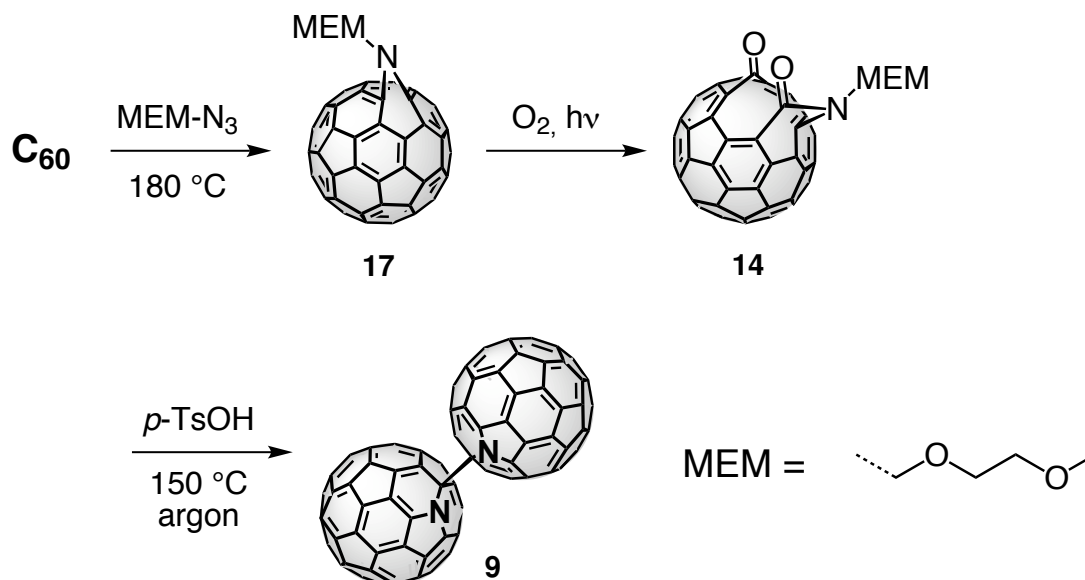


Figure 1.11: Parent azafullerenes were obtained from precursors **14** and **15**. A third method is reported that yielded azafullerene derivatives like **16**.

The available heterofullerenes $(C_{59}N)_2$ **9** and $(C_{69}N)_2$ **10** were prepared by well controlled chemical syntheses. Starting from C_{60} , appropriate precursor molecules were prepared (Figure 1.11) and finally converted to the heterofullerenes *via* acid induced fragmentation- and rearrangement-steps.^[90] The first bulk preparation of $(C_{59}N)_2$ **9** was accomplished by Wudl and coworkers (Scheme 1.1).^[83] *N*-MEM-azafulleroid **17** was prepared from MEM-azide and C_{60} in the first step of the reaction cascade (more detailed description of fullerene functionalization with azides follows in section 1.5.4 on page 22).^[91] In the next step, the cage-opened ketolactam **14** was obtained by self-sensitized photooxygenation of *N*-MEM-azafulleroid **17**.^[92] Upon treatment of the ketolactam **14** with *p*-TsOH, the desired heterofullerene $(C_{59}N)_2$ **9** was finally obtained.

It was isolated as the dimer. Substitution of one cage carbon atom by a nitrogen atom generates a radical due to the nitrogen's additional electron. The acid lability of the MEM-group was crucial to the entire process, because its acidic cleavage initiates the final transformation steps. The amino-methyl moiety was installed as break-junction already at the beginning of the synthesis. After the entire sequence the heterofullerene $(C_{59}N)_2$ **9** can be isolated and used for further investigations or reactions.

A second pathway was developed by our own group and employed A¹-A²-bisazafulleroid-aminoadduct **15** as precursor for the acid-catalyzed fragmentation process.^[84] The chemistry of nitrogen heterofullerenes, especially that of (C₅₉N)₂, was subsequently developed and a variety of even functional derivatives was prepared since then.^[93] In the past years, a third method was developed to prepare azafullerenes like **16** (Figure 1.11), but it yields only derivatives and no parent azafullerenes.^[94]



Scheme 1.1: The heterofullerene (C₅₉N)₂ **9** was prepared by the group of Wudl in three steps.

The method of Wudl usually yields (C₅₉N)₂ in higher purity and the preparation of precursor ketolactam **14** is less intricate than that of amino-adduct **15**. Thus, this synthetic pathway was adapted in several attempts to prepare C₅₈N₂ **11**, which would be the next very fundamental fullerene available in bulk quantities. Calculations have shown that the properties of C₅₈N₂ **11** depend on the relative position of the nitrogen atoms, which allows to fine-tune the performance of functional materials. Furthermore several of the 22 possible isomers should be stable and even monomeric compounds because they are no radicals like C₅₉N.^[95] This would be a great advantage in comparison to (C₅₉N)₂, because dimeric fullerene species are usually badly soluble, which hampers chemical manipulation and physical investigations. The first approach towards C₅₈N₂ was simply a twofold application of the well working Wudl method. In case of bisazafulleroids, however, the formation of the A¹-A²-isomer, like **15** is usually strongly favored, but this isomer turned out to be unsuitable because it undergoes only a single photooxygenation.^[70] It was suggested, that the azafulleroid moieties require

a certain spatial separation to undergo twofold photooxygenation.^[70] Therefore, more advanced strategies had to be considered to prepare the bisketolactam and ultimately $C_{58}N_2$. In pioneering work, Reuther evaluated two different strategies to enforce the separation of the two azafulleroid-moieties, which he called fixed-spacer- and tweezer-approach.^[85] In case of the fixed-spacer-approach (Figure 1.12), a suitable malonate, bearing two azidomethylether moieties should be attached to C_{60} in the first place. In a subsequent step, two azides should be attached to C_{60} at remote positions in intramolecular reactions. In case of the tweezer-approach, a bisazidomethylether is directly reacted with C_{60} . The steric constraints of the spacer should inhibit the A^1 - A^2 -addition pattern and install the two azafulleroid moieties at distant positions. Due to synthetic difficulties, however, Reuther was only able to prepare small amounts of a bisazafulleroid of unknown regiochemistry by the tweezer-approach (Figure 1.12). Photooxygenation to a bisketolactam failed for unknown reasons and only two monoketolactams were obtained. In case of Reuthers fixed-spacer-approach, the reaction conditions did not even allow the isolation of a suitable azidomethylether precursor.

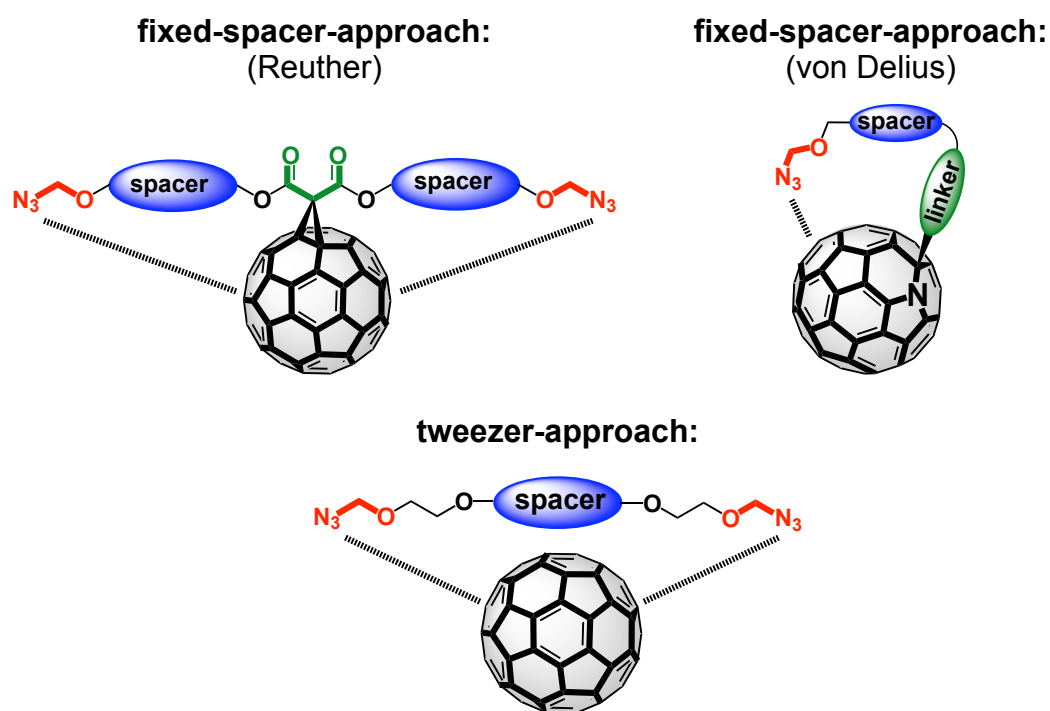
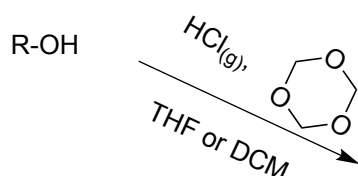


Figure 1.12: Prototypical structures that represent the different strategies that were used to gain access to $C_{58}N_2$. The spatial separation of the two nitrogen moieties is essential for success.

Von Delius followed later on a third approach, which can be classified as a kind of fixed-spacer-approach (Figure 1.12). In contrast to previous works, a $C_{59}N$ -derivative was subjected to the conditions of the Wudl method and the double photooxygenation was avoided in that way. In the end a $(C_{59}N)_2/C_{58}N_2$ product mixture was detected in the mass-spectrometer and it was shown that this strategy might be suitable to produce $C_{58}N_2$ or more exactly, derivatives therefrom.^[86] For future projects the most important discovery in his work was a new chloromethylation procedure for the formation of the necessary azidomethylethers (Figure 1.13). Instead of using gaseous HCl as before, a mild method based on TMS-Cl was found in a publication by Shipov and applied for the formation of the intermediate chloromethylethers.^[96]

Standard chloromethylation procedure:



Chloromethylation procedure according to SHIPOV:

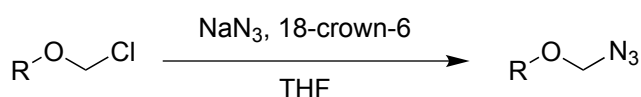
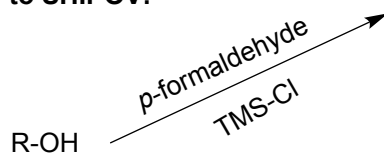
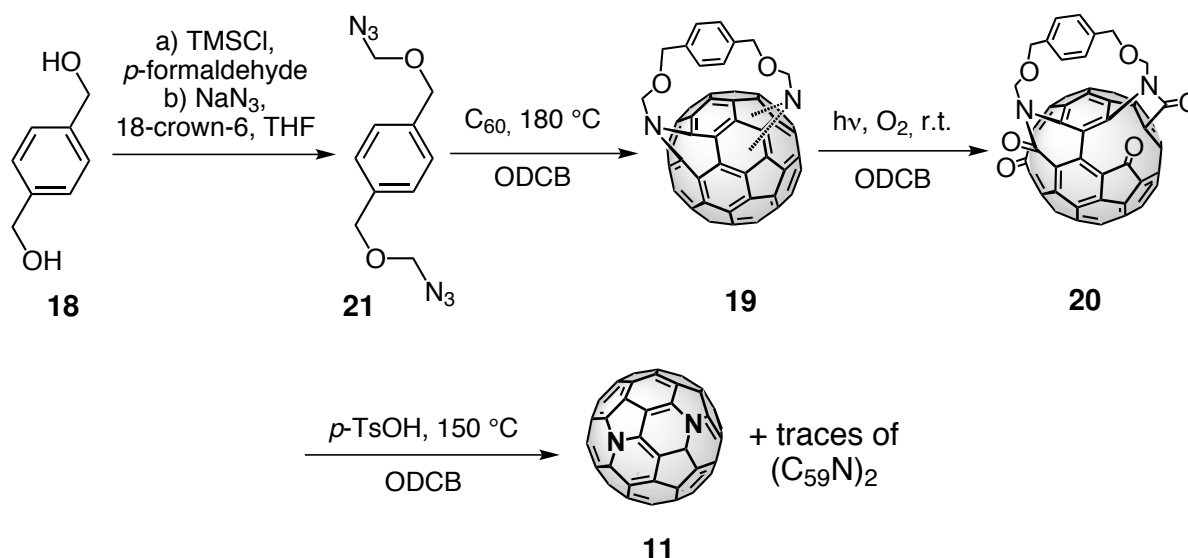


Figure 1.13: Comparison of the two methods for the crucial step of chloromethylation, during the synthesis of the essential azidomethylethers.

This chloromethylation procedure was combined with the tweezer approach in the latest attempt during the own master's thesis.^[87] Using the tweezer approach has the advantage that the parent heterofullerene $C_{58}N_2$ is immediately the product and not a derivative thereof. The knowledge of a mild chloromethylation procedure allowed the preparation of larger amounts of different precursor bisazidomethylethers and the screening of reaction conditions. In the end, the bisazidomethylether derived from 1,4-benzenedimethanol **18** was used to prepare a mixture of different regioisomers of bisazafulleroids **19**, which were successfully doubly photooxygenated in the next step (Scheme 1.2). The separation of different isomers was



Scheme 1.2: Samples of diazaheterofullerene C_{58}N_2 **11** were prepared in five steps.

attempted at that time but not possible by simple column chromatography, neither for the bisazafulleroids **19**, nor for the bisketolactams **20**. Upon acid-treatment of the bisketolactam-fraction a mixture of C_{58}N_2 **11** and $(\text{C}_{59}\text{N})_2$ was detected by MALDI-TOF-MS (Figure 1.14). A UV/Vis-spectrum of the product mixture showed new features (Figure 1.14), which in combination with the MS-data was a proof for the presence of a new fullerene compound.

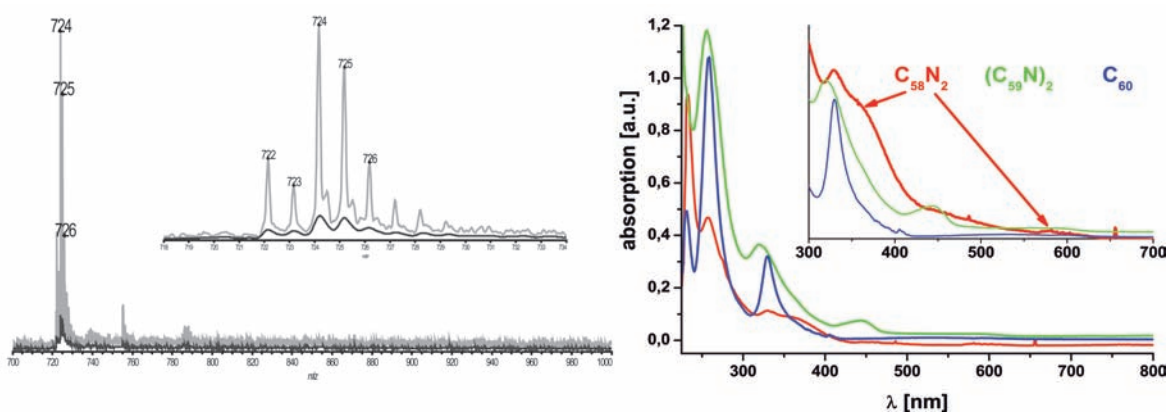


Figure 1.14: The sample of C_{58}N_2 **11** was characterized by mass-spectrometry and UV/Vis-spectroscopy in the master's thesis. MALDI-TOF-MS showed some $(\text{C}_{59}\text{N})_2$ -impurities but the UV/Vis-spectrum (DCM; r.t.; inset shows a magnification of the region between 300 nm and 700 nm) indicated the presence of a new chromophore.

1.5.4 Exohedral Functionalization

Exohedral functionalization of fullerenes is by far the most popular and widespread method of alternating their properties because it is the chemically most accessible. C_{60} can be regarded as an electron deficient, strained polyene, which explains most of its behavior in exohedral functionalization reactions. This is summarized by the following four rules:^[58]

1. C_{60} reacts preferentially with radicals, nucleophiles and in cycloadditions, because of its electron deficiency.
2. Cycloaddition reactions will usually take place at [6,6] bonds, as a consequence of the position of double bonds.
3. The major driving force of addition reactions to C_{60} is strain release of the cage due to transformation of sp^2 -carbon atoms to sp^3 -carbon atoms.
4. The formation of double bonds in five-membered rings will be avoided or at least minimized.

Halogenation reactions of fullerenes usually proceed *via* a radical mechanism. The high electron affinity of C_{60} makes it a radical scavenger or radical sponge.^[97] Halogenation was conducted with fluorine, chlorine and bromine from different sources, but not with iodine because the adducts are not stable enough.^[58, 98] The stability of the compounds increases from bromine over chlorine to fluorine and adducts up to $C_{60}F_{48}$ are reported.^[99, 100] Usually complex mixtures are obtained, which have to be separated by HPLC. The only selective example is the chlorination of C_{60} with ICl, leading to $C_{60}Cl_6$.^[101] This procedure is used to prepare the corresponding $C_{59}N$ -derivative **22** (Figure 1.15), having an isolated pyrrole substructure, surrounded by four chlorine atoms.^[102] The fluoro- and chlorofullerenes are susceptible to nucleophiles and are used in some cases as starting points for further functionalizations.^[58, 103]

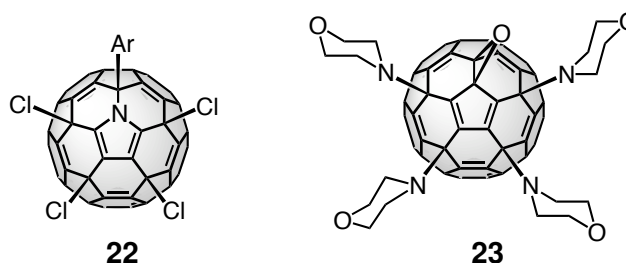
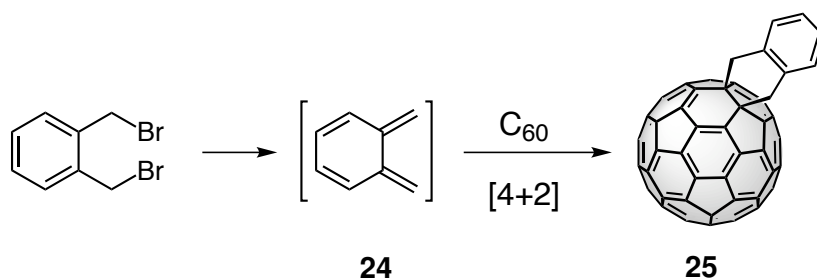


Figure 1.15: Fullerene compounds **22** and **23** were prepared by radical reactions.

Addition of amines proceeds also *via* a radical mechanism, but only few examples of defined adducts like **23** (Figure 1.15) are reported.^[104]

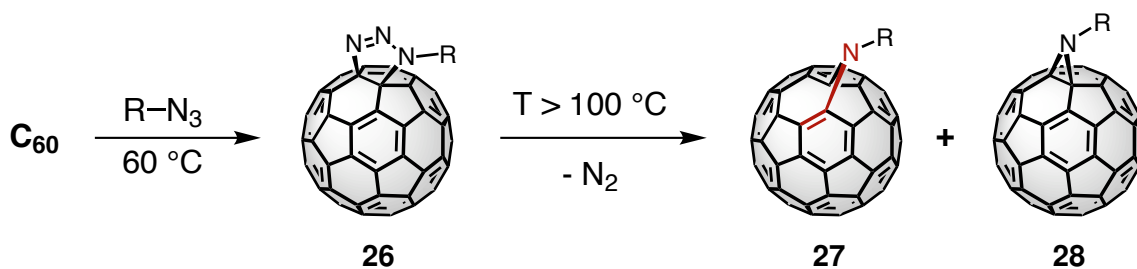
More frequent are examples for cycloadditions to C_{60} . As C_{60} is electron deficient, it acts as a good dienophile or dipolarophile in a number of reactions. Many DIELS-ALDER-reactions are reported, but they are in most cases reversible, unless a precursor is utilized, that hampers the back-reaction (Scheme 1.3).^[105, 106] This is accomplished by using *e.g.* *o*-quinodimethanes **24** as dienes, because they rearomatize upon addition to C_{60} , making a back-reaction impossible. They are usually prepared *in situ*, because they are unstable by themselves.^[107]



Scheme 1.3: DIELS-ALDER reactions with fullerenes are usually reversible, unless the products are thermodynamically trapped.

Other cycloadditions, like [3+2], [2+2] and [2+1] cycloadditions were all conducted with fullerenes.^[58] The addition of benzyne is an example for a [2+2] cycloaddition.^[108] Addition of diazoalkanes proceeds *via* a [3+2] cycloaddition and yields pyrazolinofullerenes. Depending on the further treatment, thermal or photolytic, fulleroids or methanofullerenes are formed, respectively (the analogous reaction with azides is illustrated in scheme 1.4).^[109, 110, 111] In methanofullerenes, the usual addition across a [6,6]-double bond takes place and forms a cyclopropane structure. In case of fulleroids the [5,6]-bond is bridged upon loss of N₂ from the pyrazolinofullerene and subsequent rearrangement. The [5,6]-bond is not only bridged but also opened and thus retains the π -electron network which is reflected in unchanged UV/Vis- and CV-spectra.^[109]

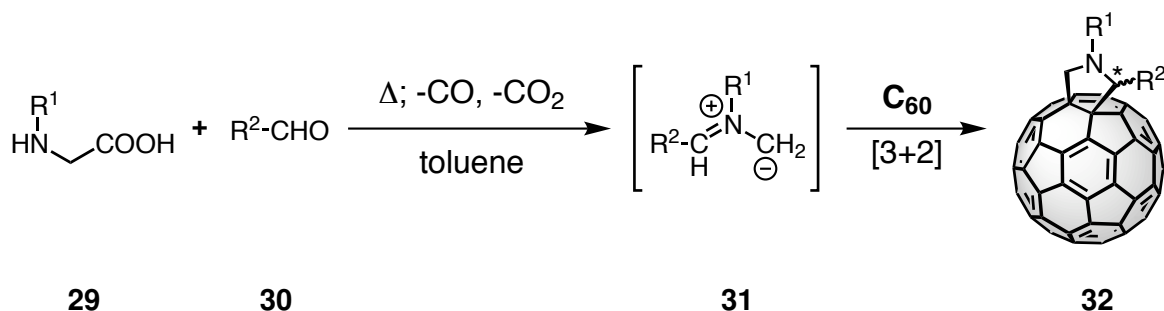
The addition of organoazides is another example for a [3+2] cycloaddition to C_{60} and yields triazolinofullerenes **26** (Scheme 1.4).^[112] Upon thermal treatment, they extrude N₂ and the [5,6]-opened azafulleroid **27** and in minor quantities the [6,6]-closed aziridinofullerene **28** are obtained. Aziridinofullerene **28** is thermally unstable towards azafulleroid **27** and can be transformed into it.^[91] Like fulleroids, azafulleroids possess a rather unperturbed π -system and their physical properties resemble those of pristine C_{60} .^[91] In azafulleroids as well as in



Scheme 1.4: The [3+2] cycloaddition between C_{60} and organoazides yields triazolinofullerenes **26** which are thermally unstable towards the aziridinofullerene **28** and the azafulleroid **27**. The activated moiety in azafulleroid **27** is highlighted.

fulleroids the [5,6]-open and the [6,6]-closed isomers are the only ones to be observed. The other two possibilities, [5,6]-closed and [6,6]-open have never been observed, because these structures lead to an unfavorable distribution of double bonds. A closer look at the bonds, surrounding the azafulleroid moiety reveals that a double bond is attached to the bridgehead atom (Scheme 1.4). This is a violation of BREDT's rule, which states that double bonds, attached to bridgehead atoms in polycyclic structures, are too strained and do not occur in stable compounds.^[113] Together with the bridging nitrogen atom, this double bond can also be considered as part of an electron-poor vinylamine moiety. These two facts together render this double bond rather reactive and are a reason for the selective oxidation and cage-opening reaction during photooxygenation towards ketolactam **14** in the heterofullerene synthesis (page 15).

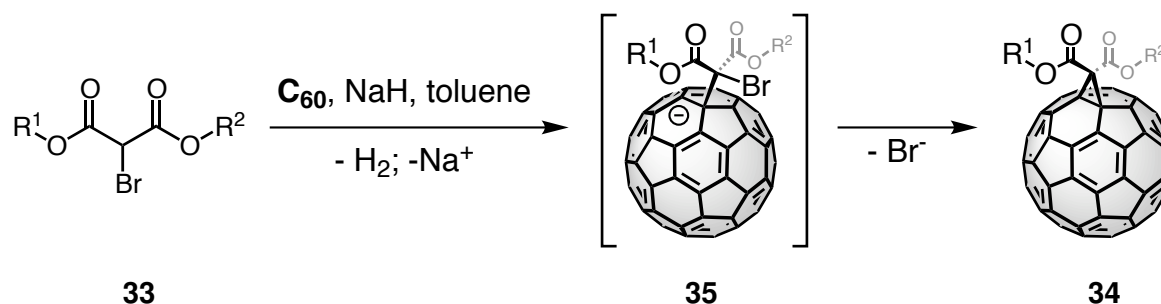
One of the most versatile cycloadditions is the [3+2] dipolar azomethine ylide cycloaddition, called PRATO-reaction (Scheme 1.5). An amino acid **29** is reacted with an aldehyde **30** to form the reactive azomethine ylide **31**, which undergoes a [3+2] dipolar cycloaddition with



Scheme 1.5: The PRATO-reaction is a [3+2] dipolar cycloaddition between C_{60} and an *in situ* generated azomethine ylide **31**.

C_{60} *in situ*.^[114] As the aldehyde or the amino acid can be attached to virtually any moiety, this allows the construction of fulleropyrrolidines **32** with a huge range of properties and appended structural motifs.^[115] The adducts are usually very stable, but the pyrrolidine ring contains a stereocenter, which can complicate the separation of isomers and which makes the NMR-spectra more complex.

An even more versatile reaction is the BINGEL-reaction, which is a nucleophilic cyclopropanation with bromomalonates **33** yielding methanofullerenes **34**.^[116] The esterification of malonates with an appropriate alcohol is an even more basic reaction than the preparation of the corresponding precursors for the PRATO-reaction and allows easy access to functional fullerene derivatives. Furthermore the BINGEL-adducts **34** are usually more symmetric, as they contain no stereocenter. In the initial protocol a bromomalonate **33** was deprotonated with NaH and reacted with C_{60} . The malonate anion attaches to a double bond of C_{60} and the new, fullerene-centered, anion **35** substitutes bromide and closes the cyclopropane ring in the last step (Scheme 1.6). Further improvements of this reaction lead to the use of DBU as non-nucleophilic base and more important the *in situ* halogenation of the malonate by elemental iodine or CBr_4 .^[47, 117, 118] Especially the *in situ* halogenation was of great benefit, because the difficult and time-consuming isolation of monobromides was no more required.



Scheme 1.6: The nucleophilic cyclopropanation of C_{60} with bromomalonates **33** is used to synthesize structurally very versatile methanofullerenes **34** (BINGEL-reaction).

1.6 Stereochemistry of C₆₀ Multiple Adducts

1.6.1 Stereochemical Nomenclature

C₆₀ being a multivalent compound gives rise to a rich collection of stereochemical phenomena. In pristine C₆₀ only the interior and the outside can be distinguished but otherwise all carbon atoms are equal due to the I_h -symmetry. Consequently, any kind of monoaddition to one of the thirty double bonds gives only a single product. In case of bisadducts, there are theoretically nine different isomers possible. For the nomenclature of multiple additions a spiral numbering system can be used to denote the absolute position of addends.^[119] Therefore the SCHLEGEL-diagram is numbered in a spiral fashion (Figure 1.16). Thus, the numbering is also chiral, which will be exploited for the absolute assignment of inherently chiral addition patterns (page 25).

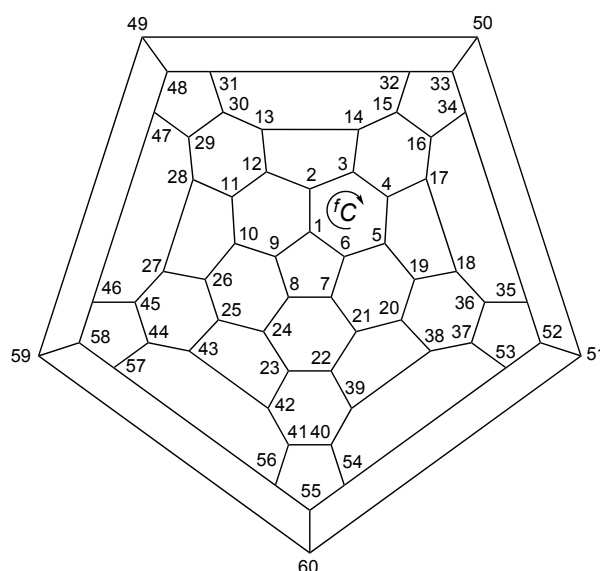


Figure 1.16: The SCHLEGEL-diagram is a two-dimensional representation of C₆₀. It is numbered in a spiral fashion to denote the position of bonds and addends. The numbering scheme is chiral by itself (fC -orientation shown here; more detailed explanation on page 25).

Most C₆₀-derivatives contain addends over [6,6]-bonds generated by the PRATO- or the BINGEL-reaction. For this purpose a more straightforward, relative nomenclature for multiadducts was proposed, resembling the *ortho/meta/para*-scheme for the nomenclature of benzene-derivatives (Figure 1.17).^[44] The fullerene sphere is divided into two hemispheres and those positions at the same hemisphere as the first addend are named *cis*-1 - *cis*-3. The positions

at the opposite hemisphere are named *trans*-1 - *trans*-4 with *trans*-1 being directly at the opposite position of the first addend. The remaining [6,6]-bonds in the equatorial plane are named *e'* and *e''*, but they are only different in case of two kinds of addends or of unsymmetrical addends. For higher adducts than bisadducts the relative positions between all the addends are stated, e.g. *e,e,e*-trisadduct, for the trisadduct isomer where all addends are in *e*-position towards each other.

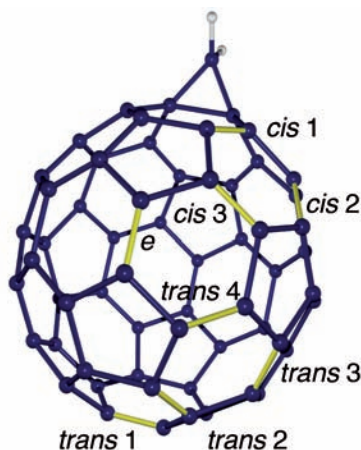


Figure 1.17: The relative position of addends at [6,6]-bonds in C_{60} -polyadducts can be described by an easy nomenclature.

Unsymmetrical addends give rise to another stereochemical phenomenon, which is a form of *in/out*-isomerism and which describes the different orientation of several addends towards each other.^[120, 121] In case of trimacrocyclic *e,e,e*-trismalonate adducts the assignment of the four isomers (*out-out-out*, *in-in-in*, *out-out-in*, *out-in-in*) is simple and intuitive (Figure 1.18) because the relative position of the free side of the malonate can be clearly determined.

In case of certain addition patterns that contain only a rotational axis as element of symmetry, the addition pattern itself is inherently chiral. The mirror images of the two isomers cannot be brought to superposition, even in case of symmetrical, achiral addends. Examples are the addition patterns *cis*-3 (C_2 -symmetry), *trans*-2 (C_2) and *trans*-3 (C_2) for bisadducts or *trans*-3,*trans*-3,*trans*-3 (D_3) and *e,e,e* (C_3) for trisadducts. In order to distinguish the two enantiomers of a given addition pattern the ^f*C*- and ^f*A*-nomenclature is used.^[122] It makes use of the fact, that the spiral numbering scheme in the SCHLEGEL-diagram is itself chiral. The prefixes describe the fashion in which the SCHLEGEL-diagram is numbered to obtain the lowest set of locants for the addends. This can be either in clockwise direction (^f*C* for fullerene clockwise, like in figure 1.16) or in anticlockwise direction (^f*A* for fullerene anticlockwise).

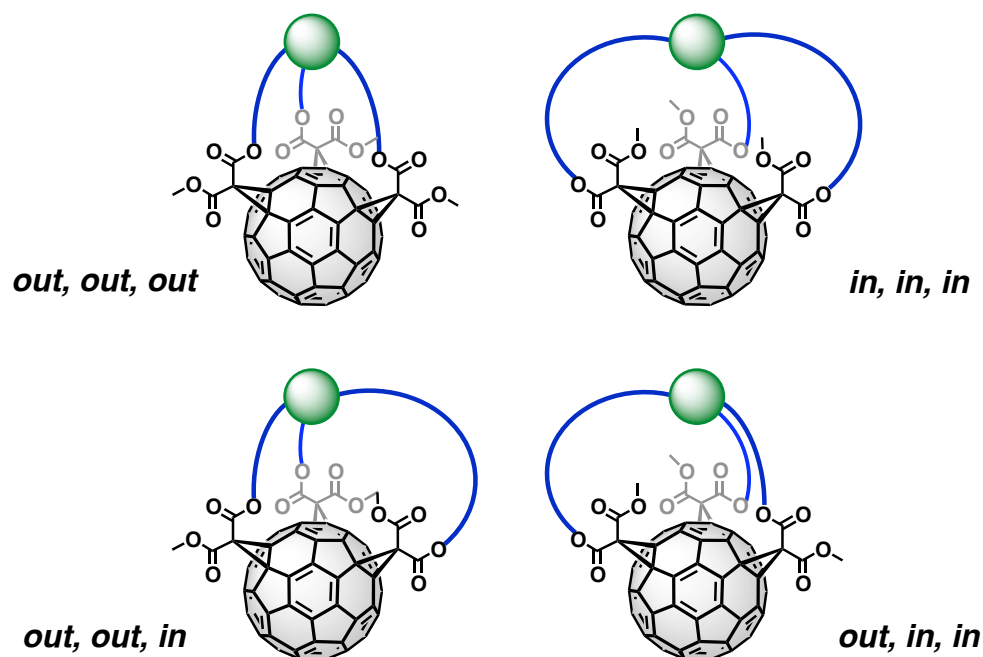


Figure 1.18: In case of unsymmetrical addends, the orientation of otherwise identical addends leads to four diastereomeric *e,e,e*-trisadducts.

1.6.2 Synthesis of Defined Multiadducts

The targeted preparation of a certain multiadduct of C₆₀ requires usually special precautions. The addition of a second independent addend to a C₆₀-monoadduct usually results in the formation of all possible isomeric bisadducts, except for *cis*-1. It is only accessible for sterically non-demanding addends. Although it was shown that the second addition of a malonate favors attachment at *e*- and *trans*-3-position a product mixture is always obtained and tedious separation procedures are necessary.^[42] The preference for the *e*- and *trans*-3-positions can be explained by increased orbital coefficients at these two positions.^[123, 42] Each additional addend in *e*-position activates the residual *e*-positions even more and facilitates the formation of the *T_h*-hexakisadducts where all addends are in an *e*-relationship to each other.^[123]

The tether-directed remote functionalization was developed by the group of Diederich to avoid time-consuming separation procedures and to prepare selectively one or a few isomers.^[124, 125] In that strategy two reactive moieties are connected by a rather rigid spacer that allows only the formation of a certain addition pattern due to steric requirements of the spacer backbone. Upon reaction of the first moiety, there is ideally only one other position possible to obtain a relaxed geometry. However, due to the irreversibility of most of the functionalization reactions,

there are sometimes more products favored for a given spacer. Today there exist suitably designed spacers to prepare all bisadducts and many trisadducts are also accessible.^[126, 127, 46] Among the latter, the highly symmetrical *e,e,e*-trisadduct is of special interest because it constitutes half-part of an even more symmetrical T_h -hexakisadduct.

Inherently chiral fullerene derivatives were also prepared in enantiomerically pure form by the use of appropriate tethers and upon removal of the template it was shown that the chiral addition pattern itself gave rise to strong COTTON-effects.^[117, 128] In another approach fullerene derivatives with a chiral addition pattern were prepared by the stepwise addition of enantiomerically pure bisoxazolines (Figure 1.19). The resulting compounds were obtained as pairs of diastereomers. They were separated on an achiral stationary phase and their optical properties were determined.^[129]

A highly selective second addition to a C_{60} -monoadduct can be observed with azafulleroids **27**. A second azide attaches selectively to the A^2 -position, directly next to the azafulleroid moiety (Scheme 1.7). The above mentioned activation by a double bond at a bridge head car-

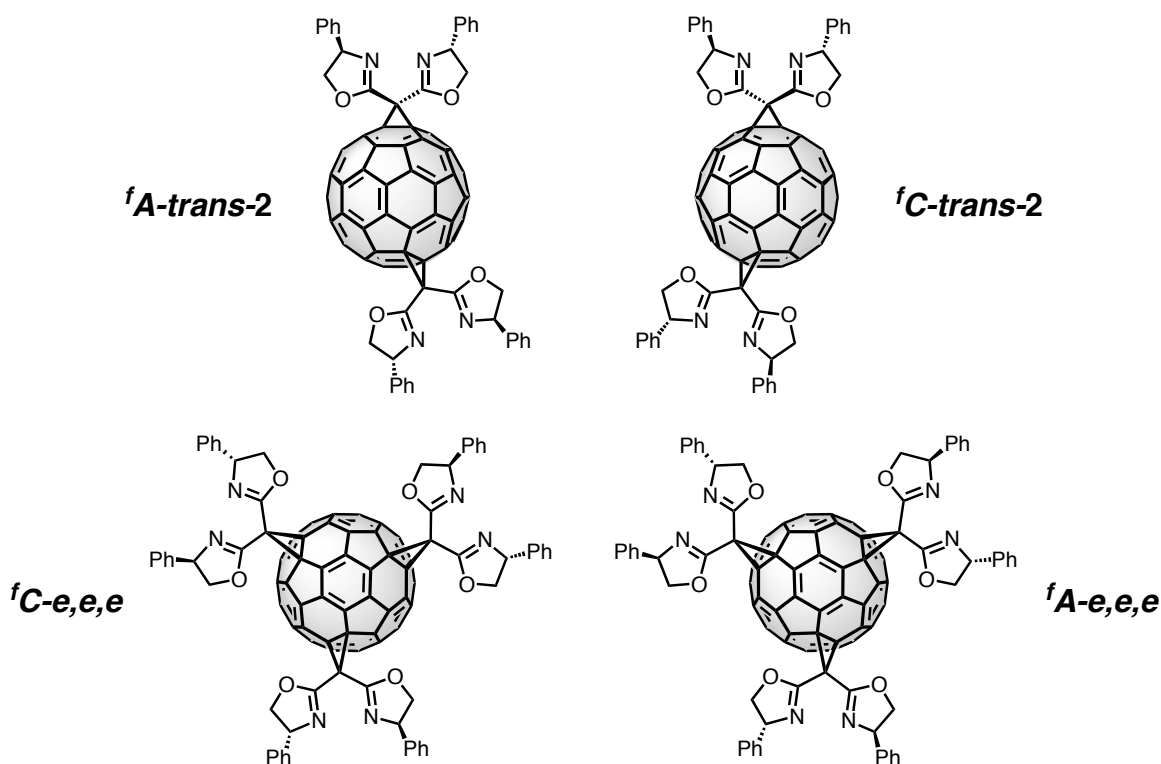
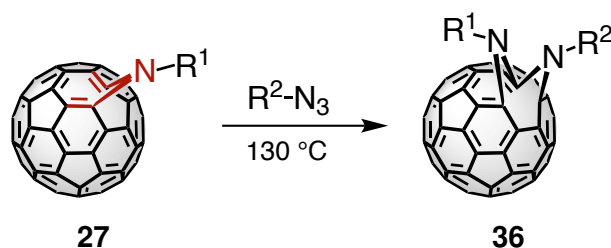


Figure 1.19: *trans*-2 and *e,e,e* are examples for inherently chiral addition patterns. If the addends are themselves chiral, the adducts are obtained as pairs of diastereomers and can be separated on an achiral stationary phase.

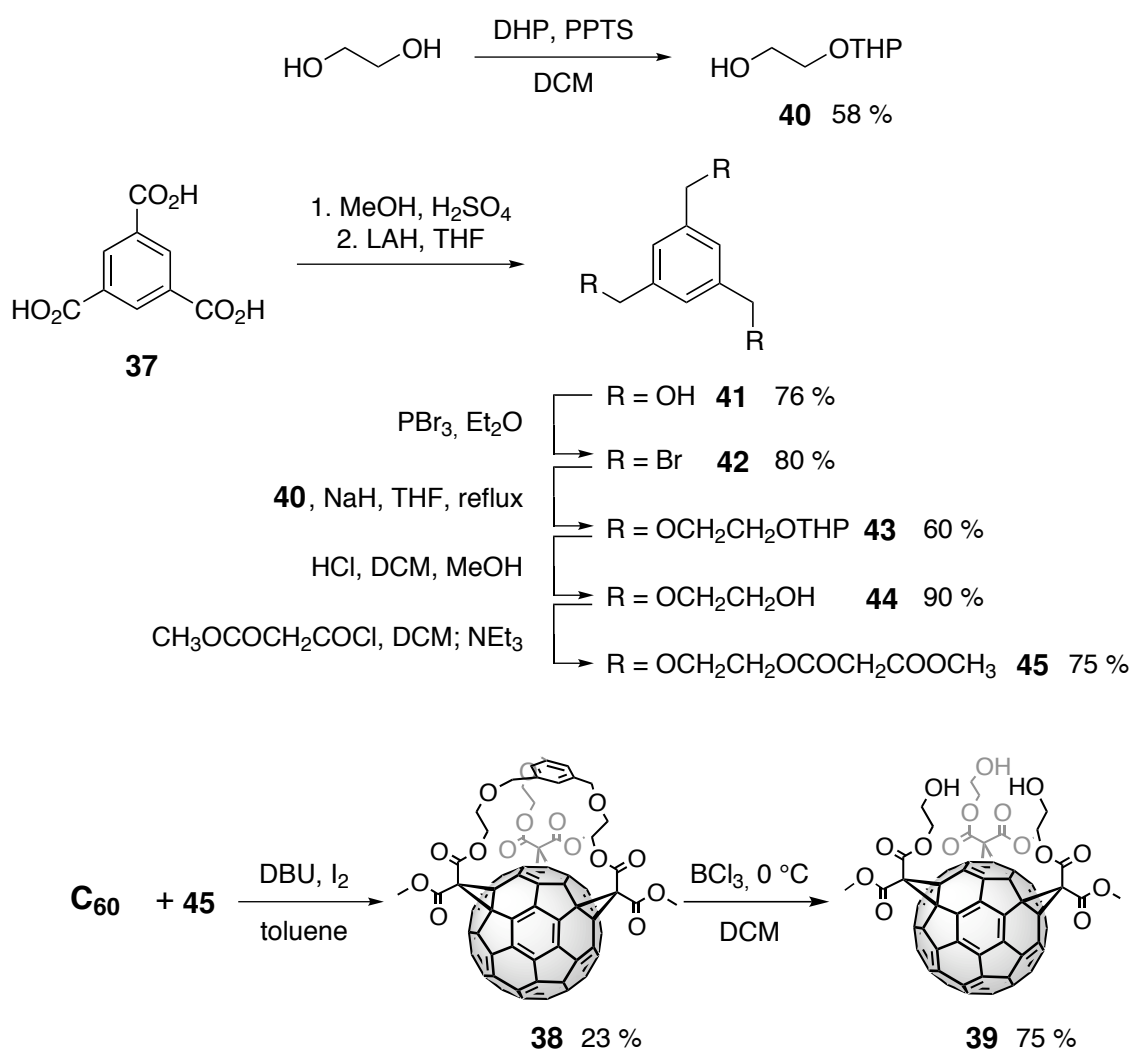


Scheme 1.7: Azafulleroids **27** are activated directly next to the nitrogen bridge and a second addition produces usually regioselectively A^1-A^2 -azafulleroids **36**.

bon atom and the electron-poor vinylamine substructure explain the selectivity (page 21).^[112] Only very rigid spacers can direct the second addition to another position and allow the isolation of other bisazafulleroid isomers.^[130, 131, 132]

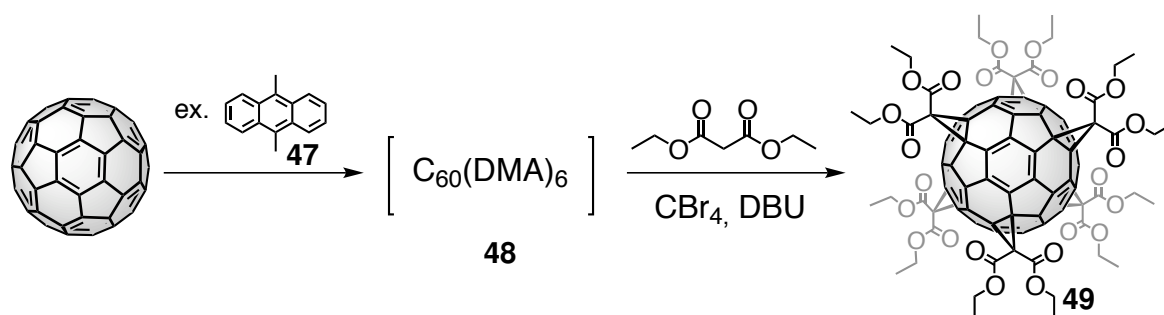
e,e,e-Trisadducts of malonates were prepared for the first time by a step-wise procedure.^[44] Later on, tethers derived from cyclotrimeratrylene or cyclo-[*n*]-alkylmalonates were developed to template selectively the formation of *e,e,e*-trisadducts.^[45, 46] This development was not only inspired by the access to this addition pattern but also by the observation, that the corresponding water-soluble *e,e,e*-hexakis acid showed promising activity as an antioxidant or neuroprotective agent.^[133, 134, 135, 136, 137, 138, 139] However, this compound was toxic due to decarboxylation during metabolism and structural analogues were sought as novel drug candidates.^[140] For this purpose systems were developed recently that allowed not only the formation of this unique addition pattern but also the removal of the template. In addition, two separately addressable and functionalizable addend zones were created. In that way, this geometry could also be incorporated in highly functional materials.^[141] One system was derived from trimesic acid **37** and allowed the formation of *e,e,e*-trisadduct **38** in eight steps and an overall yield of 3.3% (Scheme 1.8). Upon appropriate deprotection trisalcohol **39** was obtained and used as building block for the construction of various functional compounds. Highly functionalized C₆₀-hexakisadducts with T_h -symmetry are of special interest. They are not only synthetically challenging but resemble a building block with a very rare symmetry in organic chemistry. This allows the assembly of a large number of functionalities around a central core with a unique spatial arrangement. Not only hexakisadducts with one type of malonate can be prepared, but also hexakisadducts with all types of stoichiometries for two different types of adducts. This is indicated by two numbers in square brackets denoting the number of addends of each type ([5:1], [4:2], [3:3]).

e,e,e-Trisadducts allow access to mixed [3:3]-hexakisadducts and the building-block principle can be extended to these fullerene derivatives as well.^[142] The second addition of a trimalonate proceeds with even higher selectivity, as not only the template enforces the *e,e,e*-addition pattern, but the preorganized C₆₀ *e,e,e*-trisadduct is also more reactive at the remaining *e*-positions as explained above (page 26).^[123] Hexakisadducts were synthesized from *e,e,e*-trisadducts preorganized by benzene templates or cyclo-[*n*]-alkylmalonates and either another trimalonate or three independent malonates.^[142, 143]



Scheme 1.8: Trimalonate **46** was used for the templated synthesis of *e,e,e*-trisadduct **38**, which was deprotected to trisalcohol **39**. This compound serves as building block for various functional materials.

For the latter strategy another templating and activating process is beneficial that allows the preparation of T_h -symmetrical hexakisadducts from six independent malonates.^[47] For that purpose, C_{60} is first treated with 9,10-dimethylantracene (DMA) **47** to generate the DMA-hexakisadduct **48**. Unlike malonates, DMA forms reversible DIELS-ALDER-adducts with C_{60} and consequently, the entire system equilibrates. The T_h -symmetrical hexakisadduct is the thermodynamically favored isomer and as soon as the equilibrium has reached malonates are added. Once a DMA-molecule detaches from the fullerene surface, it is replaced irreversibly by a malonate at this position. This proceeds with complete regioselectivity as this is the only sterically accessible position at that moment and it is highly activated from the residual five addends. In that way, the T_h -symmetrical addition pattern is gradually established until the malonate substituted hexakisadduct **49** is obtained in the end. In recent work, it was shown, that the effect of DMA-templating can also be replaced by a large excess of CBr_4 , and a mechanism was recently presented by our group.^[144, 145] These templating mechanisms are usually employed to synthesize mixed T_h -hexakisadducts of all compositions.



Scheme 1.9: The reversible formation of the DMA-hexakisadduct **48** is a common strategy to template the formation of malonate-hexakisadducts **49** starting from C_{60} or other appropriately functionalized multiadducts.

2 Proposal

The first target of this thesis was a more detailed investigation towards the formation of diazaheterofullerene $C_{58}N_2$. In the course of its synthesis during the master's thesis,^[87] the precursor bisazafulleroids and bisketolactams were employed as mixture of isomers. These isomers had to be separated, characterized and their regiochemistry had to be determined in order to gain insight into a successful preparative strategy. In the next step, the diazaheterofullerene mixture had to be analyzed with regard to the number of isomers. They should be separated, the relative position of the nitrogen atoms should be determined and the physico-chemical properties should be investigated. As a last step, functionalization of these fundamental compounds should give insight into their chemical behavior.

A novel trifunctionalization strategy for fullerenes based on benzene templates was recently developed.^[141] It allowed a selective access to C_{60} -*e,e,e*-trisadducts with control over the spherical arrangement of unsymmetrical malonates. An important feature of these systems was the creation of two independent addend zones. As a second target of this thesis, a novel template for such systems should be developed (Figure 2.1). The search should be directed towards a faster and easier access to these fullerene multiadducts. At the same time, the template should be easy to remove because that allows the zone-selective post-functionalization.

In order to decide, which motifs fit into this geometry at all a reverse screening should be conducted in the first place. It should be tested, which moieties can be incorporated into C_{60} -*e,e,e*-trisalcohol **39**, which is already known (Scheme 1.8 on page 29). All candidates, that form stable adducts with this compound should in principle be able to template its formation. Suitable motifs to cap the polar addend zone of the trisadduct will feature tris-valent cores that attach to the hydroxyl groups.

As soon as a stable adduct is found, the forward synthesis of the corresponding trimalonate should be established, always bearing in mind that the synthesis should be easier to accomplish than that of previous systems. In a next step, the selectivity of the addition of this novel template to C_{60} should be investigated. Additionally, the influence of the spacer-length on the selectivity for a certain addition pattern should be investigated.

Removal of the template is the next step in order to equip the polar addend zone with other moieties. Depending on the nature of the template, deprotection can yield different functional groups. Their properties will guide subsequently the search for a suitable transformation that allows for the attachment of other moieties, independent of the other parts of the molecule.

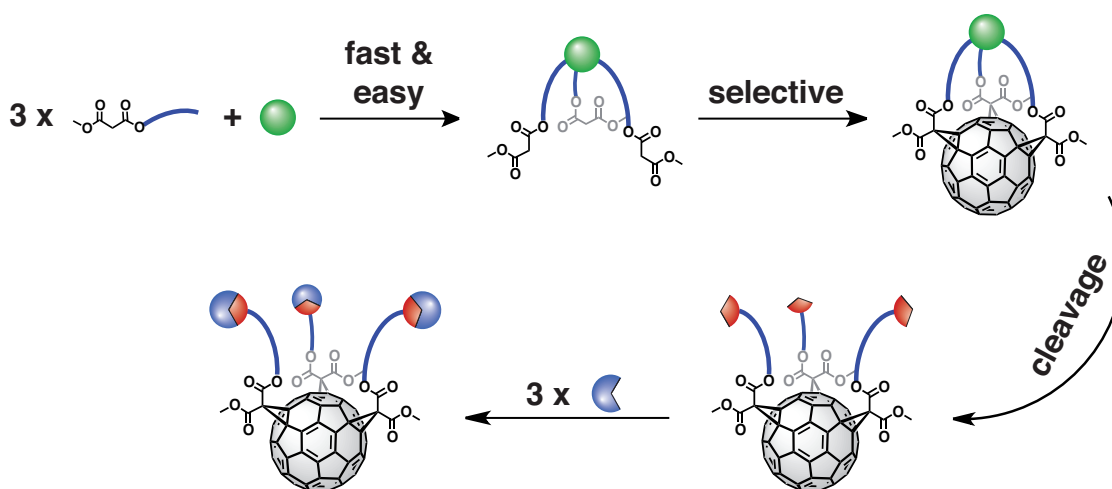


Figure 2.1: Illustration of the concept of this thesis. Three malonates should be connected fast and easily to a suitable template. Upon addition to C_{60} the *e,e,e*-addition pattern should be selectively formed. After the cleavage of the template coupling points should remain that allow the straightforward further-functionalization.

This novel template can also be used to synthesize C_{60} -[3:3]-hexakisadducts. Especially interesting in this respect is the combination with the known benzene system. Novel building blocks with two different polar addend zones will be created and they can probably be deprotected and functionalized independently on both sides. In the end of this development, versatile building blocks should be the result that provide access to a rich variety of compounds starting from a single [3:3]-hexakisadduct.

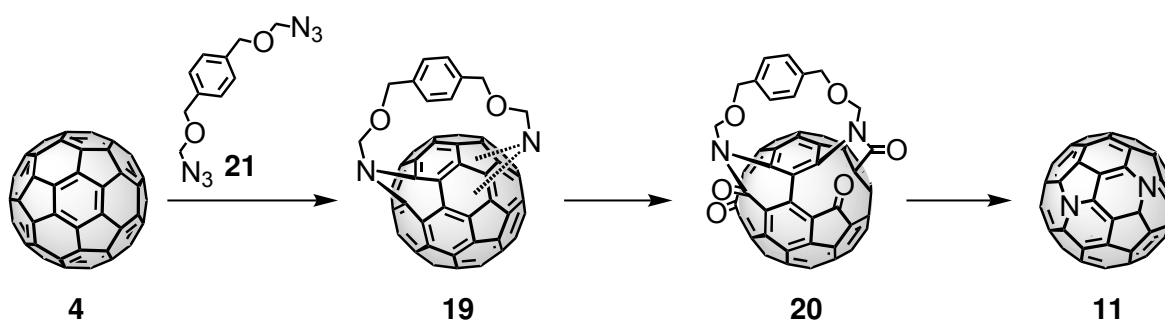
3 Results & Discussion

3.1 Investigations on $C_{58}N_2$

3.1.1 Repetition of the Synthesis

The heterofullerene $C_{58}N_2$ **11** is a highly interesting and fundamental synthetic target. It can be considered as an extension of the concept of the nitrogen substituted benzenes pyridazine, pyrimidine and pyrazine to three dimensions. Calculations have shown, that the position of the nitrogen atoms can be used to tune the properties of the resulting heterofullerenes, which is only one fundamental aspect, that makes these molecules desirable.^[95] In view of applications, this would allow to adjust the fullerene's properties to the needs of a specific application.

The first own achievements in its synthesis were reached during the master's thesis and this project should be extended in the present work.^[87] The synthetic strategy (Scheme 3.1 for a short summary) is described in the introduction (page 19) in more detail and generally follows the procedure developed by Wudl and coworkers for $(C_{59}N)_2$ **9** (Scheme 1.1 on page 16).^[83, 92] By use of bisazidomethylether **21**, C_{60} **4** was converted to bisazafulleroids **19**, which



Scheme 3.1: Intermediates in the synthesis of $C_{58}N_2$ **11** starting from C_{60} **4**. $C_{58}N_2$ **11** is represented by one of the 22 possible isomers. A more detailed description can be found in scheme 1.2 on page 19.

were immediately photooxygenated to bisketolactams **20**. Bisazafulleroid **19** was obtained as a mixture of isomers and hence, also the bisketolactams **20**. Two fractions were separated and converted to diazaheterofullerene $C_{58}N_2$ **11** by acid-catalyzed cleavage of the spacer. Thus, $C_{58}N_2$ **11** was probably obtained as a mixture of isomers, although some precursor isomers might have transformed to the same isomer of $C_{58}N_2$ **11**. Some impurities of the bisazaheterofullerene-dimer $(C_{59}N)_2$ were also detected in the product sample. Nevertheless these results were important for proof of concept. In the end, the formation of $C_{58}N_2$ **11** was verified in the master's thesis by mass spectrometry and an UV/Vis-spectrum of the heterofullerene mixture was recorded.

The aim at the beginning of this thesis was to optimize the synthesis and to prepare more material. This would have facilitated full purification of $C_{58}N_2$ **11** and its precursors and would have been essential for further characterizations and physicochemical investigations. When the synthetic procedure was repeated for several times, however, it often failed for unknown reasons. The preparation and successful detection of $C_{58}N_2$ **11** was one problem, but the bisketolactam synthesis failed also several times unpredictably. Furthermore, the obtained intermediates, be it the bisazafulleroids or the bisketolactams were not obtained in pure form due to product mixtures at all steps, which were inseparable even by HPLC. Two fractions containing bisketolactams were separated at best by flash column chromatography, but each of them contained several unseparable constituents, which was shown by analytical HPLC. It was also impossible to purify $C_{58}N_2$ **11** by column chromatography, because it was too polar and did not move at all. It was used in the first experiments as the raw reaction mixture. The only reasonable tool that could be used for the successful verification of the compounds was MALDI-TOF-MS, where the product molecular ion peaks at $m/z = 724$ for $C_{58}N_2$ **11** and at $m/z = 976$ for the bisketolactams **20** was well observed. Despite all these drawbacks, enough material of $C_{58}N_2$ **11** was obtained during the times of synthetic success to analyze the material in some basic experiments. In general the bisketolactam fractions **20** were prepared and stored. For further experiments $C_{58}N_2$ **11** was freshly prepared.

3.1.2 Stability of C₅₈N₂

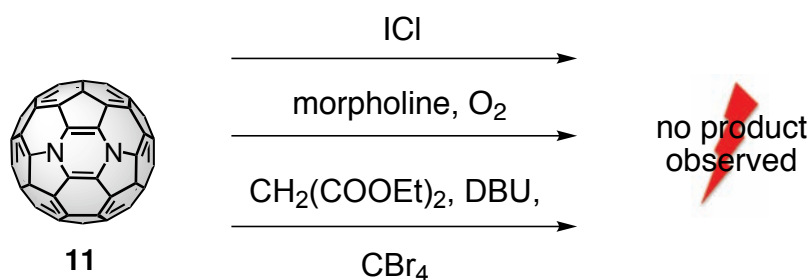
During the experiments, it turned out that diazaheterofullerene C₅₈N₂ was not long-term stable and decomposed after some time. The reasons for this were evaluated in a series of experiments, which were monitored by MALDI-TOF-MS. Therefore the crude reaction mixture of C₅₈N₂ was split in two parts. As chromatography was not possible, the first was neutralized with sodium hydrogen carbonate solution to remove *p*-TsOH, which was necessary for the synthesis of C₅₈N₂ (page 19 (introduction)) and the second one was left in its crude state. Each part was further split in two samples and one of each was dried and one of each was kept as solution. The solution stability of the heterofullerene, as well as the influence of remaining acid on the stability were thus evaluated with these four samples. MALDI-TOF mass spectra were recorded over a period of three days and the presence of the signal of C₅₈N₂ at $m/z = 724$ was compared (Table 3.1). In case of the crude sample in solution the heterofullerene had decomposed within one day and no MS-signal was observed anymore. The neutralized sample was more stable in solution and the diazaheterofullerene **11** was still detected after one day. From then on, C₅₈N₂ began to decompose. The dried samples were the most stable. No matter, whether the acid was removed before or not, the MS-signal for C₅₈N₂ was detected over the whole period of three days. As a control experiment, TFA was added to the neutralized, dried sample after three days to check the influence of acid independently. After addition, the MS-signal for C₅₈N₂ decreased gradually until it was no more observable after seven hours. The conclusion of this study was that C₅₈N₂ can be stored, at least up to three days in solid, neutralized form. It was shown that acid promotes decomposition and that it should be removed after synthesis in order to be able to store the sample for a longer time and to handle it in solution.

The instability of C₅₈N₂ **11** is probably caused by its structure. Upon insertion of two nitrogen atoms in the C₆₀-framework, [5,6] double bonds are inevitable. It is one of the basic build-

Table 3.1: Summary of the experiments on the stability of C₅₈N₂.

	crude sample	neutralized sample
solution	no detectable MS-signal at $m/z = 724$ after 24 h	stable for one day; decay until MS-signal at $m/z = 724$ disappears in background (after 56 h)
solid state	stable	stable

ing principles of stable fullerenes, that [5,6] double bonds should be avoided, because they introduce additional strain.^[16] If this cannot be avoided the corresponding double bonds are much more reactive and might be a reason for the instability of the heterofullerene. Another reactive moiety, that can be encountered in diazaheterofullerene is a vinylamine substructure. Vinylamines are by themselves reactive compounds and such a substructure within a fullerene cage will be also a preferred position of attack. For stabilization of the diazaheterofullerene cage and for saturation of these reactive substructures, several trapping experiments have been performed (Scheme 3.2). Chlorination with ICl,^[101, 102] oxidative addition of morpholine^[104] or nucleophilic cyclopropanation with malonates^[116] are all reactions that work well with pristine C₆₀ and might attack preferentially these unstable substructures. For the trapping experiments, C₅₈N₂ **11** was freshly prepared and the reagents were immediately added to the cooled reaction mixture. In case of the morpholine addition or the BINGEL-reaction, an excess of base was added to compensate for *p*-TsOH from the preparation. However, in none of these reactions with a freshly prepared sample of C₅₈N₂ an addition product was isolated or even detected.



Scheme 3.2: The reactive sites of C₅₈N₂ were attempted to saturate with different reagents, but none of these reactions was successful.

3.1.3 Electrochemical & EPR Investigations

In collaboration with the group of Lothar Dunsch at the IFW in Dresden, (spectro-)electrochemical and EPR studies were conducted to gain more information about the structure and the nature of the prepared sample of C₅₈N₂. For the investigations, C₅₈N₂ was freshly prepared, purified from acid and dried in vacuum. Before the electrochemical measurements were performed, the composition of the sample was confirmed by mass spectrometry. The electrochemical measurements were conducted in a glove box and the heterofullerene was

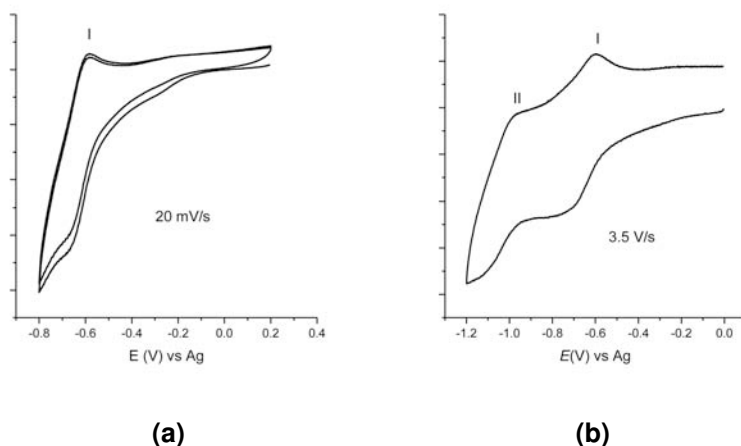


Figure 3.1: Cyclovoltammograms (ODCB, TBABF₄) of the C₅₈N₂ raw mixture at different scan rates.

dissolved in ODCB containing 0.2 M TBABF₄ as supporting electrolyte. In the last cycle ferrocene was added as standard and the spectra were referenced to the Fc/Fc⁺-couple.

One reduction wave was observed by cyclic voltammetry at low scan rate (20 mV s⁻¹) (Figure

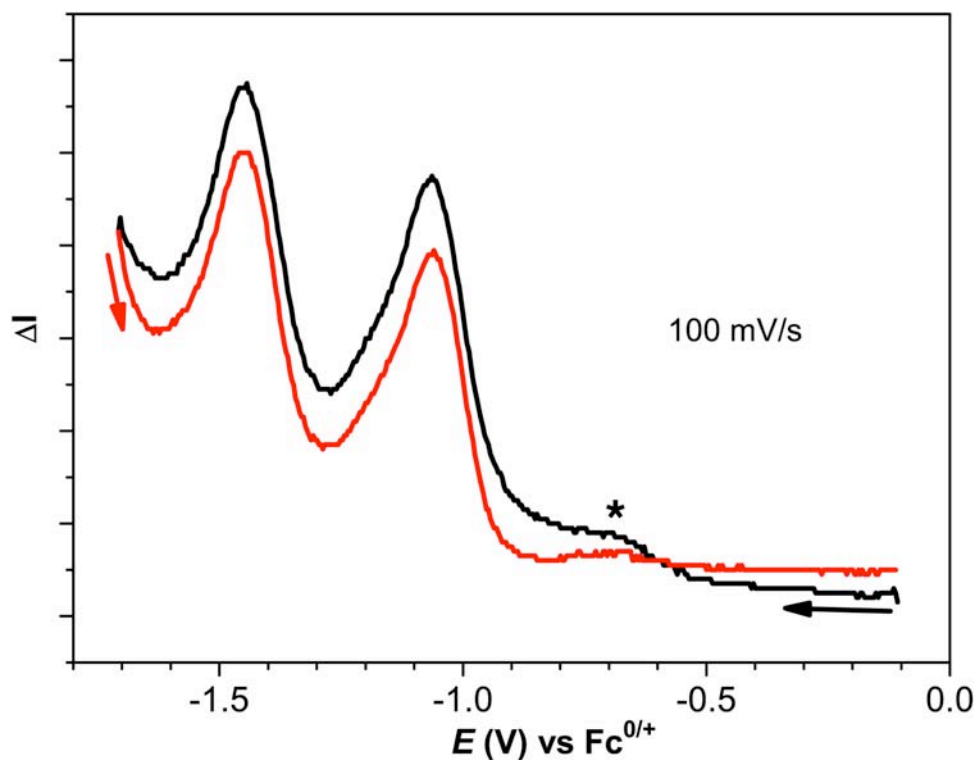


Figure 3.2: Two reduction steps can be clearly observed with square wave voltammetry (ODCB, TBABF₄) of the C₅₈N₂ raw mixture. * = reduction of impurity.

3.1a). Upon increasing the scan rate to 3.5 V s^{-1} a second reduction was detected (Figure 3.1b), but it was not very well defined. With square wave voltammetry, two reduction steps at -1.14 V and -1.58 V vs. $\text{Fc}^{0/+}$ could be observed much clearer (Figure 3.2). The reduction potentials were shifted cathodically in comparison to C_{60} (-1.12 V , -1.52 V)^[146] and $(\text{C}_{59}\text{N})_2$ (-1.00 V , -1.42 V)^[83] indicating that indeed a new compound was present.

No oxidation peaks were observed in the accessible cathodic range. A small peak at around -0.7 V was additionally observed, which was attributed to an impurity in the sample. The data showed that there was one major fullerene-based component. Several isomers of C_{58}N_2 might have been present, but as the reduction potentials depend on the position of the heteroatoms, this was unlikely from the appearance of the voltammograms.^[95] The well defined peak shape suggested, that there was either only one isomer present or eventually more but with indistinguishable redox potentials.

As the cyclic voltammetry studies showed that the first reduction step could be regarded as almost reversible at slow scan rates, the sample was also studied by EPR-spectroelectrochemistry (Figure 3.3). If a clear EPR-signal could be observed, the structure, especially the relative position of the two nitrogen atoms might be deduced in combination with DFT-calculations. By decreasing the potential, a sharp signal evolved that originated from the reduction of the impurity mentioned above. Going to more negative potentials, a broader signal appeared, which can be attributed to the heterofullerene. However, the spectrum was

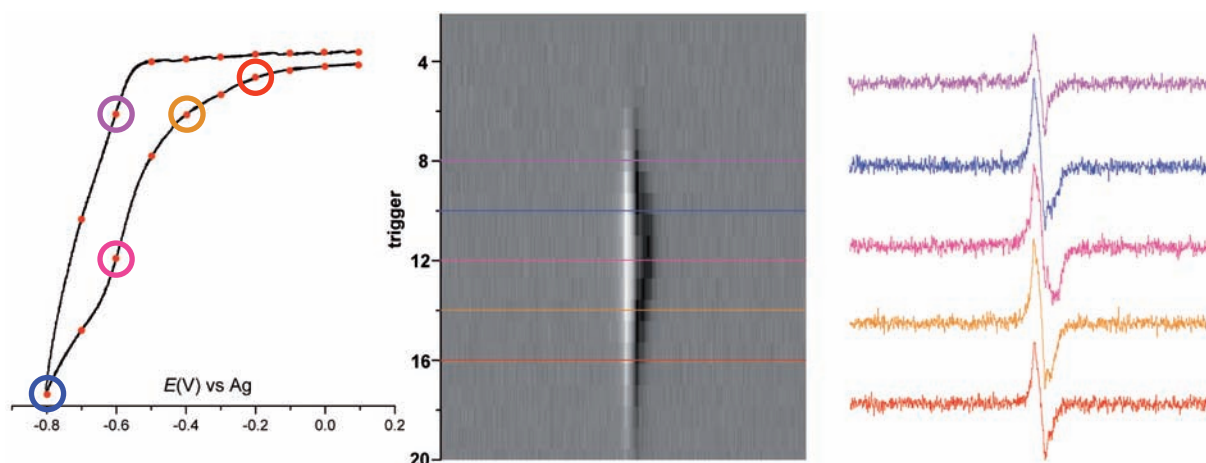


Figure 3.3: EPR-spectroelectrochemistry of the C_{58}N_2 raw mixture. left: CV curve at 5 mV/s , red dots denote the triggers to the EPR spectrometer; middle: density plot of the EPR spectra measured during CV at the first reduction peak; right: individual EPR spectra corresponding to the horizontal lines at the density plot.

largely dominated by the signal of the impurity and the fullerene signal was not very well defined. Purification of the sample was impossible because only very little amount was available that did not move visibly on the column. Conclusions on the structure could be hardly drawn from these data.

In conclusion, a new strategy on the route towards the elusive heterofullerene $C_{58}N_2$ **11** was presented. The compound was successfully prepared but it turned out that it was hard to capture and partly unstable. MALDI-TOF-MS, UV/Vis, and electrochemical data were collected and used to characterize $C_{58}N_2$ **11** partially.

3.2 Screening for a Novel Template for *e,e,e*-Trisadducts

3.2.1 Concept

The C₆₀-*e,e,e*-trisadduct **39** was previously synthesized in our group (page 29 in the introduction).^[141] In an elegant approach, the *e,e,e*-addition pattern was templated by a benzene moiety and the desired fullerene trisadduct could be isolated by simple column chromatography. The benzene template was subsequently removed and the trisalcohol **39** was obtained, which was used as a basis for further-functionalization. However, the synthesis of trismalonate precursor **50** is a time-consuming procedure, which involves seven steps with at least three chromatographic separations.

To find a new template that allowed the selective formation of C₆₀-*e,e,e*-trisadducts, a reverse screening was conducted. The idea was that a central core, which is able to template the formation of *e,e,e*-trisadducts has to fit into the polar addend zone of trisalcohol **39**. If it cannot be incorporated into this fullerene structure, because the size doesn't fit or the adduct is unstable, it will also not be able to form the macrocyclic compound from the open-chain components. Therefore, three-valent elements or those that form stable compounds with three alcohols or oxygen-donors were considered. As a first set of targets, boron-, silicon- and phosphorus-based compounds were envisaged. Boron and phosphorus intrinsically favor adducts with three ligands. In case of silicon, the four-valent trialkoxy-alkyl-silanes might be feasible targets. A potential application of trisalcohol **39** as ligand for iron atoms was also tested because the preorganization of the alcohol groups should be a good basis for complex formation.

3.2.2 Iron-Complexes

Prior to these experiments, a different application of trisalcohol **39** was tested that would not lead to templates for *e,e,e*-trisadduct formation but to another very interesting class of molecules. The hydroxyl-groups are already in very close proximity to each other and form a rigid hydrogen bonding network.^[141] The hydroxyl functionalities are preorganized by the fullerene backbone and the trisalcohol might be suitable to incorporate metal ions, which require a threefold geometry and which can be bound by oxygen donors. Metals in close proximity to the C₆₀-surface can interact with the carbon sphere and exhibit interesting magnetic or electronic properties, which was demonstrated by fullerene-porphyrin dyad **51** or by buckyferrocenes **52** (Figure 3.4).^[147, 148] Appropriately designed polyalcohols can complex

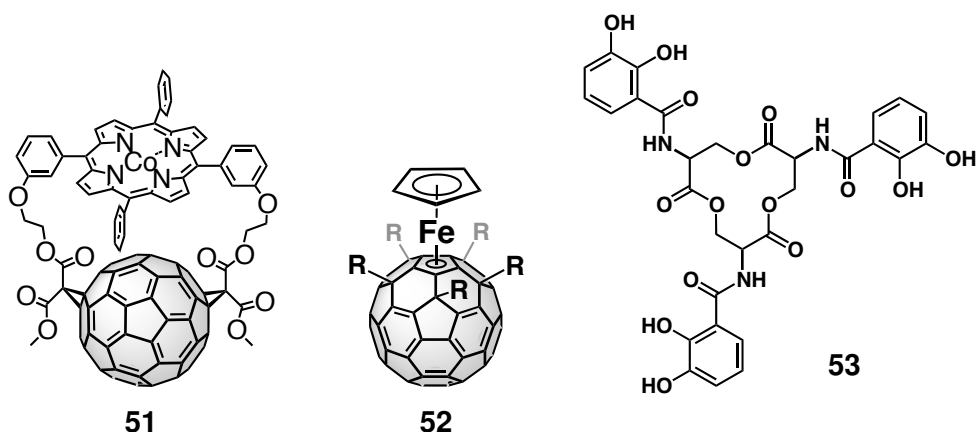
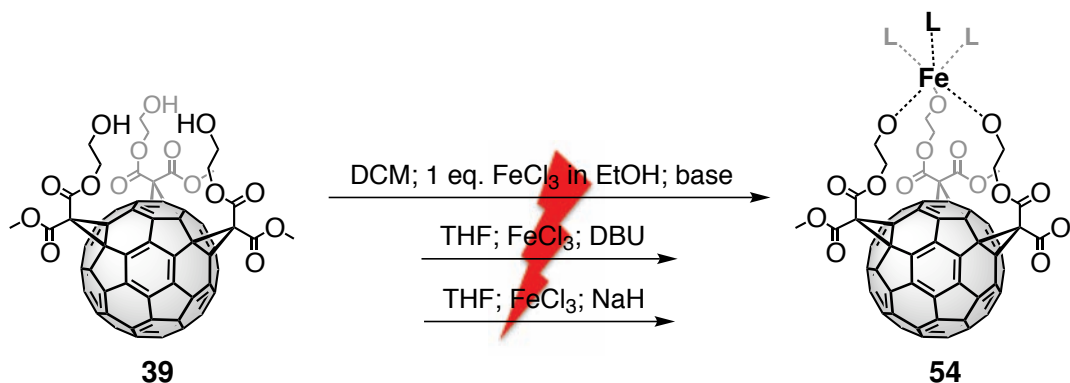


Figure 3.4: C₆₀-Co-porphyrin dyad **51** (left) and buckyferrocenes **52** (middle) are examples of C₆₀-conjugates, whose special properties originate from a close contact between the metal-ion and the fullerene sphere. Enterobactin **53** (right) is one of the strongest artificial binders of iron.

iron ions. The most important class are siderophores and they play an important role in nature for the uptake and transport of iron.^[149] They bind iron with very large affinity and solubilize it in that way. Siderophores contain three catecholate groups and the most prominent one, enterobactin **53** was synthesized by Corey and coworkers to study these phenomena in detail.^[150] Tripodal alcohol ligands were also reported to form complexes with iron.^[151] Thus, the incorporation of iron in the C₆₀-*e,e,e*-trisalcohol **39** should be feasible and yield molecules with interesting properties.



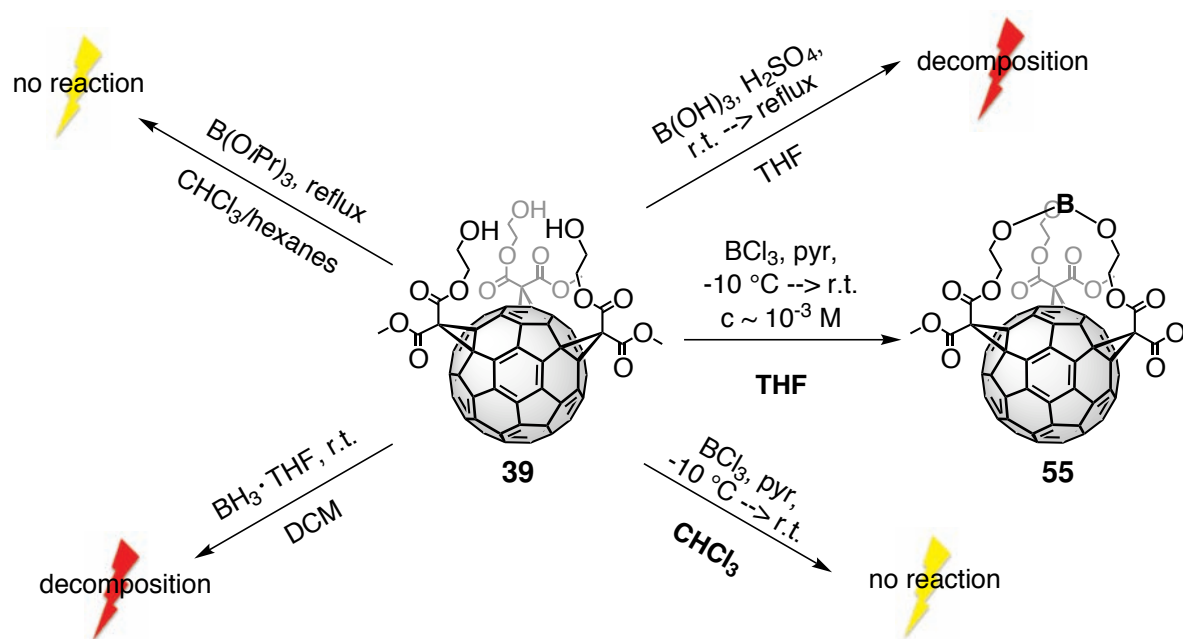
Scheme 3.3: The synthesis of iron-fullerene-complex **54** was attempted by various approaches, but none of them led to isolation of the desired product.

Preliminary studies on the synthesis of the iron complex **54** were already reported by Beuerle.^[152] Following this report, 1 eq. trisalcohol **39** was dissolved in DCM/EtOH ($c = 10^{-3}$ M) with an excess of triethylamine and 1 eq. FeCl_3 were added (Scheme 3.3) to prepare the 1:1-complex. The residual coordination sites of the iron atom would be saturated by solvent molecules or chlorine ions in this case. However, the reaction could not be reproduced, not even upon heating to reflux, most probably because triethylamine is a too weak base. DBU was subsequently added but only transesterification products with ethanol could be detected by MALDI-TOF-MS. In the next attempt the solvent was changed to THF to avoid transesterifications. In the absence of any protic components, DBU and NaH were employed in different experiments, but only black decomposition products were observed in both cases. The alcohols are clearly deprotonated, but instead of coordinating to iron, they obviously attack and decompose the C_{60} -core. The first experiments were not very promising due to the incompatibility of the formed intermediates with C_{60} . Thus, this side-project was abandoned and the focus was shifted to the main-task, finding a new template for *e,e,e*-trisadduct formation.

3.2.3 Boron-Templates

The first tris-valent element that was targeted as template for the *e,e,e*-trisadduct framework was boron. Next to the structural features, also applicational aspects are interesting in case of boron. Strained boric acid esters can serve as LEWIS-acidic catalysts for hetero DIELS-ALDER-reactions or as anion carriers in novel battery systems.^[153, 154] Their acidity can be tuned by the strain of the system, which modulates the pyramidalization at boron. Borates can be formed by a variety of different boron precursors and alcohols. The employed reagents range from BCl_3 ^[155, 156] over BH_3 ^[153] to triisopropyl borate.^[154, 157] The reaction conditions are generally very mild and in case of acidic byproducts an auxiliary base is added. All of these reaction conditions were tested with trisalcohol **39** and the results are summarized in scheme 3.4. In addition to the mentioned reaction conditions, a simple esterification with boric acid under acid catalysis was also attempted but no reaction was observed. The same is true for the transesterification with triisopropylborate in a refluxing solvent mixture of CHCl_3 /hexanes. Upon addition of the $\text{BH}_3 \cdot \text{THF}$ -complex to trisalcohol **39** only decomposition products could be obtained after one night. Presumably, the alkoxides that are formed intermediately attack preferentially the fullerene before they are trapped as a borate. BCl_3 can also be used to synthesize borates and this was first attempted in CHCl_3 -solution ($c = 10^{-3}$ M) with pyridine as auxiliary base. Boron trichloride was added at 0°C and the solution was allowed to warm

to r.t. overnight. No product could be detected by TLC (silica; DCM : MeOH = 95 : 5). Addition of more BCl_3 and pyridine or heating the solution to reflux did also not lead to any reaction. As already mentioned above, the hydroxyl groups form relatively strong hydrogen bonds among each other. As a result, strong acylating reagents like acid chlorides are necessary to induce ester formation.^[141] Because BCl_3 is the boron analogue of acid chlorides, other measures had to be considered to increase the reactivity. For example, the hydrogen bonds could be broken with more polar solvents, like THF, which is reflected in the different NMR-spectra in CDCl_3 and THF-d_8 , respectively.^[141] Thus, the reaction was conducted under identical conditions in THF. TLC-control indicated again no reaction. However, to rule out that the formed borate is hydrolyzed immediately on silica upon chromatography, the fullerenes were precipitated with pentane directly from the reaction mixture. MALDI-TOF analysis of the crude mixture then showed indeed the correct molecular ion peak for the fullerene-borate **55** at $m/z = 1208$ together with the signal for the reactant trisalcohol **39** at $m/z = 1200$. It has to be stated, that this result puts the validity of the previous experiments at least in question. The reactions with other boron sources or in CHCl_3 might have been successful, without noticing it. After the negative TLC result the samples were no more investigated in the previous experiments.



Scheme 3.4: The synthesis of borate **55** was attempted with a variety of reagents. Only BCl_3 in THF was applied successfully.

It turned out, that borate **55** was not very soluble in organic solvents. The crude product was thus washed with CHCl_3 to remove trisalcohol **39** until it was no longer detected by MALDI-TOF-MS. A sample of this compound was also analyzed by HiRes-ESI-MS on an AGILENT 6320 spectrometer and the correct molecular composition of the $[\text{M} + \text{H}]^+$ -cation was confirmed with an accuracy of 1.2 ppm. The compound was however not pure enough and not soluble enough in any solvent to obtain satisfactory NMR-spectra. The ^1H -NMR-spectra were dominated by the $\text{BCl}_3 \cdot \text{pyr}$ -adduct, which precipitated from solution together with the product.^[155] Only the ^{11}B -NMR-spectrum (128 MHz; CDCl_3 ; r.t.; $\text{BF}_3 \cdot \text{OEt}_2$ ext. ref.) could be used to gain further hints for successful product formation. It showed a weak and broad resonance at 23.04 ppm, which is in the same range as literature-known caged borates.^[154, 158] In summary, the borate capped C_{60} -*e,e,e*-trisadduct **55** could not be fully characterized due to the insolubility of the compound. Together with the sensitivity of the boric acid ester to silica gel, boron was ruled out as a practical template for the formation of C_{60} -trisadducts. However, it was not tested, whether an intermediately formed borate trisalonate might successfully attach to C_{60} in an *e,e,e*-fashion. A subsequent hydrolysis on silica would not be a problem, if the trisadduct was formed before.

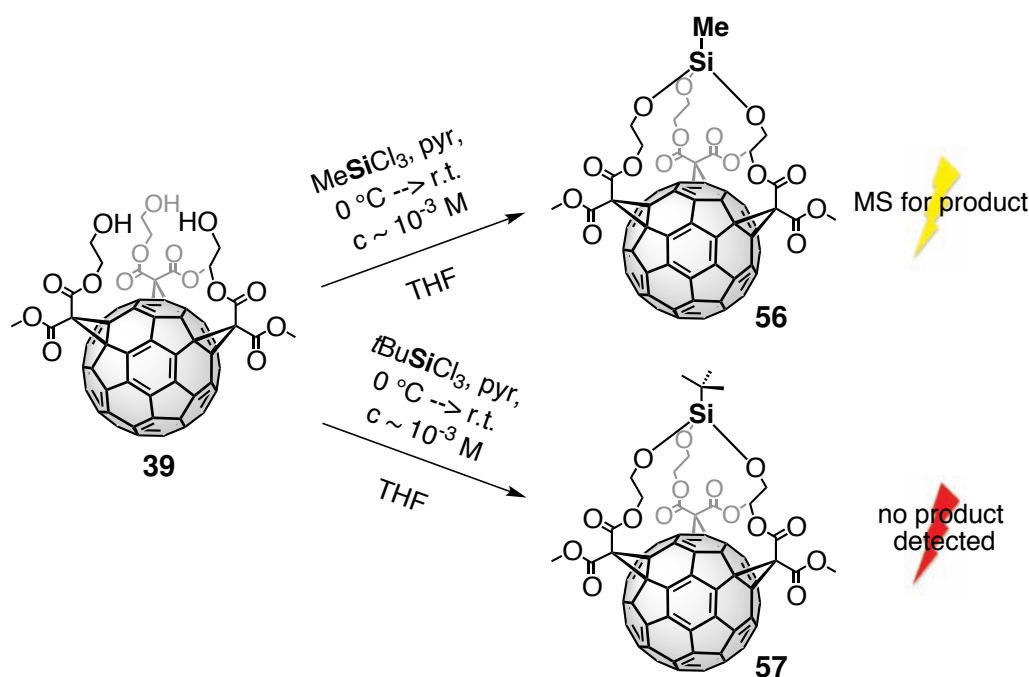
The synthesis of **55** gave valuable insights into the reactivity of trisalcohol **39** and the possible products. It was demonstrated that TLC-control is not always suitable to monitor such reactions, because the products might decompose on silica and a negative result would be misleading.

3.2.4 Silicon Templates

The experience gained from the boron experiments was then used for attempts to use silicon as the central entity. Silicon is tetravalent and next to the three Si–O-bonds that are necessary to close the macrocyclic framework at the fullerene a fourth substituent has to be attached to silicon. Thus, the commercially available trichloroalkylsilanes should be ideal reagents to accomplish this reaction (Scheme 3.5).

The capping was attempted in the same way as for C_{60} -borate **55**. Trisalcohol **39** was dissolved in THF ($c = 10^{-3} \text{ M}$) together with the auxiliary base pyridine. Methyl- and *tert*-butyltrichlorosilane were employed as silylating agents. However, the corresponding products **56** & **57** turned out to be rather unstable, probably due to hydrolysis, and column chromatography was again not possible. For workup, the solvents were removed *in vacuo* and the remaining solid was taken up in DCM and precipitated with pentane. In case of the methylsi-

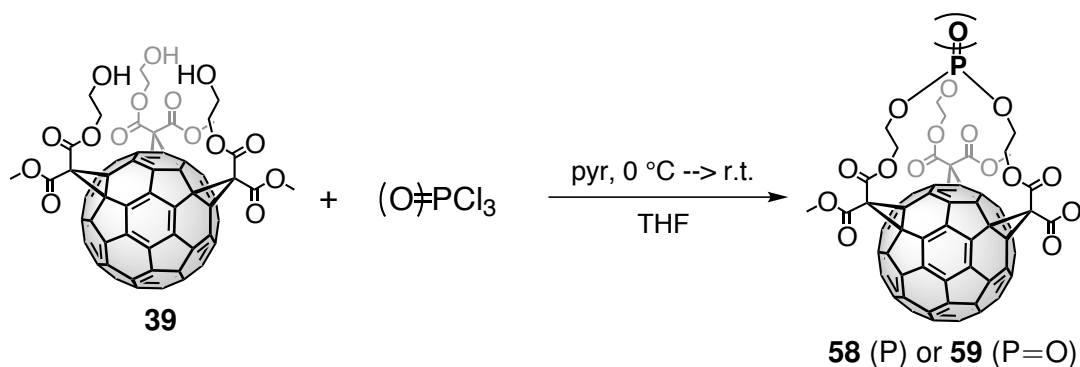
yl derivative **56** MALDI-TOF-MS of the supernatant yielded a product signal at $m/z = 1240$, whereas no signal was detected in the precipitate. This demonstrates the nonpolar character of the silanes, which is expected for this compound class. Due to the instability of the adduct and its low purity, further characterization was not accomplished. In case of the *tert*-butylsilyl derivative **57**, no product signal was detected by MALDI-TOF-MS, although the compound should be more stable towards hydrolysis due to better steric protection through the *tert*-butyl group. Despite the tripodal fullerene backbone, which might stabilize labile moieties, the silanes turned out to be very unstable. Thus, this class of compounds was also ruled out to serve as template for C₆₀-trisadduct formation.



Scheme 3.5: The capping of the fullerene pole was attempted with trichloroalkylsilanes, but no adduct was isolated. Only in case of MeSiCl₃ **56** a mass-spectrometric proof could be obtained.

3.2.5 Phosphorus-Templates

The targeted silane and borate adducts **56**, **57**, and **55**, respectively, all lacked stability or solubility to be good candidates for further investigation. Another element that connects to three alcohol moieties and that might be incorporated in the polar addend zone is phosphorus. Either the P(III) phosphites or the P(V) phosphates are stable organic molecules and promising candidates for the capping of the fullerene structure. They should be rather easily accessible



Scheme 3.6: The P(III) phosphite (**58**) as well as the P(V) phosphate (**59**) should both be stable organic molecules.

from the corresponding chlorides (PCl₃ and POCl₃) by standard procedures (Scheme 3.6). The reaction conditions were adapted from the synthesis of borate **55**. Trisalcohol **39** was dissolved in THF, pyridine was added and the solution was cooled to 0 °C. In a first experiment, a THF-solution of PCl₃ was added dropwise and the reaction was monitored by TLC (silica; DCM : MeOH = 95 : 5). After two hours, some less polar, red spots had formed. This was already a big progress to the previous attempts, as some new *e,e,e*-trisadduct products were formed that seemed to be stable on silica. The reaction mixture was allowed to warm up to r.t. overnight to allow the reaction to go to completion, but no visible changes were observed by TLC. In contrast to the previous adducts, the raw-mixture could be separated by column chromatography (silica; DCM : MeOH = 95 : 5) in this case. Subsequently, the fractions were analyzed by MALDI-TOF-MS. Unfortunately, none of the fractions yielded a signal at $m/z = 1228$ for the fullerene phosphite **58**. However, the least polar fraction yielded a signal at $m/z = 1244$. The difference of 16 corresponded exactly to an oxygen atom. Obviously, the intermediate phosphite **58** was *in situ* oxidized to the phosphate **59** (Scheme 3.7 on page 50). The correct molecular composition of the fullerenophosphate was further confirmed by HiRes-ESI-TOF mass spectrometry. A closer look at the TLC plate revealed, that there were actually two spots of very similar polarity. The two corresponding compounds were separated by automated flash column chromatography and pure **59** was obtained in 5% yield. The nature of the impurity was not further investigated.

The UV-Vis spectrum of **59** was essentially identical to that of trisalcohol **39**. It displayed the four absorptions at 251 nm, 281 nm, 380 nm and 483 nm and the two shoulders at 302 nm and 564 nm typical for *e,e,e*-trisadducts.^[43, 45] This indicated that the reaction had occurred on the sidechains and had left the fullerene core unchanged.

Further evidence for the *in situ*-reaction to the phosphate was provided by ^{31}P -NMR-spectroscopy. P(III)-nuclei in phosphites resonate around 140 ppm, whereas phosphate esters usually resonate around 0 ppm or at slightly negative values.^[159] This big difference in chemical shifts makes the distinction between the two species unambiguous and straightforward. The ^{31}P -NMR-spectrum of **59** displayed a resonance at -0.19 ppm, thus clearly supporting the phosphate and not the phosphite structure.

Due to the low hydrogen content of the molecule, the ^1H -NMR-spectrum (Figure 3.5) was supposed to be rather simple. As it displayed even less multiplets than expected, the correct assignment of the signals required 2D-NMR-spectra. The resonance of the methyl esters was clearly assigned to the signal at 3.93 ppm, which corresponded to nine hydrogen atoms. The resonances of the ethylene chain displayed a more complicated pattern. The signal at lowest field was a multiplet at 4.80 ppm, which corresponded to three hydrogens. Due to the inherent chirality of the C_3 -symmetrical addition pattern, the protons were split diastereotopically as in case of the benzene template *e,e,e*-trisadducts.^[141] The shift of the protons was not only influenced by the other addends on the chain, but mostly by their orientation towards the

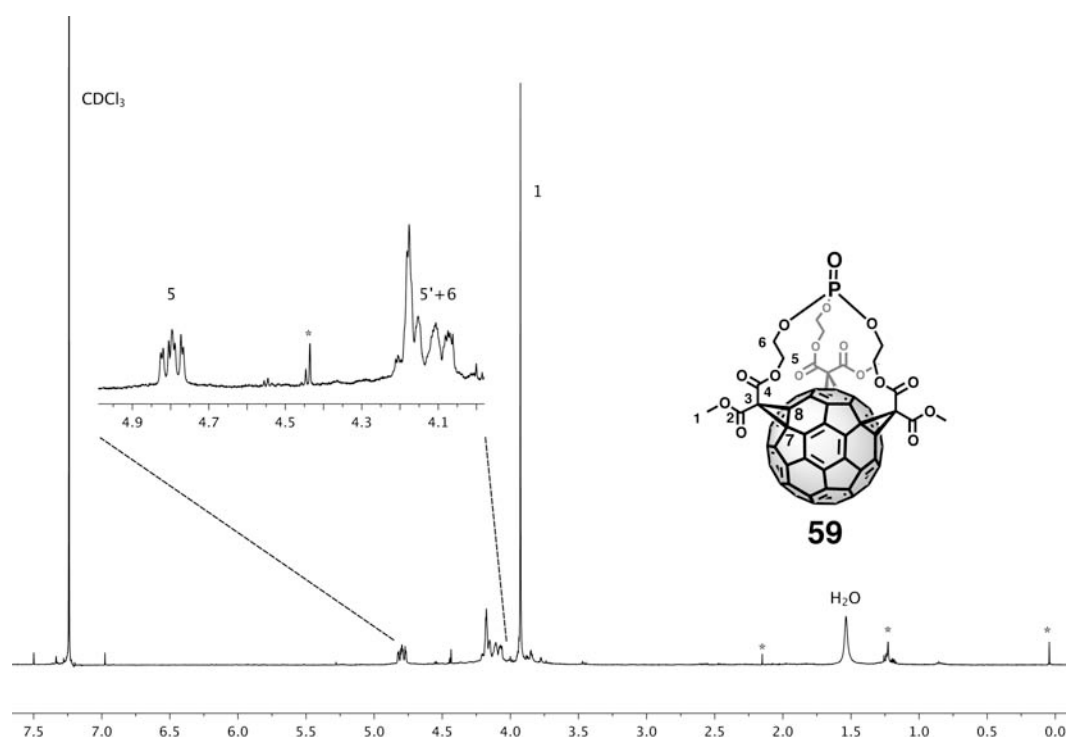


Figure 3.5: The ^1H -NMR-spectrum (400 MHz, CDCl_3 , r.t.) of the C_{60} -*e,e,e*-phosphate **59** showed diastereotopic splitting of the hydrogen atoms of the ethyl chains. * = impurity.

fullerene surface. Thus, every proton was in a different chemical environment and should yield in principle a separate signal. However, the signals of the other nine protons of the ethylene chains resonated at approximately the same position and yielded a joint multiplet at 4.13 ppm, which was not further resolved.

The ^{13}C -NMR-spectrum (Figure 3.6) confirmed the structure of **59**. Due to the C_3 -symmetry of the fullerene backbone, the spectrum was relatively simple. The six carbonyl carbon atoms yielded two signals at 163.8 ppm and 163.2 ppm, respectively. The methyl esters resonated as a single signal at 53.8 ppm and the central malonate atoms yielded a single resonance at 52.3 ppm. From the 18 expected signals for the C_{60} - sp^2 carbon atoms of an *e,e,e*-trisadduct, 17 were resolved in the range between 147.2 ppm and 140.8 ppm, thus reflecting the C_3 -symmetry again. The C_{60} - sp^3 carbon atoms yielded two resonances at 70.7 ppm and 70.0 ppm. The signal assignment was again a little more complicated for the carbon atoms of the ethylene chains. The malonate- and the phosphate-ester usually shift the resonances of the neighboring carbon atoms to similar but distinguishable positions between 60 ppm and 70 ppm (see *e.g.* the table on page 56). In case of an ethylene chain

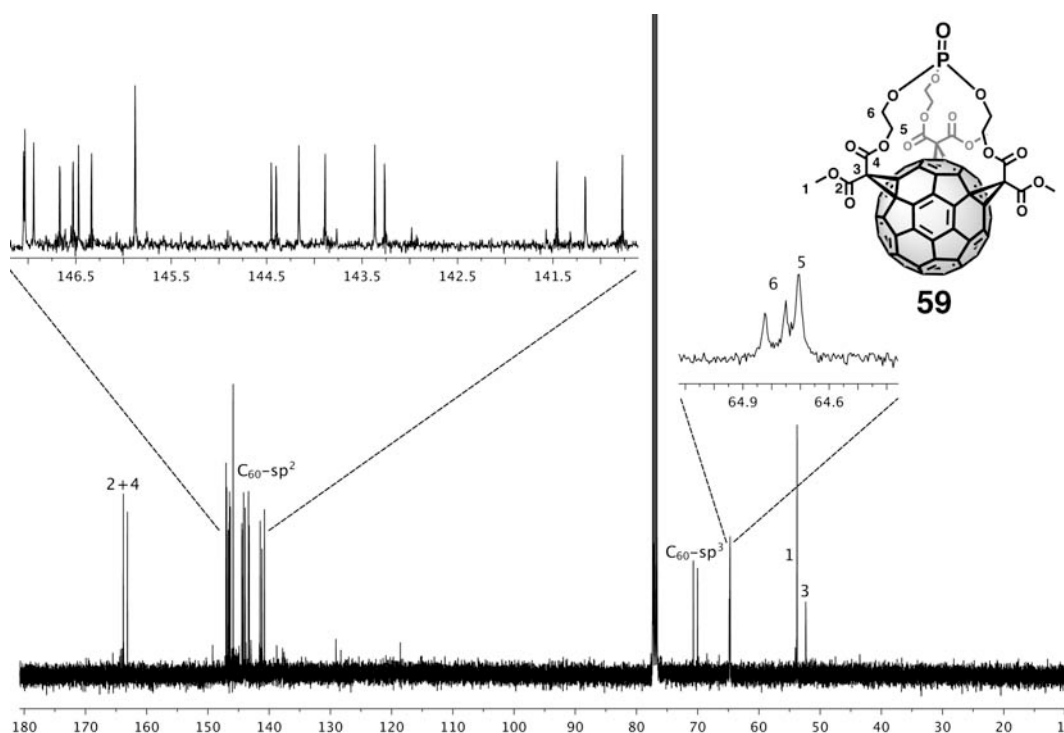


Figure 3.6: In the ^{13}C -NMR-spectrum (100 MHz, CDCl_3 , r.t.) of C_{60} -*e,e,e*-phosphate **59** the carbon resonances of the ethyl chain were scarcely separated.

separating the two entities, each carbon atom is influenced by both substituents, resulting in almost the same chemical shift for both atoms. Further on the signals for the carbon atoms in α - and β -position to the phosphate group are doublets due to coupling to the ^{31}P -core, which will become more evident in the succeeding sections (see *e.g.* page 59). In the present case, only three of the four possible resonances could be observed. From comparison with the corresponding molecules presented later on, the doublet at lower field (64.8 ppm, $^2J_{\text{C-P}} = 7.0$ Hz) was assigned to the carbon atoms at the phosphate end and the unresolved signal at 64.7 ppm was assigned to the carbon atoms at the malonate end.

In a second experiment (Scheme 3.6), the phosphate synthesis was intentionally performed using POCl_3 as the phosphorylation agent. The same reaction conditions as above were applied. Trisalcohol **39** was dissolved in THF to break up the hydrogen bonding network, pyridine was added as auxiliary base and a POCl_3 -solution was added dropwise at 0°C . After one night, no reaction was observed and more POCl_3 was added. After another night, a less polar spot was observed by TLC and subsequently isolated. As expected, the product from this reaction was the phosphate **59**, which was verified by comparison of TLC, ^1H -NMR-spectra and MALDI-TOF-MS with those from the product of the previous reaction. As the reaction with POCl_3 proceeded much slower, this synthetic pathway was, however, not further followed.

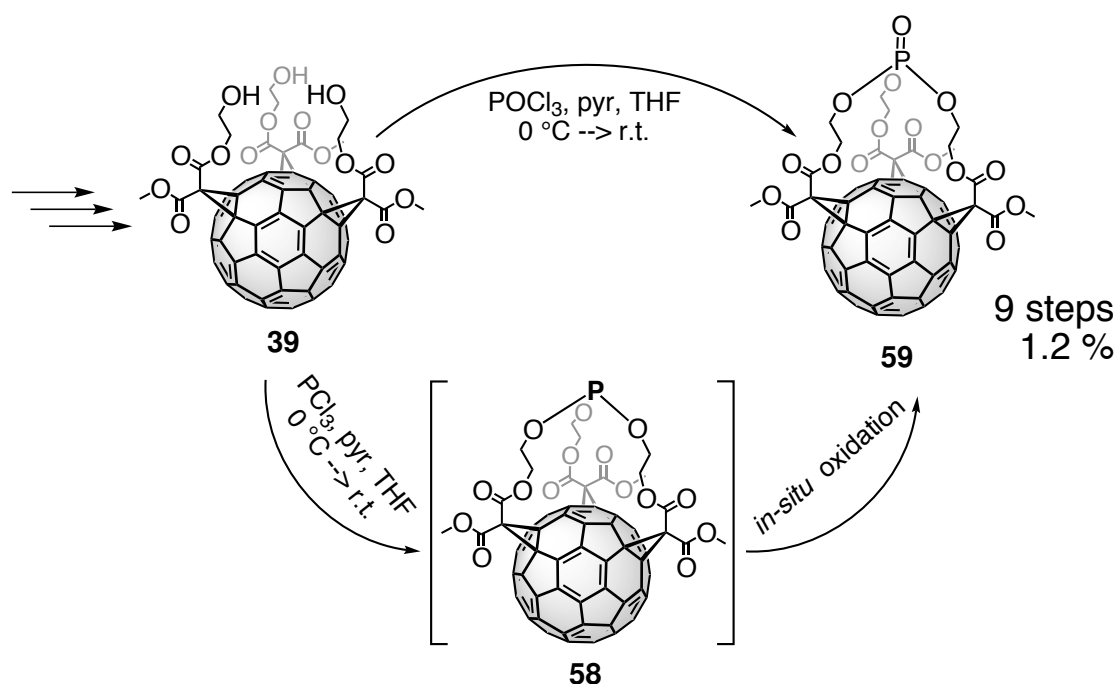
In summary, a stable adduct was identified by incorporating a phosphate atom into the polar addend zone. A first step towards easier accessible trismalonates was thus made. It was shown, that the phosphate group fits into the polar addend zone of **39**. It can bridge the three arms and it will have to be shown, that the free trismalonate can also template the formation of *e,e,e*-trisadducts in the "forward" reaction. The P(III) phosphite, however, could not be isolated, because it was *in situ* oxidized to the phosphate. Either the fullerene acted as a photosensitizer to activate oxygen or the phosphite is strained and thus activated by itself to undergo oxidation under ambient conditions.

3.3 Development of a New Trismalonate System for the Formation of C_{60} -*e,e,e*-Trisadducts

3.3.1 Proof of Concept

Two possible syntheses of phosphate trisadduct **59** were shown in the last section and are summarized in scheme 3.7. Accordingly, the phosphate moiety should be a suitable central entity for the construction of trismalonates that form *e,e,e*-trisadducts. Phosphate trismalonates should be accessible in a few steps from commercial materials in contrast to the seven-step synthesis (14% overall yield) of benzyl trismalonate **45**.^[141] Symmetrical phosphates already possess a threefold symmetry and should be able to serve as a structural template for the formation of *e,e,e*-trisadducts. To open the way to a new template system, it has to be shown, that phosphate trismalonates add to C_{60} predominantly in an *e,e,e*-addition pattern and that the resulting fullerene phosphates can be separated from byproducts, especially other isomers.

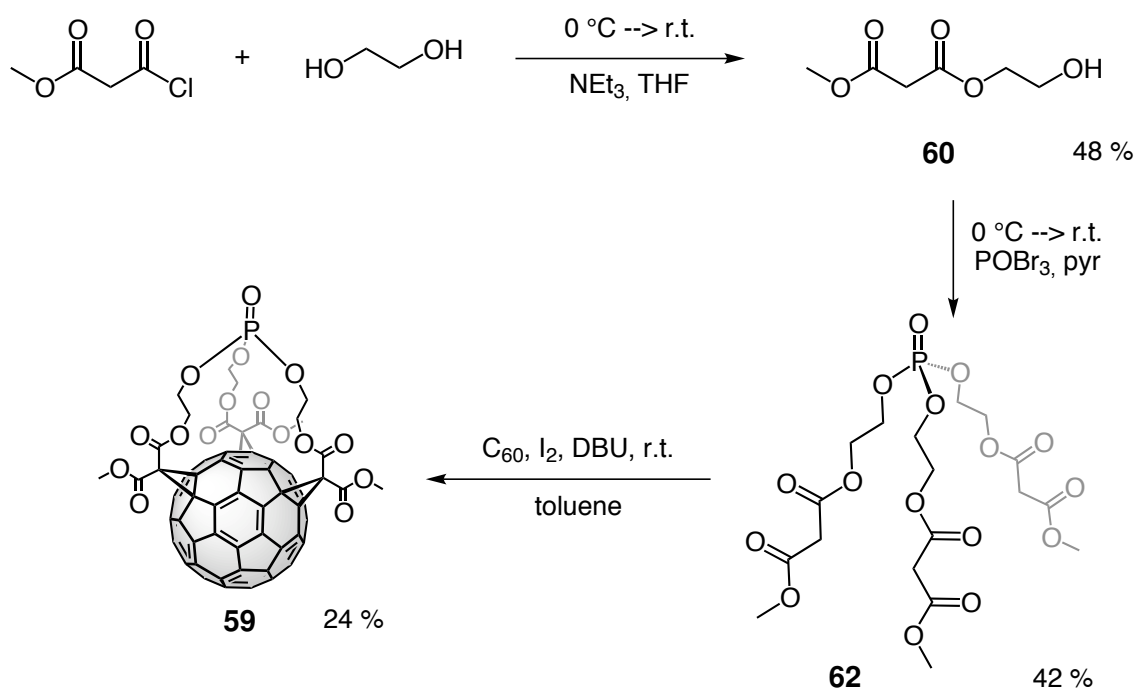
For proof of concept, the synthesis of fullerene phosphate **59** via a phosphate trismalonate



Scheme 3.7: Summary of the final steps of the synthesis of C_3 -symmetric C_{60} -phosphate-adduct **59** via previously known **39**.^[141] It is best obtained in 1.2% over 9 steps via the PCl_3 -synthesis.

was thus developed (Scheme 3.8). The first step was the preparation of 2-methylmalonyl-ethanol **60**.^[160] It was synthesized from methyl malonyl chloride, a slight excess of ethylene glycol and triethyl amine or pyridine as auxiliary base at 0 °C in THF in 48 % yield. Methyl malonyl chloride had to be added very slowly to obtain a good yield in this protocol. This prevented a high concentration of the acid chloride in the reaction mixture and thus a twofold esterification. Yet, overreaction could not be completely suppressed and the bismalonate had to be separated from the product by column chromatography.

The phosphate trismalonate **61** was subsequently formed *via* a threefold esterification of 2-methylmalonylethanol **60** with POBr₃ and pyridine in toluene at 0 °C. POBr₃ is the bromine analogue of POCl₃, which is used as a standard reagent for phosphate formation. However, by employing POCl₃ the reaction needed three days and was not even complete, while with POBr₃ complete conversion was observed after one night. After aqueous workup the product was isolated by column chromatography (silica; DCM : THF = 10 : 1) in 42 % yield.



Scheme 3.8: Novel synthetic strategy towards *e,e,e* - trisadducts.

The ¹H-NMR spectrum of **62** was as expected - details are discussed below (page 55) together with the spectra of the other phosphate trismalonates for better comparison. Yet, by use of the proton spectrum alone a clear decision, whether the phosphate unit was fully esterified or whether a mixture of differently substituted phosphates was obtained could not be

made. The sidechains are in all cases the same and the integrals have the same values. At least concerning the number of constituents of the product fraction, the ^{31}P -NMR spectrum proved, that the sample was composed of only one component, as there was only a single signal. It resonated at - 0.80 ppm, which is characteristic for fully substituted alkyl phosphates.^[159] The ^{13}C -NMR spectrum of **62** showed all expected six carbon resonances and also proved the phosphate structure. Noteworthy are only the two carbon signals of the ethylene chain at 65.3 (α) and 63.7 ppm (β) because they were split into doublets due to coupling with the ^{31}P -nucleus. The α - and the β -carbon atoms had a coupling constant of 6.5 and 7.0 Hz, respectively, which is in agreement with fully substituted alkyl phosphates.^[159] Finally, the mass spectra unequivocally proved the threefold addition. MALDI-TOF-MS showed the $[\text{M} + \text{Na}]^+$ - and the $[\text{M} + \text{K}]^+$ -peaks of trismalonate **62** at $m/z = 553$ and 569 , respectively and HiRes-ESI-MS confirmed accurately the molecular composition of **62**.

Phosphate trismalonate **62** was prepared in slightly better overall yield than the benzyl trismalonate **50** (20 % *cf.* 14%), but a big advantage was its two-step synthesis. For being fully comparable to the benzene based systems, it had to be finally investigated, if and how the phosphate trismalonate **62** adds to C_{60} and especially, if the possibly formed *e,e,e*-trisadduct could be isolated in pure form. With the experience with benzene based trisadduct **38** in mind, the cyclopropanation with iodine and DBU was attempted first. The reaction was conducted under high-dilution conditions. C_{60} , the phosphate trismalonate **62** and iodine were dissolved in toluene and a DBU-solution was added dropwise to the vigorously stirred mixture. After one night, TLC-control (silica; toluene : MeOH = 95 : 5) clearly showed a red spot, indicative for *e,e,e*-trisadducts. Pleasingly, separation from all the byproducts was good on TLC plate and posed no unexpected problems.

First, the crude mixture was subjected to a plug filtration with toluene as eluent to remove unreacted [60]-fullerene. As the fullerenophosphate **59** is substantially more polar than the benzene analogue **38**, toluene/ethyl acetate mixtures were not sufficient and toluene/MeOH mixtures had to be used to elute the product. This jump in polarity was, however, too large and even with a flat gradient, no separation could be achieved. Thus, all the products were eluted together with 5 % methanol. *e,e,e*-trisadduct **59** was isolated by a second column with DCM : THF = 95 : 5.

The spectral data of this sample were in perfect agreement with those from the previous syntheses (page 47), demonstrating that the phosphate malonate **62** forms C_{60} addition products with an *e,e,e*-pattern. No *in/out*-isomerism of the malonates was observed, which is also very unlikely for such a small addend. The yield of the cyclopropanation step was 24 %, which is in

the same range, as for the benzene analogue **38**.^[161] MALDI-TOF-MS analyses of the other fractions showed no further trisadducts, demonstrating the selectivity of the trisaddition.

The formation of a C₆₀-*e,e,e*-trisadduct through phosphate malonate **62** was thus superior to the previous approach, as it comprised only three steps and had an overall yield of 5%.

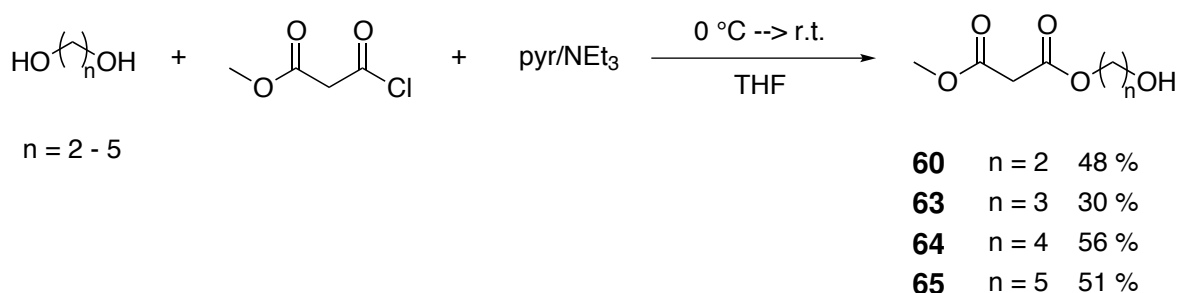
3.3.2 Synthesis of Novel Trismalonates

3.3.2.1 Synthesis of Malonate Alkanols

In order to extend the scope of the phosphate template system and to investigate the influence of the spacer length on selectivity, further phosphate trismalonates had to be synthesized. A series of alkyl chains, ranging from propyl to hexyl were incorporated as spacers instead of the previously described ethyl chain. The focus of interest was, up to which chain length *e,e,e*-trisadducts are formed and maybe, which other isomers are obtained from the threefold BINGEL-reactions.

Following the same reaction procedure as above (page 51), the *n*-propyl- to *n*-pentyl-homologues of **60** were synthesized by reacting the corresponding diol with 0.8 eq. of methyl malonyl chloride in THF (Scheme 3.9). THF was used as solvent, because it dissolved the very polar diols much better than DCM and thus allowed a higher selectivity for the monomalonate. The monomalonate was fully soluble in DCM, hence after one esterification it is better accessible in solution and a twofold esterification would be favored.

The hexanol derivative **68** was synthesized by a slightly different procedure (Scheme 3.10). In a first step 1,6-hexanediol was selectively monoprotected as THP-ether according to a literature procedure.^[162] The diol was dispersed in a 5% solution of DHP in toluene and the strongly acidic ion exchange resin Dowex[®] 50WX2 was added. The resin beads were filtered off after four hours and after aqueous workup, which removed residual traces of the

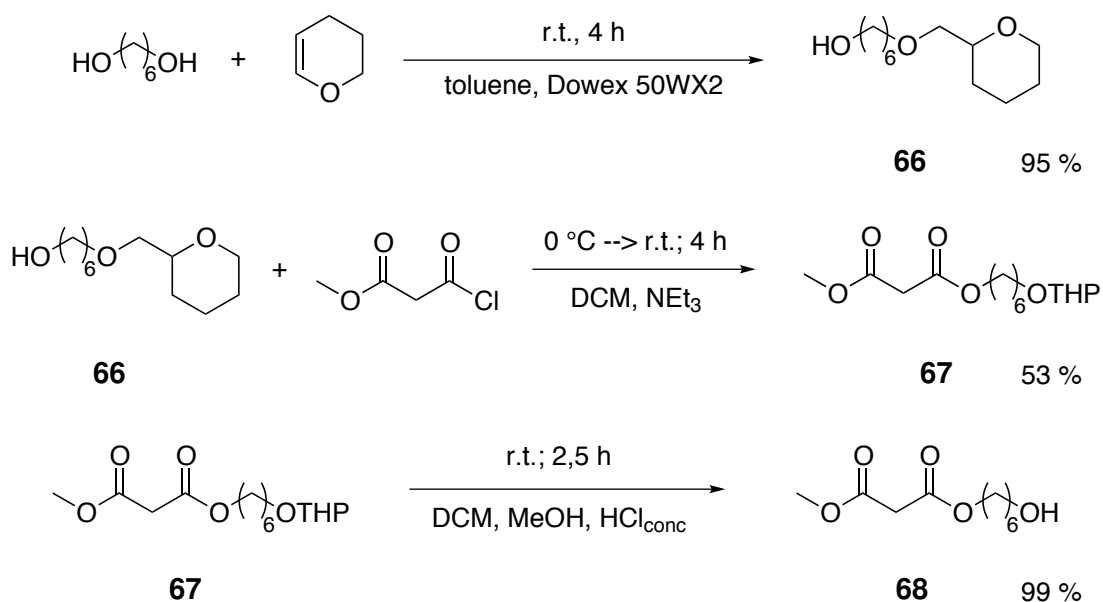


Scheme 3.9: Summary of syntheses of methylmalonylalkanols.

diol, the mono-THP-ether **66** (95% yield) was directly used for the next reaction step. The polymeric beads have a water shell on their surface, the diol is soluble therein and reaches the catalytically active sites where the reaction is initiated. The resulting mono-THP-ether is no more soluble in the water shell, diffuses to the toluene solution, is thus separated from the reactive sites and the reaction stops at the monoether stage.^[162] Thus, almost no diether is formed. This reaction performs exceptionally well with 1,6-hexanediol. The yields for the shorter homologues are not as favorable and a much higher excess of DHP has to be used, which is, why the malonate alcohols **60** - **65** were not synthesized by this procedure.

The mono-THP-ether **66** was then esterified with methylmalonylchloride by the same procedure as above and finally deprotected with HCl. The THP-malonate **67** was also pure enough after workup and was directly used for the deprotection. The only chromatographic purification step in this sequence was necessary after the final deprotection towards the desired 6-methylmalonylhexanol **68**. Thus, it was prepared in 72% yield corresponding to 1,6-hexanediol with only a single column, which made this procedure a better alternative to the direct mono-esterification of 1,6-hexanediol with methylmalonylchloride.

All the compounds were fully characterized by ¹H- and ¹³C-NMR-spectroscopy, mass spectrometry, IR-spectroscopy and elemental analysis.



Scheme 3.10: Synthesis of 6-methylmalonylhexanol **68**.

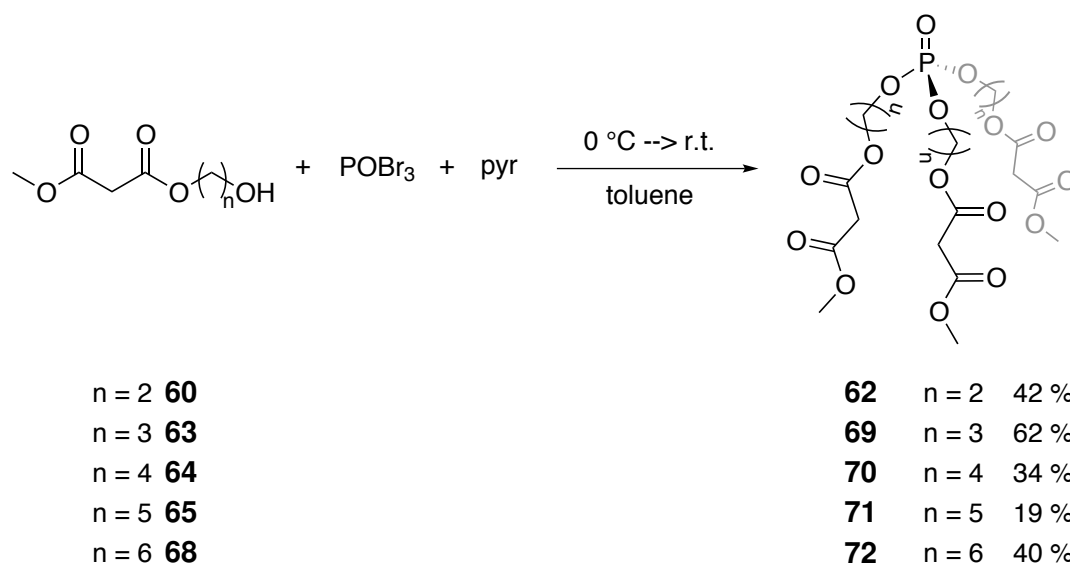
3.3.2.2 Phosphate Trismalonates

The elongated phosphate trismalonates **69** - **72** were then prepared, as described for the ethyl derivative **62** (page 51). All phosphate trismalonates were obtained in satisfactory to good yields and showed the expected spectroscopic properties.

For a full overview of the entire phosphate trismalonate series, the spectra of the previously described ethyl derivative **62** are now also included in the discussion. The peak assignments were deduced from COSY- and HETCOR-spectra in cases, where it was not evident.

The methyl ester and malonate protons resonated for all the trismalonates as two singlets (3.68 ppm, OCH_3 ; 3.33 ppm, COCH_2CO) at approximately the same chemical shift.

The protons α to the malonate group resonated between 4.34 and 4.06 ppm with decreasing values when elongating the chain. This was rationalized by the additional influence of the phosphate group. The further it is away, the weaker is its deshielding effect. For the *n*-pentyl- and the *n*-hexyl-compounds **71** & **72** the decrease was negligible. The two entities could be considered to be isolated from each other. This was also reflected in comparison to the precursor malonate alkanols **65** & **68**. The corresponding hydrogen atoms had almost the same chemical shift as in the phosphate compounds.



Scheme 3.11: Synthesis of phosphate trismalonates.

The same tendency was observed at the other side of the chain. The protons α to the phosphate group resonated between 4.23 and 3.95 ppm. Furthermore these protons did not resonate as triplet, as it would be expected from the neighbouring CH_2 -group, but as a multiplet, due to additional coupling to the ^{31}P -core.

The protons in the center of the propyl chain of **69** resonated at 1.98 ppm. For the longer chains (C4 - C6), the protons being two carbon atoms away from an electron withdrawing group resonated as one multiplet at around 1.63 ppm no matter, if it was a malonate or a phosphate group. The protons being three carbon atoms away from the phosphate or the malonate group (C5- and C6-derivative) resonated at around 1.36 ppm.

The ^{13}C -NMR spectra of the phosphate trismalonates **69** - **72** were also in analogy to that of **62**. A summary of relevant ^{13}C -shifts and ^{13}C - ^{31}P -coupling constants of the spacer is given in table 3.2. In general, the carbon atom at the malonate end resonated at higher field than the carbon atom at the phosphate end. They could be easily distinguished due to coupling to the ^{31}P -core which resulted in a doublet for the carbon atom at the phosphate end. The resonance of the carbon atom in β -position to the phosphate group was also split into a doublet, with a slightly bigger coupling constant, than the α -carbon. These facts allowed an easy assignment of the corresponding ^1H -NMR signals by HETCOR-spectra. The coupling constants were again in agreement with literature values for saturated alkyl phosphates.^[159] The ^{31}P -NMR shifts of the entire trismalonate series are also summarized in table 3.2. All compounds resonated in the typical region for alkyl phosphates at slightly negative shifts.^[159]

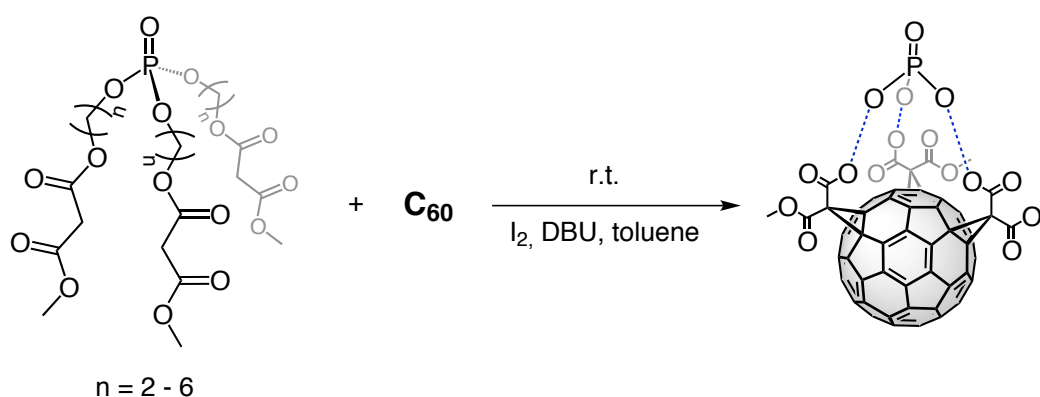
Table 3.2: Selected Chemical Shifts of the Spacer Part of the Phosphate Trismalonates.

spacer length	compound no.	$\delta(^{31}\text{P})$ [ppm]	$\delta(\text{P}_\alpha)$ [ppm]	$^2\text{J}(\text{P}_\alpha)$ [Hz]	$\delta(\text{P}_\beta)$ [ppm]	$^3\text{J}(\text{P}_\beta)$ [Hz]	$\delta((\text{C}=\text{O})_\alpha)$ [ppm]
C2	62	-0.80	65.3	6.5	63.7	7.0	63.7
C3	69	-0.59	64.1	5.7	29.3	7.1	61.3
C4	70	-0.32	66.9	6.0	26.5	7.0	64.6
C5	71	-1.55	67.2	5.9	29.6	6.8	65.0
C6	72	-0.09	67.4	6.0	30.0	6.9	65.3

3.3.3 Fullerenophosphate-*e,e,e*-Trisadducts

3.3.3.1 Synthesis of Novel *e,e,e*-Trisadducts

The phosphate trismalonates **69** - **72** were then used in the next step for the functionalization of C_{60} . The same reaction conditions as for the synthesis of **59** (page 51) were also employed (Scheme 3.12). TLC control after one night clearly displayed a red spot, which was subsequently isolated by column chromatography. In some cases, brown byproducts coeluted with the red product bands and required a very careful, second column chromatography to fully purify the desired *e,e,e*-trisadduct. During chromatography, however, a second, less polar, red band, previously invisible on TLC, was eluted. As this was the case for all four reactions and as the color is very indicative for *e,e,e*-trisadducts, this deserved further attention.



Scheme 3.12: Schematic representation of the synthesis of novel C_{60} -*e,e,e*-trisadducts.

3.3.3.2 Fullerenophosphate-*e,e,e*-Trisadducts with *n*-Propylspacer

The two red bands were subsequently investigated more thoroughly. First, the results for the *n*-propyl spacer samples **73** & **74** are described in this section. As in all cases, the more polar band was the main product. It was formed in this case in 15 % yield, while the less polar product was formed in this case in 3 % yield, which explains why it was invisible by TLC from the reaction mixture. Some more brown fractions were also isolated by column chromatography but no structure could be assigned to them, although some had the correct molecular weight for a trisadduct.

UV-Vis-spectra of the two isolated isomers are shown in figure 3.7. As the UV-Vis spectra are very indicative for a certain addition pattern, it was clearly deduced that both products were fullerene-*e,e,e*-trisadducts. Both showed the typical absorptions at 252 nm, 282 nm, 302 nm, 380 nm, 484 nm and 565 nm.^[44, 45, 46]

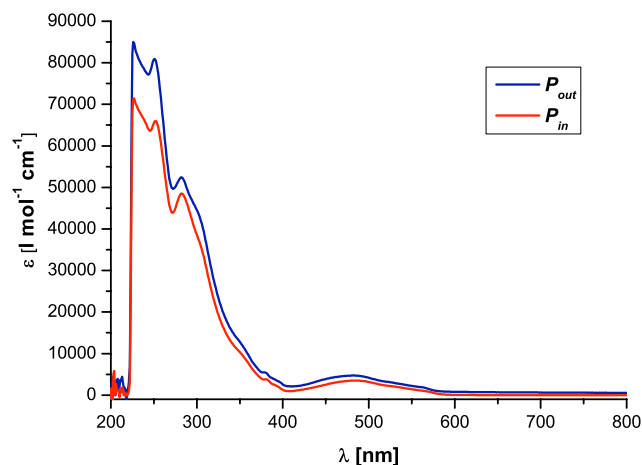


Figure 3.7: UV-Vis spectra (DCM, r.t.) of the two phosphate-*e,e,e* isomers **73** & **74**.

MALDI-TOF mass spectrometry displayed for the polar fraction the expected molecular ion peak at $m/z = 1286$, thus suggesting that it contained the desired phosphate product. However, the spectrum for the less polar fraction was exactly the same, which ruled out that decomposition with loss of phosphate or some esters had occurred. HiRes-ESI-MS also confirmed the correct molecular composition for both fractions. As a result, it can be said that both fractions contained an *e,e,e*-trisadduct with the correct mass. Which fraction contained the desired product and what the other fraction contained could not be deduced from these data alone.

Judging from a comparison on TLC between the ethyl spacer fullerophosphate **59** and the products from the reaction with the propyl spacer phosphate **69**, the more polar red band had to be the corresponding phosphate product **73**. It was slightly less polar ($R_f = 0.16$; DCM:THF = 95:5) than **59** ($R_f = 0.06$; DCM:THF = 95:5) but still in the same region, while the less polar fraction moved substantially faster on TLC ($R_f = 0.90$; DCM:THF = 95:5).

^{13}C -NMR spectroscopy revealed some more hints. The spectra (Figure 3.8) looked essentially the same for both fractions with some minor shifts of a maximum of 1 ppm for some of the signals. The ^{13}C - ^{31}P -couplings were clearly observed in both cases and 18 signals for

the fullerene sp^2 -carbon atoms clearly supported the e,e,e -addition pattern. Altogether, both spectra, together with the MS-data, confirmed the structure of a C_{60} - e,e,e -trisadduct with a phosphate group in the polar addend zone linked *via* a n -propyl-spacer. Thus, the difference in both isomers could essentially only be the orientation of the phosphate group. The only reasonable remaining possibility for two isomers with these data was an *in/out*-isomerism of the phosphate group. The two isomers, depicted in scheme 3.13, should thus be the two structures that resulted from the addition of the n -propyl phosphate **69**. For reasons of brevity, the isomerism is denoted P_{out} for **73** and P_{in} for **74**, although the stereochemical entity is rather the P=O-group and not the P-atom alone.

in/out-Isomerism is often observed in macrocyclic phosphorus compounds.^[163, 164, 165] In contrast to the corresponding amine compounds, phosphorus stereocenters are configurationally much more stable and the isomers can be isolated.^[166] Relevant literature examples to the present case are phosphite and phosphate centered cryptands (Figure 3.13).^[167, 163] The cryptands were synthesized as phosphites, which were already configurationally stable. All three isomers (*in,in*, *in,out*, *out,out*) were isolated. The orientation of the phosphorus cen-

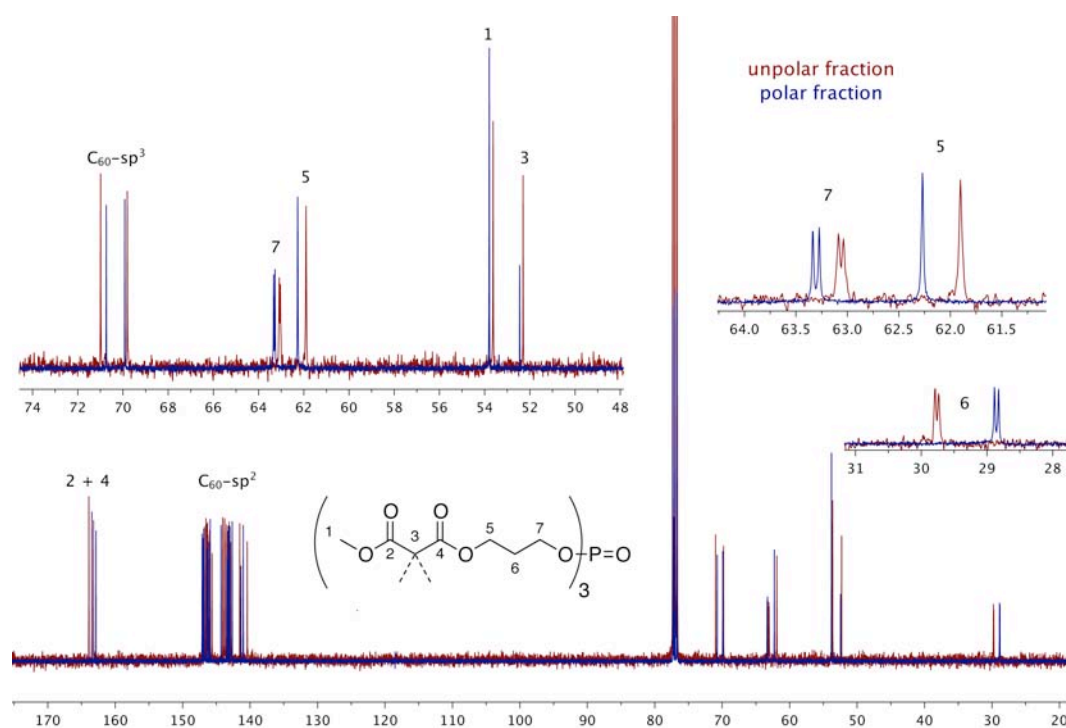
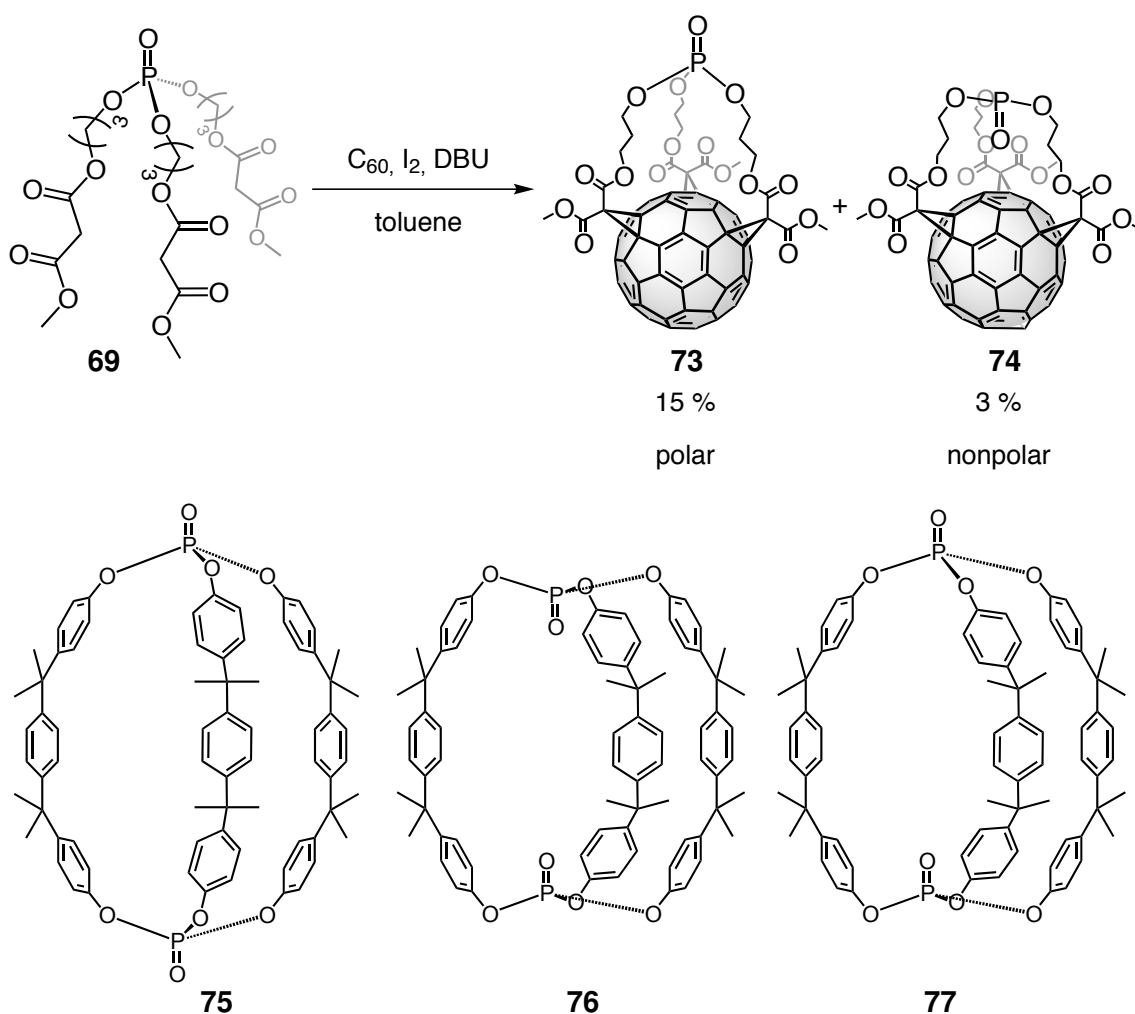


Figure 3.8: The superposition of the ^{13}C -NMR-spectra (100 MHz, CDCl_3 , r.t.) of the polar and the nonpolar fraction show their similarity. inset: magnification of the ^{13}C - ^{31}P -couplings.

ter was confirmed by X-ray crystallography.^[163, 168] The isomeric phosphorus nuclei displayed different reactivity in oxidation reactions that yielded the macrocyclic phosphates **75**, **76** and **77**. The *out*-centers reacted much faster but the *in*-centers were also oxidized. The inward orientation of the phosphorus center is of particular interest. A shielded environment of the active site was shown to be beneficial for the performance of a phosphine ligand.^[169] In an attempt to tailor the properties of the macrocycle's cavity, the *in*-phosphite corresponding to **76** was post-functionalized.^[170]

What fraction contained which isomer in our case was further clarified by ³¹P-NMR spectroscopy. The polar fraction yielded a signal at -1.23 ppm and the nonpolar isomer gave a



Scheme 3.13: The *in/out*-isomerism of phosphates is not only encountered in the synthesized fullerene derivatives **73** & **74** but also in macrobicyclic phosphates **75**, **76**, and **77** from literature.^[163]

resonance at 4.08 ppm. As the ethyl homologue **59** had a ^{31}P -resonance at -0.19 ppm and was unlikely to have the P_{in} -geometry due to steric reasons, the P_{out} -isomer **73** was assigned to the polar fraction. The P_{in} -invertomer **74** was accordingly assigned to the nonpolar fraction. Furthermore this was in accordance with the polarity and the behavior on TLC, as mentioned above. Simple considerations supported this assignment. The polar P=O-group is hidden within the cavity of the molecule in the P_{in} -isomer **74**. Thus, the molecule should be less polar. The difference in chemical shift was explained by inherent strain within the phosphate groups.^[163] The resonance in the P_{out} -isomer **73** was very close to the free addend (-0.59 ppm) and thus, the geometry should be rather relaxed. In case of the phosphate cryptands **75** - **77** mentioned above, the difference of the ^{31}P -chemical shifts between the two isomers was around 8 ppm and the *in*-isomer resonated at lower field, which was also observed in the present cases.^[163]

The ^1H -NMR spectra of the two invertomers displayed bigger differences (Figure 3.9), than the previous spectra. The signals for the methyl esters gave a single singlet at 3.91 ppm in both cases, which is shifted by 0.22 ppm to lower field in comparison to the free addend. The signals for the central protons of the methyl group were also almost identical, except that the signal from the P_{out} -isomer **73** was broader. Of special interest was the coupling pattern for the outer protons of the *n*-propyl chain. The signals were diastereotopically shifted for both isomers, as reported for the benzene system **38** and which was also observed for the ethyl homologue **59**.^[141] The assignment of the multiplets was based on the HETCOR- and COSY-spectra. As the carbons atoms close to phosphorus were split into doublets, the assignment was straightforward.

In case of the P_{out} -isomer **73**, the two multiplets for the protons at C7 were diastereotopically shifted by 0.27 ppm which meant, that they possessed a sufficiently different chemical environment. The multiplet at 4.06 ppm (H7) was almost unchanged in comparison to the free spacer, whereas the diastereotopic counterpart H7' was shifted to higher field. The protons at C5 resonated as a single multiplet at 4.28 ppm which was essentially the same value as for the free trismalonate. Thus, the chemical environment of these two protons was very similar. In case of the P_{in} -isomer **74** both sets of protons were split diastereotopically, yet on first sight, this was not apparent from the spectrum. However, examination of the HETCOR- and COSY-spectra revealed, that one multiplet of each set of signals of diastereotopic protons resonated at the same position and thus formed a joint multiplet. The signals for the protons at C5 resonated again at slightly lower field at 4.33 ppm and 4.15 ppm (diastereotopic shift = 0.18 ppm), respectively. The signals for the protons at C7 were wider separated (0.31 ppm)

and appeared at 4.15 ppm and 3.84 ppm. For this molecule the chemical environment was obviously different for every mentioned proton. In this and all the other cases an interplay between the magnetic anisotropy of the fullerene surface and the P=O-group could be used to rationalize the appearance of the spectra.^[57, 171]

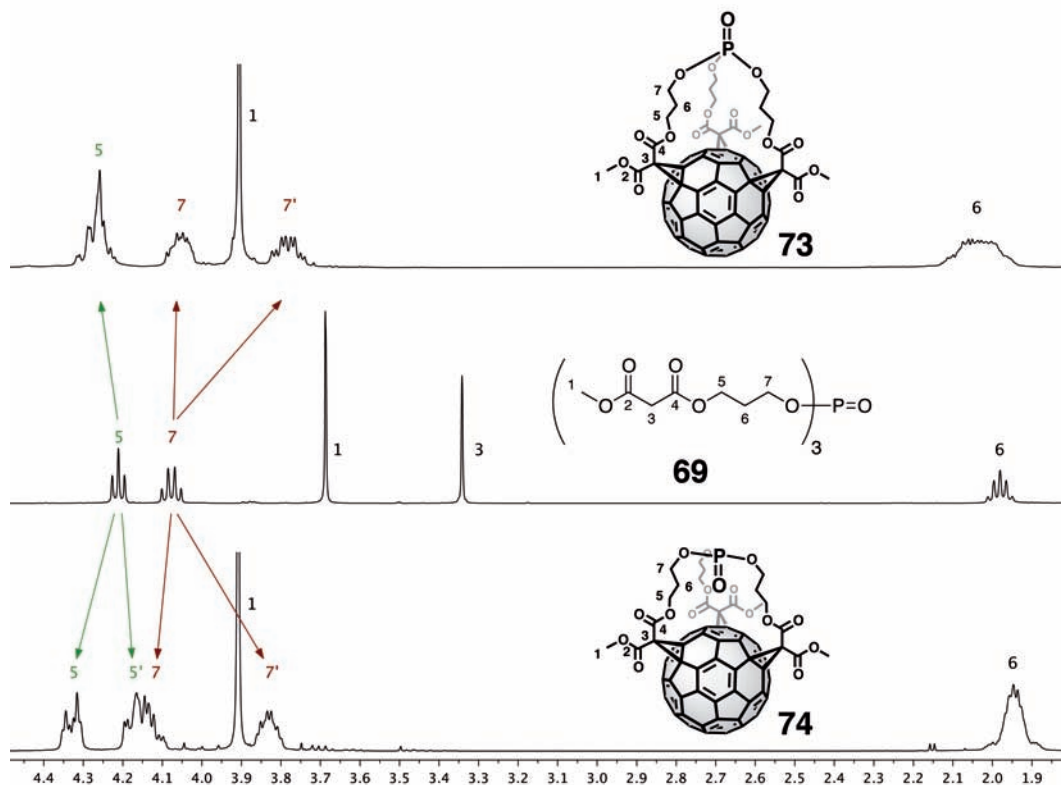


Figure 3.9: Comparison of the ^1H -NMR spectra (400 MHz, CDCl_3 , r.t.) of the P_{out} -**73** & the P_{in} -isomer **74** illustrates the different splitting patterns for both isomers.

3.3.3.3 X-Ray-Crystal Structures of Inverted Fullerenophosphate-*e,e,e*-Trisadducts

Final proof for the correct structure and the correct assignment of the fractions was obtained from X-ray crystallography. Only very rare examples of multiple C_{60} -BINGEL-adducts are reported in literature and none of them possess an *e,e,e*-addition pattern.^[47, 147, 172] A pentakisadduct with an incomplete T_h -addition pattern was recently reported by our group.^[173] The crystal structure of a C_{60} -trisadduct with malonate addends and $e_{edge}, e_{face}, trans$ -1-geometry was also recently reported.^[174] The only crystal structure of a C_{60} -*e,e,e*-trisadduct was reported by Kräutler and coworkers for a tris-DMA-adduct.^[175]

X-ray-quality crystals of the nonpolar fraction were grown from hot toluene- d_8 and finally confirmed the structure and assignment of the P_{in} -geometry (Figure 3.10). **74** crystallized in the chiral, orthorhombic space group $P2_12_12_1$ and the measured crystal was enantiomerically pure and contained only the fC - e,e,e -enantiomer. The elemental cell contained four molecules **74** and four disordered molecules toluene. The crystal structure nicely confirmed the e,e,e -addition pattern already deduced from the ^{13}C -NMR spectra, as well as the inward orientation of the P=O-group.

The C–C-bonds of the cyclopropane rings were elongated in comparison to the other [6,6]-bonds on the opposite sphere of the fullerene (Table 3.3), which demonstrated, that they had no more double-bond character. The [6,6]-bonds within the circle of cyclopropane rings, however, were slightly shorter than on the unfunctionalized part and the bond-length alternation was somewhat smaller. These values were in perfect agreement with those from the DMA- e,e,e -trisadduct.^[175] The n -propyl chains were, like the malonate groups around the fullerene core, arranged in a C_3 -symmetrical fashion (Figure 3.10 b).

The P=O-bond was almost perfectly centered above the underlying hexagon and was only slightly tilted by 2.5° ($180^\circ - \sphericalangle$ (O-P-hexane centroid)) from a perfect perpendicular orientation. The planes through the basal phosphate O-atoms and the underlying cyclohexane ring were also tilted by only 2.6° . The apical O-atom was 282.9 pm away from the underlying

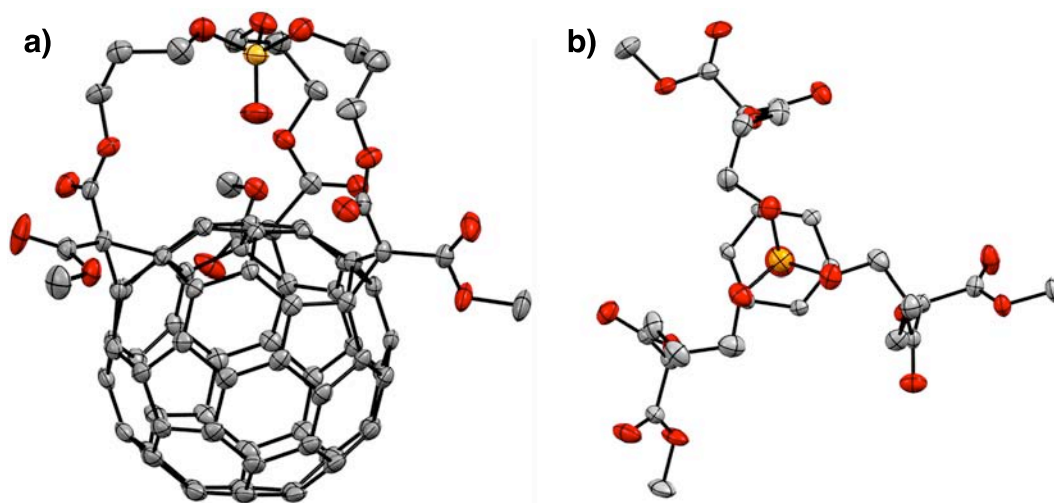


Figure 3.10: Single crystal X-ray structure of the P_{in} -isomer **74**: ORTEP representation with ellipsoids at 50% probability level (C grey, O red, P orange; hydrogen atoms and solvent molecules are omitted for clarity). a) sideview; b) top-view of the addend part with underlying hexagon of the C_{60} -sphere.

cyclohexane ring and the basal plane of phosphate O-atoms was 494.4 pm apart. The P=O-bond was 144.8 pm long while the P–O-bonds were slightly longer (156.7 pm). The angles between the P=O- and the P–O-bonds were on average 115.3° and on average 103.1° in between the P–O-bonds. The underlying structural reason was a slightly distorted tetrahedral geometry where the P=O-bond forced the other groups in a little closer proximity than in the ideal tetrahedral case.

Table 3.3: Selected bond lengths [pm] and angles of **73** and **74**. 'cluster' and 'C₆' refer to the central hexagon within the malonate addends and its centroid or the plane through it, respectively.

	<i>P_{out}</i> -isomer	<i>P_{in}</i> -isomer
∅[6,6]-bond _{cyclopropane}	159.2	159.1
∅[6,6]-bond _{cluster}	138.3	138.2
∅[6,6]-bond _{opposite}	139.5	139.0
∅[5,6]-bond _{cluster}	142.9	142.8
∅[5,6]-bond _{opposite}	144.9	144.9
P=O-bond	144.4	144.8
	162.6	156.7
P-O-bonds	155.6	157.1
	150.9	156.4
O _{P=O} -C _{6-plane} -distance	615.4	282.9
	364.2	488.3
O _P -C _{6-plane} -distances	472.2	496.0
	528.0	498.9
∠(180°-(∠O=P-C _{6-centroid}))	29.4°	2.5°
	104.9°	115.22°
∠ O=P-O	119.9°	115.29°
	120.0°	115.39°
	100.4°	102.60°
∠ O-P-O	103.4°	102.93°
	105.2°	103.66°

Single crystals, suitable for X-ray analysis, of the polar fraction were grown by slow vapor diffusion of pentane into a solution in benzene. The P_{out} -geometry of this isomer was confirmed by the crystal structure and the existence and formation of both isomers was thus established and finally verified (Figure 3.11). **73** crystallized in the triclinic space group $P\bar{1}$. The elemental cell contained two molecules **73** and two molecules of either pentane or benzene, who shared a common crystallographic site. Due to the centrosymmetry of the space group $P\bar{1}$, the crystal had to contain a racemic mixture of *e,e,e*-enantiomers. Disorder was observed for the phosphate group, where two alternative orientations were refined with site occupancies of 38.6% (not shown) and 61.4%. Further disorder was observed for one of the methoxy groups. Two alternative orientations with site occupancies of 53% and 47% (not shown) were refined. Concerning the C–C-bond lengths of the fullerene core, no major changes in comparison to the P_{in} -isomer were observed (Table 3.3). The arrangement of the *n*-propyl chains was less symmetric, which was due to the tilt of the phosphate entity, which distorted the entire molecule.

Surprisingly, the P=O-bond of the P_{out} -invertomer, was not simply oriented in the other direction than in the P_{in} -isomer but also tilted by 30.3° from a perpendicular orientation towards the hexagon and displaced off-center. This was also reflected in the angle between the planes through the basal phosphate O-atoms and the underlying cyclohexane ring, which

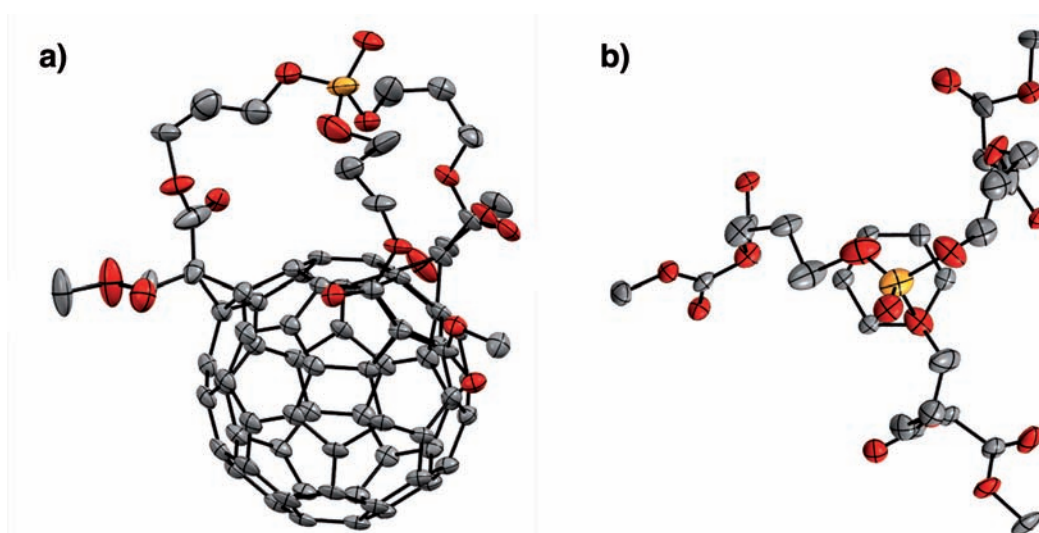


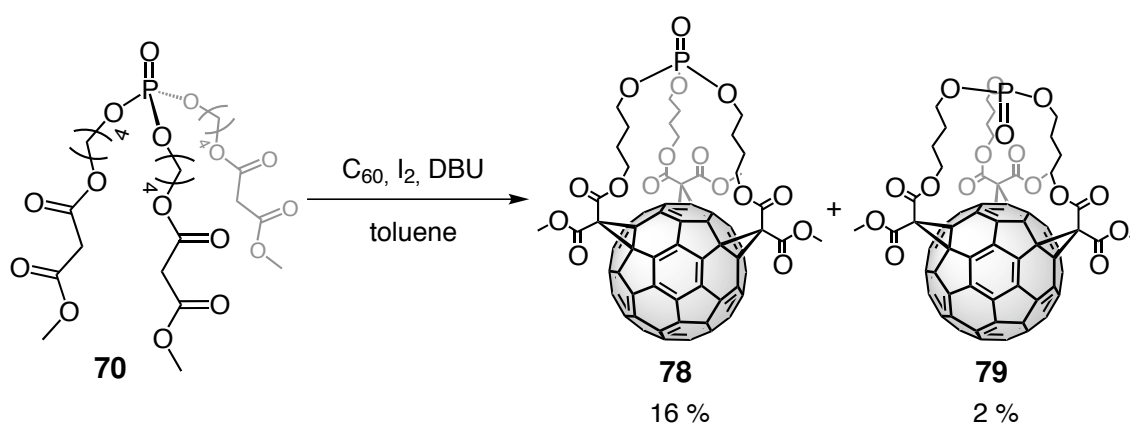
Figure 3.11: Single crystal X-ray structure of the P_{out} -isomer **73**: ORTEP representation with ellipsoids at 50% probability level (C grey, O red, P orange; hydrogen atoms and solvent molecules are omitted for clarity). a) sideview; b) top-view of the addend part with underlying hexagon of the C_{60} -sphere.

was now 29.2°. Due to the P_{out} -geometry, the apical O-atom of the phosphate group was here 623.1 pm apart from the cyclohexane plane, which was more than twice as much, as in **74**. The basal phosphate-O-atoms were between 378.2 pm and 498.9 pm away. Hence, the farthest of the O-atoms was as far away, as in the P_{in} -isomer, while the others were tilted towards the fullerene. The P=O-bond was a little shorter (139.2 pm) than in the P_{in} -isomer and one of the P–O-bonds was substantially shorter than the other two (170.2 pm, 169.1 pm and 139.5 pm). The asymmetry of the phosphate group was also reflected in the angles between the P=O- and the P–O-bonds: they ranged from 105.6° to 136.7°. A similar behavior was also found for the angles in between the P–O-bonds.

As shown, the phosphate entity in **73** was highly asymmetric in the solid state. The tilt is probably due to a conformational instability within this geometry. This can be also the reason for the disorder in some parts of the crystal structure. This is averaged in solution and the NMR-spectra show a symmetric structure. The P_{in} -isomer is probably conformationally much more stable and also had a crystal structure with higher symmetry.

3.3.3.4 Fullerenophosphate-*e,e,e*-Trisadducts with *n*-Butylspacer

The BINGEL-reaction with the *n*-butyl-phosphate-malonate **70** yielded essentially the same results as with the *n*-propyl-phosphate-malonate **69**. Two isomers **78** & **79** were isolated in 16% and 2% yield, respectively. In analogy to the *n*-propyl homologue, the P_{in} -structure **79** was assigned to the nonpolar isomer and the P_{out} -structure **78** to the polar isomer. As above, no reasonable structures could be assigned to the other fractions that were eluted, although some showed product MS-signals.



Scheme 3.14: Synthesis of the *n*-butyl spacer *e,e,e*-trisadducts **78** & **79**.

The two *e,e,e*-diastereomers possessed identical UV/Vis-spectroscopic and mass-spectrometric properties, as in case of the *n*-propyl-fullerenophosphates **73** & **74** (page 58). The ^{13}C -NMR spectra were almost identical as well, and displayed the expected signals. The ^{31}P -resonances for the nonpolar and the polar isomer were detected at -0.74 and -1.40 ppm, respectively, thus following the behavior above.

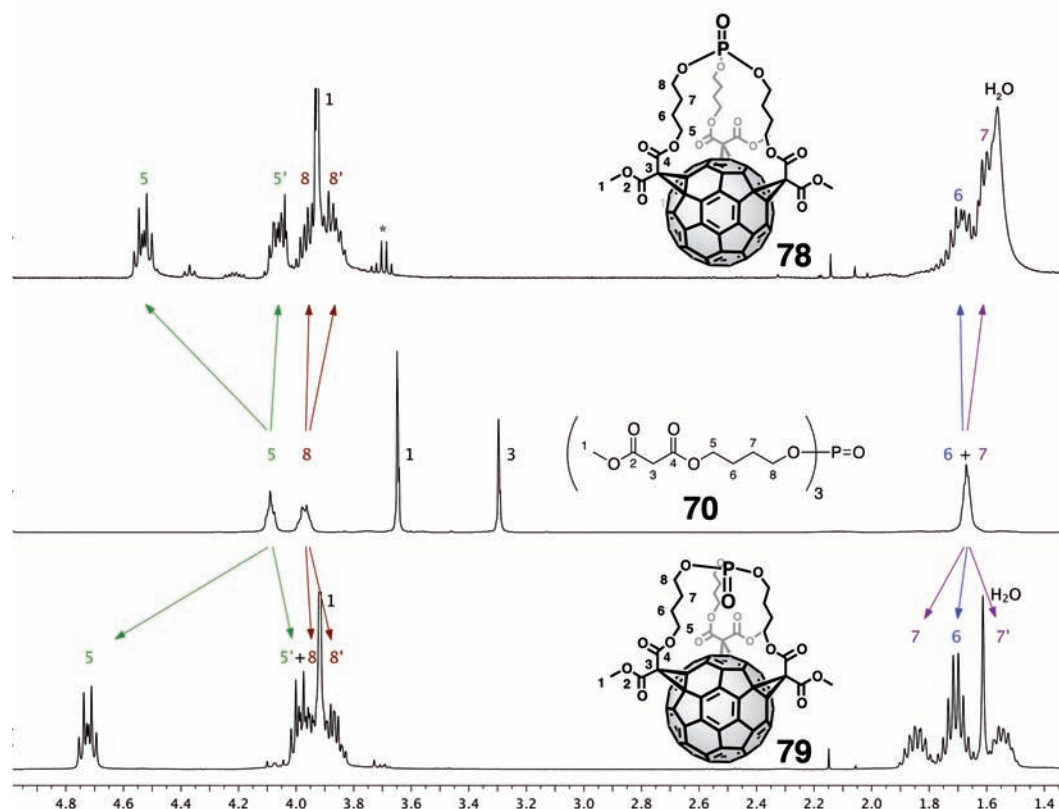


Figure 3.12: Comparison of the ^1H -NMR spectra (400 MHz, CDCl_3 , r.t.) of the P_{out} - **78** & the P_{in} -isomer **79** illustrates the different splitting patterns for both isomers.

A bigger difference between the two isomers was observed in the ^1H -NMR spectra (Figure 3.12). The protons at C5 were diastereotopically shifted in both cases. The shift was 0.47 and 0.75 ppm for the P_{out} - and the P_{in} -isomer, respectively. The multiplet at lower field was split into a doublet of triplets in both cases with coupling constants of $^2J = 10.9$ Hz and $^3J = 7.0$ Hz for **78** and $^2J = 10.7$ Hz and $^3J = 6.7$ Hz for **79**. The multiplet of the diastereotopic counterpart, however, was not as clearly resolved and overlapped with signals from H8. The resonances of the protons at C8 were only slightly diastereotopically shifted (P_{out} : 0.07 ppm; P_{in} : 0.11 ppm) and overlapped with signals from H5 and from the methyl ester. The multiplets for H6 and

H7 in **78** exhibited a complex coupling pattern and were partly hidden under the water peak. The signals for H6 and H7 in **79**, however, yielded nice multiplets with a diastereotopic shift of 0.29 ppm for H7, while H6 experienced no such an influence.

The signals were better separated and easier to observe in toluene- d_8 (exemplary comparison in figure 3.13 for **79**). Due to the ring currents of the solvent molecules the protons are deshielded differently according to their orientation in the macrocycle. Depending, whether the protons are located inside or outside the cavity, they are better or less accessible by the solvent molecules.

The diastereotopic shift of multiplets originated from a different orientation towards the fullerene surface and the inherently chiral addition pattern.^[161, 57] The coupling patterns of H5 and H8 were clearly resolved, while the protons at C6 were almost magnetically equivalent. The splitting concerned only the positions close to the nodes of the macrocycle. The diastereotopic shift was much larger for the P_{in} -isomer, which could either be explained by a different orientation towards the fullerene surface or by an additional effect of the P=O-group.

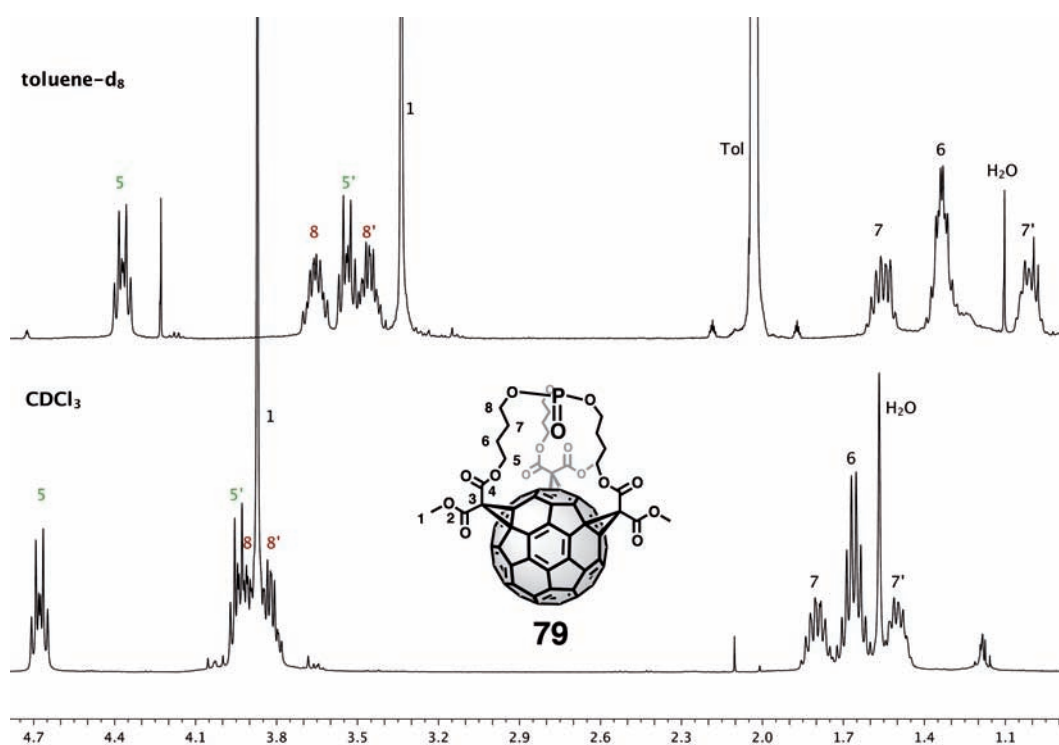
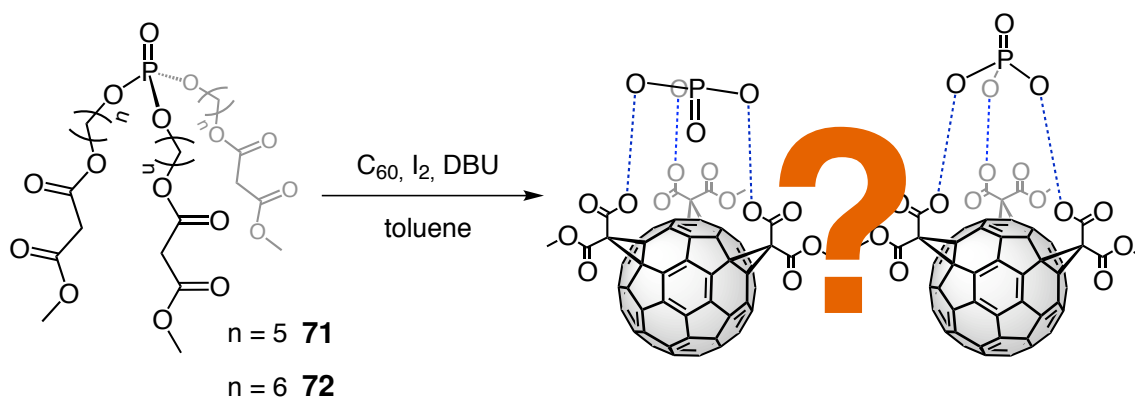


Figure 3.13: Comparison of the ^1H -NMR spectra (400 MHz, r.t.) of **79** in different solvents (top: toluene- d_8 ; bottom: CDCl_3).

3.3.3.5 Fullerenophosphate-*e,e,e*-Trisadducts with *n*-Pentyl- and *n*-Hexylspacer

The reactions above yielded the two *e,e,e*-isomers with P_{in}^- and P_{out}^- -geometry as the main products. By increasing the spacer length, as in the following cases, other addition patterns could also be possible, as the tethers are much more flexible and can, in principle, span a bigger part of the fullerene sphere.

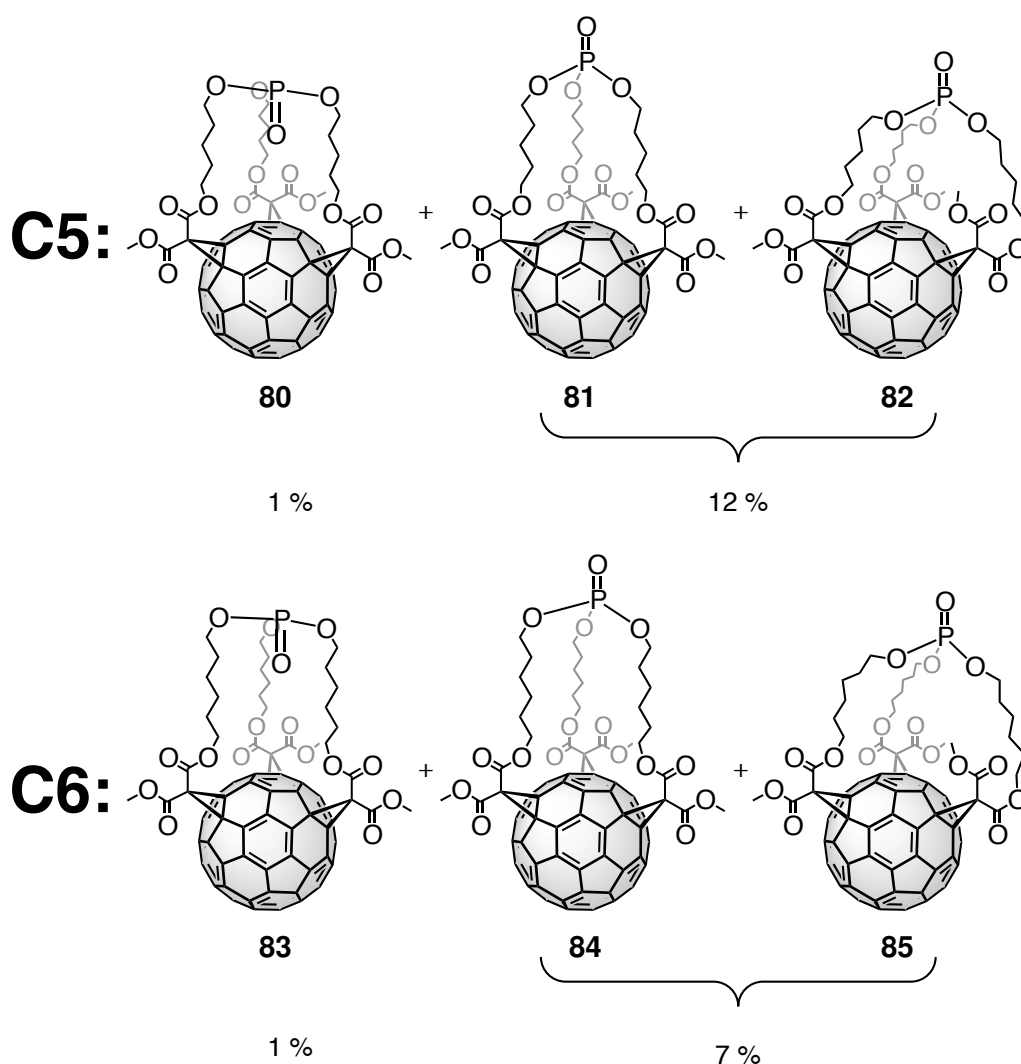


Scheme 3.15: In principle, longer tethers can favor the formation of other isomers.

Nevertheless, the reaction between the phosphate malonates **71** and **72** and C_{60} gave comparable results as with previous systems. TLC-control after one night revealed two red spots at the expected positions for the *e,e,e*- P_{in}^- and P_{out}^- -isomers. Subsequently, they were separated from the other brown fractions by column chromatography. In both cases, no other fullerene trisadduct isomers were isolated and assigned to one of the brown fractions although, MALDI-TOF analyses showed the correct molecular ion peak for some of them again. The polar main products with a C5- and a C6-chain were isolated in 12% and 7% yield, respectively. The selectivity obviously decreases with increasing chain length and thereby increasing flexibility of the spacer, which is reflected by the decreasing yield of the *e,e,e*-trisadducts.

Furthermore, the spectral data of the polar fraction were not in accordance with a pure substance. Although the mass spectra clearly showed a peak with the expected molecular weight and the UV-Vis-spectra corresponded to an *e,e,e*-addition pattern, the NMR-data did not support a single constituent. Especially the C_{60} - sp^2 -region in the ^{13}C -NMR spectra clearly showed a second set of signals, next to the 18 expected signals for an *e,e,e*-trisadduct. The ^{31}P -NMR spectrum of the mixture of pentyl adducts displayed two resonances at -2.42 ppm and -2.82 ppm. The hexyl-mixture displayed a single resonance at -2.07 ppm. In the pentyl

derivatives the strain in the two geometries was obviously sufficiently different to result in distinguishable signals. The hexyl derivatives were more flexible and the strain for both geometries was probably comparable. Neither automated flash chromatography (C5-spacer), nor HPLC (C6-spacer) were sufficient to purify the compounds. It turned out later (page 84), in another reaction step, that the polar fractions contained two isomeric P_{out} - e,e,e -trisadducts, which differed only in the orientation of one malonate group (Scheme 3.16). Thus, from n -pentyl spacer on, the alkyl chains were flexible enough to allow an inversion of one malonate group. The isomers were later (page 84) determined to be the expected malonate- out,out,out -isomers **81** & **84** and the unexpected malonate- out,out,in -isomers **82** & **85**.



Scheme 3.16: The reaction of longer tethers with C_{60} yields also less symmetrical e,e,e -trisadducts with one inverted malonate group.

In contrast, the nonpolar P_{in} -isomers **80** & **83** were isolated as pure compounds in 1 % yield, each. This underlines the somewhat more rigid character of the P_{in} -geometry, as already observed in the previous cases.

The spectral data of the P_{in} -isomers **80** & **83** were in analogy to the previously reported homologues. The ^{31}P -nuclei resonated again at slightly positive chemical shifts at 0.74 and 1.87 ppm, respectively, thus confirming the P_{in} -geometry.

The ^{13}C -NMR spectra were in analogy to the shorter systems. In the ^1H -NMR spectra, the protons at the malonate end of the alkyl chains were again diastereotopically shifted by 0.40 ppm and 0.43 ppm (C5-/C6-chain) and the multiplet at lowest field appeared again as a doublet of triplets. The protons at the phosphate end resonated again at higher field and experienced only a slight diastereotopic shift in **80** and appeared as a single multiplet in **83**. As it was in the end impossible to separate the two P_{out} -isomers in case of the n -pentyl- and n -hexyl-spacer, longer tethers were no more investigated and the series was ended with the C6-derivative. Additionally, the yields decreased from 24 % for ethano derivative **59** over 18 % (sum of yields) for the four propano and butano derivatives **73**, **74**, **78** and **79** to 8 % for the three hexano derivatives **83**, **84** and **85**, thus making it uninteresting to prepare tethers with even longer spacers.

3.3.3.6 Electrochemical Properties

The electrochemical properties of all isolated and fully purified phosphate- e,e,e -trisadducts were investigated to check, whether the phosphate-moiety had an influence on the reduction potentials and therefore interacted with the fullerene core. The compounds were investigated by cyclic voltammetry in ODCB-solution with tetrabutylammonium tetrafluoroborate (TBABF_4)

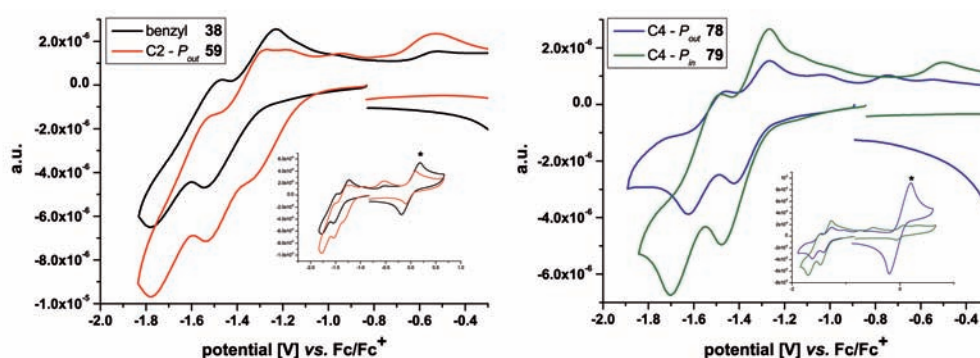


Figure 3.14: Selected cyclic voltammograms of e,e,e -trisadducts (ODCB; 0.1 M TBABF_4 at 0.1 V s^{-1} ; * = Fc/Fc^+ -couple).

as conducting salt. Selected cyclovoltammograms are shown in figure 3.14. The obtained reduction potentials (vs. Fc/Fc⁺) are summarized in table 3.4 and compared to the values of C₆₀ and the benzene-tethered trisadduct **38**.

Only the first two reduction steps were recorded, as the processes become irreversible after additional reduction steps. In contrast to C₆₀, the third reduction step becomes irreversible in C₆₀-malonate adducts due to isomerization and retro-BINGEL reactions.^[55, 176, 177] C₆₀-e,e,e-trisadducts are especially prone to isomerisation, because the dianion is very reactive.^[55] This was reflected in the cyclovoltammograms (Figure 3.14) by the small, irreversible oxidation peaks after the reductive cycle. Apart from that, two reversible reduction waves were observed for all trisadducts in the applied potential range, as it is also described for other C₆₀-trisadducts in the literature.^[54, 55] The first reduction wave was shifted cathodically by 200 mV to 300 mV in comparison to pristine C₆₀, which is in accordance with literature values.^[54] The second reduction wave was shifted by only 29 mV to 138 mV to cathodic values, which is substantially less than the literature shift of 300 mV. With increasing chain length within the *P_{out}*- & the *P_{in}*-series, the reduction potentials became more positive. The *P_{in}*-isomers with the same chain length as their corresponding *P_{out}*-isomers always had more negative reduction potentials. This indicated that the inward oxygen atom inhibited the electron uptake. The ethyl- and the *P_{in}*-propyl homologues **59** and **74**, respectively had almost the same reduction potentials, which could be attributed to an overall similar distance of the phosphate group to the fullerene surface. However, this trend was not observed for the higher homologues.

Table 3.4: Reduction potentials, as determined by cyclovoltammetry (vs. Fc/Fc⁺; ODCB-solution with 0.1 M TBABF₄ at 0.1 V s⁻¹). Values quoted: (E_{pa} + E_{pc})/2.

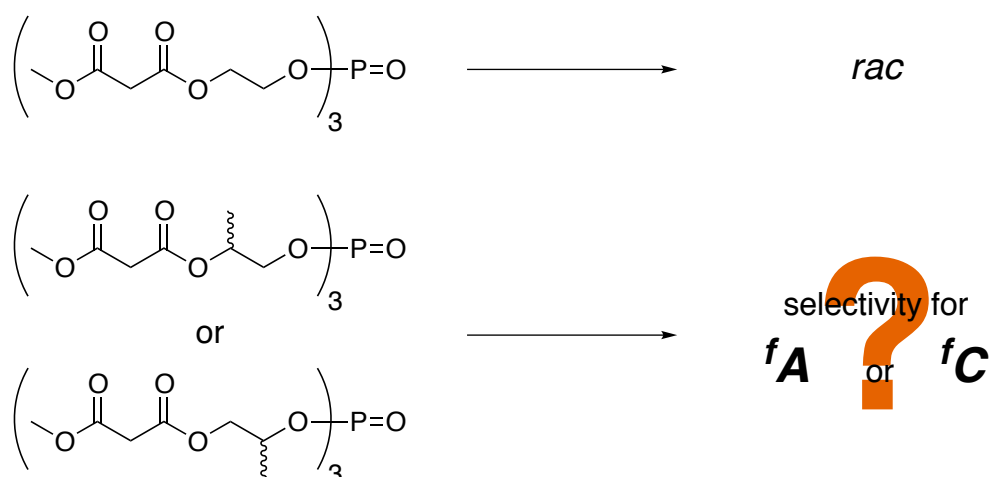
<i>P_{geometry}</i>	spacer	no.	E ₁ [V]	E ₂ [V]
C ₆₀		4	-1.106	-1.509
benzene	C2	38	-1.387	-1.623
	C2	59	-1.404	-1.631
<i>P_{out}</i>	C3	73	-1.340	-1.538
	C4	78	-1.345	-1.540
	C3	74	-1.405	-1.647
<i>P_{in}</i>	C4	79	-1.372	-1.590
	C5	80	-1.370	-1.544
	C6	83	-1.359	-1.554

The benzene reference **38** had no markedly different values than the phosphate adducts. The general electrochemical behavior was thus governed by the addition pattern and the phosphate addend only modulates the properties. With increasing chain length, the influence gets smaller and the values tend towards a limit.

3.3.3.7 Attempts for the Synthesis of Chiral Phosphate Trismalonates

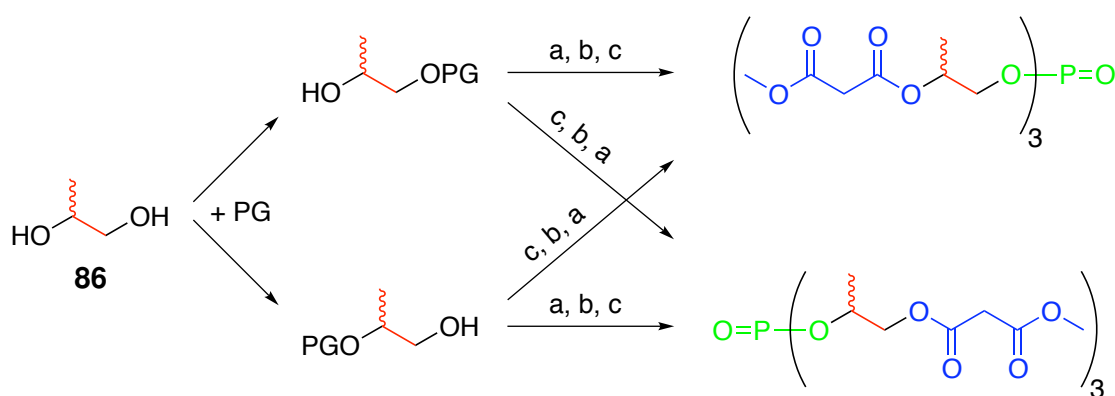
The C_{60} -*e,e,e*-addition pattern is inherently chiral, as already mentioned in the introduction (page 25). Even with three symmetrical and identical malonates, two possible enantiomers with clockwise (*fC*) and anticlockwise (*fA*) orientation of addends are possible. Examples for the corresponding enantiomers are reported for malonate and bis(oxazoline) addends (Figure 1.19 on page 27).^[43, 129] However, these compounds were prepared by stepwise addition of independent addends and required tedious purification steps. With the method described above, it should be possible to synthesize enantiomerically pure *e,e,e*-trisadducts in a single step and to create chiral functional materials in a subsequent reaction. For this purpose, chiral spacers within the phosphate trismalonates were intended to induce stereoselectivity during trisadduct formation (Scheme 3.17). Therefore, the alkylchains should be equipped with a branching unit. As a test system, the ethyl spacer should be replaced by a 1,2-propanediol spacer. Which enantiomer of the spacer would produce which fullerene *e,e,e*-enantiomer should be investigated in the next step, as well as the selectivity of the reaction.

The synthesis of the unbranched phosphate malonates started with the monoesterification of



Scheme 3.17: A stereocenter within the phosphate trismalonate could favor the formation of one C_{60} -*e,e,e*-enantiomer.

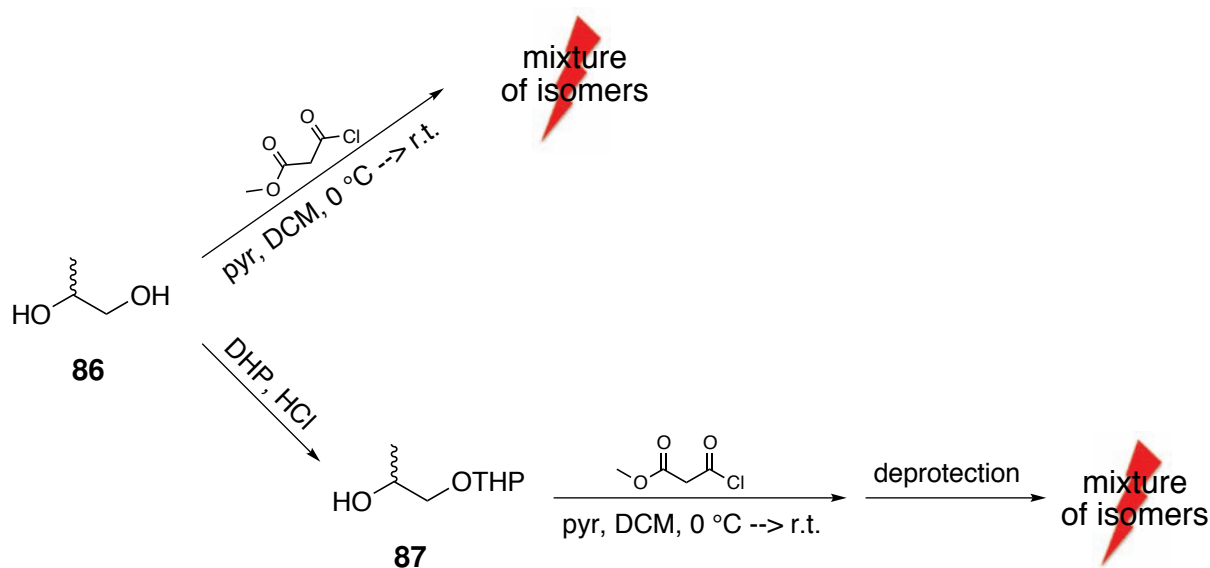
the corresponding diols. This was no big challenge, as the resulting malonate esters were the same, no matter, which of the two alcohol groups was functionalized. With 1,2-propanediol **86** as starting diol, however, this changed, as each functionalized alcohol moiety resulted in a different product. Therefore, a selective protecting group for the primary or the secondary alcohol had to be found first. The monoprotected diol could then be reacted with either methyl malonyl chloride or POBr_3 . After deprotection, the free alcohol functionality could then be reacted with the other reagent. The resulting phosphate malonates would thus have a branching unit at the malonate or the phosphate terminus of the spacer (Scheme 3.18). No matter, which alcohol group in **86** is protected in the first step, both types of addends are accessible by the proper order of functionalization steps. However, this requires mild deprotection reactions that do not lead to isomerizations.



Scheme 3.18: An unsymmetrical diol requires a protecting group strategy to obtain constitutionally pure phosphate trimalonates. PG = protecting group. a: methyl malonyl chloride, pyr, THF, 0 °C to r.t.; b: deprotection; c: POBr_3 , pyr, toluene, 0 °C to r.t.

In the first place, a selective protection for one of the alcohol groups had to be found. The corresponding test reactions were conducted with racemic 1,2-propanediol **86**, for the reason of cost-savings. In a first attempt (Scheme 3.19), the direct reaction with methyl malonyl chloride was attempted, but it turned out, as expected, that the reagent is too reactive. The mono- and the bismalonate were separated, but the monomalonate fraction contained obviously both isomers. The ^{13}C -NMR spectrum displayed four resonances for the carbonyl carbon atoms, which could only be the case, if both isomers were present. This was also verified by the ^1H -NMR spectrum. The methyl group yielded two doublets instead of one. A more promising strategy (Scheme 3.19), thus had to employ a less reactive reagent. The THP-ether is reported to be able to selectively protect the primary alcohol in (*S*)-1,2-

propanediol and was thus tested as the next alternative.^[178] The reaction was conducted, as reported, and the spectrum of the isolated monoprotected diol **87** corresponded to the reported one. Esterification with methyl malonyl chloride also proceeded smoothly. However, the ¹H-NMR-spectrum was not that clear, due to the diastereotopic product mixture that was generated, when attaching a THP-ether to a chiral molecule. Deprotection with HCl should solve this problem. Yet, the spectrum displayed again four carbonyl carbon resonances. Whether the isomerization occurred during the final deprotection step, or had already been present before and could not be detected due to the diastereotopic nature of the intermediates cannot be clearly said. In the end, this method cannot be applied for the synthesis of the desired chiral tethers.

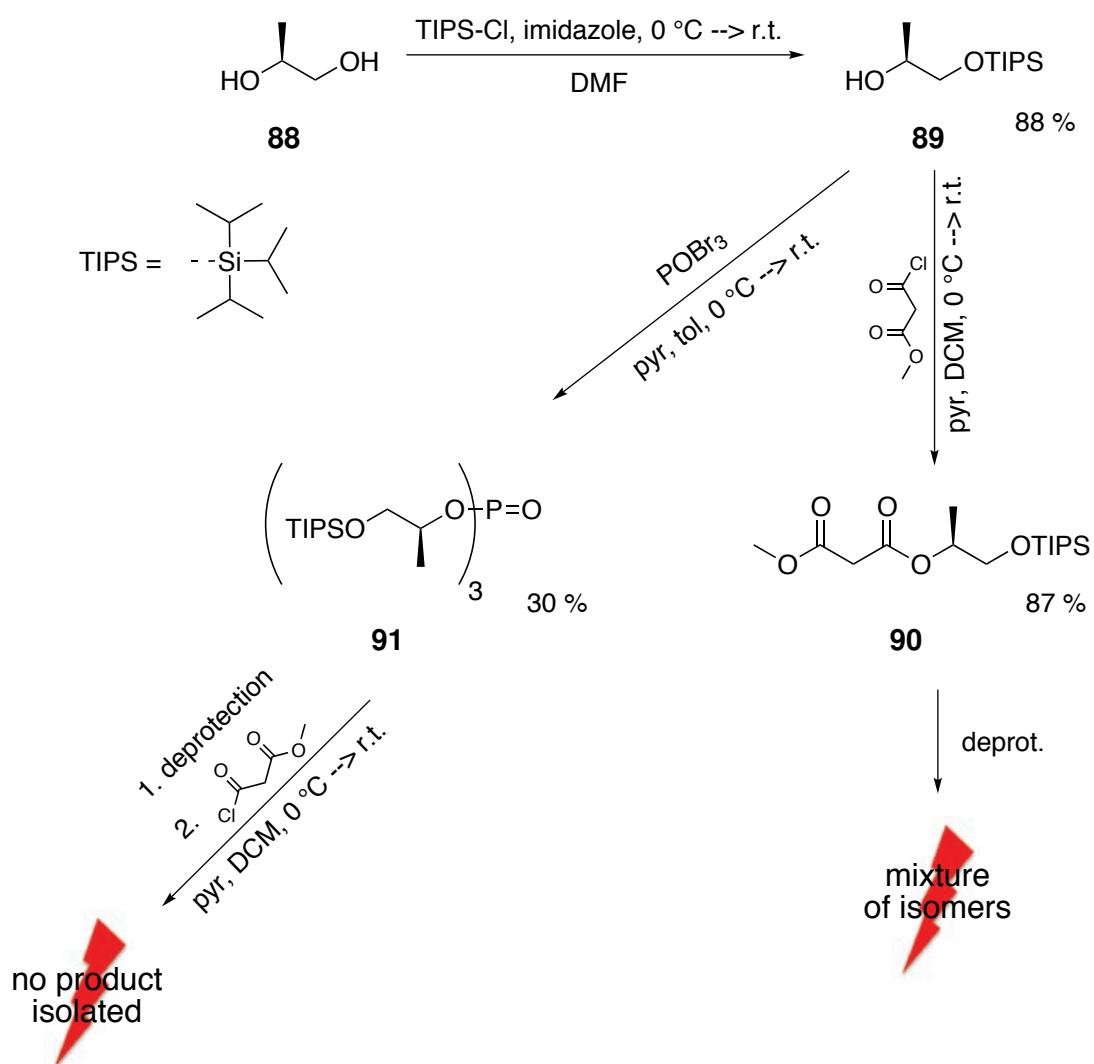


Scheme 3.19: First attempts to differentiate the primary and the secondary hydroxy group in *rac*-1,2-propanediol **86**. The products, however, always contained mixtures of the constitutional isomers.

The search for non-chiral protecting groups, differentiating between primary and secondary alcohols led in the end to silyl protecting groups. It is well known, that bulky silyl groups, like TBDMS, TBDPS or TIPS can be selectively introduced on primary alcohols in polyfunctional molecules that contain also secondary OH-groups.^[179] Furthermore they can be rather easily removed by dilute acid or fluoride ions, which could probably suppress the isomerization, that was observed above.

The monoprotection of 1,2-propanediol **86** was attempted with the TIPS-group, because the monoprotection of (*R*)-1,2-propanediol was already reported.^[180] The reaction sequence

(Scheme 3.20) was tested with the racemic diol first and then immediately applied to the (*S*)-enantiomer. (*S*)-1,2-propanediol **88** was dissolved in DMF and reacted with TIPSCI under imidazolium catalysis at 0 °C. The spectral data corresponded to the literature values and clearly confirmed the clean protection of the primary alcohol functionality. Subsequently, the free OH-group was successfully converted once to methyl malonyl ester **90** and once to phosphate **91**, according to the procedures, described for the unbranched compounds. It has to be noted, that the polarity of both products was mainly governed by the TIPS-group,

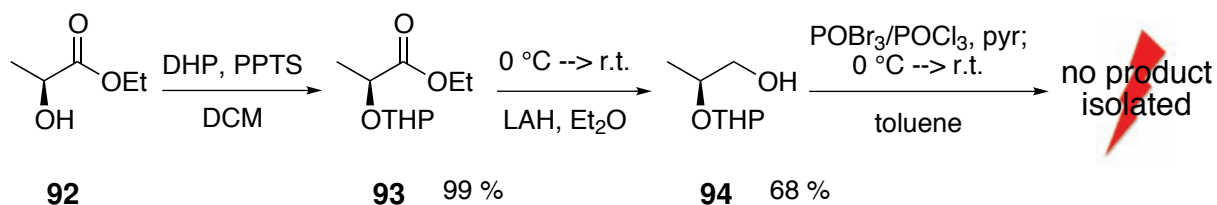


Scheme 3.20: It was possible to selectively protect the primary hydroxyl functionality with a TIPS-group, but the desired phosphate trimalonates were not obtained (for deprotection conditions, see text).

which rendered these molecules very nonpolar. Malonate **90**, e.g. had the same R_f -value as the corresponding TIPS-alcohol **89**. The identity of both compounds was clearly confirmed by their NMR-spectra. They confirmed also the selectivity of the sequence up to this point. The methyl group yielded in both compounds in the ^1H -NMR spectra one doublet at 1.23 ppm and 1.33 ppm for **90** and **91**, respectively. In the ^{13}C -NMR spectra, the carbonyl carbon atoms yielded two resonances, as expected. In the spacer part of phosphate **91** every carbon atom resonated as a doublet due to ^{13}C - ^{31}P -coupling.

For completion of the tether system, the TIPS-group had to be removed, which can be usually accomplished by dilute acid (3% HCl in EtOH or THF solution) or tetrabutylammonium fluoride (TBAF; in THF solution). However, when conducting these procedures with malonate derivative **90**, the isolated product behaved on TLC as expected but displayed again four resonances in the carbonyl region of the ^{13}C -NMR spectrum. Furthermore in the ^1H -NMR spectrum, the sidechain methyl group yielded two doublets, instead of one, as for precursor **90**. This hints to partial transesterification that had occurred during deprotection. Obviously the fluoride ion is basic enough under these conditions to catalyze the transesterification. Unfortunately, deprotection of TIPS-phosphate **91** failed as well. No product was isolated after workup, which might be due to the solubility of the phosphate trisalcohol in water. A direct conversion to the phosphate trimalonate without intermediate workup failed as well. Some of the P–O-bonds are probably cleaved by fluoride ions. At least the cleavage of phenyl-phosphates is known in the literature and is often applied in DNA syntheses, although alkyl-phosphates should be stable under these conditions.^[181, 163]

The desired chiral phosphate malonates are also accessible by a different strategy (Scheme 3.21), which starts from ethyl-*L*-lactate **92**. This approach did not require the selective reaction of one out of two very similar functional groups. Instead, the tether was built up step by step with only monofunctional intermediates. Ethyl-*L*-lactate **92** was protected as THP-ether **93** and the ester was subsequently reduced with LAH to alcohol **94**. This part of the synthe-



Scheme 3.21: The step-by-step strategy to obtain a chiral phosphate malonate failed in the end as well.

sis is already reported in literature.^[182] The strategy starting from ethyl-*L*-lactate thus yielded the orthogonally protected molecule, as the first strategy (page 75). From the experiences above, it was decided to attach the phosphate in the next step, in the hope of being not so prone to transesterification during deprotection. However, when reacting the THP-protected alcohol **94** with POBr₃ or POCl₃ no product could be isolated.

In the end, all attempts to synthesize a chiral C2-phosphate malonate failed, mainly due to the lability of the attached malonate or due to problems with purification. Thus, this approach was no longer followed, despite the promising outlook in the beginning.

3.4 Development of C₆₀-e,e,e-Building Blocks

3.4.1 Search for a Proper Deprotection Strategy

The phosphate trisadducts, described in the previous section, offered a straightforward and synthetically elegant access to C₆₀-e,e,e-trisadducts in acceptable yields. For application in novel materials, however, further functional moieties have to be attached prior or after e,e,e-trisadduct formation (Figure 3.15). The equatorial addend zone was still unchanged in comparison to the systems, introduced by Beuerle, and could be derivatized in the same way.^[141] Therefore the functional groups or their precursors would have to be introduced before the trisadduct formation. The polar addend zone, however, was completely different and a novel deprotection method for the phosphate template had to be established. The benzene template in Beuerle's systems was removed and transformed to bromides, carboxylic acids or alcohols of which the latter were further derivatized.^[141] Here, the aim is to find a suitable method to transform the phosphate group into similar, versatile functional groups that act as good anchor points for other entities.

For removal of the phosphate group in the present molecules, several procedures were tested and investigated (Figure 3.16). As model substance, the parent system **59** with an ethyl spacer was chosen. Basic hydrolysis of the phosphate ester was not considered, as the

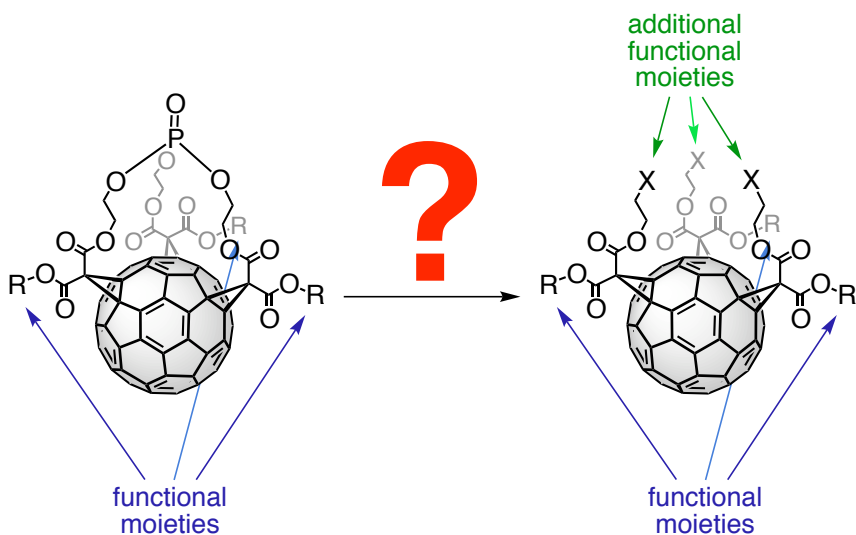


Figure 3.15: Phosphate-*e,e,e*-trisadducts can have two different functional addend zones if the template can be removed. The equatorial zone (blue) can be altered prior and the polar zone (green) can be altered after trisadduct formation.

required OH^- -ions would also attack the fullerene core.^[183] Acidic hydrolysis was attempted with concentrated hydrochloric acid in a refluxing mixture of CHCl_3 and MeOH overnight or with HBr/AcOH at r.t. overnight. None of these treatments resulted in any reaction, luckily, also in no or little decomposition. The use of BCl_3 in DCM as a Lewis-acidic reagent, which is successful for the cleavage of benzyl ethers also did not lead to any reaction. Other popular literature procedures for the deprotection of phosphate units employ TMSBr in a proper solvent, which was DCM in the present case.^[179] However, this reagent did not attack the C_{60} -phosphate-*e,e,e*-trisadduct at all within twelve hours. Changing the solvent to THF resulted only in black decomposition products. Stirring the reagents overnight in DCM and hydrolysis of eventually formed TMS esters in CHCl_3 , MeOH and water, as applied for the deprotection of phosphonates, was not successful.^[184, 185] Some other reports applied in addition to TMSBr also a base to scavenge liberated acid.^[179] Thus, equal volumes of DBU as non-nucleophilic

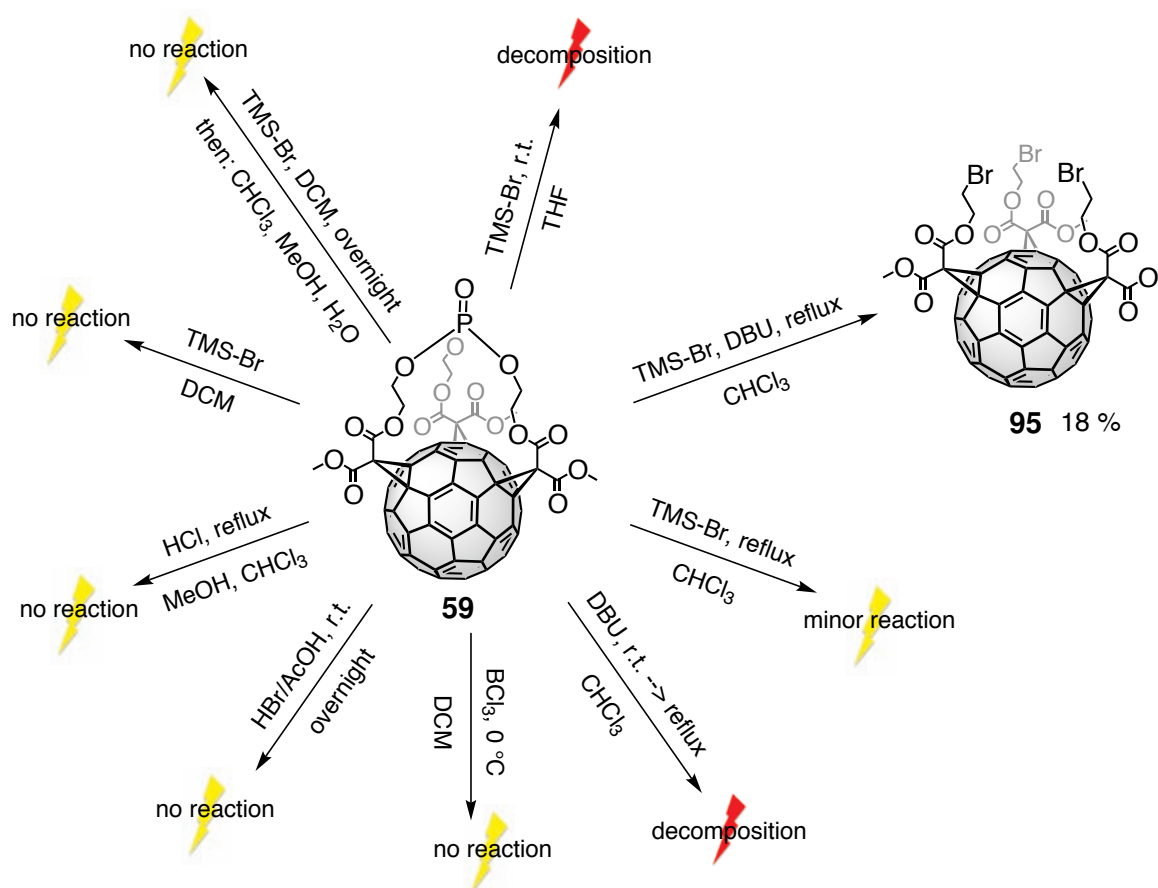


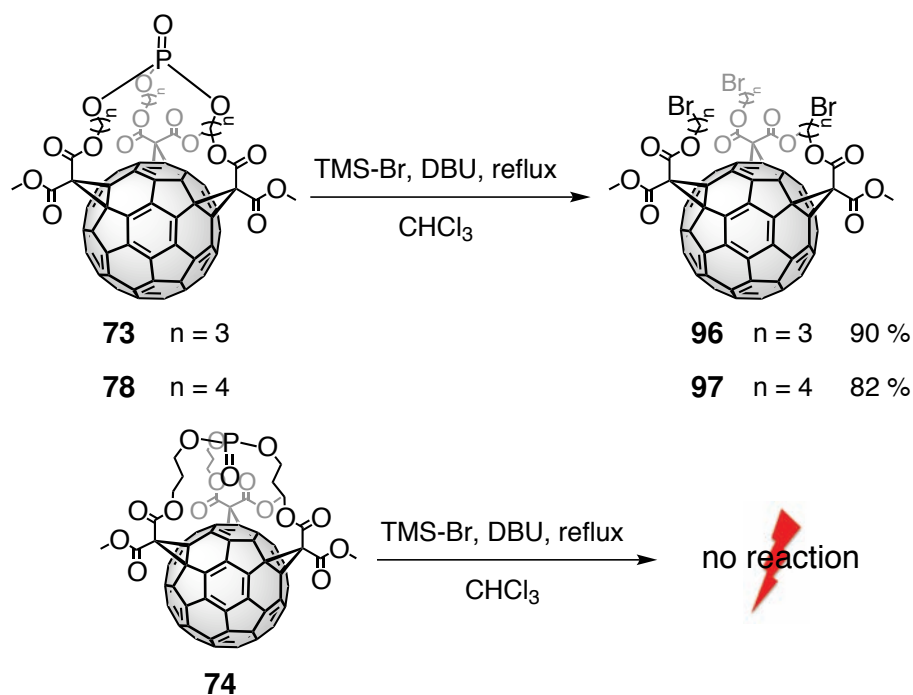
Figure 3.16: Overview of the reaction conditions that were tested to remove the phosphate group of C_{60} -phosphate trisadducts. In the end, phosphate **59** was converted to trisbromide **95**.

base and TMSBr were used and finally lead to a clean reaction of the C₆₀-phosphate. The reaction was conducted in refluxing CHCl₃ with an excess of reagents. It was complete after one night, which was observed by TLC (DCM : THF = 95 : 5), where a new red spot, substantially less polar than the reactant (R_{f, Br} = 1; R_{f, P=O} = 0.06) emerged. After purification of the product it was determined to be the trisbromo derivative **95** by the help of MS- and NMR-data. This molecule was already synthesized by Beuerle (in 77 % from **38**) in a different approach from benzene templated trisadducts and all spectra were in agreement with those from the literature compound.^[141] Additional experiments showed, that neither TMSBr, nor DBU alone resulted in a reaction. With TMSBr alone, no reaction occurred at all. With DBU alone, complete decomposition of the reactant was observed after two hours. Additionally, it is interesting to note, that some of the deprotection attempts failed without destroying the C₆₀-phosphate, which might be interesting for orthogonal functionalization strategies. Thus, *t*-butyl-esters (with formic acid), benzylic methoxy-groups (with HBr/AcOH) or benzylic ethers from a benzene templated trisadduct (with BCl₃) can be removed or transformed without affecting the phosphate moiety. Further experiments will have to show, how to effectively use the bromide-moiety for the coupling to other functional entities (page 101).

Deprotection of C₆₀-phosphate-trisadducts with TMSBr and DBU in refluxing CHCl₃ was a cornerstone in the strategy to C₆₀-based building blocks with a defined addition pattern and relative geometry of the addends. Thus, the phosphate-malonates were not only valuable for templating the formation of *e,e,e*-trisadducts but possibly allowed the incorporation of this geometry in more complex assemblies. Functional materials with well defined arrangement of components would be accessible, if the bromide moiety could be used for further functionalization.

3.4.2 Synthesis of a Homologous Series of *e,e,e*-Trisbromides

The reaction conditions established for the ethyl spacer derivative **59** were subsequently applied to the higher homologues. The *n*-propyl- and *n*-butyl-derivatives **73** and **78** were subjected to the same reaction conditions and the corresponding trisbromides **96** and **97** were obtained in 90 % and 82 % yield, respectively (Scheme 3.22). The reaction times decreased with increasing chain length (Table 3.5) from one night (ethyl **59**) over 2.5 hours (*n*-propyl **73**) to 1.5 hours (*n*-butyl **78**). This could be ascribed to a better accessibility and more vibrational freedom of the phosphate moiety with longer spacers. The shorter reaction times were probably also the reason for the higher yields of **96** and **97**, because decomposition was reduced.



Scheme 3.22: The C_{60} -trisbromides **96** & **97** were readily obtained from the corresponding P_{out} -precursors. The P_{in} -isomer **74** did not react at all.

Another interesting aspect of the C_{60} -phosphates in terms of reactivity was the fact, that only the P_{out} -isomers reacted. The P_{in} -propyl derivative **74** was used as a test system and did not react even after one night, although the P_{out} -isomer reacted completely within 2.5 hours. Additional amounts of reagents also did not change this fact and the reactant was recovered

Table 3.5: The reaction times for the removal of the phosphate template decrease with increasing chain length. reaction conditions: TMSBr, DBU, CHCl_3 , reflux.

spacer-length	P -geometry	compound no.	reaction time	yield
C2	P_{out}	59	overnight	18%
C3	P_{out}	73	2.5 h	90%
	P_{in}	74	—	—
C4	P_{out}	78	1.5 h	82%
C5	P_{out}	81 & 82	1 h	43% & 26%
C6	P_{out}	84 & 85	45 min	33% & 31%

unchanged after this treatment. The phosphate group of the P_{in} -isomer is well protected by the alkyl chains and the fullerene backbone and hidden within the cavity. This is nicely illustrated by the space-filling representation of the X-ray structures of **74** and **73** (Figure 3.17).

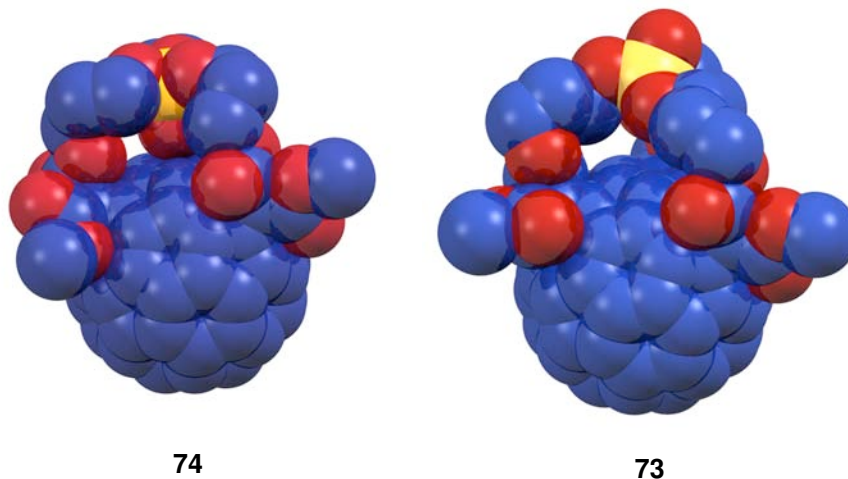


Figure 3.17: The space-filling representations of the X-ray crystal structures of **74** (left) and **73** (right) illustrate the protection of the internal P=O-group.

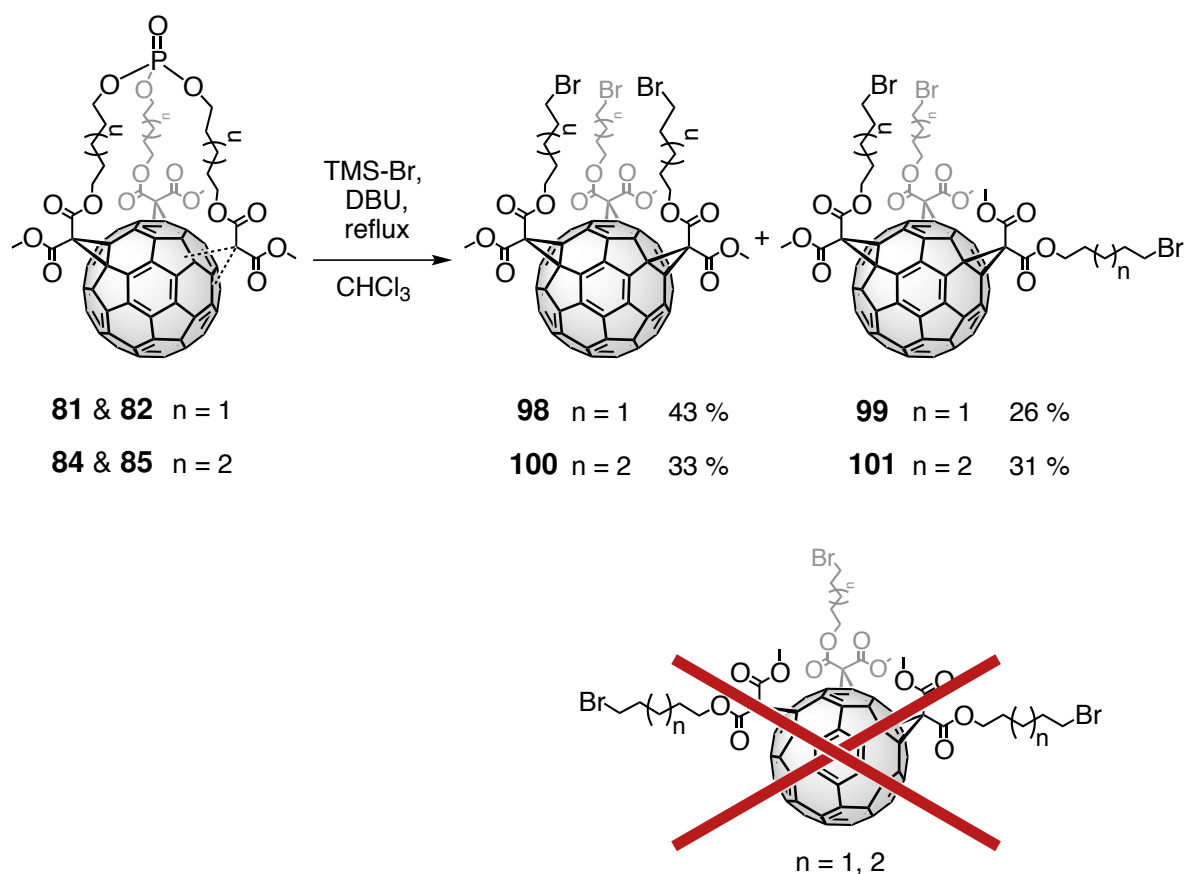
Purification of the trisbromides was accomplished by column chromatography with DCM as eluent. Furthermore, the brown impurities that were hard to remove on the phosphate stage were removed easily on the bromide stage. This implicated that the phosphate reactant did not have to be entirely pure, as the deprotection served as a purification step. This accelerated the overall synthesis of the trisbromides.

The spectral data of all new trisbromides were according to expectations. (HiRes)MS- and UV-data confirmed the molecular composition and the unchanged addition pattern of the trisbromides **96** and **97**. No more P-resonance was observed and the ^{13}C -NMR spectra displayed no more ^{13}C - ^{31}P -couplings. Instead the bromide bearing C-atoms resonated at around 30 ppm. The ^1H -NMR spectra displayed no more diastereotopic splittings, which indicated, that the three sidechains could move freely. Only the chain-protons closest to the malonate showed small splitting. They were probably too close to the fullerene surface and were stronger influenced by it. The protons in neighborhood to the bromide substituent resonated as the expected triplet at around 3.4 ppm.

The *n*-pentyl- and *n*-hexyl- P_{out} -phosphates **81**, **82**, **84** and **85** were not obtained as pure compounds, as mentioned above (page 70). At the phosphate stage, the nature of the impu-

rity was unclear and it could not be removed. As mentioned above, the deprotection served as a kind of purification, which was subsequently attempted with the *n*-pentyl- and *n*-hexyl-phosphate mixtures. The reaction times decreased further (Table 3.5), as already observed for the *n*-propyl- and *n*-butyl-derivatives **73** and **78**. Interestingly, the reaction yielded two *e,e,e*-products, as indicated by TLC (silica; DCM). They were isolated in similar amounts (*n*-pentyl-spacer: 43%, 26%; *n*-hexyl-spacer: 33%, 31%; Scheme 3.23). As a matter of fact, they could be easily separated by column chromatography (silica; toluene : DCM = 1:1). Their structures were subsequently determined by spectroscopy and hence also the nature of the precursor mixture.

The less polar compounds turned out to be the C_3 -symmetrical trisadducts **98** and **100**, which corresponded to the other bromides of the series. Their spectra were in perfect analogy to



Scheme 3.23: The *n*-pentyl- and *n*-hexyl-phosphates **81**, **82**, **84** & **85** were not obtained pure, but turned out to be mixtures of *out,out,out*- and *out,out,in*-isomers when converted to trisbromides. These were readily separated and it was excluded that the *out,in,in*-configuration was formed.

them. The more polar compounds, however, had slightly more complicated spectra that helped to deduce what had happened during the threefold cyclopropanation. The $^1\text{H-NMR}$ spectra (Figure 3.18 for the hexyl derivative) displayed a second set of resonances for H1 and H5, with a ratio of 2:1, while the other signals showed no major changes. The spectrum was interpreted to resemble one misoriented malonate entity. During threefold cyclopropanation it was not attached with relative *out*- but with relative *in*-geometry. The protons closest to the fullerene core (H1 and H5) were thus distinguishable, depending on their orientation, while the other protons were far enough away from the influence of the fullerene. Chemical intuition prompted to assume, that the unsymmetrical isomer was the *out, out, in*-isomer, because the isomer with *out, in, in*-configuration would have been too strained in case of the closed phosphate structure. This was underlined by semi-empirical calculations on the PM6-level for the pentyl derivative.^[186, 187] Geometry optimization of the symmetrical phosphate **98** yielded a heat of formation of $22.48 \text{ kcal mol}^{-1}$. The *out, out, in*-isomer **99** had a heat of formation of $24.91 \text{ kcal mol}^{-1}$ and the *out, in, in*-isomer of $36.00 \text{ kcal mol}^{-1}$. Thus, an *e, e, e*-trisadduct with

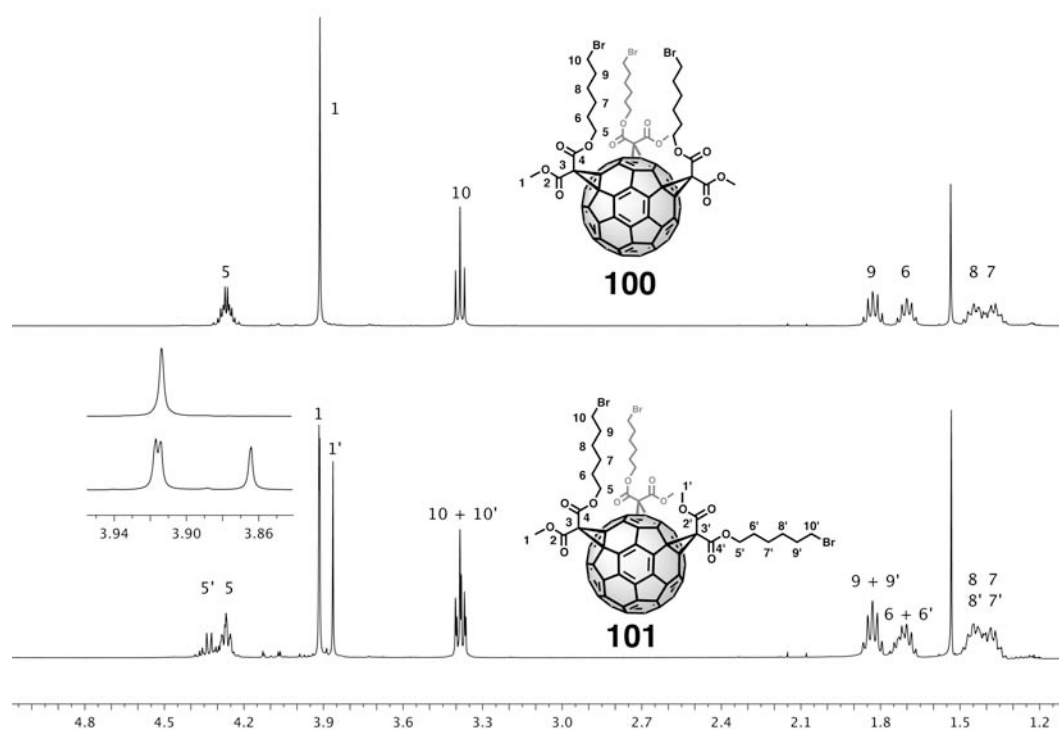


Figure 3.18: The more polar trisubstituted isomer (in case of *n*-pentyl and *n*-hexyl spacers) had an unsymmetrical configuration (bottom), as can be seen in the $^1\text{H-NMR}$ -spectrum (here for *n*-hexyl-derivatives; 400 MHz; CDCl_3 ; r.t.). The position of the methyl ester signals and the multiplets of H5 confirmed the assignment of the *out, out, in*-geometry.

two twisted malonate groups was very unlikely to be formed, because it is too strained. This assignment was further supported by a closer look at the $^1\text{H-NMR}$ signals of the methyl esters of the trisbromides (inset in figure 3.18 for the hexyl derivatives **100** and **101**). As already mentioned there were two signals with a ratio of 2:1 for the unsymmetrical trisbromides **99** and **101**. The signal with double intensity was further split into two signals and resonated at the same position as the methyl esters of the symmetrical trisbromides **98** and **100**. This was clear evidence that two of the methyl esters are pointing outwards, as in the symmetrical case. Hence, the unsymmetrical trisadducts had to have the *out,out,in*-configuration. The pentyl- and hexyl-phosphate malonates **71** and **72** were flexible enough to allow one malonate group to be twisted and to form another isomer. The pentyl spacer was more rigid and a little more selective for the symmetrical isomer, as demonstrated by the yields. In the end the entire homologous series of C_{60} -*e,e,e*-trisbromides from ethyl- to hexyl-spacers was isolated. As it was already mentioned for the ethyl spacers bromide **95**, they could be possibly used as building blocks for architectures with a defined geometry (examples can be found from page 100 on or in the literature^[141, 142]). In that case, the different spacer length will allow the fine-tuning of properties and the unsymmetrical trisbromides **99** and **101** would allow even more sophisticated arrangements.

3.5 Extension Towards Hexakisadducts

3.5.1 Hexakisadducts with Mixed Templates

C_{60} -*e,e,e*-trisadducts could be considered as incomplete part or precursor of a highly symmetric hexakisadduct with octahedral addition pattern (Figure 3.19). In extension of the presented strategy, the addition of a second trismalonate to an *e,e,e*-trisadduct would lead selectively to hexakisadducts.^[142] They serve as versatile structural templates, like *e,e,e*-trisadducts. Shape-persistent micelles are only one example for their interesting and unprecedented properties.^[188] The concept of equatorial and polar addend zones is also applicable to hexakisadducts. They possess two addend zones of each kind and each can be functionalized independently, if the trismalonates are properly predesigned.^[142] As the trisbromides, presented above, can, in principle, serve as building blocks for more complex structures, the formation of the corresponding hexakisadducts was targeted in the next step.

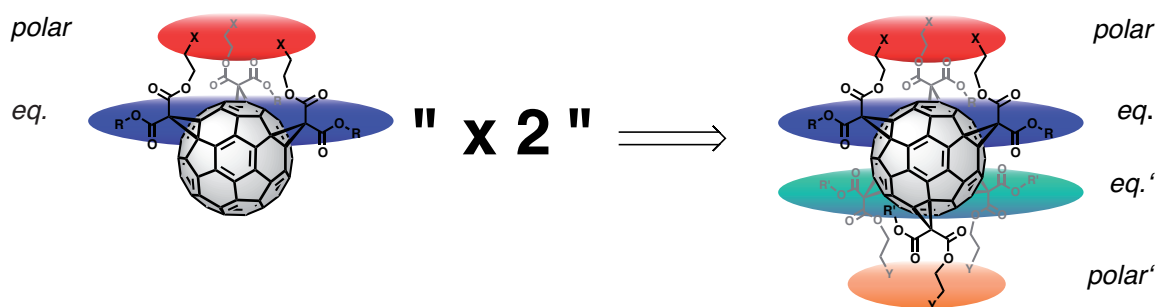
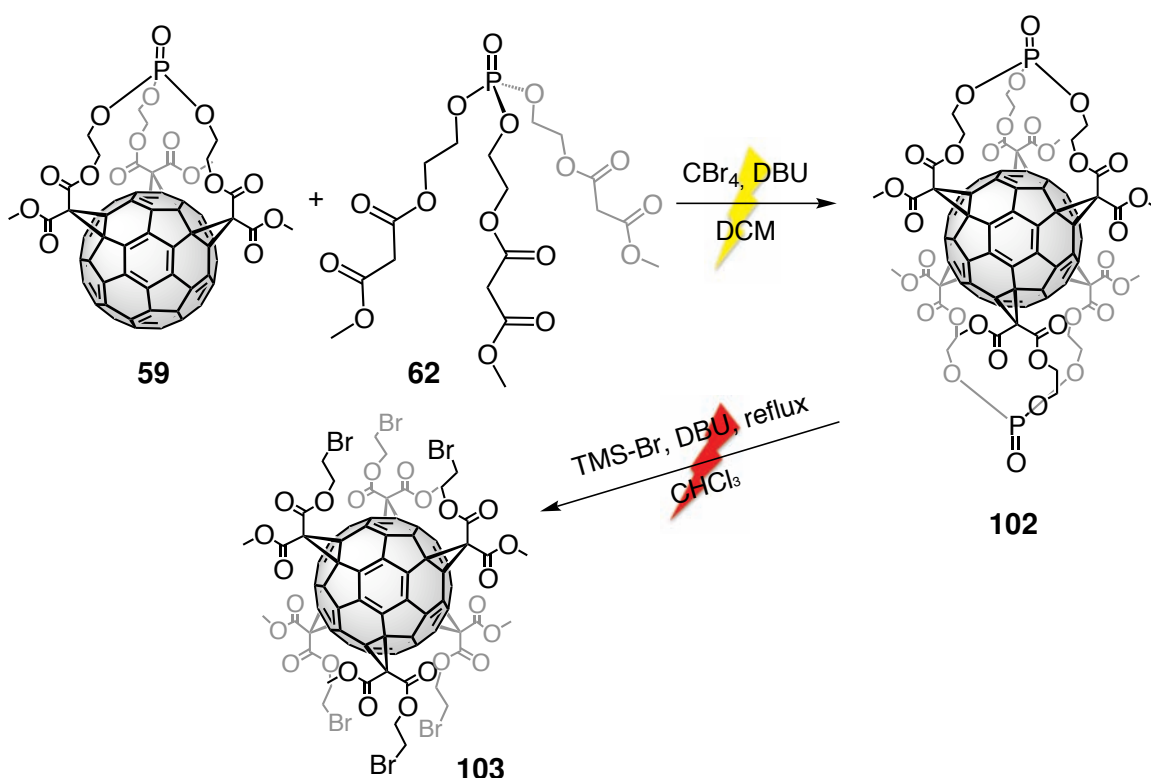


Figure 3.19: C_{60} -*e,e,e*-trisadducts can be considered as half-part of an octahedrally substituted hexakisadduct. The concept of polar (*polar*) and equatorial (*eq.*) addend zones can be applied in the same way.

The first goal was to synthesize symmetrical hexakisadduct **102**, derived from ethyl-spacer phosphate trismalonate **62** as proof of concept. The corresponding C_{60} -trisadduct **59** was reacted with trismalonate **62** in dry DCM. The use of iodine as halogenation reagent was attempted, but yielded no product at all. The fullerene sphere of *e,e,e*-trisadducts has probably already lost enough strain, so that iodomalonates are not reactive enough for a successful functionalization. As in most cases in literature, CBr_4 was the better choice for hexakisadduct formation and yielded the target compound. However, the product was not isolated in pure form. MALDI-TOF and HiRes-ESI-MS measurements confirmed the formation of **102**, but the 1H -NMR- as well as the ^{31}P -NMR-spectra showed several impurities next to the product

signals. The C₆₀-phosphate maybe is not stable enough towards the basic conditions, which was already shown during the deprotection attempts towards the trisbromides (Figure 3.16 on page 80). Treatment of C₆₀-phosphate **59** with DBU in CHCl₃ solution lead to a quick decomposition of the fullerene, which probably also happened, at least partially, in this case. The sideproducts were inseparable from the product. A purification attempt by conversion to hexabromide **103** was made due to the good experiences in the trisadduct case (page 83), but it failed in this case. Partial consumption of bisphosphate **102** was observed by TLC (silica; DCM : MeOH = 95 : 5), but no hexabromide **103** was detected, not even by mass spectrometry. Only signals of residual reactant were detected.



Scheme 3.24: The symmetrical bisphosphate hexakisadduct **102** was not obtained in pure form. "Purification" towards hexabromide **103** failed.

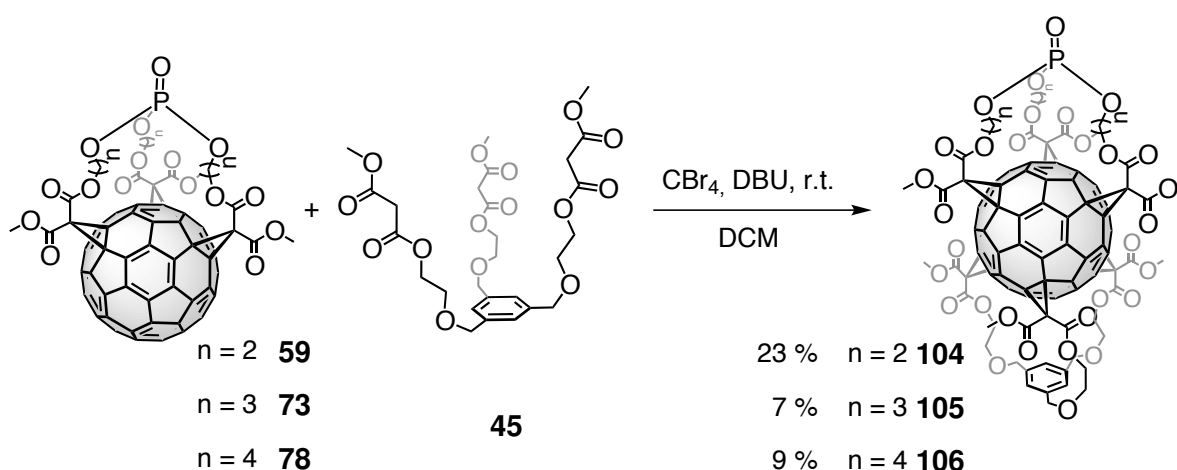
As the symmetrical hexakisadduct was not obtained, the next target was the mixed hexakisadduct **104** (Scheme 3.25). It consisted of one phosphate- and one benzene-templated hemisphere. As it did not consist of two phosphate entities and as its polarity was different from the symmetrical counterpart **102**, it was expected to be easier to purify, partly due to less decomposition during the reaction. Furthermore, it was a much more interesting building block. It has two different polar addend zones, which could probably be deprotected inde-

pendently. TMSBr and DBU should not cleave the benzylic ethers and BCl_3 was shown not to attack the phosphate moiety (page 80). Thus, the hexakisadducts could be orthogonally deprotected and functionalized and this building block would provide easy access to a wide variety of structurally diverse molecules.

The synthesis was attempted, starting from phosphate- **59** and benzene-templated trisadduct **38** and by applying either iodine or CBr_4 as halogenation reagent. The only successful combination, that lead to substantial product amounts was cyclopropanation of phosphate trisadduct **59** (1 eq.) with CBr_4 (9 eq.). They were dissolved together with benzene trismalonate **45** (1.5 eq.) in DCM and a DBU-solution (9 eq.) was added dropwise. After stirring overnight, no more reactant was observed and the product was isolated by column chromatography. It turned out to be beneficial for purification to use MeOH as the polar component instead of THF. **104** was fully purified by column chromatography by using DCM : MeOH = 98 : 2 as eluent. The mixed hexakisadduct **104** was finally isolated in 23% yield.

The homologous hexakisadducts with *n*-propyl (**105**) and *n*-butyl spacer (**106**) were synthesized by the same strategy (Scheme 3.25) and purified under the same conditions. They were obtained in 7% and 9% yield, respectively. Although the components of this reaction were already strongly preorganized, the yield was rather low. This was attributed to a slight instability of the phosphate moiety under the reaction conditions, as already pointed out above.

All compounds were fully characterized. MALDI-TOF and HiRes-ESI-TOF mass spectrometry confirmed the correct molecular weight and composition. The UV/Vis-spectra (Figure



Scheme 3.25: Mixed hexakisadducts with different polar addend zones were available from the corresponding phosphate trisadducts.

3.20) showed the typical hexakisadduct absorption features with maxima at 244 nm, 273 nm, 281 nm, 315 nm and 334 nm. This is another proof of purity, as even slight impurities from incomplete additions lead to flattening of the shoulders at 315 nm and 334 nm and their disappearance.

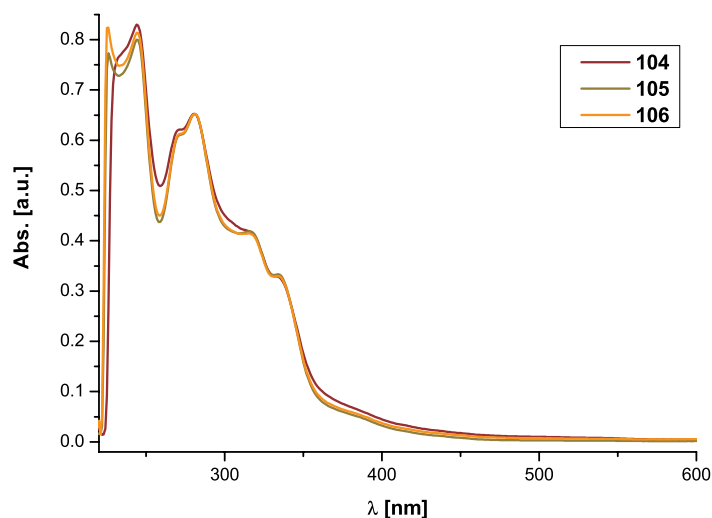


Figure 3.20: UV/Vis-spectra (DCM; r.t.) of mixed hexakisadducts **104**, **105**, **106**. The spectra were normalized to the absorption at 281 nm.

The ^{31}P -nuclei resonated again at slightly negative shifts between -1.62 ppm to -1.20 ppm, which is in the same range as for the trisadducts.

The ^{13}C -NMR-spectra confirmed the correct hexakisaddition pattern furthermore. Two sets of 8 carbon resonances were detected in the fullerene- sp^2 -region, which corresponded to the C_3 -symmetry of the hexakisadducts. The two different sets of addends were also reflected in the four C_{60} - sp^3 - and the four malonate carbonyl-carbon resonances. The other signals matched almost perfectly a superposition of the two corresponding trisadduct spectra, which is illustrated exemplarily in figure 3.21 for **106**. The ^{13}C - ^{31}P -couplings were in the hexakisadducts also well resolved. The only signals that were shifted to a greater extent, in comparison to the trisadduct spectra were those of the central malonate carbon atoms (7.3 ppm to higher field) and to a smaller extent those of the C_{60} - sp^3 -carbon atoms (~ 1 ppm). In summary, only the signals from the fullerene core and the central malonate carbon atoms experienced a shift, which was due to less strain in a higher functionalized fullerene sphere. The carbon atoms' signals of the addends remained unchanged.

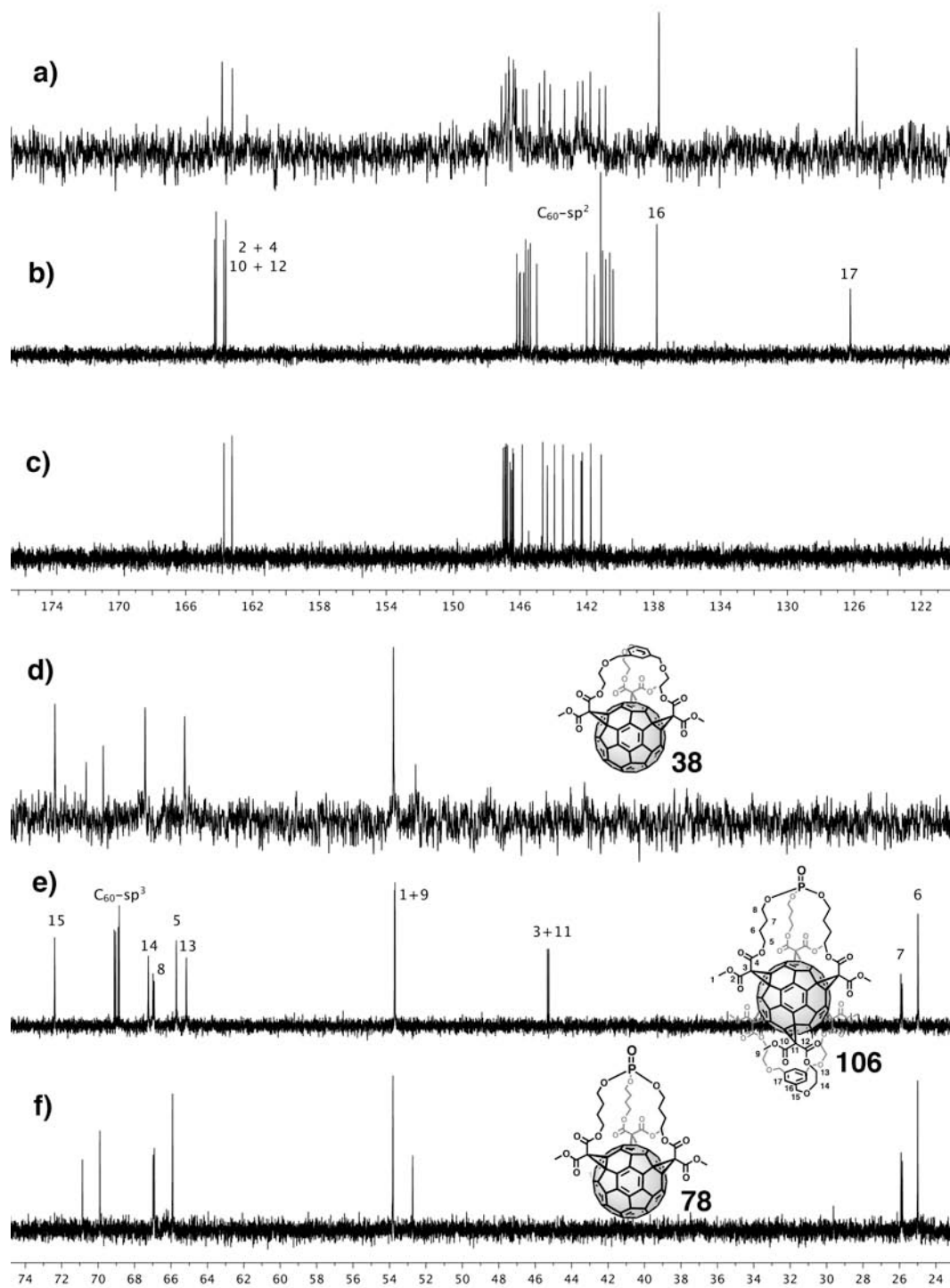


Figure 3.21: The ^{13}C -NMR-spectrum (100 MHz; CDCl_3 ; r.t.) of mixed hexakisadduct **106** (b lowfield region and e highfield region) was a superposition of the spectra of the two constituting trisadducts **38** (a and d) and **78** (c and f).

The ^1H -NMR-spectra (Figure 3.22) appeared as superposition of the single trisadduct spectra as well. All diastereotopic splittings of the spacers, from the malonate, as well as from the phosphate side, were retained, although they were sometimes overlaid. Due to a more relaxed fullerene geometry, the signals were generally slightly shifted. Notably, the methyl esters resonated at slightly higher field and thus the diastereotopic splitting patterns of H8 were observed clearer because they were no more entirely overlaid. Although both sets of methyl ester protons resonated at almost the same position, the two singlets were observed.

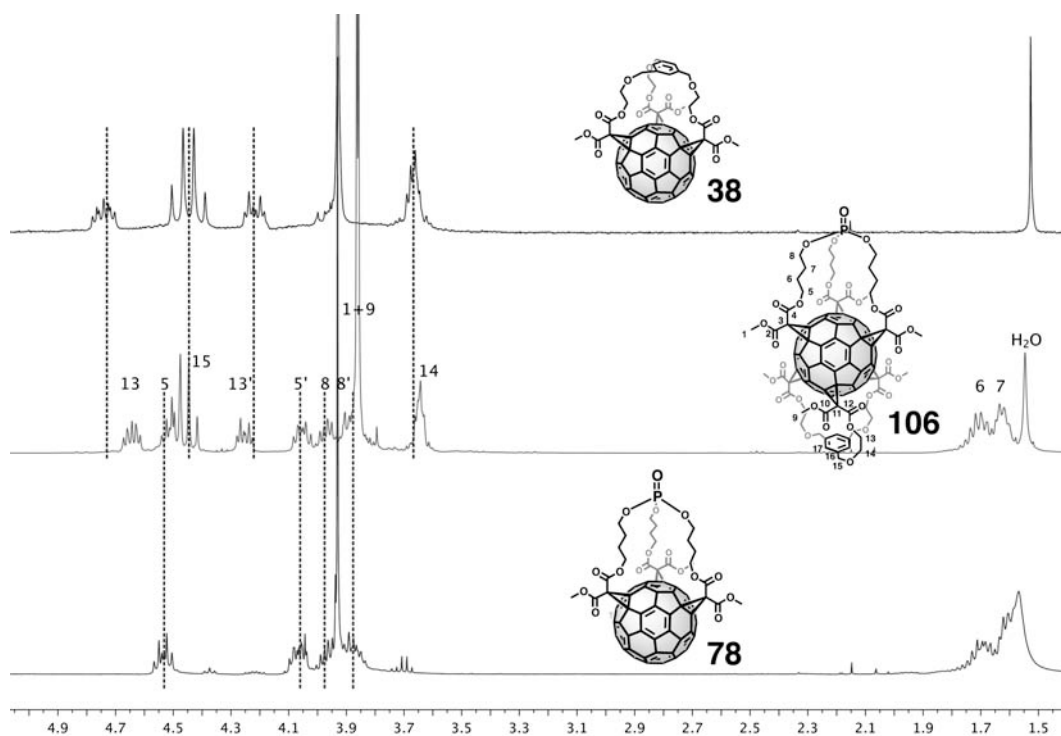


Figure 3.22: The ^1H -NMR-spectrum (400 MHz; CDCl_3 ; r.t.) of the mixed hexakisadduct **106** (middle) is a superposition of the spectra of the two constituting trisadducts **38** (top) and **78** (bottom).

3.5.2 Hexakisadduct Building Blocks

As it was possible to synthesize hexakisadducts with mixed templates, the zone-selective deprotection was demonstrated in the next step (Figure 3.23). The accessible hexakisadducts would be valuable building blocks because each pole could be functionalized independently in the presence of the other functionality. Starting from one mixed hexakisadduct a variety of different compounds would be accessible.

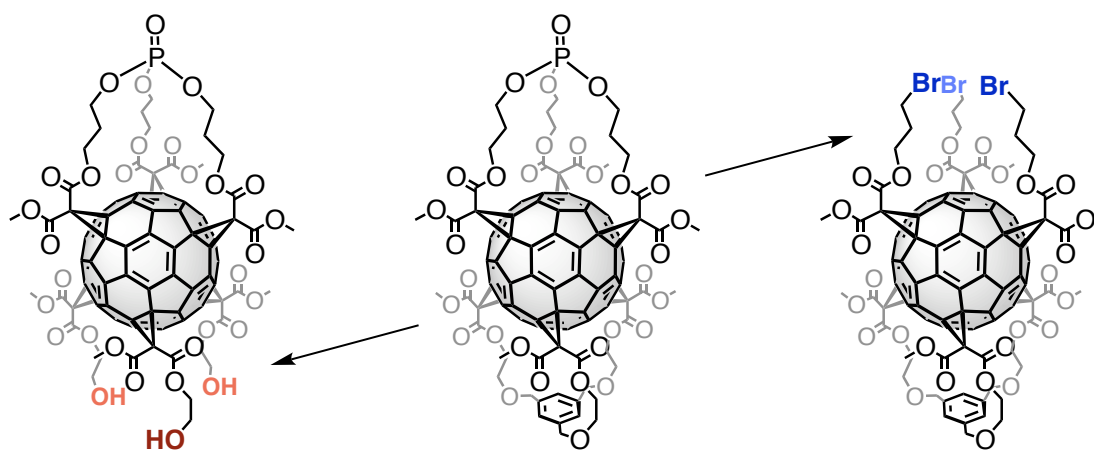
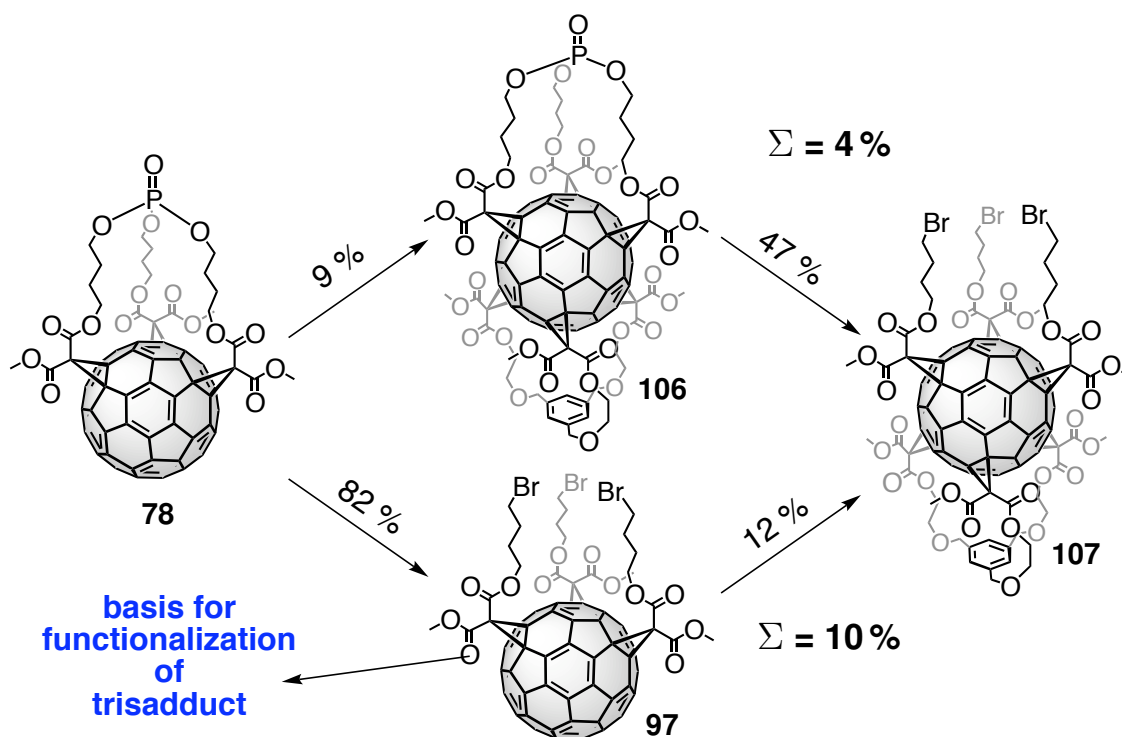


Figure 3.23: By applying the reaction conditions, developed for the corresponding trisadducts, the two polar addend zones of a mixed hexakisadduct should be deprotected independently.

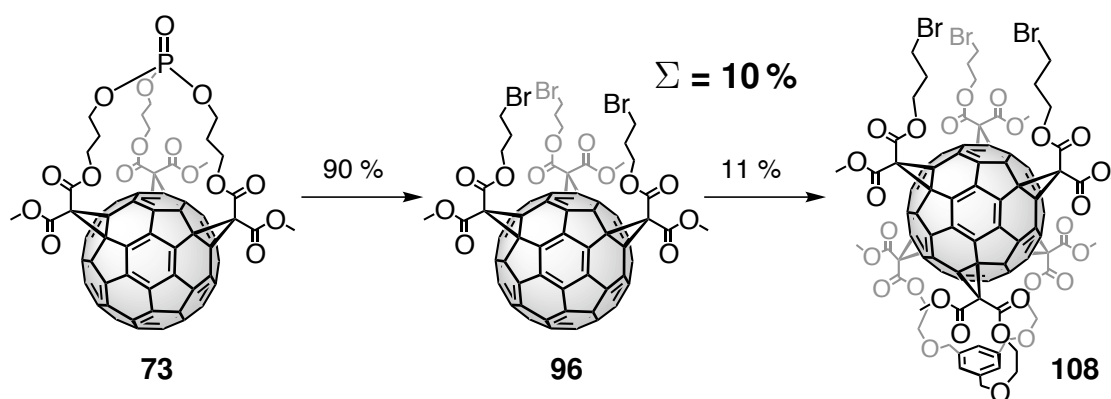
The orthogonal deprotection had to begin with the removal of the phosphate moiety, as the reaction conditions were not compatible with free hydroxyl groups that resulted from the removal of the benzene moiety. On the one hand, TMSBr would silylate the alcohol groups and on the other hand, DBU would deprotonate the alcohol groups and the resulting nucleophiles would attack the fullerene core or the ester groups. Thus, in a first step, it was accomplished to transfer the phosphate deprotection from the trisadducts to the hexakisadducts. As the deprotection proceeded faster with longer alkyl chains, this step was demonstrated with the butyl spacer system (Scheme 3.26 *vide supra*). The reaction conditions and time remained the same as for the trisadduct and the product **107** was obtained in 47% yield. The purification by column chromatography (silica; DCM : THF = 98 : 2) was easier than in case of the phosphate hexakisadducts because it separated better from more polar impurities. The ^1H -, as well as the ^{13}C -NMR-spectra could be again described as superposition of the corresponding trisadduct spectra with all the slight deviations, that were already observed for the phosphate hexakisadducts. The successful deprotection was additionally confirmed by the absence of any ^{31}P -resonance and by the correct molecular ion peak in the mass spec-

tra. The addition pattern was unaffected, which was demonstrated by the unchanged UV/Vis spectrum.

A second synthetic pathway for hexakisadduct **107** could be envisaged and was realized (Scheme 3.26 *vide infra*). Starting with bromo trisadduct **97** the corresponding hexakisadduct was prepared through cyclopropanation with benzene trismalonate **45**. The identity of the products of the two reaction pathways was confirmed by their $^1\text{H-NMR}$ -, MALDI-TOF- and HiRes-ESI-TOF-data. Product **107** was obtained in this reaction in 12% yield. Starting from phosphate trisadduct **78** bromo hexakisadduct **107** was isolated in an overall yield of 10% *via* bromo trisadduct **97** and in 4% overall yield *via* the phosphate hexakisadduct **106**. In general, the synthesis of this kind of compounds should be accomplished *via* the intermediate bromo trisadduct. Apart from the higher yield of this reaction sequence, it had the advantage that the bromo intermediate could be easier obtained in a purer form and the bromo hexakisadduct is easier to purify than the phosphate hexakisadduct. Furthermore the bromo trisadduct might be necessary anyway for functional trisadduct derivatives and this



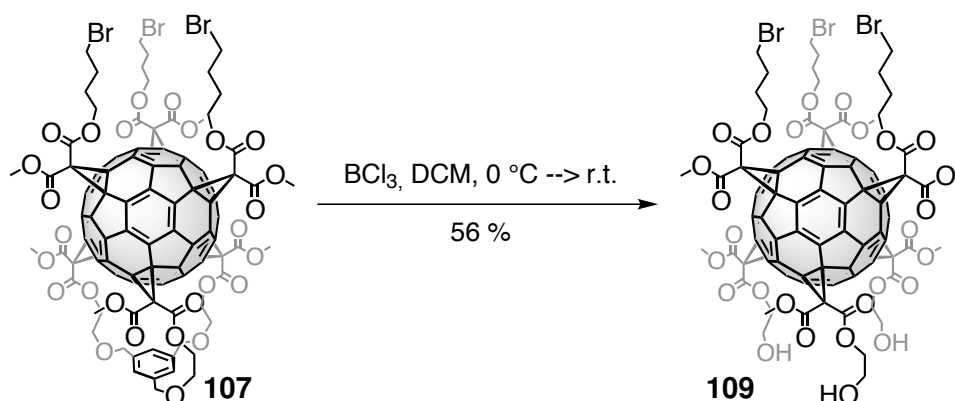
Scheme 3.26: Valuable building block **107** was obtained *via* two different strategies. Intermediate **97** can also serve as a building block for further functionalizations, which makes the bottom strategy, in addition to the higher yield, the preferred synthetic pathway.



Scheme 3.27: Building block **108** was readily obtained by the previously established procedure.

intermediate could thus be used for multiple reactions. To show the generality of this reaction sequence, the corresponding bromo hexakisadduct with a *n*-propyl spacer (**108**) was successfully synthesized by the second reaction sequence (Scheme 3.27). The spectral data contained no surprises and confirmed clearly the product structure. Thus, the properties of functional derivatives of these kinds of hexakisadducts could be fine tuned by the spacer length.

The second step towards a fully deprotected hexakisadduct was subsequently accomplished with cleavage of the benzylic ethers of bromo hexakisadduct **107**. As the amounts of available hexakisadducts of this kind were very limited, this step was only demonstrated with the butyl spacer derivative, but it could surely be applied to derivatives with different spacer length. The deprotection followed the reported procedure for the corresponding trisadducts



Scheme 3.28: After removing the phosphate template, the benzene template was successfully removed from **107** and bifunctional building block **109** was obtained.

and is depicted in scheme 3.28.^[141] A solution of hexakisadduct **107** in dry DCM was cooled to 0 °C and a solution of BCl₃ was added under vigorous stirring. After TLC indicated complete conversion, the solution was hydrolyzed and the raw product was purified by column chromatography (silica; DCM : MeOH = 95 : 5). Product **109** was obtained in 56 % yield.

The mass spectral data confirmed the correct composition of the compound and the NMR-spectra showed the same characteristics as for the other hexakisadducts. They were again a superposition of the single trisadduct spectra with only minor shifts in comparison to the constituents. In case of the ¹H-NMR-spectrum (Figure 3.24) the effects of hydrogen bonding between the hydroxyl-functionalities were also observed, as already reported for trisadduct **39**.^[141] This could be seen by the diastereotopic splitting of the ethyl chain hydrogens which could be explained by a rigid structure, that is held together by hydrogen bonding. In summary, this compound was a valuable building block as it could be functionalized on both poles independently. It is already reported that the alcohol pole can be functionalized with acid chlorides.^[141] Thus the functionalization reaction of this pole is already compatible with the

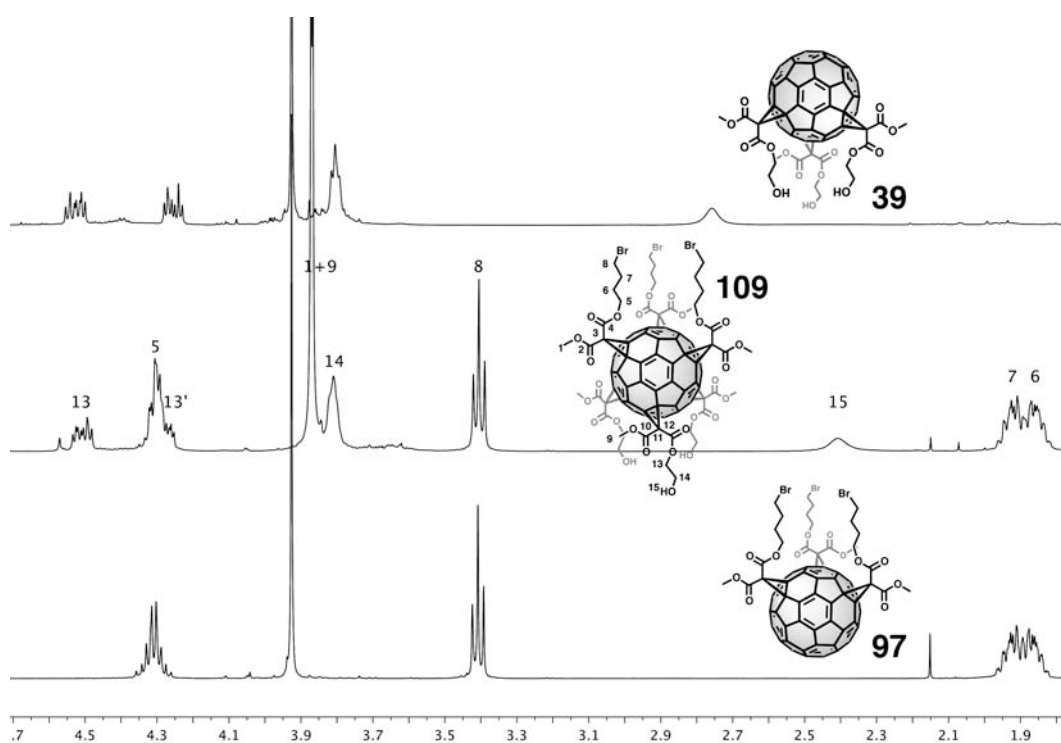
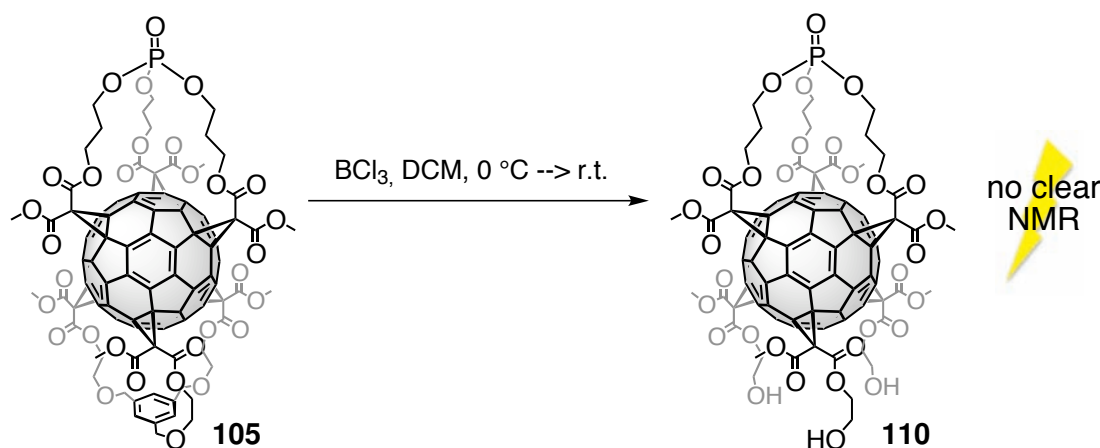


Figure 3.24: The ¹H-NMR-spectrum (400 MHz; CDCl₃; r.t.) of **109** was again a superposition of the spectra of the constituting trisadduct spectra. The hydrogen bonding at the hydroxy-functionalized pole was reflected in the diastereotopic splitting of the otherwise free sidechains.

bromine groups. Functionalization of the bromine pole is described in the next section (page 101) and should be compatible with the hydroxyl moieties. Starting from a single molecule like this kind, a variety of differently functionalized compounds with a well established spatial orientation could then be accessed.

The last combination in this molecular tool box is a hexakisadduct with a phosphate group on one side and hydroxyl functionalities on the other side. It was already demonstrated above (page 80) that selective removal of the benzylic ethers should be possible because the phosphate group is not attacked by BCl_3 . Thus, the same deprotection reaction, as described above (Scheme 3.28), was also applied to **105** (Scheme 3.29). The reaction proceeded well, all the product was consumed and a clear, yellow compound was isolated by column chromatography and automated flash chromatography (silica; DCM : MeOH = 95 : 5). The MALDI-TOF-spectrum showed the expected molecular ion peak at $m/z = 1766$ as well as the $[\text{M} + \text{Na}]^+$ - and $[\text{M} + \text{K}]^+$ -peaks at $m/z = 1789$ and $m/z = 1806$, respectively. HiRes-ESI-TOF mass spectrometry confirmed further on the correct molecular composition with an accuracy of 1.4 ppm for $\text{C}_{99}\text{H}_{51}\text{O}_{31}\text{PNa}$. The ^1H -NMR spectrum, however, gave only hints to a successful hexakisadduct formation. The spectral pattern corresponded to a 1:1 mixture of the constituting trisadducts **73** and **39** but the integrals did not fit. A better resolved spectrum could not be obtained due to the limited amounts of the compound. This made it also impossible to record a ^{13}C -NMR spectrum. The limited amounts of the compound (0.6 mg) resulted from the small starting amount (6 mg) and the repetitive chromatographic workup.



Scheme 3.29: Undoubtful proof for the formation of hexakisadduct **110** was not obtained.

3.6 Further Functionalization of C₆₀-e,e,e-Trisbromides

3.6.1 Transformation to Azides

The C₆₀-e,e,e-trisbromides and C₆₀-trisbromide hexakisadducts that were presented in the sections above had a well defined arrangement of bromide groups. A wide variety of molecules were available (Figure 3.25) with varying distance to the fullerene core and with varying relative orientation. Compounds with different moieties on the opposite pole, including coupling points for other entities were also available. However, to exploit this preorganization for the creation of building blocks, the bromide groups had to be transformed into another entity that allowed the connection to functional units. Benzene templated trisadducts like **39** possessed hydroxyl groups after appropriate removal of the template and further functionalization was

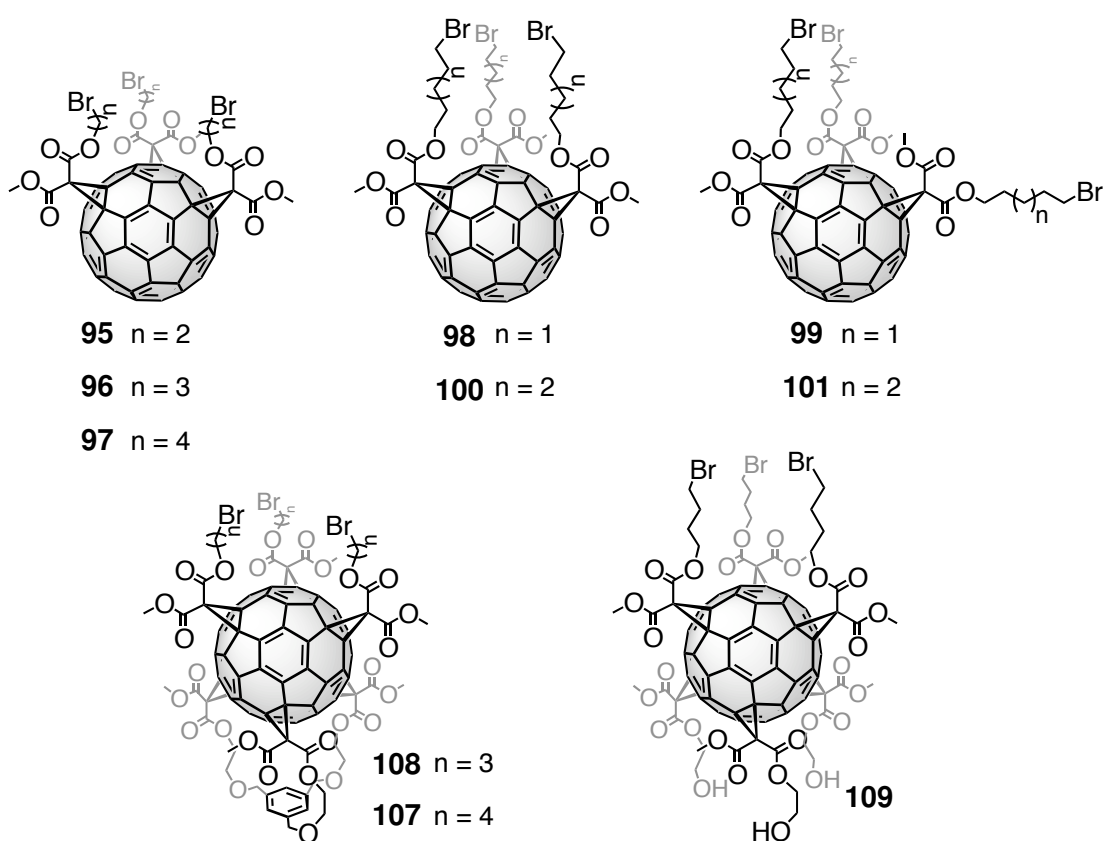


Figure 3.25: Overview of the different types of synthesized bromides. The building blocks offer the possibility to generate functional materials with varying distance and orientation of appended entities and the introduction of a second series of functional entities on the opposite pole.

straightforwardly accomplished by acid chloride coupling.^[141] Esterification is a very versatile and mild reaction, and the coupling counterpart has to bear only an acide group. Bromide groups on the other hand are not as direct coupling points as hydroxyl groups. They can be directly transformed only into a limited number of other functional groups but not coupled to other moieties, at least not under mild conditions that are compatible with the fullerene core. Bromide groups in the equatorial addend zone were e.g. transformed into pyridinium groups, thus generating water soluble fullerene derivatives, but this type of reaction cannot be considered to be very variable.^[141] A substitution of bromide groups through hydroxyl groups seemed also not feasible as the necessary hydroxide ions are too nucleophilic and would attack the fullerene framework. Thus, soft nucleophiles would have to be applied for the transformation of the bromide group into a coupling point for other entities.

The HUISGEN Cu(I)-catalyzed 1,3-dipolar cycloaddition between azides and alkynes (CuAAC), is a very versatile and functional group tolerant reaction and the prime example of a CLICK-reaction.^[189] Thus, it would be the ideal choice for the synthesis of functional derivatives of the preorganized *e,e,e*-trisadducts. Therefore the bromides had to be converted either to acetylenes or to azides. As a substitution reaction with anionic acetylide fragments usually requires hard nucleophiles this option was not investigated. On the other hand, the azide anion is probably the ideal choice, as it is a good, but also soft nucleophile that would only substitute the bromide group and not attack the fullerene. CLICK-chemistry with fullerenes has already been extensively explored and established by Nierengarten and coworkers with fullerenes bearing either terminal alkynes or azides (Figure 3.26 for illustration).^[144, 190] They

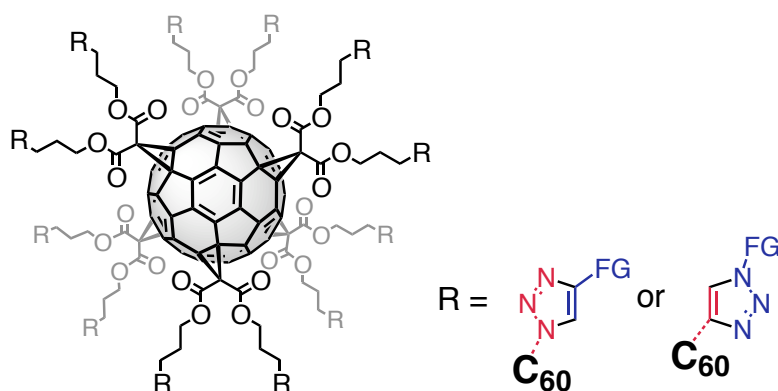


Figure 3.26: "Clicked" hexakisadducts, that were developed by Nierengarten and coworkers. The malonates were initially functionalized either with alkynes or azides, but had to be symmetric to obtain single products. FG = added functional group.

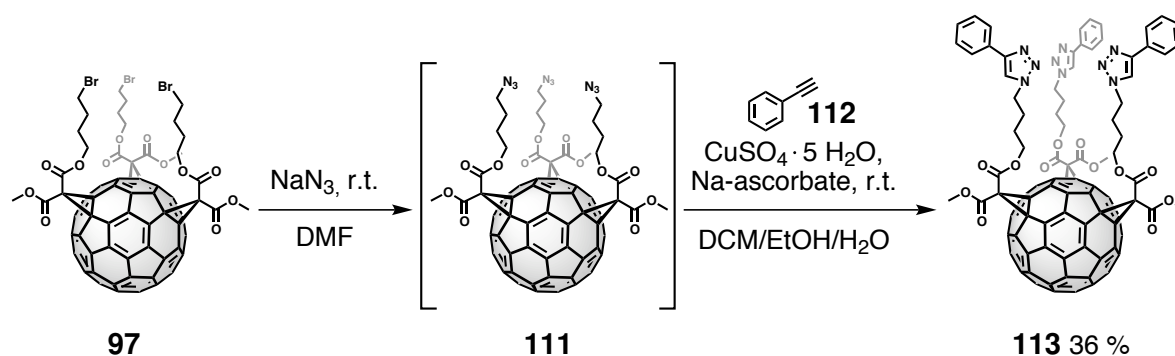
employed symmetrical malonates already bearing the desired acetylenes or azides for the synthesis of hexakisadducts as a first step. A distinction between the equatorial and the polar addend zone was not possible by this approach and thus, symmetrical malonates had to be used to obtain a single product. The corresponding hexakisadducts were variable building blocks because they could be successfully "clicked" with a variety of substrates in a second step.

The trisbromides, that were described above, would grant access to more sophisticated structures. The equatorial and the polar addend zone were distinguishable and the influence of the position of the addends could in principle be investigated. Additionally, each addend zone could bear different functionalities. However, the substitution reaction with sodium azide had to be tested first. The butyl derivative **97** was chosen as a test system as it was the easiest to access in terms of yield and reaction times. In a first attempt a substitution in THF with excess of sodium azide and catalytic amounts of 18-crown-6 was attempted, but the concentration of azide ions in solution was too low and no reaction was observed. Changing the solvent to DMF increased the concentration of sodium azide in solution dramatically without having to employ the expensive crown-ether. The reaction was conducted successfully in this way. Within 2.5 hours complete conversion of the reactant was observed by TLC (silica; DCM). Interestingly even partially substituted intermediates were observed in the meantime. With increasing reaction time, more and more polar spots were observed by TLC until in the end, only the most polar spot remained. In principle, partially substituted trisadducts could probably also be isolated and the corresponding [2:1]-trisadducts might be accessible. After completed reaction and subsequent aqueous workup the solvent was removed under reduced pressure. However, when attempting to dissolve the red solid again after one night, this turned out to be impossible with any type of solvent. The azido fullerene was probably already partially decomposed or polymerized. For a successful conversion the CLICK-reaction would have to follow the isolation of the azides immediately, or is even better attempted *in situ*. In this context, the group of Nierengarten also reported that the azido fullerene is more stable in solution and suggested to use it immediately to minimize losses.^[144]

3.6.2 CLICK-Reaction with Phenylacetylene

This strategy was finally followed and C₆₀-e,e,e-trisazide **111** was not isolated but immediately reacted with an alkyne (Scheme 3.30). For test-purposes phenylacetylene **112** was used and the corresponding adduct **113** was successfully isolated. Therefore two different

strategies for the direct conversion were attempted. Two parallel experiments with 10 mg trisbromide **97** each, were conducted and the azide was synthesized as described above. For reasons of simplicity it was tested in a first experiment, if the catalyst ($\text{CuSO}_4 \cdot 5\text{H}_2\text{O}$ & sodium ascorbate) and phenylacetylene **112** could simply be added to the reaction mixture of trisazide **111** in DMF. The catalyst amounts were chosen, according to the procedures of the Nierengarten group (0.1 eq. $\text{CuSO}_4 \cdot 5\text{H}_2\text{O}$ & 0.3 eq. sodium ascorbate), but an excess of phenylacetylene **112** was used.^[144] After one night, no reaction had occurred and little water was added to the reaction mixture, as sodium ascorbate did not dissolve very well in DMF. There was still no reaction observable and more catalyst, phenylacetylene **112** and water (up to a ratio of $\text{DMF} : \text{H}_2\text{O} = 1 : 1$) were added. In the course of three hours, all trisazide **111** was consumed and after another hour, toluene and water were added for workup. The organic phase was washed with water and the raw product was purified by flash column chromatography (silica; $\text{DCM} : \text{THF} = 95 : 5$). Unfortunately, the product decomposed gradually during evaporation of the solvent in the rotary evaporator. Another chromatography was necessary to remove the decomposition product and subsequently the solvent was carefully removed *in vacuo* without heating the sample. The product contained probably some remnants of DMF or sodium azide in the first place, which degraded the product upon heating.



Scheme 3.30: Trisbromide **97** was converted to the corresponding trisazide **111** and *in situ* clicked with phenylacetylene **112**.

This drawback was circumvented in the second experiment. Water was added to the reaction mixture after complete conversion to trisazide **111** and the product precipitated. It was separated from the solution, now containing the salts and DMF and washed with water. The intermediate was dissolved in a mixture of DCM (7 mL) and ethanol (4 mL) and vigorously stirred. The two catalyst components (same amounts as above) were dissolved separately in water (total of 5 mL) and combined. A firstly yellow, then brownish precipitate formed which

was added to the reaction flask. After stirring overnight, the reactant was completely consumed and a more polar product spot was observed by TLC (silica; DCM : THF = 95 : 5). After aqueous workup, the raw product was purified by flash column chromatography (silica; DCM : THF = 10 : 1) and the solvent was removed *in vacuo* to avoid decomposition. After reprecipitation, product **113** was obtained in 36 % yield as a red powder. Subsequently, a small amount of the product was dissolved in the eluent, which was then removed at a rotary evaporator. No decomposition was observed, which indicated that the interfering compounds were removed sufficiently in this case. For further CLICK-reactions this second strategy was thus followed.

The product was fully characterized by ^1H - and ^{13}C -NMR-spectroscopy, MALDI-TOF- and HiRes-ESI-TOF mass spectrometry and UV- and IR-spectroscopy. The ^1H -NMR spectrum (Figure 3.28 on page 104) of the butyl spacer part of **113** did not change significantly in comparison to trisbromide **97**. Only the protons of the spacer that were previously attached to the bromine atoms were shifted from 3.41 ppm to 4.37 ppm indicating the successful transformation from an alkyl bromide to an alkyl triazole moiety. The triazole proton resonated at 7.75 ppm, which was in agreement with the values from the Nierengarten group.^[144] The additional phenyl ring protons resonated as three multiplets at 7.80 ppm, 7.39 ppm and 7.30 ppm. The ^{13}C -NMR spectrum of **113** showed equal changes in comparison to the reactant. The trisadduct core remained the same, except for the spacer carbon atom, bearing the triazole moiety. It was shifted from 32.8 ppm in trisbromide **97** to 49.6 ppm. The two new triazole carbon atoms resonated at 148.0 ppm and 119.7 ppm, respectively, confirming the successful formation of the triazole ring. The additional phenyl ring yielded four more carbon resonances at 130.6 ppm, 128.9 ppm, 128.2 ppm and 125.8 ppm, respectively, thus proofing the successful adduct formation.

3.6.3 Complexation Attempts with Zn(II)

The CuAAC is not only a versatile conjugation method for the connection of two entities, but the formed 1,4-substituted 1,2,3-triazoles are functional units in their own right. They can be considered, *e.g.* as a new motif in anion recognition, extending the pool of traditional motifs like amines, pyrroles, ureas and amides.^[191] Furthermore, the triazole unit has three different donor sites ($N2$, $N3$, $C5$) for metal coordination, which makes this ligand very versatile (Figure 3.27). Together with the easy access and variation of the appended groups, this has attributed to the rising attention for triazoles as transition metal ligands.^[192] The most

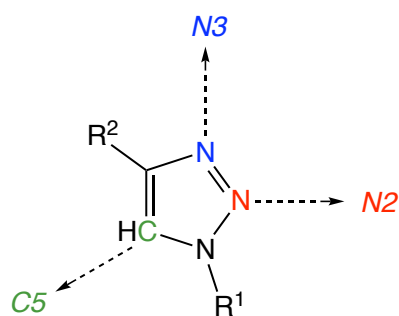
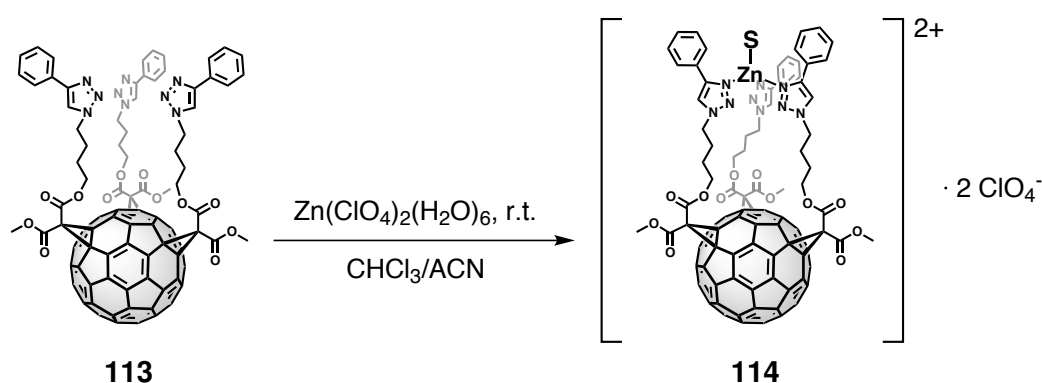


Figure 3.27: The triazole group is a very versatile ligand for metal coordination and contains three different coordination sites.

common coordination mode is *via* N3. An impressive example is a calix[6]arene bearing three triazole units which are capable of coordinating Zn(II) and Cu(I).^[193] A cavitand bearing four triazole groups is also reported in literature. Upon complexation of Cu(I) or Fe(II) these cavitands even become water soluble and the iron compound is capable to perform C–H-oxidations.^[194] The clicked phenyl trisadduct **113** might thus also be a promising candidate for the complexation of metal ions because of the circular arrangement of the triazole units.

Zn(II) was chosen as a first target because the calix[6]arene, prepared by Colasson *et al.*, demonstrated the successful complexation of Zn(II) by three triazole groups in a circular arrangement.^[193] Furthermore Zn(II) is diamagnetic and allows the use of ¹H-NMR-spectroscopy. For complex formation (Scheme 3.31) fullerene ligand **113** was dissolved in equal volumes of CHCl₃ and ACN. Excess Zn(ClO₄)₂(H₂O)₆ was added as the Zn(II)-source and the solution was stirred until the salt had completely dissolved. Complex **114** was precipitated with diethyl ether, centrifuged and the solvent was decanted. The obtained red powder



Scheme 3.31: Several hints were found, that trisadduct **113** was capable to form complexes with Zn(II). S = coordinated solvent or water.

was no more soluble in CHCl_3 , which was a first hint for successful complex formation, because the resulting complex should have been doubly charged and was therefore expected to be no longer soluble in CHCl_3 . More polar solvents like THF, ACN or MeOH were successfully applied to dissolve the complex again and underlined the polar nature of the compound.

Investigations by mass spectrometry gave more proof for the successful formation of complex **114**. In a MALDI-TOF mass spectrometry measurement the complex was detected with one additional perchlorate ion ($m/z([\text{M} + \text{ClO}_4]^+) = 1828$). Only a small proof for the correct molecular composition was found with HiRes-ESI-TOF mass spectrometry. A very small peak was detected at the corresponding m/z -value, but the accuracy and the intensity of the peak were not very convincing.

Further proof for complex formation was obtained from $^1\text{H-NMR}$ experiments. The fullerene ligand **113** was dissolved in equal volumes of CDCl_3 and CD_3CN in an NMR-tube. One equivalent of $\text{Zn}(\text{ClO}_4)_2(\text{H}_2\text{O})_6$ was separately dissolved in the same solvent mixture and added to the NMR tube. After mixing the solutions, the spectrum was recorded (Figure 3.28). Almost

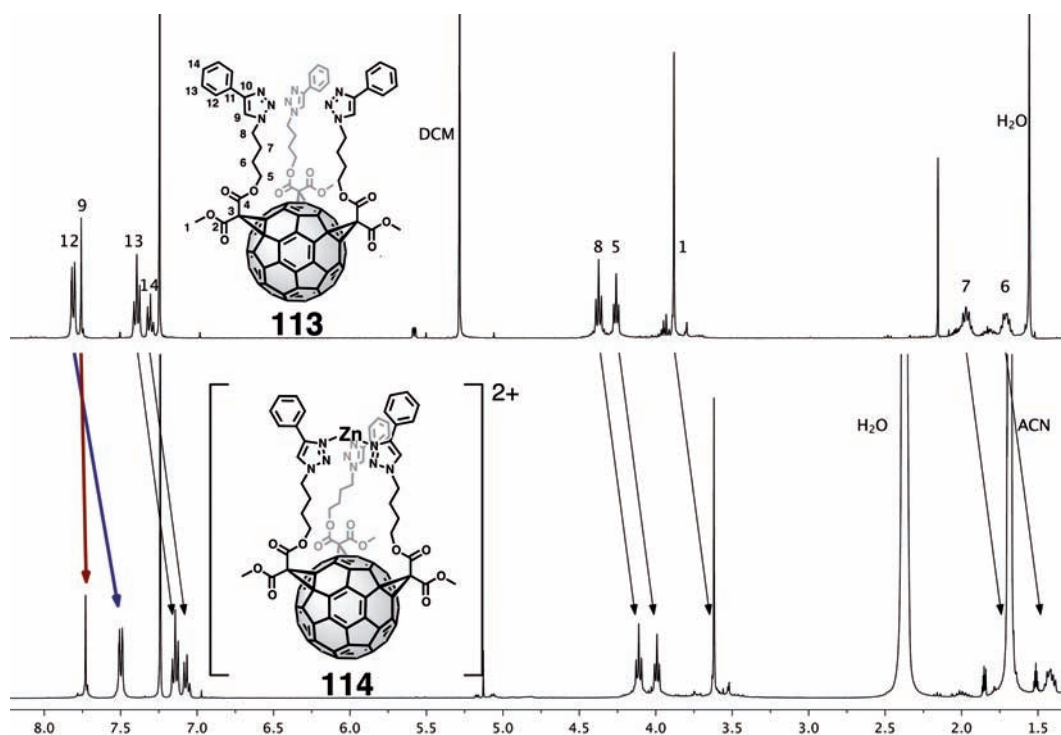


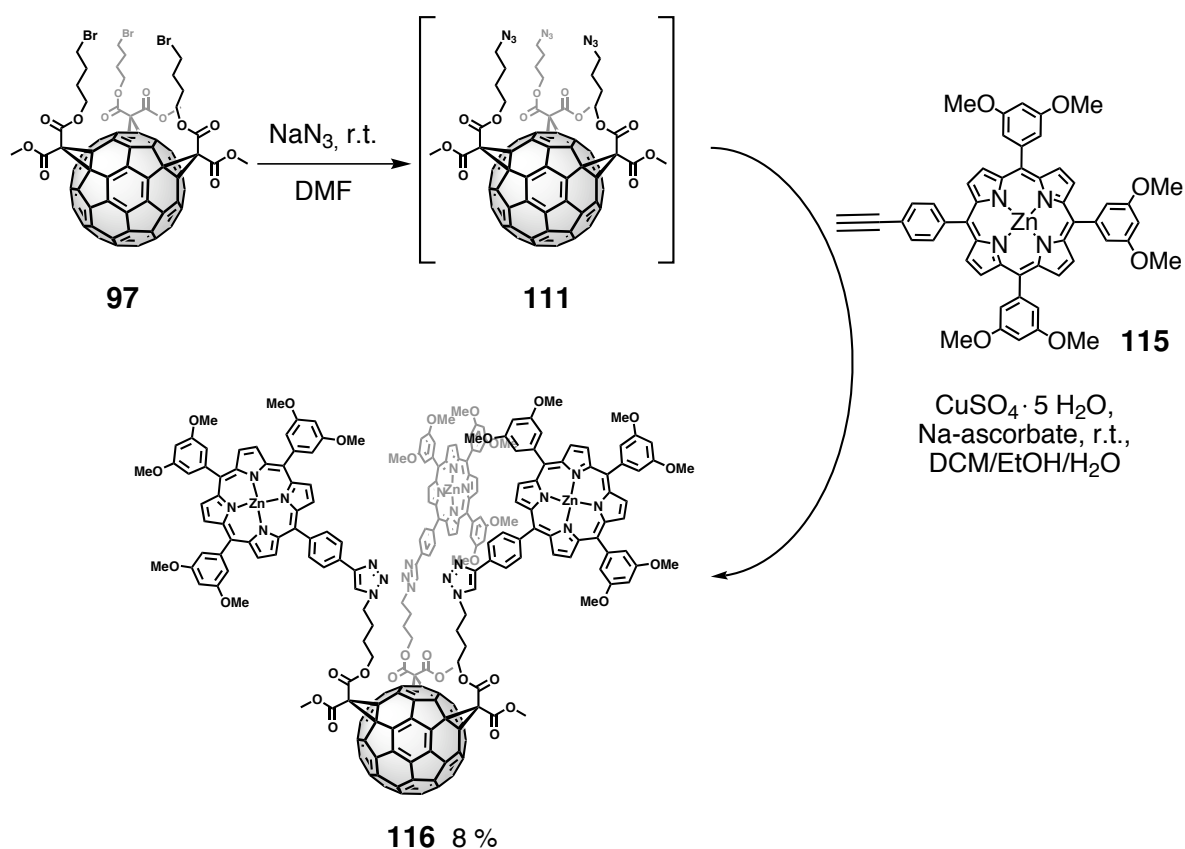
Figure 3.28: The spectral changes in the $^1\text{H-NMR}$ -spectrum of **113** (400 MHz; CDCl_3 (top) or CDCl_3/ACN 1:1 (bottom); r.t.) upon addition of $\text{Zn}(\text{II})$ were partially attributed to the change in solvent (black arrows) and partially to the complexation of the metal ion (colored arrows).

all signals were shifted by 0.26 ppm to higher field in comparison to the ligand spectrum in pure CDCl_3 , which was ascribed to the different character of the NMR-solvents. Only the signals of the triazolyl proton and the two *ortho*-protons of the phenyl ring were exceptions to this behavior. They were shifted by 0.02 ppm and 0.31 ppm to higher field, respectively. The triazolyl proton was now the most downfield shifted signal and no more that of the *ortho*-protons. Thus, the geometry must have been distorted to adapt to the complexed metal ion. On the other hand it was surprising that the signals of the spacer showed no diastereotopic shifts, as it would have been expected for a capped structure. Probably coordination to zinc allowed more flexibility and reversibility of the bonds as it was obviously the case for the covalently bound phosphate group. The coordination ability of triazoles is strongly influenced by the electronic structure of the appended groups and can be fine-tuned by them.^[195, 196] An aromatic substituent, as in **113** could lower the electron density in the triazole ring by delocalization of the electron density over the entire aromatic system.^[193] Thus, coordination was probably rather weak, and the Zn ion could not fix the structure on the NMR time-scale. A substituent, which interrupted the cross-delocalization like benzyl or a more electron rich substituent, like anisyl might have improved the coordination strength of the system.^[193] In summary, these experiments could be considered as a first step towards triazole bearing fullerenes that host metal ions. Due to the limited amount of the available ligand further experiments with different metals were not conducted.

3.6.4 Synthesis of a Fullerene-Trisporphyrin Tetrad

The reaction conditions for a CLICK-reaction starting from C_{60} -trisbromides were established with the test system phenylacetylene. In the next step, a functional trisadduct, bearing three porphyrin substituents was synthesized (Scheme 3.32). Fullerene-porphyrin hybrids are interesting test systems to mimic basic processes of charge separation in nature.^[197] Furthermore charge separation in these conjugates may also be used to power organic photovoltaic cells.^[198] The geometry of the present trisadducts will result in a cup-like geometry of the entire molecule which brings the porphyrin units in close proximity. The cavity might also be able to accept guest molecules and to form supramolecular complexes. Zinc-porphyrin **115** was chosen as coupling counterpart for fullerene **97**. It was previously synthesized in our group and was generously provided in this case by Astrid Herrmann.^[199] The synthesis was conducted as described above with phenylacetylene and an intermediate aqueous workup was applied, as described above (page 101). However, azide **111** did not precipitate upon

addition of water and was extracted with THF and brine, instead. After removal of solvent, trisazide **111** was immediately dissolved in DCM and the CLICK-reaction was performed, as described above. More catalyst was added after one night, as no conversion was observed and after 48 hours, consumption of the reactants was observed. As the reaction was still very slow, THF was added to reduce aggregation of the zinc-porphyrins and after another four hours all reactants were consumed. After aqueous workup the product **116** was finally purified by repetitive column chromatography and obtained in 8% yield. The product was fully characterized by ^1H - and ^{13}C -NMR-spectroscopy, MALDI-TOF- and HiRes-ESI-TOF-mass spectrometry and UV- and IR-spectroscopy.



Scheme 3.32: Tetrad **116** was successfully built up by CLICK-chemistry.

In the ^1H -NMR spectrum of **116** (Figure 3.29), the fullerene part remained again mostly unchanged in comparison to the reactant bromide **97** or the phenyl analogue **113**. The three triazole protons were shifted high field to 7.35 ppm and the additional porphyrin protons were assigned by comparison to the reactant spectrum. The β -pyrrolic protons resonated as two multiplets at 8.92 ppm and 8.80 ppm in a ratio of 3:1, which was in agreement with the

values of the reactant porphyrin **115**. The twelve protons (H12 & H13) of the phenyl rings that connected the triazole and the porphyrin units resonated as two doublets at 7.91 and 7.52 ppm, respectively with a coupling constant of $^3J = 8.1$ Hz. The proton resonances of the other phenyl rings around the porphyrin core appeared as two sets of signals in a ratio of 2:1, which reflected the local symmetry around the porphyrin core. The phenyl ring opposite to the triazole connection possessed only half the protons of the other two phenyl rings. Therefore the *ortho*-protons (H22 & H32) resonated as two doublets at 7.20 and 7.16 ppm, respectively and the *para*-protons (H24 & H34) resonated as two triplets at 6.60 ppm and 6.50 ppm, respectively. The porphyrin MeO-protons resonated approximately at the same position as the methyl ester protons of the malonates and yielded a joint multiplet at 3.72 ppm. There is actually one peak more than there would be expected. However, it is not clear, whether it originates from an impurity or from a hindered rotation of the porphyrins or parts from them. The protons of the butyl-spacer (H8, H7, H6, H5) resonated at the same positions (4.30, 1.69, 1.88, 4.20 ppm) as in phenyl analogue **113**.

The signals in the ^{13}C -NMR spectrum of **116** (Figure 3.30) were subsequently assigned by comparison to the reactant porphyrin and the phenyl analog's spectrum. Only the porphyrin

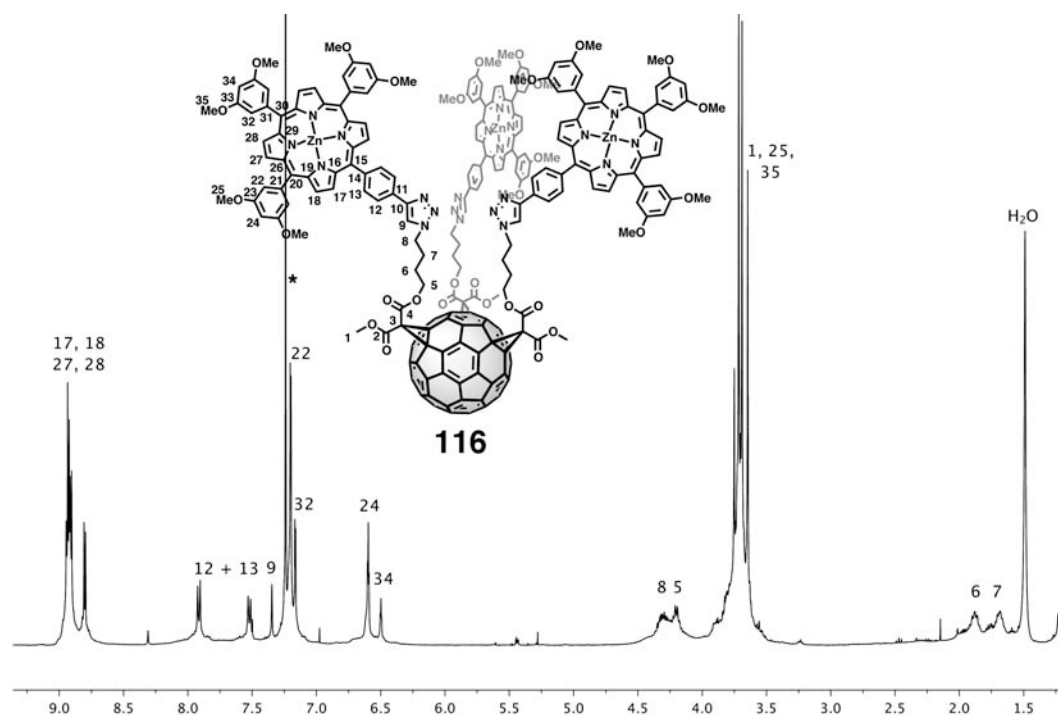


Figure 3.29: ^1H -NMR-spectrum of tetrad **116** (400 MHz; CDCl_3 ; r.t.).

resonances were additionally observed in comparison to the phenyl analog **113**. The other signals remained at the same positions. Hence, only the porphyrin signals are mentioned here. The porphyrin's C-atoms, resonating at lowest field, were those from the phenyl rings, where the methoxy groups were bound (C23 & C33). They yielded two signals at 158.6 and 158.5 ppm for the two types of phenyl rings. The α -pyrrolic carbons gave four signals at around 150.0 ppm and the β -pyrrolic C-atoms yielded two signals at 132.1 ppm and 131.8 ppm. The *ipso*-C-atoms of the methoxy-phenyl rings yielded two signals at 144.7 ppm and 144.6 ppm in between the C_{60} - sp^2 -range. The phenyl ring that was connected to the triazole unit yielded four resonances at 135.0 ppm, 134.8 ppm, 129.2 ppm and 123.6 ppm. The *meso*-C-atoms of the porphyrin resonated at 120.8 ppm, 120.7 ppm and 120.5 ppm in which the signal at 120.8 ppm had double intensity. The *ortho*-carbon atoms of the methoxy-phenyl rings resonated as a single resonance at 113.8 ppm and the *para*-C-atoms at 99.9 ppm. In this case the chemical environment was obviously no more different enough to distinguish between the two types of appended phenyl rings. The last remaining signal of the porphyrin unit was that of the methoxy-groups which resonated as a single signal at 55.5 ppm.

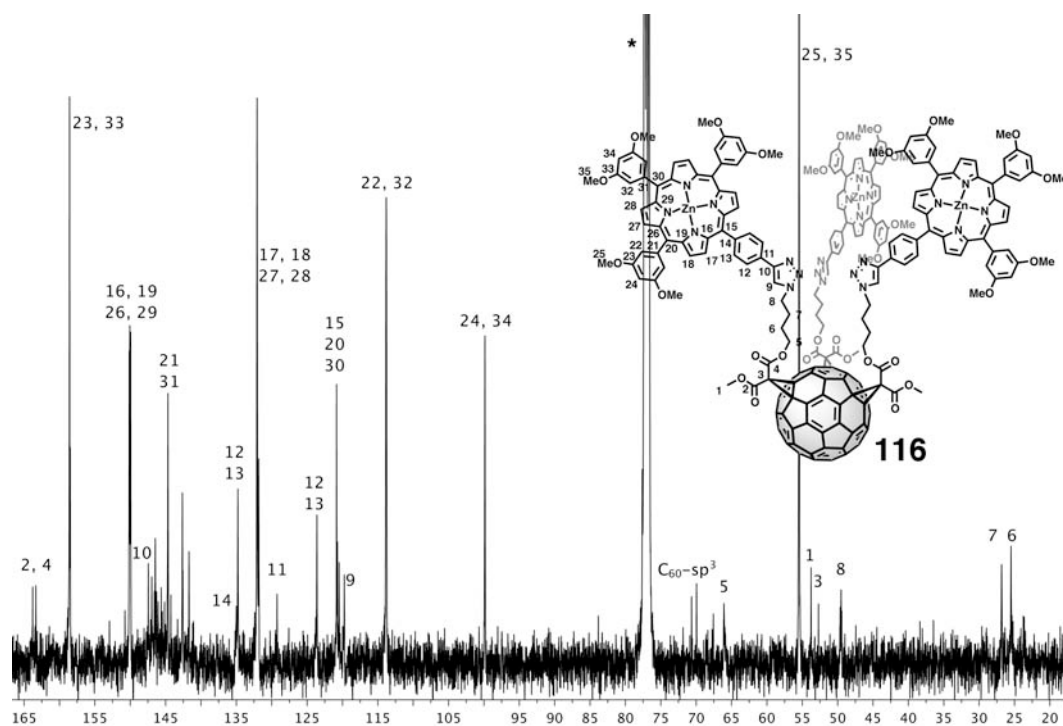


Figure 3.30: ^{13}C -NMR-spectrum of tetrad **116** (100 MHz; CDCl_3 ; r.t.; label for C_{60} - sp^2 C-atoms (18 signals around 140 ppm) omitted for clarity).

The spectra, especially the $^1\text{H-NMR}$ -spectrum, might indicate that the compound might not have been fully purified. However, due to the limited amounts a better quality of the spectra and a more reliable conclusion was not possible.

In MALDI-TOF mass spectrometry the molecular ion peak at $m/z = 4000$ was detected and further confirmed the correct molecular composition. With high-resolution mass spectrometry the molecular composition was confirmed. The signal was detected as the $[\text{M}+2\text{Na}]^{2+}$ cation, instead of the $[\text{M} + \text{Na}]^+$ cation, as for all other compounds. Hence, the m/z -value was found at half mass of the compound at $m/z = 2022.93639$ and differed by only -0.6 ppm from the calculated value.

3.6.5 UV/Vis- and Fluorescence-Studies of the C_{60} -Trisporphyrin-Tetrad

Fullerene-porphyrin-conjugates are well-known model compounds for the basic events of charge separation in photosynthesis and a large number of examples are reported.^[200, 201] Thus, some basic photophysical investigations were conducted with the present C_{60} -trisporphyrin-conjugate **116** to investigate some of its photophysical properties.

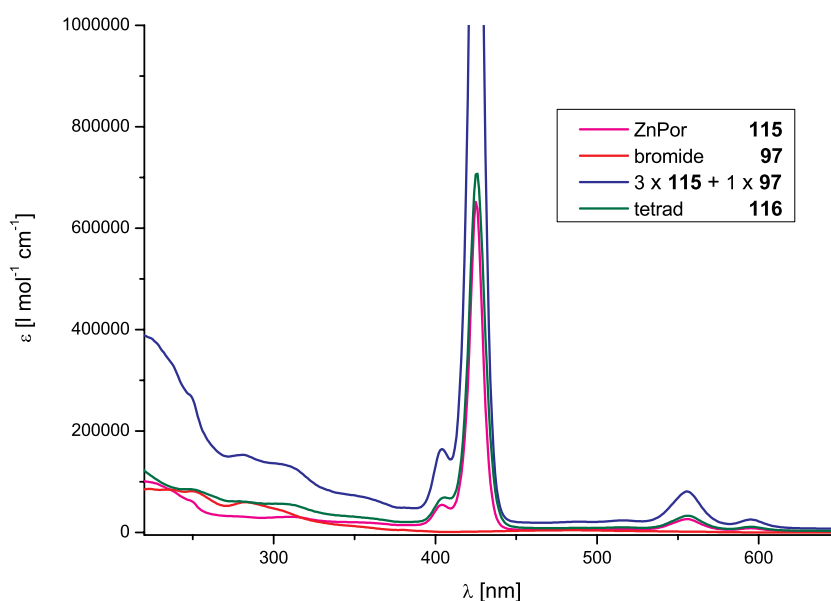


Figure 3.31: The UV/Vis-spectrum (THF; r.t.) of tetrad **116** (green) was less than the sum-spectrum of its components (blue). The spectrum was dominated by the features of precursor zinc porphyrin **115**.

The UV/Vis-spectrum of **116** was recorded in solvents of different polarity and the extinction coefficients were determined (Figure 3.31 for THF). All spectra had the same shape and could be considered as superposition of the spectra of the single components. The main features matched those of the precursor zinc porphyrin, which were the Soret-band and two Q-bands at 422 nm, 550 nm and 586 nm in DCM.^[199] In toluene and THF those absorptions were bathochromically shifted to 426 nm, 552 nm and 592 nm and 426 nm, 556 nm and 595 nm, respectively, due to the different polarity of the solvents. Yet, the UV/Vis-spectrum was not the sum of the component spectra, which is illustrated in figure 3.31 for the spectra of conjugate **116**, precursor porphyrin **115**, and precursor fullerene **97** in THF. The sum would have been three times the porphyrin absorption plus once the fullerene trisadduct absorption, but it was rather in the order of magnitude of once the porphyrin's absorption and once the fullerene's absorption. Figure 3.31 illustrates also nicely that the main features of the absorption spectrum originate from the porphyrin part, as its extinction coefficient was much larger over most of the spectral range.

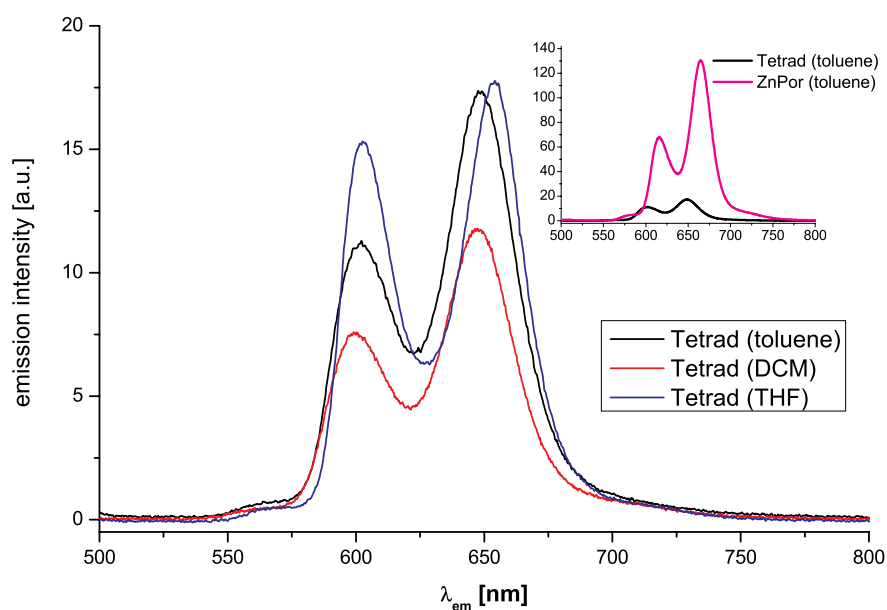
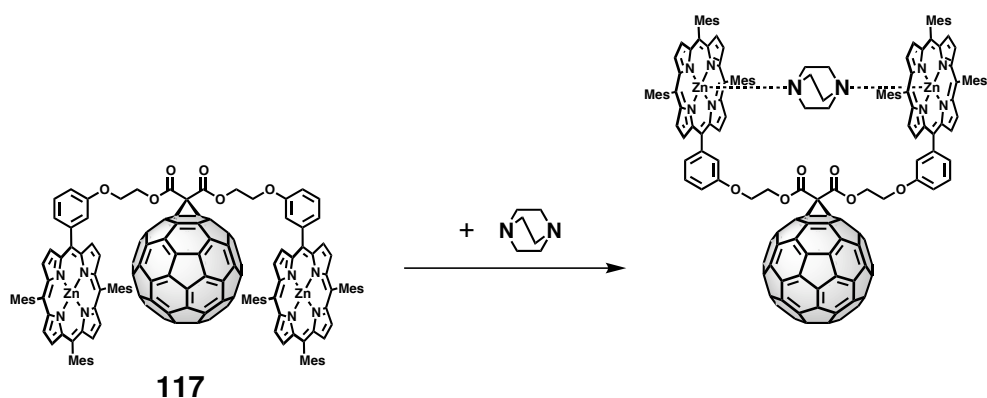


Figure 3.32: Qualitative comparison of the fluorescence spectra of tetrad **116** in different solvents. The samples were excited at the wavelength of the porphyrin's Soret-band in the corresponding solvents. inset: Comparison of emission of tetrad **116** and precursor zinc-porphyrin **115** in toluene of samples with comparable absorption.

The emission spectra of tetrad **116** (Figure 3.32) were recorded in the same solvents as the UV/Vis-spectra. Upon excitation of the Soret-band, the typical emission bands of zinc-porphyrins at around 600 nm and 650 nm were observed in all three solvents. Nevertheless, the fluorescence was strongly quenched. A qualitative comparison of the emission spectrum of **116** with a sample of precursor porphyrin **115** with comparable absorption illustrates this nicely (Figure 3.32, inset). This behavior was in agreement with the reported fullerene-bisporphyrin triad **117** (Scheme 3.33).^[201] π -stacking between the components lead to intramolecular energy- or charge-transfer-processes in that case and thus prevented emission mostly.^[200, 201] The same effects can be considered to play a role in this case although it cannot be excluded that a minor impurity (page 107) caused the fluorescence quenching.

3.6.6 Complexation-Studies of *s*-Triazine with the Fullerene-Trisporphyrin-Tetrad

The three porphyrin units of **116** were prearranged around the polar region of a C₆₀-*e,e,e*-trisadduct yet still flexible due to the butyl spacers. These might be good prerequisites for the adaption to guests and their inclusion in the cavity. Fullerene-Bisporphyrin Triad **117** is a smaller example of such a system from literature and it was shown to form complexes with DABCO-guests (Scheme 3.33).^[201] The triad underwent a conformational change upon complexation, which moved the porphyrin arms from their π -stacked orientation to a more remote position and restored the porphyrin emission. This phenomenon should be investigated with the current tetrad **116** by UV/Vis-, fluorescence- and ¹H-NMR-spectroscopy. As the present



Scheme 3.33: Literature compound **117** complexed DABCO, upon which its fluorescence was restored.^[201]

molecule contained three porphyrins a planar, C_3 -symmetric guest was necessary and *s*-triazine was chosen as complementary structure (Figure 3.33). Together with the previously mentioned complexation of metal ions, this compound would be a modular, bifunctional host. Metal ions could be complexed on the lower rim of triazole units and nitrogen-donors could be complexed in the upper cavity by the Zn-porphyrin units. The two processes would probably interact with each other and give the opportunity to modulate each phenomenon by the other.

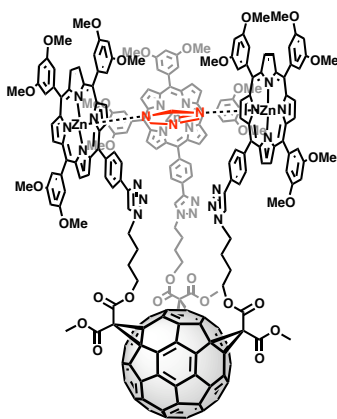


Figure 3.33: Representation of a complex between tetrad **116** and *s*-triazine.

A DCM-solution of *s*-triazine was titrated to a solution of **116** in DCM ($c = 9 \times 10^{-7}$ M) and the changes were monitored by UV/Vis- and fluorescence spectroscopy. In the beginning portions of 0.2 eq. *s*-triazine were added until one equivalent was reached. The spectra were recorded after 15 minutes of equilibration. No changes in the spectra were observed that allowed to deduce a coordination of *s*-triazine to the zinc-porphyrins. Thus, ten more equivalents of *s*-triazine were added and allowed to equilibrate, but no change in the spectra was observed. Only upon addition of a very large excess of *s*-triazine by adding some solid *s*-triazine to the solution in the cuvette coordination related changes were observed (Figure 3.34). The porphyrin's Soret-band was red-shifted by 8 nm and the Q-bands were red-shifted by 7 nm and 11 nm, respectively, which was in agreement with previous reports for the coordination of amine-donors to zinc-porphyrins.^[202] However, the Soret-band displayed a shoulder at its original position at 422 nm, indicating a mixed system of coordinated and uncoordinated porphyrins. Clear conclusions could not be drawn from these results alone. It could be assumed that *s*-triazine was coordinating only very weakly to the zinc-porphyrins and the large excess was necessary to drive the equilibrium towards the complex. However, not all zinc sites were occupied, which was apparent from the shoulder of the Soret-band.

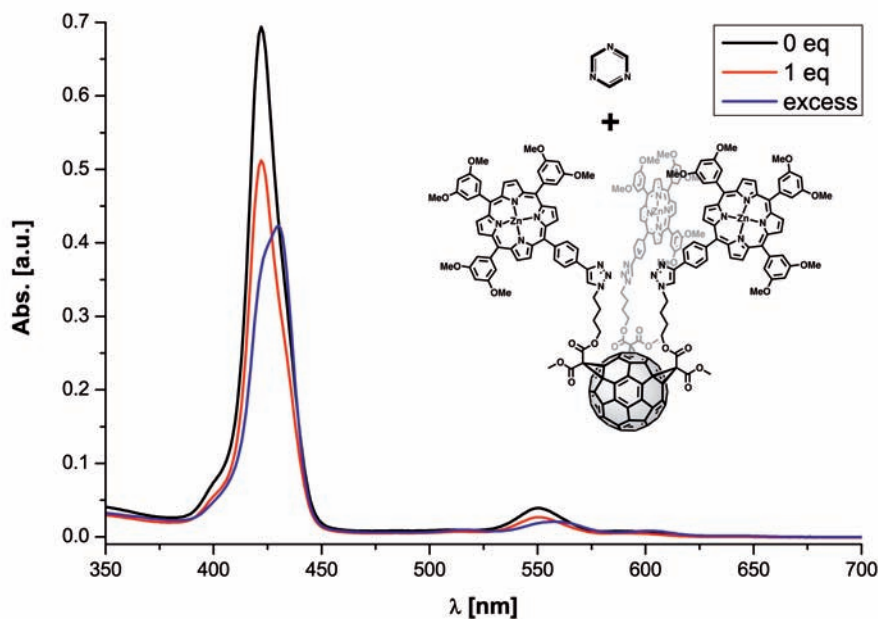


Figure 3.34: Only upon addition of a large excess of *s*-triazine, spectral changes could be observed in the UV/Vis-spectra (DCM) of **116**.

In case of literature system **117** coordination of DABCO to the host restored most of the emission intensity of the porphyrin.^[201] In case of tetrad **116**, the emission remained quenched, even when a large excess of *s*-triazine was added. The bands were slightly shifted to longer wavelengths but the intensity did not increase significantly. An inclusion of *s*-triazine in the cavity of the three porphyrins and a fixation of the porphyrins in a certain distance to the fullerene core had to be doubted. *s*-triazine was maybe not big enough or not strongly enough bound to bridge the three porphyrins in the polar region of the fullerene and the spectral changes described above probably originated from *s*-triazine-molecules coordinated to only one or two porphyrins or just on the outside and not in the proposed manner.

The complexation phenomena were investigated in a rather low concentration regime in the UV/Vis- and fluorescence-experiments ($\sim 10^{-6}$), which might have been a reason for the small effects, that were observed. In $^1\text{H-NMR}$ -experiments much higher concentration ranges are usually assessed ($\sim 10^{-3}$) and therefore different phenomena might be observed. For the conducted titration experiments 0.65 mL of a CDCl_3 -solution ($c = 1.5 \times 10^{-3} \text{ M}$) were titrated with a $11.2 \times 10^{-3} \text{ M}$ solution of *s*-triazine in CDCl_3 . After addition of *s*-triazine, the samples were allowed to equilibrate for approximately 45 min before the $^1\text{H-NMR}$ -spectrum was

recorded (400 MHz; r.t.). Upon addition of the first portion of *s*-triazine (0.1 eq.) a new singlet was observed at 7.87 ppm (Figure 3.35). The signal was shifted by 1.33 ppm to higher field in comparison to free *s*-triazine ($\delta(\text{CDCl}_3) = 9.20$ ppm). The signal appeared still as a singlet, which was a first hint towards internal complexation, although it was very little shifted in comparison to literature reports of amine donors complexed to porphyrins.^[203, 202]

Coordination of *s*-triazine to only one porphyrin would result in two signals, as the protons closer to the porphyrin would be stronger deshielded, than those farther away.^[203, 202] Upon addition of increasing amounts of *s*-triazine, the signal was increasing and shifted downfield. Some of the protons of the porphyrin (*e.g.* H12 & H13) and the triazolyl protons (H9) were also shifted, but to a much lesser extent (Figure 3.35). No other additional signals emerged in comparison to pristine tetrad **116**, which was another hint for the formation of a 1:1-complex. However, when plotting the chemical shifts vs. the mole fraction of added *s*-triazine, only a linear relationship was found (Figure 3.36). For a 1:1-complex a sigmoidal shape with a plateau, starting at one equivalent would have been expected. A rationalisation of these data

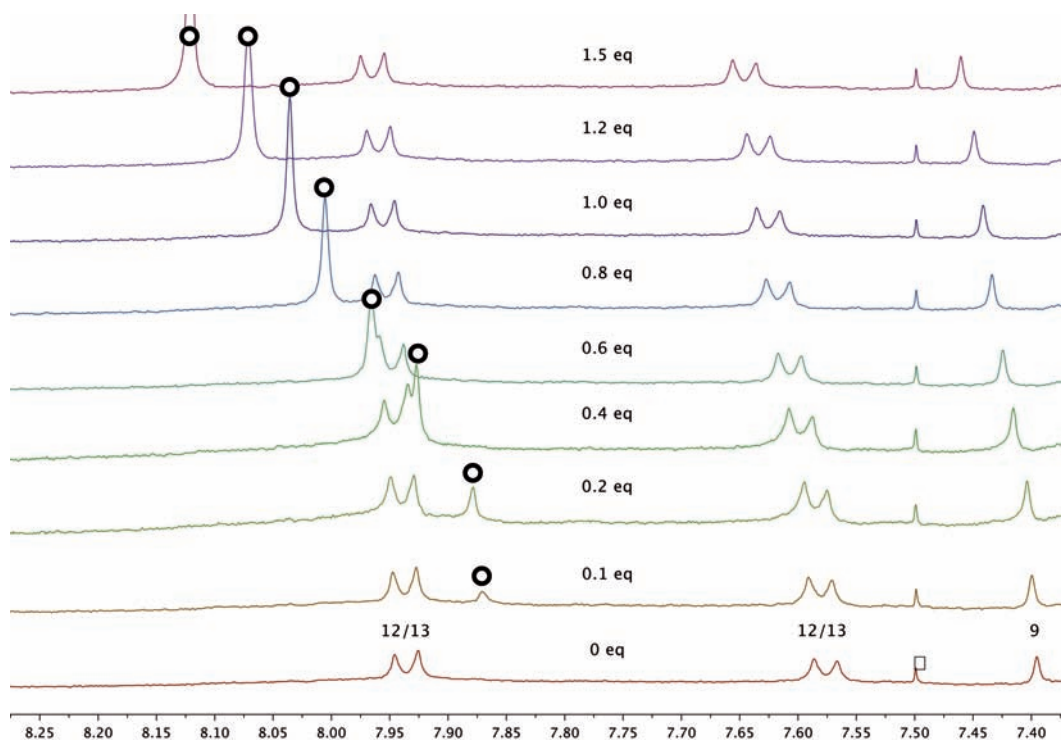


Figure 3.35: Selected region of ^1H -NMR-spectra (CDCl_3 ; 400 MHz; r.t.) of tetrad **116** upon addition of *s*-triazine. The resonance of *s*-triazine (○) was shifted highfield in comparison to the free compound and was moving downfield with increasing concentration. For assignment of the atom-numbers, see figure 3.29. * = impurity.

could be that tetrad **116** complexed several molecules *s*-triazine. Taking the UV/Vis- and fluorescence-data also into account, it had to be assumed that tetrad **116** was too flexible and the space between the zinc-centers was too large to complex a single molecule of *s*-triazine. Furthermore *s*-triazine is probably not a good enough donor. There were probably several molecules *s*-triazine weakly bound to different porphyrins and all these states were in fast equilibrium, which might explain the occurrence of a single and only little shifted signal.

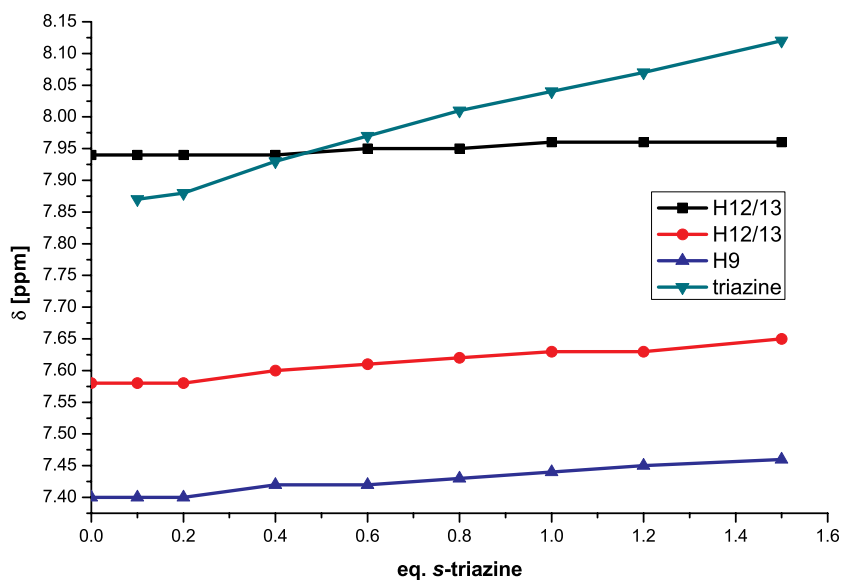


Figure 3.36: Plot of the ^1H -NMR-shifts of selected protons against the mole fraction of added *s*-triazine. The linear relationship pointed to the coordination of single *s*-triazine-molecules to each porphyrin.

4 Summary

In the first part of this thesis, additional investigations on the elusive heterofullerene $C_{58}N_2$ **11** were conducted. Although the results of the master's thesis gave reason for big hope, it turned out that the diazaheterofullerene is rather unstable under the given conditions, which prevented its full purification. Double bonds within pentagons and vinylamine moieties are thought to account for the instability, but all efforts to stabilize and saturate these structures were unsuccessful. Additionally, its synthetic preparation contained uncontrollable hurdles and was not very reliable. Nevertheless, $C_{58}N_2$ **11** was reasonable stable under solvent- and acid-free conditions. The raw mixture obtained directly after synthesis could thus be used to conduct investigations on its stability and its physicochemical properties. The reduction potentials of $C_{58}N_2$ **11** were determined by square-wave voltammetry. They were found to be clearly different from those of C_{60} **4** and $(C_{59}N)_2$ **9**, indicating the presence of a novel fullerene structure. The data suggested that there was probably only one isomer present.

In the second part of this thesis, a novel template structure for the synthesis of C_{60} -*e,e,e*-trisadducts was developed, which was faster accessible than known systems. It guaranteed control over the spatial orientation of unsymmetrical malonates and divided the carbon sphere in defined addend zones. Further conversion yielded valuable building blocks for the preparation of functional materials. The system was based on a central phosphate moiety, which exhibited additionally *in/out*-isomerism.

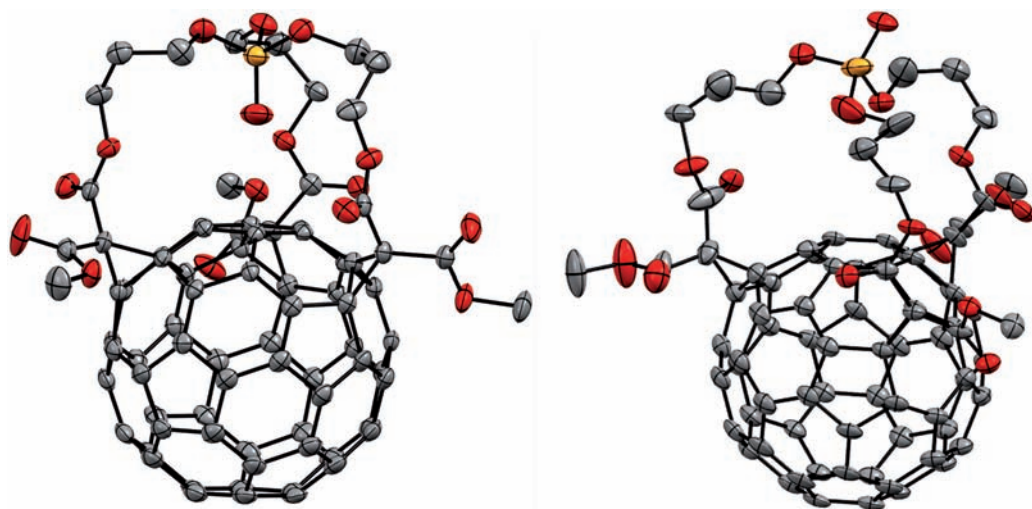
A reverse screening was conducted in advance to determine a suitable template structure. Therefore, the capping of known *e,e,e*-trisalcohol **39** was attempted to check the feasibility of the reaction and the compatibility with the structure of the fullerene backbone. Boric acid esters and silanes turned out to be unsuitable, but phosphate esters were successfully incorporated into the polar addend zone.

In a next step, the forward synthesis was successfully accomplished. The phosphate tris-malonate **62** was easily accessible by a two-step synthesis. Upon BINGEL-reaction with C_{60} the corresponding *e,e,e*-fullerenophosphate **59** was obtained as the single product. As this synthetic pathway proved feasible, the influence of the spacer length on selectivity and addi-

tion pattern was investigated. The phosphate trismalonates **69** - **72** were synthesized, having chain lengths from propyl to hexyl and the corresponding *e,e,e*-fullerenophosphates **73**, **78**, **118** and **119** were all obtained as the main product. In case of the propyl- and butyl-spacer the *e,e,e*-trisadducts were fully purified, but for the pentyl- and hexyl-derivatives an impurity with switched orientation of one malonate group could not be removed.

For all tether systems, except for the ethyl derivative, a second set of *e,e,e*-fullerenophosphates was obtained. It turned out, that the adduct geometry also allowed an inward orientation of the P=O-group. All P_{in} -isomers **74**, **79**, **80** and **83** were isolated as pure compounds, also the pentyl- and hexyl-derivative, and fully characterized. The P_{in} -isomers were substantially less polar than the P_{out} -counterparts but exhibited otherwise almost identical spectroscopic properties.

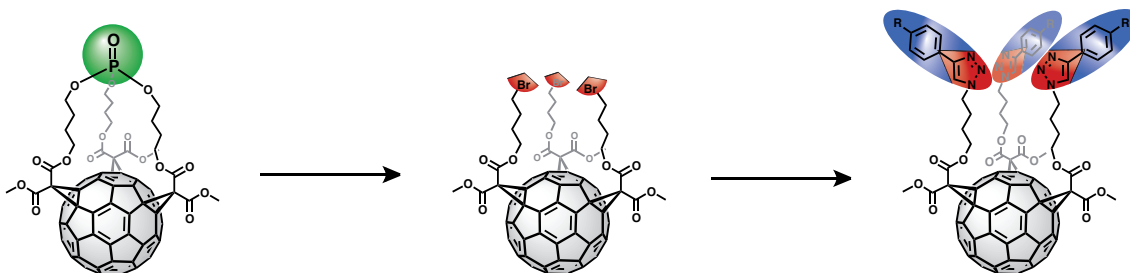
Unequivocal proof for the correct structural assignment, especially the orientation of the phosphate group, was obtained from the X-ray crystal structures of the two propyl isomers **73** and **74**. These are the first crystal structures for a BINGEL-*e,e,e*-trisadduct that are reported. The P_{in} -isomer is highly symmetric in the crystal and the P=O-group points almost perpendicular to the fullerene surface, whereas in case of the P_{out} -isomer the P=O-group is significantly tilted.



The next target was the removal of the phosphate template, in order to obtain building blocks for functional materials, which featured a well defined spatial arrangement of addends. The phosphate group was successfully removed and transformed into bromide groups, which allow further functionalization. The deprotection was accomplished for all spacer length from ethyl to hexyl, and the symmetrical tribromides **95**, **96**, **97**, **98** and **100** were all obtained. In

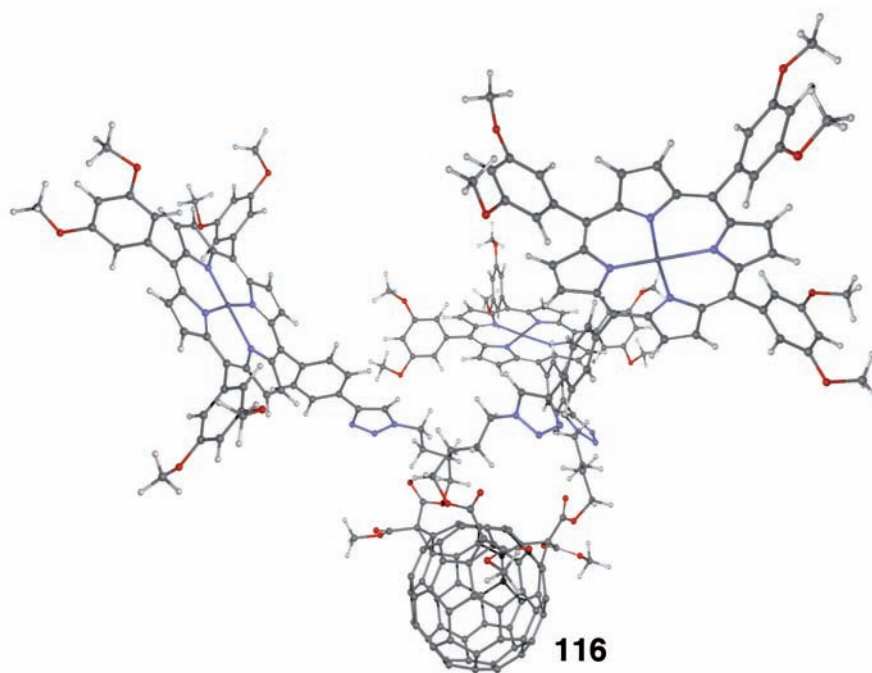
case of the pentyl- and hexyl-derivatives, the impurity from the phosphate compounds could be determined to be the corresponding malonate-*out,out,in*-isomers **99** and **101**, which were separated and characterized at the bromide stage. The deprotection proceeded faster and easier with longer spacers. The P_{in} -isomers proved to be inert to the conditions of deprotection, and the phosphate group can be considered to be protected inside the molecule's cavity.

The versatile concept of phosphate-centered tethers was subsequently extended to fullerene hexakisadducts. Based on phosphate trisadducts, the opposite hemisphere was functionalized with benzyl-capped trismalonates. The obtained hexakisadducts **104**, **105** and **106** are even more versatile building blocks. The two different polar addend zones can be deprotected and functionalized independently, which was shown by the synthesis of partially deprotected hexakisadducts **107** and **110** and of fully deprotected hexakisadduct **109**.



For a full proof of the versatility of the obtained systems a coupling scheme had to be established, that allowed the attachment of virtually any moiety to the polar addend zone. The Cu-catalyzed azide-alkyne cycloaddition (CuAAC) was chosen as ideal target for this purpose. For proof of concept, the reaction conditions were established with the butyl-spacered *e,e,e*-trisbromide **97**. It was successfully converted to the trisazide **111** and coupled with a phenyl- and a Zn-porphyrin substituent. First results towards the complexation of Zn-ions by the three preorganized triazole-moieties were obtained with the phenyl-derivative **113**. Porphyrin-derivative **116** is even a potential bifunctional host, because it can complex metal ions on the lower rim through the triazole moieties and nitrogen guests on the upper rim through the Zn-porphyrins. Preliminary complexation experiments with *s*-triazine revealed that this compound is not a good enough donor and probably too small to be encapsulated by the three Zn-porphyrin moieties but bigger nitrogen donors might be more promising.

These molecules show nevertheless the huge potential of the entire strategy. It grants easy and selective access to the *e,e,e*-addition pattern. The fullerene compound can then be used as structural template for the well-defined arrangement of various functionalities. Especially the arrangement of the triazole moieties can be used as an additional basis for novel functionalities.



5 Zusammenfassung

Im ersten Teil dieser Arbeit wurde das Diazaheterofulleren $C_{58}N_2$ **11** weitergehend untersucht. Nach den sehr positiven Ergebnissen aus der Masterarbeit, konnten diese aber nicht sehr viel weiter vertieft werden. Es stellte sich heraus, dass $C_{58}N_2$ unter den Bedingungen der Synthese nicht stabil ist und es nicht vollständig aufgereinigt werden konnte. Doppelbindungen in Fünfringen und Vinylaminteilstrukturen destabilisieren dieses neue Heterofulleren. Alle Versuche, diese Strukturen abzusättigen scheiterten im weiteren Verlauf. Erschwert wurde das Projekt zusätzlich dadurch, dass die Synthese nicht zuverlässig reproduziert werden konnte. Eine Probe des Diazaheterofullerens $C_{58}N_2$ **11** kann nur für kurze Zeit als stabil angesehen werden, am Besten im trockenen, neutralisierten Zustand. Für einige grundlegende Untersuchungen konnte die ungetrennte Rohmischung dennoch verwendet werden. Mit ihr wurden die Stabilität und einige physikochemischen Eigenschaften des Diazaheterofullerens $C_{58}N_2$ **11** bestimmt. Die Redoxpotentiale wurden mittels 'square wave'-Voltammetrie bestimmt, wobei sich zeigte, dass sie sich von denen von C_{60} **4** und von $(C_{59}N)_2$ **9** unterscheiden. Dies deutet auf einen neuen Fullertyp hin. Aus den Voltammogrammen lässt sich außerdem ableiten, dass vermutlich nur ein Isomer gebildet wurde.

Im zweiten Teil dieser Arbeit wurde ein neues Templatsystem entwickelt, das einen besseren Zugang als bisherige Systeme zu C_{60} -*e,e,e*-Trisaddukten ermöglicht. Mit ihnen konnte zusätzlich die räumliche Anordnung von unsymmetrischen Malonaten kontrolliert werden. Diese Fulleren-trisaddukte besitzen definierte Addendenzonen und darauf aufbauend wurden Bausteine für funktionelle Materialien entwickelt. Die Phosphatgruppe stellte sich als geeignetes Templat heraus. Im starren Gerüst des Fullerenadduktes wies sie *in/out*-Isomerie auf.

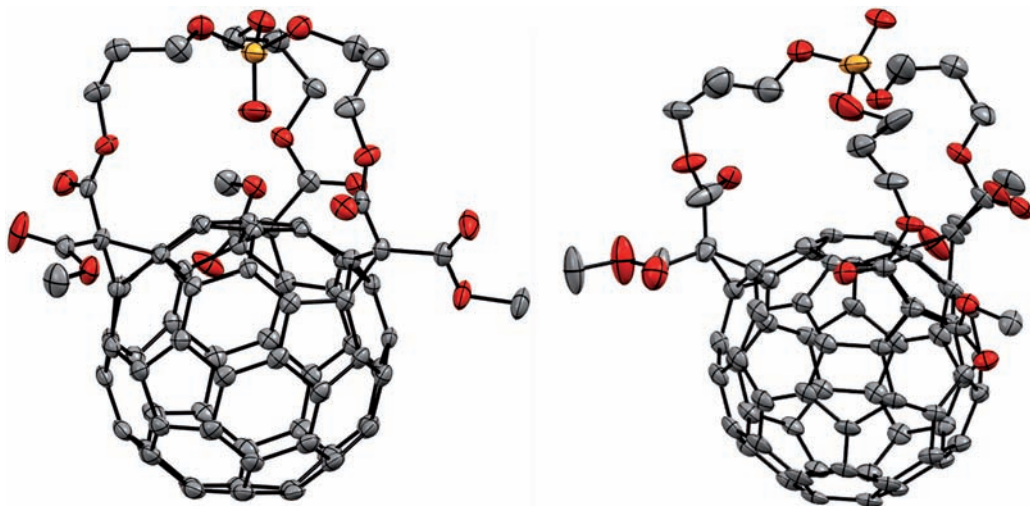
Zunächst musste diese zentrale Einheit gefunden werden. Dazu wurde eine vorhandene *e,e,e*-Struktur genutzt. Der bekannte *e,e,e*-Trisalkohol **39** diente dazu als Wirt für die zu untersuchenden Templatmotive. Dies garantierte, dass die Templatstruktur zum Additionsmuster passte und zu den strukturellen Anforderungen des restlichen Moleküles kompatibel war. Als zentrale Elemente wurden Borsäureester und Silane getestet, die sich aber beide

als ungeeignet herausstellten. Ein Phosphorsäureester konnte schließlich stabil eingebaut werden.

Nach der Definition der Zielstruktur wurde diese von einfachen Bausteinen ausgehend synthetisiert. Zunächst wurde das entsprechende Phosphatrimonalonat **59** dargestellt, womit anschließend gezeigt werden konnte, dass es selektiv mit einem *e,e,e*-Additionsmuster an C_{60} addiert.

Hiermit war bewiesen, dass das System geeignet war, C_{60} -*e,e,e*-Trisaddukte zu templatisieren. Anschließend wurde der Einfluß der Spacerlänge auf Selektivität und Additionsmuster untersucht. Die entsprechenden Phosphatrimonalonate mit Propyl- (**69**), Butyl- (**70**), Pentyl- (**71**) und Hexylkette (**72**) wurden synthetisiert und anschließend an C_{60} addiert. Dabei konnten die entsprechenden *e,e,e*-Fullerenophosphate **73**, **78**, **81** und **84** als Hauptprodukte isoliert werden. Im Fall der Pentyl- und Hexylkette stellte sich jedoch heraus, dass die gewünschten symmetrischen *e,e,e*-Additionsprodukte **81** und **84** noch Verunreinigungen enthielten, die sich später als die unsymmetrischen *e,e,e*-Isomere **82** und **85** erwiesen.

Neben diesen Hauptprodukten entstanden bei der Addition der Propyl- bis Hexyl-Trismalonate noch die analogen *e,e,e*-Fullerenophosphate mit invertierter P=O-Geometrie, die P_{in} -Isomere **74**, **79**, **80** und **83**. Im Gegensatz zu den P_{out} -Isomeren konnten sie alle als Reinstoff erhalten werden. Sie waren wesentlich unpolarer als die Hauptprodukte, ähnelten ihnen aber ansonsten in allen spektroskopischen Eigenschaften.

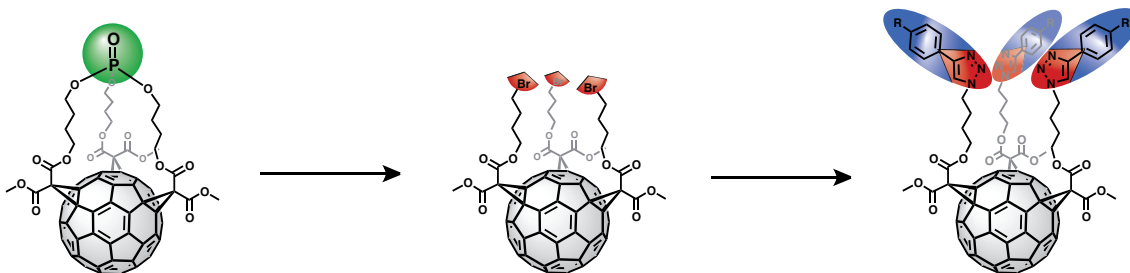


Der endgültige Beweis für die isomeren Strukturen und deren korrekte Zuweisung lieferten schließlich Kristallstrukturanalysen der beiden Propylisomere **73** und **74**. Deren Kristallstrukturen bestätigten nicht nur die Existenz dieser beiden Isomeren, sondern waren auch die

ersten Kristallstrukturen überhaupt von C_{60} -*e,e,e*-Trisaddukten mit Malonataddenden. Das P_{in} -Isomer lag dabei in einer hochsymmetrischen Konformation vor, bei der die P=O-Bindung nahezu senkrecht zur Kugeloberfläche stand. Die P=O-Bindung im P_{out} -Isomer ist dagegen deutlich verkippt zur Oberflächennormalen und die gesamte Struktur weit weniger symmetrisch.

Um die *e,e,e*-Trisaddukte als Bausteine für Materialien verwenden zu können, wurde im nächsten Schritt gezeigt, dass das Phosphattemplat bei allen P_{out} -Isomeren entfernt werden kann. Dabei entstanden die Bromide **95**, **96**, **97**, **98**, **100**, die nun die Möglichkeit zur Weiterfunktionalisierung bieten. Im Falle der Phosphate mit Pentyl- und Hexylspacer konnten auf der Bromidstufe die symmetrischen von den unsymmetrischen Trisbromiden **99** und **101** getrennt werden und deren Struktur zweifelsfrei bestimmt werden. Im Umkehrschluss war damit auch die Zusammensetzung der Phosphatgemische geklärt. Bei der Entschützung wurden Unterschiede in der Reaktivität der verschiedenen Phosphataddukte festgestellt. Die Entschützung war mit größerer Kettenlänge zunehmend leichter und es wurde außerdem gezeigt, dass die P_{in} -Isomere inert gegenüber den Reaktionsbedingungen sind.

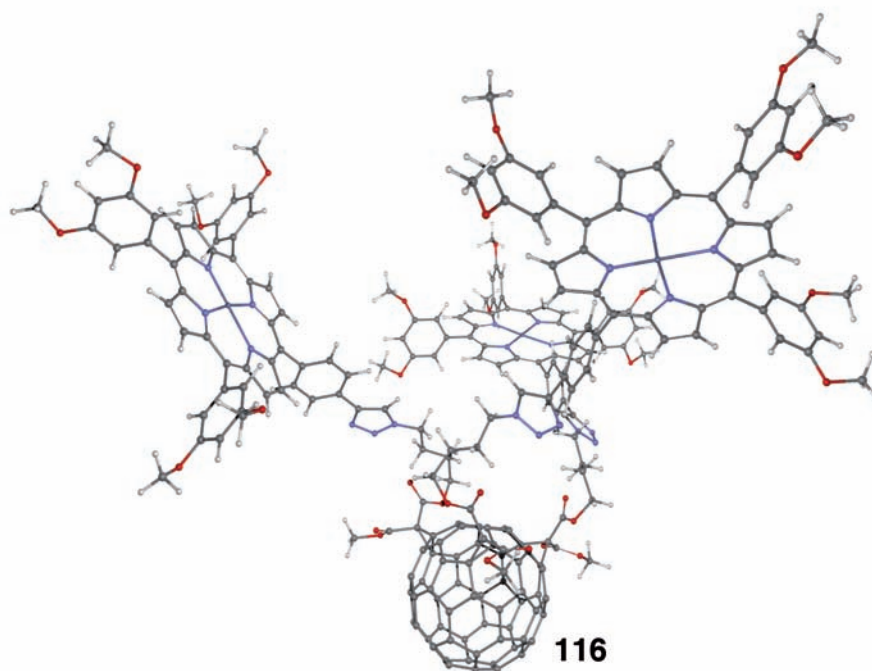
Das Konzept der Phosphattemplate wurde weiterhin auf die Synthese von C_{60} -Hexakisaddukten erweitert. Hierfür wurde, ausgehend von den *e,e,e*-Fullerenophosphaten, die gegenüberliegende Hemisphäre mit einem anderen Trismalonat funktionalisiert. Dadurch erhielt man die Hexakisaddukte **104**, **105** und **106**, die zwei unabhängige polare Addendenzonen besitzen, die getrennt voneinander entschützt und in dieser Form dann auch funktionalisiert werden können. Dies wurde anhand der Darstellung der teilweise entschützten Hexakisaddukte **107** und **110** und des vollständig entschützten Hexakisaddukts **109** gezeigt. Die letztgenannte Verbindung ist ein vielseitig einsetzbarer Baustein aus dem zahlreiche funktionale Moleküle mit definierter Anordnung der Substituenten in der Peripherie aufgebaut werden können.



Der letzte Schritt bestand darin, eine Methode zu entwickeln, mit der die erhaltenen *e,e,e*-Trisbromidbausteine tatsächlich mit weiteren Einheiten gekoppelt werden können. Es kann

te, ausgehend von Trisbromid **97**, gezeigt werden, dass nach Umwandlung in das Trisazid **111** mit Hilfe der Kupfer katalysierten Azid-Alkin-Cycloaddition weitere Einheiten angekoppelt werden können. Dabei wurden Verbindungen mit Phenyl- und Zinkporphyrinsubstituenten dargestellt. Im Falle des Phenylderivats **113** wurden außerdem erste Ergebnisse im Hinblick auf die Komplexierung von Zinkionen durch die drei vororganisierten Triazoleinheiten erzielt. Das Zinkporphyrinderivat **116** kann in diesem Zusammenhang als bifunktionelle Einheit aufgefasst werden, da es durch die Triazoleinheiten nicht nur Metallionen binden kann, sondern durch die drei Zinkporphyrine auch *N*-Donoren. Dies wurde mit *s*-Triazin getestet, wobei sich aber herausstellte, dass es ein zu schwacher Donor und zu klein ist, um effektiv eingeschlossen zu werden.

Gerade diese letzten Moleküle verdeutlichen das enorme Potential dieser Strategie. Sie ermöglicht schnellen Zugang zu *e,e,e*-Trisaddukten mit gleichzeitiger Kontrolle über die räumliche Orientierung der Addenden. Diese grundlegende Struktur kann als Baustein für die Organisation verschiedenster Funktionen dienen. Durch die Weiterfunktionalisierung entstehende Triazoleinheiten stellen ein weiteres Bindungsmotiv in solchen Architekturen dar.



6 Experimental Section

6.1 Materials and Chemicals

All reagents were purchased from chemical suppliers and used without further purification. Solvents, except for ODCB, were distilled prior to use. Ethylacetate and dichloromethane were distilled over potassium carbonate. HPLC-grade solvents were purchased from VWR and used as obtained. C₆₀ was either purchased from IOLITEC NANOMATERIALS (99.0% purity) or provided by the former Hoechst AG, (now Sanofi-Aventis), Germany as a C₆₀/C₇₀ mixture, which was separated by plug filtration (see page 132).^[204, 205]

Silica gel for column chromatography: Kieselgel 60 M, deactivated (0.04 - 0.063 mm / 230-400 mesh ASTM) MACHEREY-NAGEL, Düren, Germany.

TLC-sheets: Silica gel 60 F₂₅₄ TLC-aluminium foils, MERCK, Darmstadt, Germany.

6.2 Technical Equipment

NMR-spectroscopy: JEOL Alpha 500, JEOL EX 400, JEOL GX 400, BRUKER Avance 300, BRUKER Avance 400. Chemical shifts are indicated in ppm in relation to the particular internal standard (¹H-NMR: 7.24 ppm for CDCl₃, 2.08 ppm for acetone-d₆, 2.03 ppm for toluene-d₈, 1.73 ppm for THF-d₈; ¹³C-NMR: 77.0 ppm for CDCl₃, 29.8 ppm for acetone-d₆, 25.2 ppm for THF-d₈). Signal multiplicities are denoted as *s* (singlet), *d* (doublet), *t* (triplet), *q* (quartet), *m* (multiplet), *br* (broad signals) or a combination of the latter. Processing of the raw data was performed with the program MestReNova 5.3.2.

If a chemical shift is stated twice, the two corresponding signals can be clearly distinguished in the spectrum, but the peak positions are rounded to the same value. In case of signals that originate from multiple atoms the assigned atom numbers are connected by "+" if two

resonances coincide in one multiplet. In case of signals for similar atoms, where the exact assignment is ambiguous, the attributed atom numbers are connected by "/".

UV/Vis-Spectroscopy: VARIAN Cary 5000 UV/Vis-NIR spectrophotometer, AGILENT TECHNOLOGIES, München, Germany. Spectra were recorded in the indicated solvents. The absorption maxima λ_{\max} are given in [nm], the extinction coefficients are given in [$M^{-1}cm^{-1}$], shoulders are denoted as sh.

Fluorescence-Spectroscopy: SHIMADZU RF-5301PC Spectrofluorophotometer. Spectra were recorded in the indicated solvents with the indicated excitation wavelength λ_{ex} in [nm]. The emission maxima λ_{\max} are given in [nm].

IR-spectroscopy: BRUKER FTIR Tensor 27 (Pike MIRacle ATR). The ATR unit was equipped with a diamond crystal plate and high-pressure clamp. Spectra were recorded neat. All absorptions $\bar{\nu}$ are given in wavenumbers [cm^{-1}].

Elemental Analysis: CE Instruments, EA 1110 CHNS.

Mass-spectrometry:

MALDI-TOF: SHIMADZU Axima Confidence (nitrogen UV-laser, 50 Hz, 337 nm). matrices: Sinapic acid (SIN), 2,5-Dihydroxybenzoic acid (DHB), Dithranol (DITH), *t*-2-(3-(4-*t*-Butylphenyl)-2-methyl-2-propenylidene)malononitrile (DCTB)).

ESI-TOF: BRUKER micrOTOF II. The difference in ppm between the calculated and the measured value is given as $\Delta = \text{mass}(\text{measured}) - \text{mass}(\text{calc.})$.

EI: VARIAN MAT 311 A in EI-mode.

X-Ray crystallography: AGILENT SuperNova Dual, Atlas diffractometer.

BRUKER Kappa APEX 2 $I\mu S$ Duo diffractometer.

Automated flash chromatography: INTERCHIM puriFlash 430. PuriFlash Column 15 silica HP-silica 15 μ (80.0 g).

Analytical High Performance Liquid Chromatography (HPLC): VARIAN 940-LC Liquid Chromatograph with Scale-Up Module 445-LC, Column Oven Model 510 and Fraction Collector 440-LC, AGILENT TECHNOLOGIES, München, Germany.

Solvents were purchased from ACROS ORGANICS and VWR in HPLC quality.

Columns: COSMOSIL, Buckyprep Waters 4.6 x 250 mm, NACALAI TESQUE; Nucleosil 200 x 4 mm, 5 μ m, MACHEREY-NAGEL, Düren, Germany.

Preparative High Performance Liquid Chromatography: SHIMADZU CORPORATION, ANALYTICAL INSTRUMENTS DIVISION, Kyoto, Japan: 2 pumps LC-8 A, Autoinjector SIL-10 A, BUS-Module CBM 10 A, UV-Detector SPD-10 A, fraction collector FRC-10 A.

Solvents were distilled prior to use.

Columns: COSMOSIL, Buckyprep Waters 250 x 20 mm, NACALAI TESQUE, Japan (purchased from PHENOMENEX, Aschaffenburg); Nucleosil 250 x 21 mm, 5 μ m, MACHEREY NAGEL, Düren, Germany.

Cyclic voltammetry: Potentiostat Autolab PGSTAT 30, METROHM, Filderstadt, Germany. Electrochemical measurements were conducted in a glass cell under an argon atmosphere. The necessary amount of the compounds was dissolved in 3 mL dry ODCB to obtain a concentration of 10^{-3} M. TBABF₄ was employed as a conducting salt in a concentration of 0.1 M. The solution was purged with argon prior to measurement and a flow of argon was passed over the solution during measurement. The setup consisted of a polished Pt-working electrode, a Pt-counter electrode and a silver wire as reference electrode. For a typical measurement three cycles of the desired potential range were measured. After the measurement, ferrocene was added to the solution as an internal standard and one more cycle was measured. The potentiostat was controlled with the Autolab Nova software package.

6.3 General Procedures

General Procedure for the Formation of Methylmalonylalkanols (GP I)

The entire reaction was conducted under an inert atmosphere and in dried glassware. One equivalent of the corresponding diol was dissolved in dry THF and the solution was cooled to 0 °C with an ice-bath. An excess of dry pyridine or triethyl amine was added. 0.8 equivalents of methyl malonyl chloride were dissolved in dry THF in a dropping-funnel. The solution of methyl malonyl chloride was slowly added at 0 °C within four hours under vigorous stirring. The solution was allowed to warm up overnight and afterwards the precipitate was filtered off. The filtrate was washed with a solution of citric acid. Brine and ethyl acetate were added to the mixture to aid the phase-separation. The organic phase was washed twice with water and dried over magnesium sulfate. The raw-product was purified by column chromatography (silica; hexanes : THF = 3 : 1).

General Procedure for the Formation of Tris((methylmalonyl)alkanyl)-phosphates (GP II)

The entire reaction was conducted under an inert atmosphere and in dried glassware. Three equivalents of the corresponding methylmalonylalkanol were dissolved in the necessary volume of dry toluene to obtain a concentration of approximately 0.15 M. The reaction mixture was cooled to 0 °C with an ice-bath and six equivalents of dry pyridine were added. A 0.15 M solution of POBr₃ in dry toluene was added dropwise at 0 °C during one hour. The solution was allowed to warm up overnight. The precipitated pyridinium salts were filtered off and the filtrate was washed consecutively with bicarbonate solution, a solution of citric acid and twice with water. The organic phase was separated and dried over magnesium sulfate. The crude product was purified by flash column chromatography (silica; DCM : THF = 10 : 1).

General Procedure for the Formation of *polar*-Phosphate-*e,e,e*-trisadducts (GP III)

The reaction was carried out under modified HIRSCH-BINGEL-conditions with iodine for the *in situ* halogenation of the phosphate-malonates following in general the procedure, developed by Beuerle.^[141] As the reaction can be considered a macrocyclization reaction between a tritopic (phosphate malonate) and a polytopic compound (C₆₀), the reaction was carried out under high-dilution conditions. Therefore approximately 2.7 mL toluene per mg C₆₀ were used

to dissolve the fullerene and to obtain a solution with a concentration of 5 mmol/L. DBU was dissolved in 0.7 mL toluene per μL DBU to obtain a concentration of approximately 9 mmol/L. Special care for the exclusion of water had not to be taken, but for protection, the reaction was carried out under a nitrogen-atmosphere. For the reaction, HPLC-grade toluene was degassed for 15 minutes in a Schlenk-flask before C_{60} (1 eq.) was added. After dissolution of C_{60} the respective phosphate malonate (0.95 eq.) and iodine (3.1 eq.) were added and the content of the flask was protected from light by an aluminum-foil. The flask was equipped with a dropping-funnel, and a solution of DBU (7.5 eq.) in the necessary amount of HPLC-grade toluene was degassed therein for 15 minutes. The DBU solution was added under vigorous stirring over 5 - 8 hours to the reaction mixture. It was stirred overnight under ambient conditions. The crude reaction mixture was purified by plug filtration to remove DBU-salts and other polar by-products. The entire mixture was directly subjected to the silica-plug because prior evaporation was reported to result in substantial loss of product.^[141] Traces of unreacted C_{60} were eluted with pure toluene. Afterwards the eluent was changed to toluene: MeOH = 95:5. First, unreacted iodine was removed as a pink band and afterwards, all the product-fractions were eluted together as a red-brown band. The one or two isomers of the desired *e,e,e*-trisadducts were finally purified by a second column as stated for the specific compounds and reprecipitated from chloroform with pentane.

General Procedure for the Removal of the Phosphate Group (GP IV)

The synthesis of the trisbromoalkyl derivatives from the corresponding phosphate trisadducts was carried out in heat-dried glassware and under nitrogen atmosphere. One equivalent of the corresponding phosphate-*e,e,e*-trisadduct was dissolved in HPLC-grade CHCl_3 and an excess of TMSBr and DBU were added by a syringe. The mixture was heated to reflux and the reaction was monitored by TLC (silica; DCM : THF = 95 : 5). If reflux overnight did not result in complete conversion, which was sometimes the case for the ethyl- and propyl-derivatives, more TMSBr and DBU were added and the reaction was continued until no reactant could be detected anymore. After the solution had cooled to room-temperature, the entire volume was directly subjected to column chromatography (silica; DCM). In case, where the phosphate-mixture contained two isomers and hence, there were two trisbromoalkyl-isomers formed, toluene : DCM = 1:1 was used as eluent, to achieve separation.

General Procedure for the Formation of [3:3] Hexakisadducts from *e,e,e*-trisadducts (GP V)

The same considerations as for the synthesis of *e,e,e*-trisadducts also hold true for the synthesis of [3:3] hexakisadducts. The only difference was, that the use of iodine as halogenation reagent resulted in very little, or no product formation at all. This can be explained by the reduced reactivity of *e,e,e*-trisadducts, because the strain in the carbon sphere is already diminished by the first three addends. Therefore many synthetic protocols for the formation of fullerene hexakisadducts employ CBr_4 as halogen source. This was also successfully employed in the present case and the more reactive bromomalonates could be successfully attached to the *e,e,e*-trisadducts. The much stronger phosphazene base $\text{P}_1\text{-}^t\text{Bu}$ is also regularly used in the synthesis of [3:3] hexakisadducts but only led to undesired sideproducts for these kinds of substrates. The synthesis was conducted under nitrogen atmosphere and under exclusion of light. 1 eq. *e,e,e*-trisadduct was dissolved in HPLC-grade DCM (ca. 1.2 mL/mg) and 1.5 eq. of the tritopic malonate and approximately 9 eq. CBr_4 were added to the reaction mixture. 9 eq. DBU were dissolved in HPLC-grade DCM (0.4 mL DCM / μL DBU) in a dropping-funnel and added dropwise within an hour. The reaction was stirred until no reactant could be observed anymore by TLC, which was usually the case after one night. The entire reaction mixture was subjected to column chromatography (silica; DCM) without evaporation of solvent beforehand. After all the products were adsorbed to silica, the eluent was changed to a more polar mixture as stated for the single compounds. If necessary, a second column chromatography was applied and finally, the products were reprecipitated from CHCl_3 / pentane.

6.4 General Remarks

The organic compounds are named in accordance with the IUPAC nomenclature. The fullerene compounds are not named according to the recent IUPAC recommendation for the nomenclature of fullerenes but by a trivial system, suggested by Beuerle.^[206, 152] The addends in the different regions are listed with the prefix *polar* or *eq* to designate the polar or the equatorial addend zone, respectively, to which the addend belongs. The term *e,e,e*-trisadduct is then added. In the case of [3:3] hexakisadducts the four addend zones are indicated with *polar*, *polar'*, *eq* and *eq'* and [3:3] hexakisadduct is added after the listed addends.

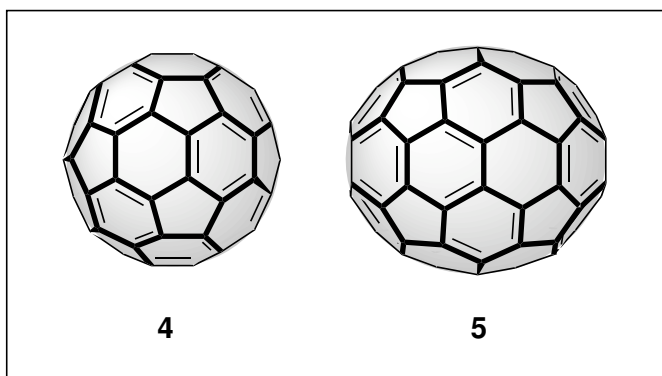
The following compounds were prepared according to literature procedures. The synthetic procedures and spectroscopic data can be found in the original publication. Changes to the described procedures are stated in the text above.

- 2-Methylmalonylethanol **60**^[160]
- 6-(Tetrahydro-2*H*-pyran-2-yloxy)-hexanol **66**^[162]
- (*S*)-1-(Triisopropylsilyloxy)propan-2-ol **89**^[180]
- (*S*)-(-)-Ethyl-2-(Tetrahydropyranyloxy)propionate **93**^[182]
- (*S*)-(-)-2-(Tetrahydropyranyloxy)propanol **94**^[182]
- 1,3,5-Tris-(2'-methylmalonyl)ethoxymethylbenzene **45**^[141]
- *polar*-1,3,5-Tris-(2'-ethoxy)methylbenzene-1,3,5-triyl-*eq*-trimethyl-*e,e,e*-trisadduct **38**^[141]
- *polar*-Tris-2-hydroxyethyl-*eq*-trimethyl-*e,e,e*-trisadduct **39**^[141]
- 5-(4-Ethynyl-phenyl)-10,15,20-tris(3,5-dimethoxy-phenyl)-porphyrinato zinc(II) **115**^[199]

6.5 Synthetic Procedures & Analytical Data

Separation of a C₆₀/C₇₀-mixture:

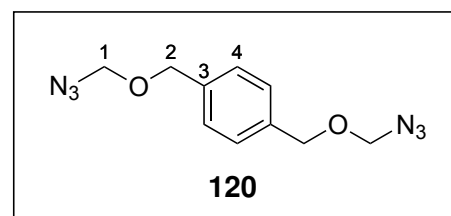
This separation technique is a combination of two methods previously described.^[204, 205] 25 g of the fullerene mixture are dissolved in 10 L of toluene by vigorous stirring for 1.5 days. Undissolved residues are removed by filtering through a Büchner funnel and can be recycled in the next separation. For the plug filtration, a



glass filter frit with a diameter of 19 cm is used. The filter plate is covered with a paper filter to prevent soiling of the glass frit. Afterwards, the filter is charged with a slurry of 370 g of Darco-G60 (purchased from Fluka) and 735 g of silica gel in toluene to produce a plug of 9 cm in height. The plug surface is carefully covered with filter paper to avoid any disturbance to the plug surface. It must be ensured that the plug does not run dry, because this would lead to an unsuccessful separation. The plug is charged with the toluene solution and eluted with toluene (by applying vacuum at the aspirator bottle) until the main part of the C₆₀ is obtained in its pure form and the eluted toluene is almost colorless. The C₆₀ fraction is evaporated to dryness, and the resulting microcrystalline solid is washed several times with pentane. After drying in vacuum 15 g of pure C₆₀ (> 98 % purity as determined by HPLC) can be obtained.

1,4-Bis(azidomethoxymethyl)benzene 120:

A 25-mL-round-bottom flask was evacuated and heat-dried prior to use. The flask was flushed with nitrogen and 2.00 g (14.5 mmol) 1,4-benzenedimethanol were added. The flask was evacuated for another 10 minutes, 14.7 mL (12.58 g; 115.8 mmol; 8 eq) trimethylsilylchloride and 0.96 g (31.8 mmol; 2.2 eq) *p*-formaldehyde were added. The mixture was stirred for 4.5 hours. The diol was dissolved after about half an hour and the *p*-formaldehyde was successively consumed. Excess trimethylsilylchloride was removed un-



der reduced pressure and the formation of the chloromethylether was checked by NMR. The crude chloromethylether was dissolved in 12 mL dry THF. 5.64 g (86.9 mmol; 6 eq) sodium-azide and 0.38 g (1.4 mmol; 0.1 eq) 18-crown-6 were added and the suspension was stirred over night. Excess sodium-azide was filtered off and the solvent was removed on a rotary evaporator. The yellow liquid was purified by column chromatography (silica; hexanes : ethyl-acetate = 4 : 1) and yielded the product as a colorless liquid.

1,4-Bis(azidomethoxymethyl)benzene 120: Colorless liquid; Yield: 1.57 g (6.68 mmol), 44 % corresponding to 1,4-benzenedimethanol.

- **Empirical Formula:** $C_{10}H_{12}N_6O_2$
- **Molecular Weight:** M_w [g/mol] = 248.24.
- **1H -NMR (CDCl₃, 400 MHz):** δ [ppm] = 7.35 (s, 4H, **4**), 4.69 (s, 4H, **1**), 4.67 (s, 4H, **2**).
- **^{13}C -NMR (CDCl₃, 100 MHz):** δ [ppm]= 136.6 (2C, **3**), 128.2 (4C, **4**), 81.8 (2C, **1**), 70.6 (2C, **2**).
- **MS (MALDI-TOF, SIN):** m/z = 248 [M]⁺, 207 [M-N₃]⁺.
- **IR (NaCl):** $\bar{\nu}$ [cm⁻¹]: 3332, 2953, 2893, 2437, 2115, 1617, 1517, 1465, 1424, 1374, 1224, 1075, 1021, 878, 813, 696.
- **UV/Vis (DCM):** λ_{max} [nm]: 235, 262, 266, 272.
- **Elemental Analysis:** Found: C, 47.75; H, 4.9, N, 33.15%. Calc. for $C_{10}H_{12}N_6O_2 \times 1/18 CH_2Cl_2$: C, 47.7; H, 4.8; N, 33.2%.

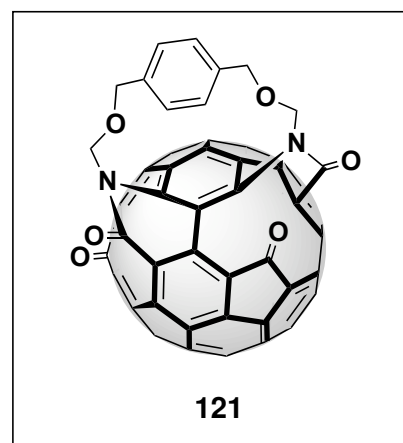
General procedure for the photooxygenation of azafulleroids:

The solid azafulleroid is taken up in little ODCB and transferred to a Schlenk tube of appropriate size. The tube is immersed in a 2-L-beaker, which contains a basic, aqueous solution of potassium chromate. The solution in the Schlenk tube must lie under the level of the yellow chromate solution. The reaction mixture is stirred and irradiated with two halogen flood lights (500 W each). The potassium chromate solution serves as a light filter and must also be vigorously stirred. During the irradiation a steady, slow stream of oxygen from a gas bottle is passed through the solution by means of a pipette. As the chromate bath would be

heavily heated up by the flood lights, a cryostat is used to keep the chromate bath at a constant temperature of 18 °C. The progress of the reaction can be monitored by TLC (silica; toluene : ethylacetate = 95 : 5). The formed ketolactam is always more polar than the starting azafulleroids.

Bisketolactam 121:

1.00 g (1.39 mmol) C₆₀ was dissolved in 250 mL ODCB and preheated to 180 °C. 345 mg (1.39 mmol, 1eq.) 1,4-bis(azidomethoxy)methylbenzene were dissolved in approximately 2 mL ODCB and added to the preheated solution. The mixture was stirred for 30 minutes at 180 °C. Afterwards it was quickly cooled to room temperature and concentrated. The products were separated by column chromatography (5 x 24 cm; silica; toluene). After the elution of C₆₀, four bands of grey-green, yellow, grey-purple and pink color were collected. These four bands were



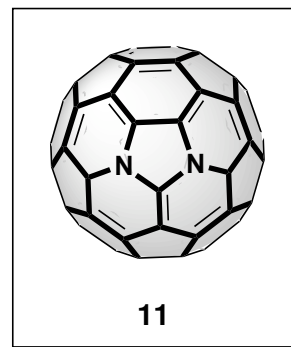
combined and the solvent was removed. The product was taken up in ODCB, filled into a 100 mL Schlenk tube and photooxygenated. The progress of the reaction was monitored by TLC. After 5.5 h, the reaction was stopped and the solution was concentrated. Column chromatography (5 x 13 cm; silica; toluene : ethylacetate = 95 : 5) yielded four fractions. A small fraction of reactants was eluted first. Afterwards the monoketolactam was eluted in a broad, brown band and finally, two bisketolactam fractions were collected as very weak, yellow-brown bands. The product fractions were evaporated to dryness.

Bisketolactam 121: Yellow-brown powder; Yield: not determined.

- **Empirical Formula:** C₇₀H₁₂N₂O₆
- **Molecular Weight:** M_w [g/mol] = 976.85.
- **UV/Vis (DCM):** λ_{max} [nm]: 235, 258, 320, 580.
- **MS (MALDI-TOF, DCTB(-)):** m/z = 976 [M]⁻.

Diazaheterofullerene 11:

Bisketolactam **121** was taken up in 5 mL ODCB and filled into a 25-mL round-bottom flask. The solution was thoroughly degassed and purged with argon. 17 mg (0.09 mmol) *p*-TsOH were added to the solution and the flask was immersed into an oilbath, which was preheated to 150 °C. A slight stream of argon was passed through the flask. The progress of the reaction was controlled by TLC (silica; toluene : ethylacetate = 95 : 5). After two hours, the reactant had disappeared and the reaction was stopped. For neutralisation, the reaction mixture was washed with sodium bicarbonate solution and water. The organic phase was dried over magnesium sulfate and evaporated to dryness. The product was obtained as yellow powder.

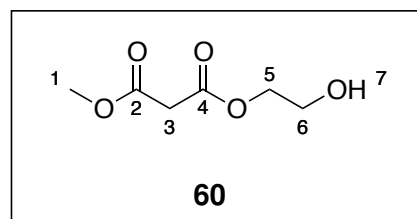


Bisazaheterofullerene 11: Yellow powder; Yield: not determined.

- **Empirical Formula:** C₅₈N₂
- **Molecular Weight:** M_w [g/mol] = 724.63.
- **UV/Vis (DCM):** λ_{max} [nm]: 232, 257, 329, 357, 576.
- **MS (MALDI-TOF, SIN):** *m/z* = 724 [M]⁺.

2-Methylmalonylethanol 60:

2-Methylmalonylethanol **60** was synthesized according to **GP I** from 3.10 mL (3.45 g; 55.5 mmol; 1 eq.) ethylene glycol, 4.80 mL (6.07 g; 44.5 mmol; 0.8 eq.) methyl malonyl chloride and 7.20 mL (7.04 g; 88.9 mmol; 1.6 eq.) dry pyridine in dry THF (180 + 50 mL). After purification



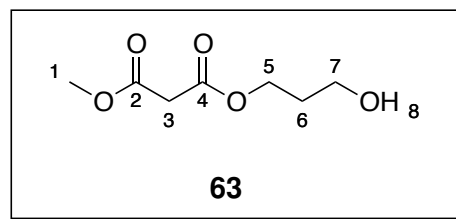
by flash column chromatography (silica; hexanes : THF = 3 : 1; R_f = 0.17) **60** was obtained as a colorless oil.

2-Methylmalonylethanol 60: Colorless oil; Yield: 4.33 g (26.7 mmol), 48 % corresponding to methyl malonyl chloride.

- **Empirical Formula:** C₆H₁₀O₅
- **Molecular Weight:** M_w [g/mol] = 162.14.
- **¹H–NMR (CDCl₃, 400 MHz):** δ [ppm] = 4.22 (t, ³J = 4.7 Hz, 2H, **5**), 3.75 (t, ³J = 4.7 Hz, 2H, **6**), 3.69 (s, 3H, **1**), 3.41 (s, 2H, **3**), 2.82 (s, 1H, **7**).
- **¹³C–NMR (CDCl₃, 100 MHz):** δ [ppm] = 167.3, 166.6 (2C, **2/4**), 66.8 (1C, **5**), 60.4 (1C, **6**), 52.5 (1C, **1**), 41.0 (1C, **3**).
- **MS (EI):** m/z = 145 [M–OH]⁺, 132 [M–OMe]⁺, 101 [M–OCH₂CH₂OH]⁺.
- **IR (neat):** ν̄ [cm⁻¹]: 3468, 2957, 2853, 1727, 1439, 1376, 1336, 1276, 1200, 1148, 1078, 1025, 955, 884.
- **UV/Vis (DCM):** λ_{max} [nm]: 230, 256.
- **Elemental Analysis:** Found: C, 44.16; H, 6.52 %. Calc. for C₆H₁₀O₅: C, 44.45; H, 6.22 %.

3-Methylmalonylpropanol **63**:

3-Methylmalonylpropanol **63** was synthesized according to **GP I** from 6.00 mL (6.32 g; 83.0 mmol; 1 eq.) 1,3-propanediol, 7.10 mL (8.92 g; 66.4 mmol; 0.8 eq.) methyl malonyl chloride and 11.2 mL (8.13 g; 80.4 mmol; 1 eq.) dry triethylamine in dry THF (400 + 50 mL). After purification by flash column chromatography (silica; hexanes : THF = 3 : 1; R_f = 0.14) **63** was obtained as a colorless oil.



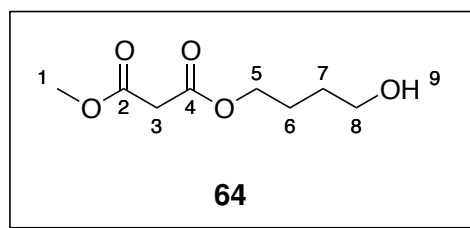
3-Methylmalonylpropanol **63:** Colorless oil; Yield: 3.54 g (20.1 mmol), 30 % corresponding to methyl malonyl chloride.

- **Empirical Formula:** C₇H₁₂O₅
- **Molecular Weight:** M_w [g/mol] = 176.17.
- **¹H–NMR (CDCl₃, 400 MHz):** δ [ppm] = 4.16 (t, ³J = 5.9 Hz, 2H, **5**), 3.62 (s, 3H, **1**), 3.55 (t, ³J = 5.7 Hz, 2H, **7**), 3.28 (s, 2H, **3**), 2.87 (s, 1H, **8**), 1.76 (m, 2H, **6**).

- **^{13}C -NMR (CDCl_3 , 100 MHz):** δ [ppm]= 167.0, 166.5 (2C, 2/4), 62.4 (1C, 5), 58.5 (1C, 7), 52.3 (1C, 1), 41.0 (1C, 3), 31.1 (1C, 6).
- **MS (EI):** m/z = 159 $[\text{M}-\text{OH}]^+$, 146 $[\text{M}-\text{OMe}]^+$, 101 $[\text{M}-\text{OCH}_2\text{CH}_2\text{CH}_2\text{OH}]^+$.
- **IR (neat):** $\bar{\nu}$ [cm^{-1}]: 3435, 2957, 1728, 1438, 1336, 1274, 1200, 1149, 1048, 1019, 850, 685.
- **UV/Vis (DCM):** λ_{max} [nm]: 231, 252.
- **Elemental Analysis:** Found: C, 46.76; H, 7.29 %. Calc. for $\text{C}_7\text{H}_{12}\text{O}_5$: C, 47.72; H, 6.87 %.

4-Methylmalonylbutanol **64**:

4-Methylmalonylbutanol **64** was synthesized according to **GP I** from 4.20 mL (4.27 g; 47.4 mmol; 1 eq.) 1,4-butanediol, 4.00 mL (5.09 g; 37.3 mmol; 0.8 eq.) methyl malonyl chloride and 5.20 mL (3.78 g; 37.3 mmol; 0.8 eq.) dry triethylamine in dry



THF (400 + 150 mL). After purification by flash column chromatography (silica; hexanes : THF = 3 : 1; R_f = 0.02) **64** was obtained as a colorless oil.

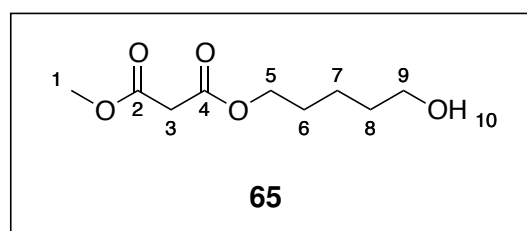
4-Methylmalonylbutanol 64: Colorless oil; Yield: 3.95 g (20.7 mmol), 56 % corresponding to methyl malonyl chloride.

- **Empirical Formula:** $\text{C}_8\text{H}_{14}\text{O}_5$
- **Molecular Weight:** M_w [g/mol] = 190.19.
- **^1H -NMR (CDCl_3 , 400 MHz):** δ [ppm]= 4.13 (*t*, 3J = 6.5 Hz, 2H, 5), 3.69 (*s*, 3H, 1), 3.60 (*t*, 3J = 6.4 Hz, 2H, 8), 3.33 (*s*, 2H, 3), 2.05 (*s*, 1H, 9), 1.69 (*m*, 2H, 6), 1.56 (*m*, 2H, 7).
- **^{13}C -NMR (CDCl_3 , 100 MHz):** δ [ppm]= 167.0, 166.5 (2C, 2/4), 65.3 (1C, 5), 62.0 (1C, 8), 52.4 (1C, 1), 41.2 (1C, 3), 28.8 (1C, 7), 24.8 (1C, 6).
- **MS (EI):** m/z = 174 $[\text{M}-\text{OH}]^+$, 159 $[\text{M}-\text{OMe}]^+$, 143 $[\text{M}-\text{OH}-\text{OMe}]^+$, 101 $[\text{M}-\text{O}(\text{CH}_2)_4\text{OH}]^+$.

- **IR (neat):** $\bar{\nu}$ [cm^{-1}]: 3435, 2954, 1729, 1438, 1412, 1390, 1335, 1274, 1200, 1149, 1018, 850, 786.
- **UV/Vis (DCM):** λ_{max} [nm]: 230, 250.
- **Elemental Analysis:** Found: C, 48.28 ; H, 7.40 %. Calc. for $\text{C}_8\text{H}_{14}\text{O}_5 \times 1/7 \text{CH}_2\text{Cl}_2$: C, 48.34; H, 7.12 %.

5-Methylmalonylpentanol **65**:

5-Methylmalonylpentanol **65** was synthesized according to **GP I** from 4.90 mL (4.86 g; 46.6 mmol; 1 eq.) 1,5-pentandiol, 4.00 mL (5.09 g; 37.3 mmol; 0.8 eq.) methyl malonyl chloride and 3.80 mL (3.69 g; 46.6 mmol; 1 eq.) dry



pyridine in dry THF (400 + 70 mL). After purification by flash column chromatography (silica; hexanes : THF = 3 : 1; R_f = 0.23) **65** was obtained as a colorless oil.

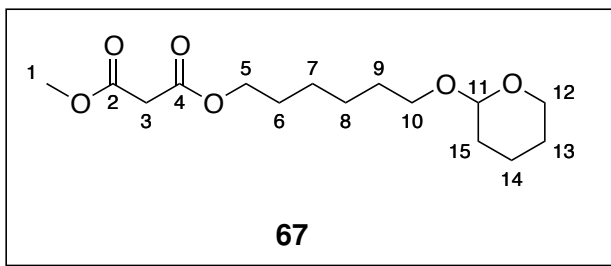
5-Methylmalonylpentanol 65: Colorless oil; Yield: 3.89 g (19.1 mmol), 51 % corresponding to methyl malonyl chloride.

- **Empirical Formula:** $\text{C}_9\text{H}_{16}\text{O}_5$
- **Molecular Weight:** M_w [g/mol] = 204.22.
- **^1H -NMR (CDCl_3 , 400 MHz):** δ [ppm]= 4.06 (*t*, 3J = 6.6 Hz, 2H, **5**), 3.65 (*s*, 3H, **1**), 3.53 (*t*, 3J = 6.5 Hz, 2H, **9**), 3.29 (*s*, 2H, **3**), 2.26 (*s*, 1H, **10**), 1.59 (*m*, 2H, **6**), 1.49 (*m*, 2H, **8**), 1.34 (*m*, 2H, **7**).
- **^{13}C -NMR (CDCl_3 , 100 MHz):** δ [ppm]= 167.0, 166.5 (2C, **2/4**), 65.3 (1C, **5**), 62.2 (1C, **9**), 52.3 (1C, **1**), 41.1 (1C, **3**), 31.9 (1C, **8**), 28.0 (1C, **6**), 21.9 (1C, **7**).
- **MS (MALDI-TOF, DHB):** m/z = 227 [$\text{M} + \text{Na}$] $^+$.
- **IR (neat):** $\bar{\nu}$ [cm^{-1}]: 3399, 2927, 2866, 1730, 1457, 1438, 1412, 1391, 1336, 1273, 1200, 1150, 1056, 1022, 887, 850, 735.
- **UV/Vis (DCM):** λ_{max} [nm]: 226.

- **Elemental Analysis:** Found: C, 52.83; H, 7.75%. Calc. for C₉H₁₆O₅: C, 52.93; H, 7.90 %.

1-(Methylmalonyl)-6-(tetrahydro-2H-pyran-2-yloxy)hexane 67:

The entire reaction was conducted under inert and dry conditions. 3.93 g (19.4 mmol; 1 eq.) mono-THP protected 1,6-hexanediol **66** was dissolved in 200 mL dry dichloromethane in a two-necked 500-mL round-bottom Schlenk-flask. The



solution was cooled to 0 °C with an ice-bath and 3.25 mL (2.36 g; 23.3 mmol; 1.2 eq.) dry triethylamine were added. 2.30 mL (2.92 g; 21.4 mmol; 1.1 eq.) methyl malonyl chloride were dissolved in 50 mL dry dichloromethane in a dropping-funnel and added within two hours. The reaction mixture was kept at 0 °C for another 30 minutes and was allowed to warm up to room temperature within another 1.5 hours. The solution was washed four times with water and dried over magnesium sulfate. After evaporation of the solvent the product was already pure enough for further conversions. To obtain the spectroscopically pure compound, the raw product was purified by column chromatography (silica; hexanes : THF = 3 : 1; R_f = 0.78) to yield a colorless oil.

1-(Methylmalonyl)-6-(tetrahydro-2H-pyran-2-yloxy)hexane 67: Colorless oil; Yield after chromatography: 3.14 g (10.4 mmol), 53 % corresponding to 6-(tetrahydro-2H-pyran-2-yloxy)-hexanol **66**.

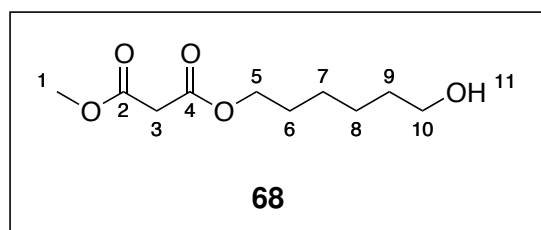
- **Empirical Formula:** C₁₅H₂₆O₆
- **Molecular Weight:** M_w [g/mol] = 302.36.
- **¹H-NMR (CDCl₃, 400 MHz):** δ [ppm]= 4.45 (*m*, 1H, **11**), 4.03 (*t*, ³*J* = 6.7 Hz, 2H, **5**), 3.74 (*m*, 1H, **12**), 3.63 (*s*, 3H, **1**), 3.61 (*m*, 1H, **10**), 3.38 (*m*, 1H, **12'**), 3.27 (*s*, 2H, **3**), 3.26 (*m*, 1H, **10'**), 1.70 (*m*, 1H, **6/9/13/14/15**), 1.48 (*m*, 9H, **6/9/13/14/15**), 1.28 (*m*, 4H, **7 + 8**).
- **¹³C-NMR (CDCl₃, 100 MHz):** δ [ppm]= 166.8, 166.3 (2C, **2/4**), 98.6 (1C, **11**), 67.1 (1C, **10**), 65.3 (1C, **5**), 62.1 (1C, **12**), 52.2 (1C, **1**), 41.1 (1C, **3**), 30.5 (1C, **13/14/15**), 29.4

(1C, **9**), 28.2 (1C, **6**), 25.6, 25.4 (2C, **7/8**), 25.3 (1C, **13/14/15**), 19.4 (1C, **13/14/15**).

- **MS (MALDI-TOF, SIN):** $m/z = 325 [M + Na]^+$, $341 [M + K]^+$.
- **IR (neat):** $\bar{\nu} [cm^{-1}]$: 2939, 2864, 1734, 1438, 1334, 1273, 1139, 1076, 1022, 904, 868, 813, 685.
- **UV/Vis (DCM):** $\lambda_{max} [nm]$: 230.
- **Elemental Analysis:** Found: C, 59.11; H, 8.71%. Calc. for $C_{15}H_{26}O_6 \times 1/27 CH_2Cl_2$: C, 59.12; H, 8.60 %.

6-Methylmalonylhexanol **68**:

2.53 g (8.35 mmol) of purified 1-(Methylmalonyl)-6-(tetrahydro-2*H*-pyran-2-yloxy)hexane **67** were dissolved in a 250-mL round-bottom flask in 50 mL dichloromethane and 50 mL methanol. 0.5 mL concentrated hydrochloric acid were added and the mixture was stirred at room tem-



perature for 2.5 hours. The solution was neutralized with solid sodium hydrogen carbonate and filtered. The residue was washed with methanol, DCM was added to the filtrate and it was washed with water. The aqueous phase was extracted three times with DCM and dried over magnesium sulfate. The solvent was removed and the pure product was obtained by flash column chromatography (silica; hexanes : THF = 3 : 1; $R_f = 0.19$) as a colorless oil.

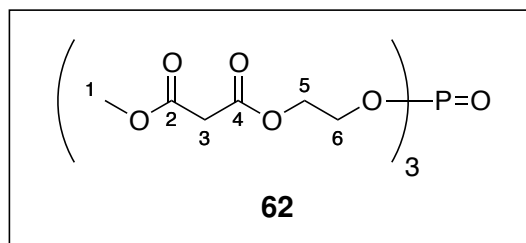
6-Methylmalonylhexanol 68: Colorless oil; Yield: 1.80 g (8.27 mmol), 99 % corresponding to 1-(Methylmalonyl)-6-(tetrahydro-2*H*-pyran-2-yloxy)hexane **67**.

- **Empirical Formula:** $C_{10}H_{18}O_5$
- **Molecular Weight:** $M_w [g/mol] = 218.25$.
- **1H -NMR ($CDCl_3$, 400 MHz):** $\delta [ppm] = 4.07 (t, {}^3J = 6.6 \text{ Hz}, 2H, \mathbf{5})$, $3.67 (s, 3H, \mathbf{1})$, $3.55 (t, {}^3J = 6.6 \text{ Hz}, 2H, \mathbf{10})$, $3.31 (s, 2H, \mathbf{3})$, $2.02 (s, 1H, \mathbf{11})$, $1.59 (m, 2H, \mathbf{6})$, $1.49 (m, 2H, \mathbf{9})$, $1.31 (m, 4H, \mathbf{7 + 8})$.

- **^{13}C -NMR (CDCl₃, 100 MHz):** δ [ppm]= 167.0, 166.5 (2C, 2/4), 65.4 (1C, 5), 62.4 (1C, 10), 52.3 (1C, 1), 41.2 (1C, 3), 32.4 (1C, 9), 28.2 (1C, 6), 25.4, 25.2 (2C, 7/8).
- **MS (MALDI-TOF, OM):** m/z = 241 [M + Na]⁺, 257 [M + K]⁺.
- **IR (neat):** $\bar{\nu}$ [cm⁻¹]: 3402, 2937, 2862, 1731, 1438, 1335, 1273, 1200, 1149, 1057, 1018, 849, 685.
- **UV/Vis (DCM):** λ_{max} [nm]: 229.
- **Elemental Analysis:** Found: C, 54.72; H, 8.52%. Calc. for C₁₀H₁₈O₅: C, 55.03; H, 8.31 %.

Tris(2-(methylmalonyl)ethyl)-phosphate **62**:

Tris(2-(methylmalonyl)ethyl)-phosphate **62** was synthesized according to **GP II** from 973 mg (6.00 mmol; 3 eq.) 2-methylmalonylethanol **60**, 573 mg (2.00 mmol; 1 eq.) POBr₃ and 0.97 mL (949 mg; 12.0 mmol; 6 eq.) dry pyridine in dry toluene (35 + 12 mL). After purification by flash column chromatography (silica; DCM : THF = 10 : 1; R_f = 0.28) **62** was obtained as a colorless oil.



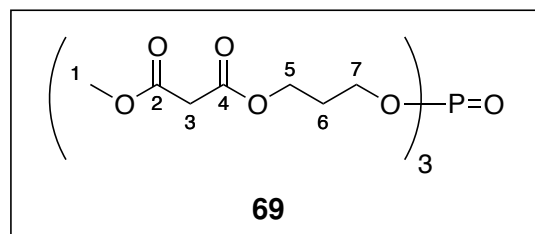
Tris(2-(methylmalonyl)ethyl)-phosphate **62:** Colorless oil; Yield: 440 mg (0.830 mmol), 42 % corresponding to 2-methylmalonylethanol **60**.

- **Empirical Formula:** C₁₈H₂₇O₁₆P
- **Molecular Weight:** M_w [g/mol] = 530.37.
- **^1H -NMR (CDCl₃, 400 MHz):** δ [ppm]= 4.34 (*m*, 6H, 5), 4.23 (*m*, 6H, 6), 3.71 (*s*, 9H, 1), 3.40 (*s*, 6H, 3).
- **^{13}C -NMR (CDCl₃, 100 MHz):** δ [ppm]= 166.6, 166.2 (6C, 2/4), 65.3 (*d*, $^2J_{\text{C-P}}$ = 6.5 Hz, 3C, 6), 63.7 (*d*, $^3J_{\text{C-P}}$ = 7.0 Hz, 3C, 5), 52.5 (3C, 1), 41.0 (3C, 3).
- **^{31}P -NMR (CDCl₃, 162 MHz):** δ [ppm]= - 0.80.

- **MS (MALDI-TOF, SIN):** $m/z = 553 [M + Na]^+$, $569 [M + K]^+$.
- **HiRes-MS (ESI-TOF):** $m/z = \text{calc. for } C_{18}H_{27}O_{16}PNa: 553.09289; \text{found: } 553.09347$ ($\Delta = 1.0 \text{ ppm}$).
- **IR (neat):** $\bar{\nu} [cm^{-1}]: 2958, 1731, 1439, 1412, 1376, 1336, 1268, 1199, 1148, 1062, 1028, 982, 844, 683$.
- **UV/Vis (DCM):** $\lambda_{\text{max}} [nm]: 230, 289$.
- **Elemental Analysis:** Found: C, 40.31; H, 5.31 %. Calc. for $C_{18}H_{27}O_{16}P \times 1/9 CH_2Cl_2$: C, 40.30; H, 5.08 %.

Tris(3-(methylmalonyl)propyl)-phosphate **69**:

Tris(3-(methylmalonyl)propyl)-phosphate **69** was synthesized according to **GP II** from 3.00 g (17.0 mmol; 3 eq.) 3-methylmalonylpropanol **63**, 1.62 g (5.65 mmol; 1 eq.) $POBr_3$ and 2.80 mL (2.74 g; 34.6 mmol; 6 eq.) dry pyridine in dry toluene (100 + 30 mL). After purification by flash column chromatography (silica; DCM : THF = 10 : 1; $R_f = 0.30$) **69** was obtained as a colorless oil.



Tris(3-(methylmalonyl)propyl)-phosphate **69:** Colorless oil; Yield: 2.02 g (3.52 mmol), 62 % corresponding to 3-methylmalonylpropanol **63**.

- **Empirical Formula:** $C_{21}H_{33}O_{16}P$
- **Molecular Weight:** $M_w [g/mol] = 572.45$.
- **1H -NMR ($CDCl_3$, 400 MHz):** $\delta [ppm] = 4.21 (t, {}^3J = 6.2 \text{ Hz}, 6H, \mathbf{5})$, $4.08 (m, 6H, \mathbf{7})$, $3.69 (s, 9H, \mathbf{1})$, $3.34 (s, 6H, \mathbf{3})$, $1.98 (m, 6H, \mathbf{6})$.
- **^{13}C -NMR ($CDCl_3$, 100 MHz):** $\delta [ppm] = 166.8, 166.3 (6C, \mathbf{2/4})$, $64.1 (d, {}^2J_{C-P} = 5.7 \text{ Hz}, 3C, \mathbf{7})$, $61.3 (3C, \mathbf{5})$, $52.5 (3C, \mathbf{1})$, $41.1 (3C, \mathbf{3})$, $29.3 (d, {}^3J_{C-P} = 7.1 \text{ Hz}, 3C, \mathbf{6})$.
- **^{31}P -NMR ($CDCl_3$, 162 MHz):** $\delta [ppm] = -0.59$.

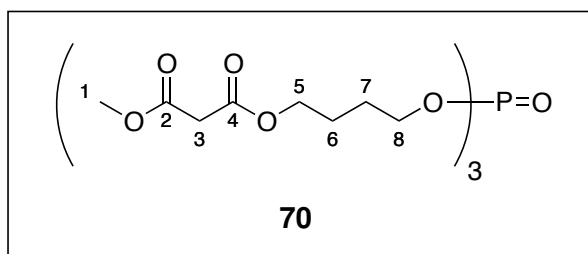
- **MS (MALDI-TOF, DHB):** $m/z = 595 [M + Na]^+$, $611 [M + K]^+$.
- **HiRes-MS (ESI-TOF):** $m/z = \text{calc. for } C_{21}H_{33}O_{16}PNa: 595.13984; \text{found: } 595.13801$ ($\Delta = -3.1 \text{ ppm}$).
- **IR (neat):** $\bar{\nu} [cm^{-1}]: 2959, 2853, 1730, 1438, 1413, 1337, 1268, 1199, 1150, 1012, 906, 849, 689$.
- **UV/Vis (DCM):** $\lambda_{\text{max}} [nm]: 231$.
- **Elemental Analysis:** Found: C, 44.33; H, 6.12 %. Calc. for $C_{21}H_{33}O_{16}P$: C, 44.06; H, 5.81 %.

Tris(4-(methylmalonyl)butyl)-phosphate **70**:

Tris(4-(methylmalonyl)butyl)-phosphate **70**

was synthesized according to **GP II** from 2.50 g (13.1 mmol; 3 eq.) 4-methylmalonylbutanol **64**, 1.26 g (4.38 mmol; 1 eq.) $POBr_3$ and 2.10 mL (2.05 g; 26.3 mmol; 6 eq.) dry pyridine in dry

toluene (75 + 25 mL). After purification by flash column chromatography (silica; DCM : THF = 10 : 1; $R_f = 0.17$) **70** was obtained as a colorless oil.



Tris(4-(methylmalonyl)butyl)-phosphate **70:** Colorless oil; Yield: 0.922 g (1.50 mmol), 34 % corresponding to 4-methylmalonylbutanol **64**.

- **Empirical Formula:** $C_{24}H_{39}O_{16}P$
- **Molecular Weight:** $M_w [g/mol] = 614.53$.
- **1H -NMR ($CDCl_3$, 400 MHz):** $\delta [ppm] = 4.10 (m, 6H, \mathbf{5})$, $3.98 (m, 6H, \mathbf{8})$, $3.65 (s, 9H, \mathbf{1})$, $3.30 (s, 6H, \mathbf{3})$, $1.67 (m, 12H, \mathbf{6 + 7})$.
- **^{13}C -NMR ($CDCl_3$, 100 MHz):** $\delta [ppm] = 166.9, 166.4 (6C, \mathbf{2/4})$, $66.9 (d, {}^2J_{C-P} = 6.0 \text{ Hz}, 3C, \mathbf{8})$, $64.6 (3C, \mathbf{5})$, $52.3 (3C, \mathbf{1})$, $41.0 (3C, \mathbf{3})$, $26.5 (d, {}^3J_{C-P} = 7.0 \text{ Hz}, 3C, \mathbf{7})$, $24.5 (3C, \mathbf{6})$.
- **^{31}P -NMR ($CDCl_3$, 162 MHz):** $\delta [ppm] = -0.32$.

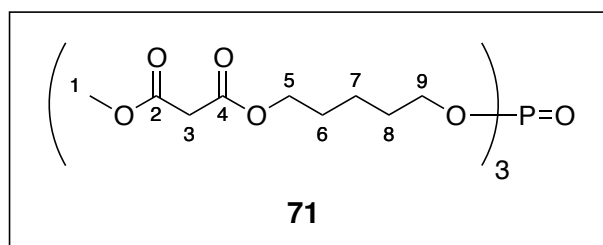
- **MS (MALDI-TOF, SIN):** $m/z = 615 [M + H]^+$, $637 [M + Na]^+$, $653 [M + K]^+$.
- **HiRes-MS (ESI-TOF):** $m/z = \text{calc. for } C_{24}H_{39}O_{16}PNa: 637.18679; \text{found: } 637.18469$ ($\Delta = -3.3 \text{ ppm}$).
- **IR (neat):** $\bar{\nu} [cm^{-1}]: 2956, 2922, 2853, 1730, 1438, 1413, 1387, 1336, 1261, 1201, 1149, 1014, 850, 805, 684$.
- **UV/Vis (DCM):** $\lambda_{\text{max}} [nm]: 230$.
- **Elemental Analysis:** Found: C, 46.31; H, 6.34 %. Calc. for $C_{24}H_{39}O_{16}P \times 1/8 CH_2Cl_2$: C, 46.35; H, 6.33 %.

Tris(5-(methylmalonyl)pentyl)-phosphate **71**:

Tris(5-(methylmalonyl)pentyl)phosphate **71**

was synthesized according to **GP II** from 2.00 g (9.79 mmol; 3 eq.) 5-methylmalonylpentanol **65**, 0.936 g (3.26 mmol; 1 eq.) $POBr_3$ and 1.60 mL (1.55 g; 19.6 mmol; 6 eq.) dry pyridine in dry

toluene (60 + 20 mL). After purification by flash column chromatography (silica; DCM : THF = 10 : 1; $R_f = 0.43$) **71** was obtained as a colorless oil.



Tris(5-(Methylmalonyl)pentyl)-phosphate **71:** Colorless oil; Yield: 0.404 g (0.615 mmol), 19 % corresponding to 5-methylmalonylpentanol **65**.

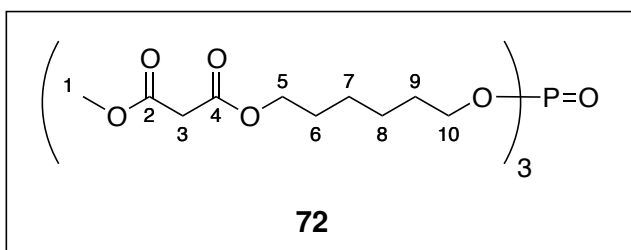
- **Empirical Formula:** $C_{27}H_{45}O_{16}P$
- **Molecular Weight:** $M_w [g/mol] = 656.61$.
- **1H -NMR ($CDCl_3$, 400 MHz):** $\delta [ppm] = 4.06 (t, {}^3J = 6.6 \text{ Hz}, 6H, \mathbf{5})$, $3.95 (m, 6H, \mathbf{9})$, $3.66 (s, 9H, \mathbf{1})$, $3.29 (s, 6H, \mathbf{3})$, $1.62 (m, 12H, \mathbf{6 + 8})$, $1.37 (m, 6H, \mathbf{7})$.
- **^{13}C -NMR ($CDCl_3$, 100 MHz):** $\delta [ppm] = 166.8, 166.3 (6C, \mathbf{2/4})$, $67.2 (d, {}^2J_{C-P} = 5.9 \text{ Hz}, 3C, \mathbf{9})$, $65.0 (3C, \mathbf{5})$, $52.3 (3C, \mathbf{1})$, $41.1 (3C, \mathbf{3})$, $29.6 (d, {}^3J_{C-P} = 6.8 \text{ Hz}, 3C, \mathbf{8})$, $27.8 (3C, \mathbf{6})$, $21.7 (3C, \mathbf{7})$.
- **^{31}P -NMR ($CDCl_3$, 162 MHz):** $\delta [ppm] = -1.55$.

- **MS (MALDI-TOF, DHB):** $m/z = 657 [M + H]^+$, $679 [M + Na]^+$, $695 [M + K]^+$.
- **HiRes-MS (ESI-TOF):** $m/z = \text{calc. for } C_{27}H_{45}O_{16}PNa: 679.23374; \text{found: } 679.23256$ ($\Delta = -1.7 \text{ ppm}$).
- **IR (neat):** $\bar{\nu} [cm^{-1}]: 2955, 2869, 1730, 1437, 1413, 1390, 1335, 1268, 1200, 1148, 994, 849, 733, 685$.
- **UV/Vis (DCM):** $\lambda_{\text{max}} [nm]: 227$.
- **Elemental Analysis:** Found: C, 49.30; H, 7.15 %. Calc. for $C_{27}H_{45}O_{16}P$: C, 49.39; H, 6.91 %.

Tris(6-(methylmalonyl)hexyl)-phosphate **72**:

Tris(6-(methylmalonyl)hexyl)phosphate **72**

was synthesized according to **GP II** from 2.10 g (9.63 mmol; 3 eq.) 6-methylmalonylhexanol **68**, 0.920 g (3.21 mmol; 1 eq.) $POBr_3$ and 1.60 mL (1.55 g; 19.6 mmol; 6 eq.) dry pyridine in dry



toluene (53 + 18 mL). After purification by flash column chromatography (silica; DCM : THF = 95 : 5; $R_f = 0.33$) **72** was obtained as a colorless oil.

Tris(6-(methylmalonyl)hexyl)-phosphate **72:** Colorless oil; Yield: 0.905 g (1.30 mmol), 40 % corresponding to 6-methylmalonylhexanol **68**.

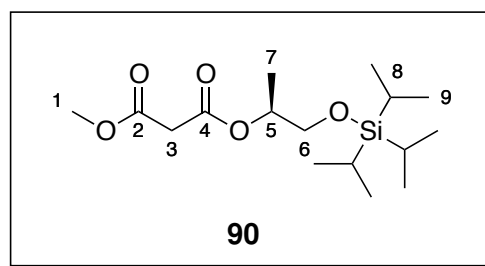
- **Empirical Formula:** $C_{30}H_{51}O_{16}P$
- **Molecular Weight:** $M_w [g/mol] = 698.69$.
- **1H -NMR ($CDCl_3$, 400 MHz):** $\delta [ppm] = 4.08 (t, {}^3J = 6.7 \text{ Hz}, 6H, \mathbf{5})$, $3.96 (m, 6H, \mathbf{10})$, $3.69 (s, 9H, \mathbf{1})$, $3.32 (s, 6H, \mathbf{3})$, $1.61 (m, 12H, \mathbf{6 + 9})$, $1.34 (m, 12H, \mathbf{7 + 8})$.
- **^{13}C -NMR ($CDCl_3$, 100 MHz):** $\delta [ppm] = 166.9, 166.4 (6C, \mathbf{2/4})$, $67.4 (d, {}^2J_{C-P} = 6.0 \text{ Hz}, 3C, \mathbf{10})$, $65.3 (3C, \mathbf{5})$, $52.4 (3C, \mathbf{1})$, $41.2 (3C, \mathbf{3})$, $30.0 (d, {}^3J_{C-P} = 6.9 \text{ Hz}, 3C, \mathbf{9})$, $28.2 (3C, \mathbf{6})$, $25.2, 25.0 (6C, \mathbf{7/8})$.
- **^{31}P -NMR ($CDCl_3$, 162 MHz):** $\delta [ppm] = -0.09$.

- **MS (MALDI-TOF, SIN):** $m/z = 699 [M + H]^+$, $721 [M + Na]^+$, $737 [M + K]^+$.
- **HiRes-MS (ESI-TOF):** $m/z = \text{calc. for } C_{30}H_{51}O_{16}PNa: 721.280693; \text{found: } 721.281706$ ($\Delta = 1.4 \text{ ppm}$).
- **IR (neat):** $\bar{\nu} [cm^{-1}]: 2952, 2861, 1731, 1437, 1413, 1390, 1335, 1265, 1198, 1148, 999, 850, 685$.
- **UV/Vis (DCM):** $\lambda_{\text{max}} [nm]: 232$.
- **Elemental Analysis:** Found: C, 50.75; H, 7.51 %. Calc. for $C_{30}H_{51}O_{16}P \times 1/6 CH_2Cl_2$: C, 50.83; H, 6.26 %.

(S)-1-(Triisopropylsilyloxy)-2-(methylmalonyl)propan 90:

The reaction was conducted under nitrogen atmosphere and in dried glassware. 2.01 g (8.65 mmol; 1 eq.) (S)-1-(Triisopropylsilyloxy)propan-2-ol **89** were dissolved in 80 mL dry DCM and cooled to 0 °C. 1.50 mL (1.50 g; 19.02 mmol; 2.2 eq.) dry pyridine were added. 1.00 mL (1.30 g; 9.51 mmol; 1.1 eq.)

methyl malonyl chloride was dissolved in 30 mL dry DCM and added dropwise within an hour. The solution was allowed to warm up overnight and then washed twice with saturated sodium hydrogen carbonate solution and once with water. The organic phase was dried over magnesium sulfate the raw product was purified by column chromatography (silica; hexanes : THF = 8 : 1; $R_f = 0.76$) and dried in vacuum.



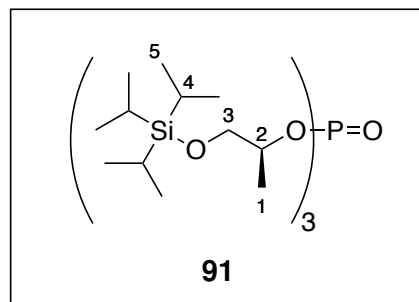
(S)-1-(Triisopropylsilyloxy)-2-(methylmalonyl)propan-2-ol 90: Colorless oil; Yield: 2.50 g (7.51 mmol), 87 % corresponding to (S)-1-(Triisopropylsilyloxy)propan-2-ol **89**.

- **Empirical Formula:** $C_{16}H_{32}O_5Si$
- **Molecular Weight:** $M_w [g/mol] = 332.51$.
- **1H -NMR ($CDCl_3$, 400 MHz):** $\delta [ppm] = 5.00 (m, 1H, 5)$, $3.71 (s, 3H, 1)$, $3.68 (m, 2H, 6)$, $3.33 (s, 2H, 3)$, $1.23 (d, ^3J = 6.4 \text{ Hz}, 3H, 7)$, $1.02 (m, 21H, 8 + 9)$.

- **^{13}C -NMR (CDCl_3 , 100 MHz):** δ [ppm]= 167.0, 166.0 (2C, **2/4**), 72.8 (1C, **5**), 65.6 (1C, **6**), 52.4 (1C, **1**), 41.5 (1C, **3**), 17.9 (6C, **9**), 16.1 (1C, **7**), 11.9 (3C, **8**).
- **HiRes-MS (ESI-TOF):** m/z = calc. for $\text{C}_{16}\text{H}_{33}\text{O}_5\text{Si}$: 333.20918; found: 333.20894 ($\Delta = -0.7$ ppm); calc. for $\text{C}_{16}\text{H}_{32}\text{O}_5\text{SiNa}$: 355.19112; found: 355.19127 ($\Delta = 0.4$ ppm); calc. for $\text{C}_{32}\text{H}_{64}\text{O}_{10}\text{Si}_2\text{Na}$: 687.39302; found: 687.39145 ($\Delta = -2.3$ ppm).
- **IR (neat):** $\bar{\nu}$ [cm^{-1}]: 2943, 2867, 1756, 1737, 1462, 1438, 1329, 1269, 1150, 1111, 1064, 1015, 882, 836, 786, 681, 659.
- **UV/Vis (DCM):** λ_{max} [nm]: 229, 423.
- **Specific Rotation (c = 0.1 g cm^{-3} , DCM):** $[\alpha]_{\text{D}}^{20} = -15^\circ$.

Tris-((*S*)-1-(triisopropylsilyloxy)propan-2-yl)phosphate **91**:

The reaction was conducted under nitrogen atmosphere and in dried glassware. 2.01 g (8.65 mmol; 3 eq.) (*S*)-1-(Triisopropylsilyloxy)propan-2-ol **89** were dissolved in 50 mL dry toluene and cooled to 0 °C. 1.40 mL (1.37 g; 17.3 mmol; 6 eq.) dry pyridine were added. 0.826 g (2.88 mmol; 1 eq.) POBr_3 were dissolved in 15 mL dry toluene and added dropwise within two hours. The solu-



tion was allowed to warm up overnight. The white precipitate was filtered off and washed with toluene and ethyl acetate. The filtrate was washed with saturated sodium hydrogen carbonate solution, a solution of citric acid and twice with water. The organic phase was dried over magnesium sulfate, the raw product was purified by column chromatography (silica; DCM : hexanes = 8 : 2; $R_f = 0.32$) and dried in vacuum.

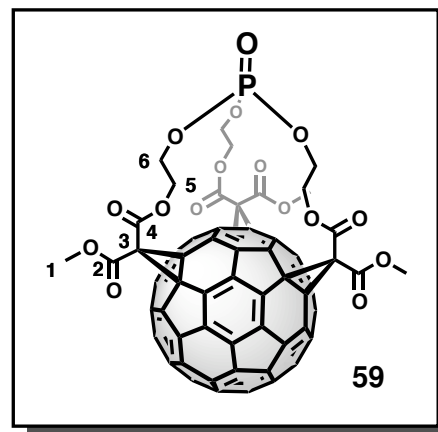
Tris-((*S*)-1-(triisopropylsilyloxy)propan-2-yl)phosphate **91:** Colorless oil; Yield: 0.632 g (0.853 mmol), 30 % corresponding to (*S*)-1-(Triisopropylsilyloxy)propan-2-ol **89**.

- **Empirical Formula:** $\text{C}_{36}\text{H}_{81}\text{O}_7\text{PSi}_3$
- **Molecular Weight:** M_w [g/mol] = 741.25.
- **^1H -NMR (CDCl_3 , 400 MHz):** δ [ppm]= 4.45 (*m*, 3H, **2**), 3.79 (*m*, 3H, **3**), 3.58 (*m*, 3H, **3'**), 1.33 (*d*, $^3J = 6.3$ Hz, 9H, **1**), 1.03 (*m*, 63H, **4 + 5**).

- ^{13}C -NMR (CDCl_3 , 75 MHz): δ [ppm]= 75.3 (*d*, $^2J_{\text{C-P}} = 6.0$ Hz, 3C, **2**), 66.7 (*d*, $^3J_{\text{C-P}} = 7.2$ Hz, 3C, **3**), 18.4 (*d*, $^3J_{\text{C-P}} = 3.5$ Hz, 3C, **1**), 17.9 (18C, **5**), 11.9 (9C, **4**).
- ^{31}P -NMR (CDCl_3 , 121 MHz): δ [ppm]= - 1.25.

polar-Tris-(2-ethyl)-phosphate-*eq*-trimethyl-*e,e,e*-trisadduct 59:

e,e,e-trisadduct **59** was synthesized according to **GP III** from 288 mg (0.543 mmol; 0.95 eq.) tris-malonate **62**, 412 mg (0.572 mmol; 1 eq.) C_{60} , 450 mg (1.77 mmol; 3.1 eq.) iodine and 640 μL (0.652 g; 4.28 mmol; 7.5 eq.) DBU in HPLC-grade toluene (1100 + 470 mL). Final purification by column chromatography (silica; DCM : THF = 95 : 5; $R_f = 0.06$) yielded **59** as a red solid.



polar-Tris-(2-ethyl)-phosphate-*eq*-trimethyl-*e,e,e*-trisadduct 59: Red solid; Yield: 159 mg (0.128 mmol), 24 % corresponding to malonate **62**.

- **Empirical Formula:** $\text{C}_{78}\text{H}_{21}\text{O}_{16}\text{P}$
- **Molecular Weight:** M_w [g/mol] = 1244.97.
- ^1H -NMR (CDCl_3 , 400 MHz): δ [ppm]= 4.80 (*m*, 3H, **5**), 4.13 (*m*, 9H, **5'** + **6**), 3.93 (*s*, 9H, **1**).
- ^{13}C -NMR (CDCl_3 , 100 MHz): δ [ppm]= 163.8, 163.2 (6C, **2/4**), 147.2, 147.1, 147.0, 146.7, 146.5, 146.5, 146.4, 145.9 (2x), 144.5, 144.4, 144.2, 143.9, 143.4, 143.3, 141.5, 141.2, 140.8 (54C, $\text{C}_{60}\text{-sp}^2$), 70.7, 70.0 (6C, $\text{C}_{60}\text{-sp}^3$), 64.8 (*d*, $^2J_{\text{C-P}} = 7.0$ Hz, 3C, **6**), 64.7 (3C, **5**), 53.8 (3C, **1**), 52.3 (3C, **3**).
- ^{31}P -NMR (CDCl_3 , 162 MHz): δ [ppm]= - 0.19.
- **MS (MALDI-TOF, DCTB):** $m/z = 1244$ [M] $^+$.
- **HiRes-MS (ESI-TOF):** $m/z = \text{calc. for } \text{C}_{78}\text{H}_{21}\text{O}_{16}\text{PNa}: 1267.04594; \text{found}: 1267.04423$ ($\Delta = -1.3$ ppm).

- **IR (neat):** $\bar{\nu}$ [cm^{-1}]: 2950, 1745, 1434, 1372, 1235, 1213, 1104, 1074, 1055, 980, 756, 731, 703.
- **UV/Vis (DCM):** λ_{max} (ϵ) [nm ($\text{M}^{-1}\text{cm}^{-1}$)]: 251 (86952), 281 (59524), 302 (sh, 47373), 380 (4726), 483 (4344), 564 (sh, 1143).

polar- P_{in} - & P_{out} -Tris-(3-propyl)-phosphate-*eq*-trimethyl-*e,e,e*-tris-
adducts **74 & **73**:**

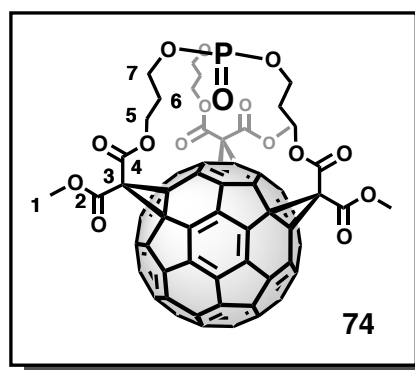
e,e,e-trisadducts **74** & **73** were synthesized according to **GP III** from 340 mg (0.594 mmol; 0.95 eq.) trismalonate **69**, 450 mg (0.625 mmol; 1 eq.) C_{60} , 492 mg (1.93 mmol; 3.1 eq.) iodine and 701 μL (0.714 g; 4.69 mmol; 7.5 eq.) DBU in HPLC-grade toluene (1250 + 550 mL). Final purification by column chromatography (silica; DCM : THF = 95 : 5; $R_f(P_{in})$ = 0.90; $R_f(P_{out})$ = 0.16) yielded **74** & **73** as red solids.

Single crystals of the P_{in} -isomer **74** suitable for X-ray crystallography were grown from hot toluene- d_8 .

Single crystals of the P_{out} -isomer **73** suitable for X-ray crystallography were grown by slow vapor diffusion of pentane into a benzene solution of **73**.

polar- P_{in} -Tris-(3-propyl)-phosphate-*eq*-trimethyl-*e,e,e*-trisadduct **74**: Red solid; Yield: 22 mg (0.017 mmol), 3 % corresponding to malonate **69**.

- **Empirical Formula:** $\text{C}_{81}\text{H}_{27}\text{O}_{16}\text{P}$
- **Molecular Weight:** M_w [g/mol] = 1287.05.
- **^1H -NMR (CDCl_3 , 400 MHz):** δ [ppm]= 4.33 (*dt*, 2J = 10.9 Hz, 3J = 3.4 Hz, 3H, **5**), 4.15 (*m*, 6H, **5'** + **7'**), 3.91 (*s*, 9H, **1**), 3.84 (*m*, 3H, **7**), 1.95 (*m*, 6H, **6**).
- **^{13}C -NMR (CDCl_3 , 100 MHz):** δ [ppm]= 163.9, 163.2 (6C, **2/4**), 146.9, 146.8, 146.8, 146.6, 146.4, 146.3, 146.2, 146.0, 145.6, 144.1, 144.0, 143.8, 143.7, 143.5, 143.1, 142.9, 141.5, 140.4 (54C, $\text{C}_{60}\text{-sp}^2$), 71.0, 69.8 (6C, $\text{C}_{60}\text{-sp}^3$), 63.1 (*d*, $^2J_{\text{C-P}}$ = 4.8 Hz, 3C, **7**), 61.9 (3C, **5**), 53.6 (3C, **1**), 52.3 (3C, **3**), 29.8 (*d*, $^3J_{\text{C-P}}$ = 5.5 Hz, 3C, **6**).

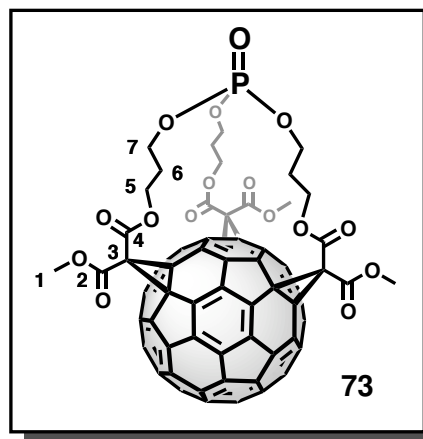


- **^{31}P -NMR (CDCl₃, 162 MHz):** δ [ppm]= 4.08.
- **MS (MALDI-TOF, DCTB):** $m/z = 1286$ [M]⁺.
- **HiRes-MS (ESI-TOF):** $m/z = \text{calc. for } \text{C}_{81}\text{H}_{27}\text{O}_{16}\text{PNa}: 1309.0929; \text{found}: 1309.0928$ ($\Delta = -0.1$ ppm).
- **IR (neat):** $\bar{\nu}$ [cm⁻¹]: 2955, 2898, 1741, 1456, 1434, 1389, 1274, 1235, 1212, 1113, 1067, 995, 907, 745, 703, 666.
- **UV/Vis (DCM):** λ_{max} (ϵ) [nm (M⁻¹cm⁻¹)]: 252 (66008), 282 (48511), 305 (sh, 35661), 380 (3839), 484 (3512), 565 (sh, 990).
- **X-ray crystallography:** CCDC 915455

Red crystal (linear dimensions: 0.0616 x 0.0501 x 0.0311 mm³); Crystal Data: C₈₈H₃₅O₁₆P, $M = 1379.13$, $\rho_{\text{calc}} = 1.509$ mg/mm³, orthorhombic, space group $P2_12_12_1$ (no. 19), $Z = 4$, $a = 13.8911(3)$ Å, $b = 17.0928(4)$ Å, $c = 25.5724(5)$ Å, $V = 6071.9(2)$ Å³, $T = 173(1)$ K, $\mu(\text{CuK}\alpha) = 1.099$, 18727 reflections measured, 11199 unique ($R_{\text{int}} = 0.0267$) which were used in all calculations. Final $R_1 = 0.0541$, $wR_2 = 0.1455$ for 937 parameters and 11199 reflections with $I > 2\sigma(I)$ and an index range of $6.22^\circ < 2\theta < 140.86^\circ$ (corresponding R values based on all 18727 reflections are 0.0623 and 0.1545, respectively). The asymmetric unit contained one molecule toluene. The absolute structure was determined.

The X-ray data were collected on a AGILENT SuperNova Dual, Atlas diffractometer. The crystal was kept at 173 K during data collection with a CuK α radiation ($\lambda = 1.5418$ Å). Using Olex2,^[207] the structure was solved with the ShelXS^[208] structure solution program using direct methods and refined with the ShelXL^[208] refinement package using full-matrix least-squares minimisation on F^2 with use of an analytical absorption correction. The hydrogen atoms were fixed in ideal positions using a riding model.

polar- P_{out} -Tris-(3-propyl)-phosphate-*eq*-trimethyl-*e,e,e*-trisadduct **73:** Red solid; Yield: 111 mg (0.086 mmol), 15 % corresponding to malonate **69**.



- **Empirical Formula:** $C_{81}H_{27}O_{16}P$
- **Molecular Weight:** M_w [g/mol] = 1287.05.
- **1H -NMR ($CDCl_3$, 400 MHz):** δ [ppm]= 4.28 (*m*, 6H, **5**), 4.06 (*m*, 3H, **7**), 3.91 (*s*, 9H, **1**), 3.79 (*m*, 3H, **7'**), 2.04 (*m*, 6H, **6**).
- **^{13}C -NMR ($CDCl_3$, 100 MHz):** δ [ppm]= 163.5, 162.8 (6C, **2/4**), 147.1, 147.0, 147.0, 146.8, 146.4, 146.4, 146.2, 145.9, 145.9, 144.3, 143.5, 143.3, 143.2, 143.2, 143.0, 142.7, 141.4, 141.0 (54C, $C_{60}-sp^2$), 70.7, 69.9 (6C, $C_{60}-sp^3$), 63.3 (*d*, $^2J_{C-P} = 6.3$ Hz, 3C, **7**), 62.3 (3C, **5**), 53.8 (3C, **1**), 52.5 (3C, **3**), 28.9 (*d*, $^3J_{C-P} = 6.3$ Hz, 3C, **6**).
- **^{31}P -NMR ($CDCl_3$, 162 MHz):** δ [ppm]= - 1.23.
- **MS (MALDI-TOF, DCTB):** $m/z = 1286$ [M] $^+$.
- **HiRes-MS (ESI-TOF):** $m/z =$ calc. for $C_{81}H_{27}O_{16}PNa$: 1309.0929; found: 1309.0906 ($\Delta = - 1.8$ ppm).
- **IR (neat):** $\bar{\nu}$ [cm^{-1}]: 2955, 2900, 1743, 1434, 1387, 1236, 1213, 1068, 1017, 905, 726, 703.
- **UV/Vis (DCM):** λ_{max} (ϵ) [nm ($M^{-1}cm^{-1}$)]: 251 (80929), 282 (52441), 302 (sh, 43679), 380 (5419), 482 (4709), 564 (sh, 1826).
- **X-ray crystallography:** CCDC 915467

Orange plates were coated with protective perfluoropoly-alkylether oil on a microscope slide. A suitable single crystal of approximate dimensions 0.20 x 0.14 x 0.03 mm³ was selected and mounted on a MiTeGen micromount. Intensity data were collected at 120 K on a Bruker Kappa APEX 2 $I\mu S$ Duo diffractometer using MoK_{α} radiation ($\lambda = 0.71072 \text{ \AA}$, QUAZAR focusing Montel optics). Data were corrected for Lorentz and polarization effects, a semi-empirical absorption correction on the basis of multiple scans was applied (SADABS, 2008/1, Bruker AXS, Inc., 2009). The structure was

solved by direct methods and refined by full-matrix least-squares procedures on F^2 (SHELXTL NT 6.12, Bruker AXS, Inc., 2002). Disorder was observed in the range of the substituted phosphate where two alternative orientations were refined resulting in site occupancies of 61.4(4) % for O2, O65, O75, O85, O61A, O62A, C63A, C64A, and C65A and of 38.6(4) % for the alternative site with O1, O60, O70, O80, O61, O62, C63, C64 and C65. Further disorder affected one of the methoxy groups. Here again two alternative orientations were refined resulting in site occupancies of 53(2) % for O64, C67 and 47(2) % for O64A, C67A, respectively. The compound crystallized with a mixture of benzene and *n*-pentane solvent molecules sharing a common crystallographic site. Refined site occupancies were 68(1) % for the *n*-pentane (C101 – C105) and 32(1) % for the benzene molecule (C111 – C116). SIMU and ISOR restraints were applied in the refinement of the disordered structure parts.

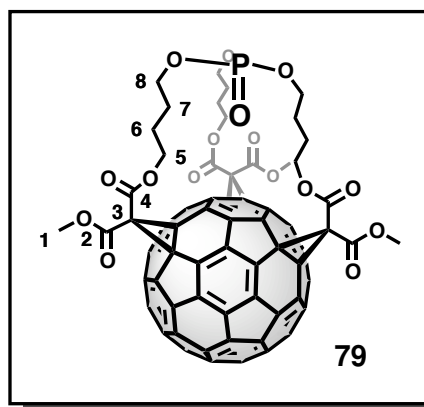
Crystal Data: $C_{86.32}H_{37.08}O_{16}P$, $M = 1361.05$, $\rho_{\text{calc}} = 1.563 \text{ mg/mm}^3$, triclinic, space group $P\bar{1}$ (Nr. 2), $a = 11.860(4) \text{ \AA}$, $b = 14.985(5) \text{ \AA}$, $c = 18.715(6) \text{ \AA}$, $\alpha = 106.643^\circ(6)$, $\beta = 91.258^\circ(6)$, $\gamma = 113.267^\circ(6)$, $V = 2892(2) \text{ \AA}^3$, $Z = 2$, $T = 120 \text{ K}$, $\mu(\text{MoK}\alpha) = 0.135 \text{ mm}^{-1}$, 40936 reflections measured, 10919 unique ($R_{\text{int}} = 0.0885$) of which 5911 were observed ($I > 2\sigma(I)$), 2θ range $4.6^\circ < 2\theta < 51.4^\circ$, final $\Delta\rho_{\text{max/min}} = 0.747 / -0.823 \text{ e\AA}^{-3}$. The least-squares refinement converged normally with residuals of $R_1 = 0.0716$ ($I > 2\sigma(I)$), $wR_2 = 0.2104$ and GooF = 1.099 (all data) for 1072 parameters and 10919 reflections.

***polar-P_{in}*- & *P_{out}*-Tris(4-butyl)-phosphate-*eq*-trimethyl-*e,e,e*-tris-adducts **79** & **78**:**

e,e,e-trisadducts **79** & **78** were synthesized according to **GP III** from 339 mg (0.552 mmol; 0.95 eq.) trismalonate **70**, 418 mg (0.581 mmol; 1 eq.) C₆₀, 456 mg (1.80 mmol; 3.1 eq.) iodine and 651 μL (0.663 g; 4.36 mmol; 7.5 eq.) DBU in HPLC-grade toluene (1150 + 500 mL). Final purification by column chromatography (silica; DCM : THF = 95 : 5; R_f(*P_{in}*) = 0.50; R_f(*P_{out}*) = 0.14) yielded **79** & **78** as red solids. The *in*-isomer **79** had to be purified once again with DCM : THF = 98 : 2.

***polar-P_{in}*-Tris(4-butyl)-phosphate-*eq*-trimethyl-**

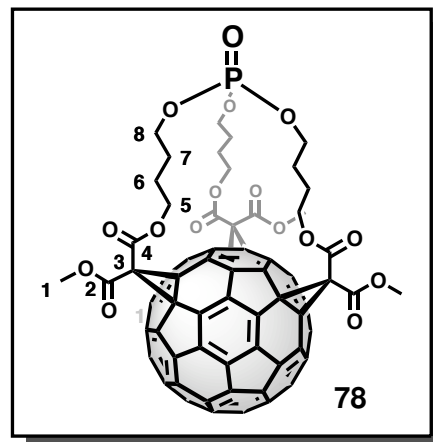
***e,e,e*-trisadduct **79**:** Red solid; Yield: 14 mg (0.011 mmol), 2 % corresponding to malonate **70**.



- **Empirical Formula:** C₈₄H₃₃O₁₆P
- **Molecular Weight:** M_w [g/mol] = 1329.12.
- **¹H-NMR (CDCl₃, 400 MHz):** δ [ppm]= 4.72 (*dt*, ²J = 10.7 Hz, ³J = 6.7 Hz, 3H, **5**), 3.97 (*m*, 6H, **5'** + **8'**), 3.92 (*s*, 9H, **1**), 3.86 (*m*, 3H, **8**), 1.84 (*m*, 3H, **7**), 1.71 (*m*, 6H, **6**), 1.55 (*m*, 3H, **7'**).
- **¹³C-NMR (CDCl₃, 100 MHz):** δ [ppm]= 163.9, 163.2 (6C, **2/4**), 146.9, 146.9, 146.8, 146.6, 146.4, 146.3, 146.3, 146.2, 145.6, 144.5, 144.4, 144.1, 143.3, 142.5 (2x), 142.2, 142.0, 140.8 (54C, C₆₀-sp²), 71.0, 69.9 (6C, C₆₀-sp³), 66.7 (*d*, ²J_{C-P} = 6.0 Hz, 3C, **8**), 65.7 (3C, **5**), 53.7 (3C, **1**), 52.7 (3C, **3**), 26.3 (*d*, ³J_{C-P} = 3.9 Hz, 3C, **7**), 24.5 (3C, **6**).
- **³¹P-NMR (CDCl₃, 162 MHz):** δ [ppm]= - 0.74.
- **MS (MALDI-TOF, DCTB):** *m/z* = 1329 [M + H]⁺.
- **HiRes-MS (ESI-TOF):** *m/z* = calc. for C₈₄H₃₃O₁₆PNa: 1351.1398; found: 1351.1390 (Δ = - 0.6 ppm).
- **IR (neat):** $\bar{\nu}$ [cm⁻¹]: 2952, 2893, 1742, 1433, 1391, 1234, 1212, 1102, 1063, 1008, 733, 702.

- **UV/Vis (DCM):** λ_{\max} (ϵ) [nm ($M^{-1}\text{cm}^{-1}$): 251 (99371), 283 (71002), 306 (sh, 51351), 380 (6135), 483 (5229), 565 (sh, 1519).

polar- P_{out} -Tris(4-butyl)-phosphate-*eq*-trimethyl-*e,e,e*-trisadduct 78: Red solid; Yield: 115 mg (0.087 mmol), 16 % corresponding to malonate **70**.



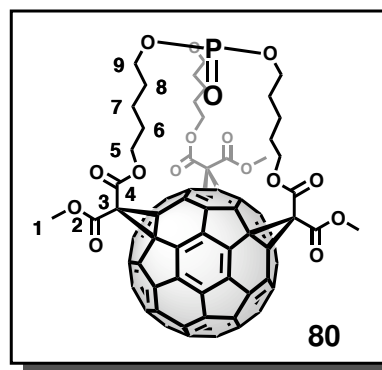
- **Empirical Formula:** $C_{84}H_{33}O_{16}P$
- **Molecular Weight:** M_w [g/mol] = 1329.12.
- **^1H -NMR (CDCl_3 , 400 MHz):** δ [ppm]= 4.54 (*dt*, $^2J = 10.9$ Hz, $^3J = 7.0$ Hz, 3H, **5**), 4.07 (*m*, 3H, **5'**), 3.96 (*m*, 3H, **8**), 3.93 (*s*, 9H, **1**), 3.89 (*m*, 3H, **8'**), 1.70 (*m*, 6H, **6**), 1.60 (*m*, 6H, **7**).
- **^{13}C -NMR (CDCl_3 , 100 MHz):** δ [ppm]= 163.7, 163.2 (6C, **2/4**), 147.0, 146.9, 146.8, 146.8, 146.6, 146.5, 146.4, 146.4, 145.9, 144.6, 144.4, 143.9, 143.4, 142.8, 142.3, 142.3, 141.8, 141.1 (54C, $C_{60}-sp^2$), 70.9, 70.0 (6C, $C_{60}-sp^3$), 66.9 (*d*, $^2J_{C-P} = 5.9$ Hz, 3C, **8**), 65.9 (3C, **6**), 53.8 (3C, **1**), 52.7 (3C, **3**), 25.9 (*d*, $^3J_{C-P} = 7.2$ Hz, 3C, **7**), 25.0 (3C, **6**).
- **^{31}P -NMR (CDCl_3 , 162 MHz):** δ [ppm]= - 1.40.
- **MS (MALDI-TOF, DCTB):** $m/z = 1329$ [M + H] $^+$.
- **HiRes-MS (ESI-TOF):** $m/z = \text{calc. for } C_{84}H_{33}O_{16}PNa: 1351.13984; \text{found: } 1351.14332$ ($\Delta = 2.6$ ppm).
- **IR (neat):** $\bar{\nu}$ [cm^{-1}]: 2952, 1741, 1433, 1236, 1213, 1102, 1066, 987, 736, 702, 664.
- **UV/Vis (DCM):** λ_{\max} (ϵ) [nm ($M^{-1}\text{cm}^{-1}$): 251 (91318), 282 (60943), 305 (sh, 47222), 379 (5279), 483 (4596), 563 (sh, 1408).

polar- P_{in} - & P_{out} -Tris(5-pentyl)-phosphate-*eq*-trimethyl-*e,e,e*-tris-
adducts **80, **81** & **82**:**

e,e,e-trisadducts **80**, **81** & **82** were synthesized according to **GP III** from 326 mg (0.496 mmol; 0.95 eq.) trismalonate **71**, 376 mg (0.523 mmol; 1 eq.) C_{60} , 411 mg (1.62 mmol; 3.1 eq.) iodine and 586 μ L (0.597 g; 3.92 mmol; 7.5 eq.) DBU in HPLC-grade toluene (1000 + 430 mL). The P_{in} - and P_{out} -*e,e,e*-isomers were first separated from all the other by-products by column chromatography (silica; DCM : THF = 95 : 5; $R_f(P_{in}) = 0.72$; $R_f(P_{out}) = 0.21$). The P_{in} -isomer **80** was fully purified by column chromatography with DCM : THF = 98 : 2. The P_{out} -isomers were further purified by automated flash chromatography by applying a gradient from toluene to toluene : methanol = 98 : 2 within two minutes and then keeping the ratio constant. It turned out, however, that the fraction contained two isomers, namely malonate-*out,out,out* **81** and malonate-*out,out,in* **82** which were inseparable.

polar- P_{in} -Tris(5-pentyl)-phosphate-*eq*-trimethyl-

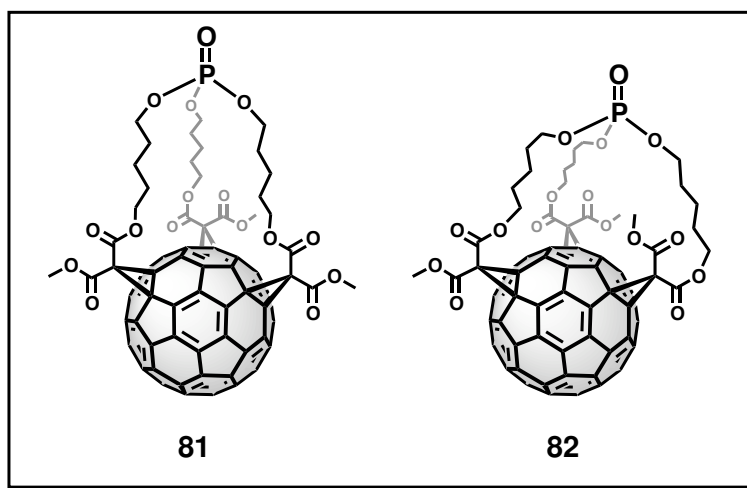
***e,e,e*-trisadduct **80**:** Red solid; Yield: 4 mg (0.003 mmol), 1 % corresponding to malonate **71**.



- **Empirical Formula:** $C_{87}H_{39}O_{16}P$
- **Molecular Weight:** M_w [g/mol] = 1371.20.
- **1H -NMR ($CDCl_3$, 400 MHz):** δ [ppm]= 4.51 (*dt*, $^2J = 11.0$ Hz, $^3J = 6.8$ Hz, 3H, **5**), 4.11 (*m*, 3H, **5'**), 3.98 (*m*, 3H, **9**), 3.91 (*s*, 9H, **1**), 3.87 (*m*, 3H, **9'**), 1.69 (*m*, 12H, **6 + 8**), 1.38 (*m*, 6H, **7**).
- **^{13}C -NMR ($CDCl_3$, 100 MHz):** δ [ppm]= 164.0, 163.3 (6C, **2/4**), 147.1, 146.8, 146.8, 146.6, 146.4, 146.4, 146.2, 146.1, 145.6, 144.5, 144.4, 144.2, 143.4, 142.6, 142.6, 142.2, 142.1, 140.9 (54C, $C_{60}-sp^2$), 71.0, 70.0 (6C, $C_{60}-sp^3$), 68.5 (3C, **9**), 66.7 (3C, **5**), 53.7 (3C, **1**), 53.0 (3C, **3**), 29.1 (*d*, $^3J_{C-P} = 5.0$ Hz, 3C, **8**), 27.3 (3C, **6**), 21.5 (3C, **7**).
- **^{31}P -NMR ($CDCl_3$, 162 MHz):** δ [ppm]= 0.74.
- **MS (MALDI-TOF, DCTB):** $m/z = 1370$ [M] $^+$, 1393 [M + Na] $^+$.
- **HiRes-MS (ESI-TOF):** $m/z =$ calc. for $C_{87}H_{39}O_{16}PNa$: 1393.18679; found: 1393.18591 ($\Delta = -0.6$ ppm).

- **IR (neat):** $\bar{\nu}$ [cm^{-1}]: 2951, 1742, 1454, 1433, 1236, 1213, 1103, 1066, 987, 939, 734, 703.
- **UV/Vis (DCM):** λ_{max} (ϵ) [nm ($\text{M}^{-1}\text{cm}^{-1}$)]: 251 (65903), 283 (46631), 304 (sh, 34815), 380 (3936), 485 (3406), 565 (sh, 1012).

P_{out} -e,e,e-trisadducts: Mixture of malonate-*out,out,out* **81** and malonate-*out,out,in* **82** isomers; Red solid; Yield: 84 mg (0.062 mmol), 12 % corresponding to malonate **71**.

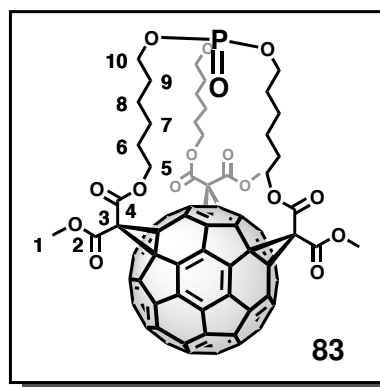


- **Empirical Formula:** C₈₇H₃₉O₁₆P
- **Molecular Weight:** M_w [g/mol] = 1371.20.
- **³¹P-NMR (CDCl₃, 162 MHz):** δ [ppm] = - 2.42, - 2.82.
- **MS (MALDI-TOF, DCTB):** m/z = 1370 [M]⁺.
- **HiRes-MS (ESI-TOF):** m/z = calc. for C₈₇H₃₉O₁₆PNa: 1393.18679; found: 1393.18442 (Δ = - 1.7 ppm).
- **UV/Vis (DCM):** λ_{max} (ϵ) [nm]: 251, 282, 305 (sh), 380, 481, 563 (sh).

polar- P_{in} - & P_{out} -Tris(6-hexyl)-phosphate-*eq*-trimethyl-*e,e,e*-tris-
adducts **83, **84** & **85**:**

e,e,e-trisadducts **83**, **84** and **85** were synthesized according to **GP III** from 290 mg (0.415 mmol; 0.95 eq.) trismalonate **72**, 315 mg (0.437 mmol; 1 eq.) C_{60} , 344 mg (1.35 mmol; 3.1 eq.) iodine and 490 μ L (0.499 g; 3.28 mmol; 7.5 eq.) DBU in HPLC-grade toluene (840 + 360 mL). The P_{in} - and P_{out} -*e,e,e*-isomers were first separated from all the other by-products by column chromatography (silica; DCM : THF = 95 : 5; $R_f(P_{in}) = 0.70$; $R_f(P_{out}) = 0.25$). The P_{in} -isomer **83** was fully purified by a second column with DCM : THF = 95 : 5. The P_{out} -isomers were further purified by preparative HPLC (Nucleosil; DCM : THF = 97 : 3; 20 mL/min). It turned out, however, that the fraction contained two isomers, namely malonate-*out,out,out* **84** and malonate-*out,out,in* **85** which were inseparable and eluted as a single peak.

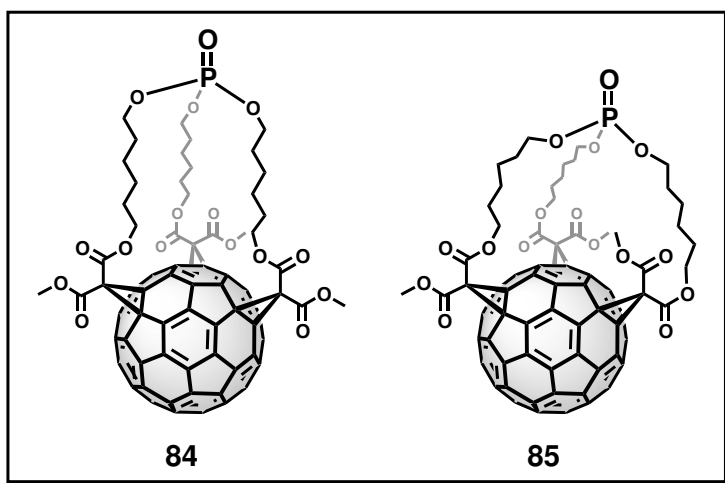
polar- P_{in} -Tris(6-hexyl)-phosphate-*eq*-trimethyl-*e,e,e*-tris-
adduct **83**: Red solid; Yield: 4 mg (0.003 mmol), 1 %
 corresponding to malonate **72**.



- **Empirical Formula:** $C_{90}H_{45}O_{16}P$
- **Molecular Weight:** M_w [g/mol] = 1413.28.
- **1H -NMR ($CDCl_3$, 400 MHz):** δ [ppm]= 4.49 (*dt*, $^2J = 10.6$ Hz, $^3J = 6.9$ Hz, 3H, **5**), 4.06 (*m*, 3H, **5'**), 4.00 (*m*, 6H, **10**), 3.93 (*s*, 9H, **1**), 1.66 (*m*, 6H, **6**), 1.56 (*m*, 6H, **9**), 1.30 (*m*, 12H, **7 + 8**).
- **^{13}C -NMR ($CDCl_3$, 100 MHz):** δ [ppm]= 164.0, 163.4 (6C, **2/4**), 147.1, 146.9, 146.9, 146.7, 146.5, 146.5, 146.4, 146.2, 145.7, 144.8, 144.5, 144.3, 143.5, 142.7, 142.6, 142.2, 141.9, 141.0 (54C, $C_{60}-sp^2$), 70.9, 70.1 (6C, $C_{60}-sp^3$), 67.4 (*d*, $^2J_{C-P} = 5.7$ Hz, 3C, **10**), 66.5 (3C, **5**), 53.7 (3C, **1**), 52.8 (3C, **3**), 29.9 (*d*, $^3J_{C-P} = 4.3$ Hz, 3C, **9**), 28.0 (3C, **6**), 24.5, 24.3 (6C, **7/8**).
- **^{31}P -NMR ($CDCl_3$, 162 MHz):** δ [ppm]= 1.87.
- **MS (MALDI-TOF, DCTB):** $m/z = 1412$ [M] $^+$.
- **HiRes-MS (ESI-TOF):** $m/z =$ calc. for $C_{90}H_{45}O_{16}PNa$: 1435.2337; found: 1435.2345 ($\Delta = 0.5$ ppm).

- **IR (neat):** $\bar{\nu}$ [cm^{-1}]: 2949, 2859, 1742, 1456, 1433, 1389, 1237, 1214, 1104, 1067, 996, 744, 704, 667.
- **UV/Vis (DCM):** λ_{max} (ϵ) [nm ($\text{M}^{-1}\text{cm}^{-1}$)]: 251 (73118), 282 (49011), 305 (sh, 36609), 380 (4625), 484 (3480), 565 (sh, 1081).

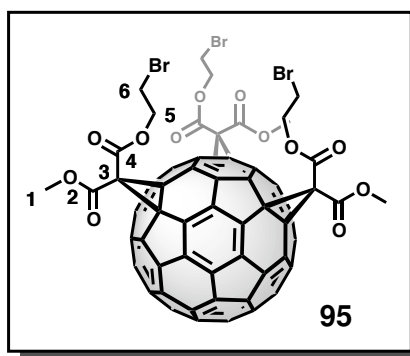
P_{out} -e,e,e-trisadducts: Mixture of malonate-*out,out,out* **84** and malonate-*out,out,in* **85** isomers; Red solid; Yield: 42 mg (0.029 mmol), 7 % corresponding to malonate **72**.



- **Empirical Formula:** C₉₀H₄₅O₁₆P
- **Molecular Weight:** M_w [g/mol] = 1413.28.
- **³¹P-NMR (CDCl₃, 162 MHz):** δ [ppm] = - 2.07.
- **MS (MALDI-TOF, DCTB):** m/z = 1412 [M]⁺.
- **HiRes-MS (ESI-TOF):** m/z = calc. for C₉₀H₄₅O₁₆PNa: 1435.2337; found: 1435.2340 (Δ = 0.2 ppm).
- **UV/Vis (DCM):** λ_{max} (ϵ) [nm]: 250, 282, 304 (sh), 380, 481, 564 (sh).

polar-Tris-2-bromoethyl-*eq*-trimethyl-*e,e,e*-trisadduct 95:

Compound **95** was synthesized according to **GP IV** from 10.0 mg (8.03 μmol ; 1 eq.) trisadduct **59**, 0.50 mL (0.580 g; 3.79 mmol; 472 eq.) TMSBr and 0.50 mL (0.510 g; 3.35 mmol; 417 eq.) DBU in 4 mL HPLC-grade CHCl_3 . The reaction mixture was refluxed overnight. The product was purified by column chromatography (silica; DCM; $R_f = 0.33$).

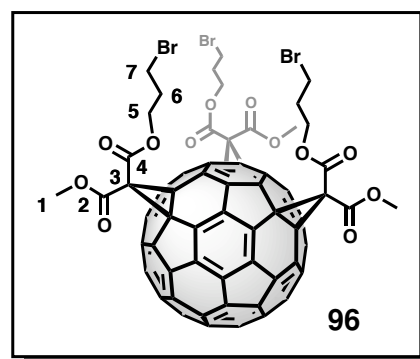


polar-Tris-2-bromoethyl-*eq*-trimethyl-*e,e,e*-trisadduct 95: Red solid; Yield: 2 mg (1.44 μmol), 18 % corresponding to trisadduct **59**.

- **Empirical Formula:** $\text{C}_{78}\text{H}_{21}\text{O}_{12}\text{Br}_3$
- **Molecular Weight:** M_w [g/mol] = 1389.71.
- **^1H -NMR (CDCl_3 , 400 MHz):** δ [ppm]= 4.57 (t, $^3J = 5.9$ Hz, 6H, **5**), 3.94 (s, 9H, **1**), 3.54 (t, $^3J = 6.0$ Hz, 6H, **6**).
- **^{13}C -NMR (CDCl_3 , 100 MHz):** δ [ppm]= 162.9, 162.5 (6C, **2/4**), 147.0, 146.9, 146.7, 146.7, 146.6, 146.5, 146.3, 146.0, 145.7, 145.4, 145.0, 144.7, 144.4, 143.5, 142.5, 141.9, 141.5, 141.0 (54C, $\text{C}_{60}\text{-sp}^2$), 70.5, 69.8 (6C, $\text{C}_{60}\text{-sp}^3$), 66.0 (3C, **5**), 53.9 (3C, **1**), 52.3 (3C, **3**), 27.7 (3C, **6**).
- **MS (MALDI-TOF, DCTB):** $m/z = 1386$ [M] $^+$.
- **HiRes-MS (ESI-TOF):** $m/z = \text{calc. for } \text{C}_{78}\text{H}_{22}\text{O}_{12}\text{Br}_3: 1386.86559; \text{found: } 1386.86047$ ($\Delta = -3.7$ ppm).
- **IR (neat):** $\bar{\nu}$ [cm^{-1}]: 1745, 1433, 1383, 1344, 1280, 1242, 1213, 1105, 1073, 1011, 990, 938, 818, 741, 705.
- **UV/Vis (DCM):** λ_{max} [nm]: 251, 280, 306 (sh), 380, 480, 565 (sh).

polar-Tris-3-bromopropyl-*eq*-trimethyl-*e,e,e*-trisadduct 96:

Compound **96** was synthesized according to **GP IV** from 12.0 mg (9.32 μmol ; 1 eq.) trisadduct **73**, 0.10 mL (0.116 g; 0.758 mmol; 81 eq.) TMSBr and 0.10 mL (0.102 g; 0.669 mmol; 71 eq.) DBU in 10 mL HPLC-grade CHCl_3 . The reaction mixture was refluxed for 2.5 hours. The product was purified by column chromatography (silica; DCM; $R_f = 0.71$).

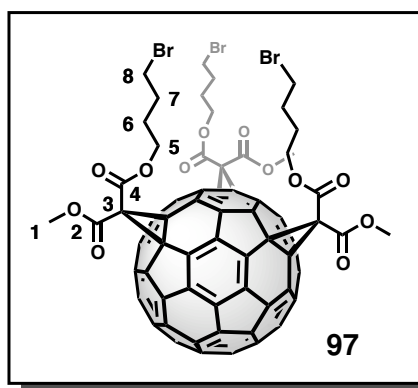


polar-Tris-3-bromopropyl-*eq*-trimethyl-*e,e,e*-trisadduct 96: Red solid; Yield: 12 mg (8.38 μmol), 90 % corresponding to trisadduct **73**.

- **Empirical Formula:** $\text{C}_{81}\text{H}_{27}\text{O}_{12}\text{Br}_3$
- **Molecular Weight:** M_w [g/mol] = 1431.79.
- **^1H -NMR (CDCl_3 , 400 MHz):** δ [ppm] = 4.42 (*m*, 6H, **5**), 3.93 (*s*, 9H, **1**), 3.43 (*t*, $^3J = 6.4$ Hz, 6H, **7**), 2.23 (*m*, 6H, **6**).
- **^{13}C -NMR (CDCl_3 , 100 MHz):** δ [ppm] = 163.7, 163.1 (6C, **2/4**), 147.0, 146.8, 146.7, 146.6, 146.5, 146.5, 146.3, 145.7, 145.5, 145.0, 144.7, 144.4, 143.4, 142.6, 142.5, 141.9, 141.6, 141.0 (54C, $\text{C}_{60}\text{-sp}^2$), 70.7, 69.9 (6C, $\text{C}_{60}\text{-sp}^3$), 64.6 (3C, **5**), 53.8 (3C, **1**), 52.5 (3C, **3**), 31.2 (3C, **6**), 28.9 (3C, **7**).
- **MS (MALDI-TOF, DCTB):** $m/z = 1428$ [M] $^+$, 1451 [$\text{M} + \text{Na}$] $^+$.
- **HiRes-MS (ESI-TOF):** $m/z = \text{calc. for } \text{C}_{81}\text{H}_{27}\text{O}_{12}\text{Br}_3\text{Na}: 1450.8945$; found: 1450.8932 ($\Delta = -0.9$ ppm).
- **IR (neat):** $\bar{\nu}$ [cm^{-1}]: 2922, 2851, 1741, 1434, 1389, 1352, 1280, 1235, 1214, 1104, 1067, 1011, 994, 906, 861, 730, 703, 666.
- **UV/Vis (DCM):** λ_{max} [nm]: 249, 283, 303 (sh), 378, 477, 562 (sh).

polar-Tris-4-bromobutyl-*eq*-trimethyl-*e,e,e*-trisadduct 97:

Compound **97** was synthesized according to **GP IV** from 74.0 mg (55.7 μmol ; 1 eq.) trisadduct **78**, 0.10 mL (0.116 g; 0.758 mmol; 14 eq.) TMSBr and 0.10 mL (0.102 g; 0.669 mmol; 12 eq.) DBU in 15 mL HPLC-grade CHCl_3 . The reaction mixture was refluxed for 1.5 hours. The product was purified by column chromatography (silica; DCM; $R_f = 0.48$).



polar-Tris-4-bromobutyl-*eq*-trimethyl-*e,e,e*-trisadduct 97: Red solid; Yield: 67 mg (45.0 μmol), 82 % corresponding to trisadduct **78**.

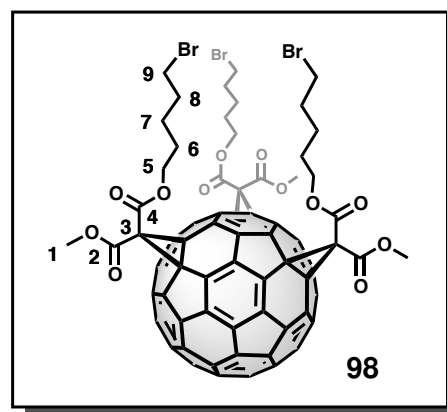
- **Empirical Formula:** $\text{C}_{84}\text{H}_{33}\text{O}_{12}\text{Br}_3$
- **Molecular Weight:** M_w [g/mol] = 1473.87.
- **¹H-NMR (CDCl₃, 400 MHz):** δ [ppm]= 4.31 (*m*, 6H, **5**), 3.93 (*s*, 9H, **1**), 3.41 (*t*, $^3J = 6.3$ Hz, 6H, **8**), 1.93 (*m*, 6H, **7**), 1.86 (*m*, 6H, **6**).
- **¹³C-NMR (CDCl₃, 100 MHz):** δ [ppm]= 163.8, 163.3 (6C, **2/4**), 147.1, 146.8, 146.7, 146.6, 146.5, 146.4, 146.3, 145.6, 145.4, 145.1, 144.8, 144.3, 143.4, 142.7, 142.4, 141.7, 141.5, 141.0 (54C, C₆₀-sp²), 70.7, 69.9 (6C, C₆₀-sp³), 66.0 (3C, **5**), 53.8 (3C, **1**), 52.6 (3C, **3**), 32.8 (3C, **8**), 29.0 (3C, **7**), 27.1 (3C, **6**).
- **MS (MALDI-TOF, DCTB):** $m/z = 1470$ [M]⁺.
- **HiRes-MS (ESI-TOF):** $m/z = \text{calc. for } \text{C}_{84}\text{H}_{33}\text{O}_{12}\text{Br}_3\text{Na}: 1492.94144; \text{found}: 1492.94172$ ($\Delta = 0.2$ ppm).
- **IR (neat):** $\bar{\nu}$ [cm⁻¹]: 2952, 2850, 1740, 1433, 1390, 1278, 1233, 1213, 1103, 1066, 1013, 989, 919, 878, 816, 799, 754, 732, 703, 665.
- **UV/Vis (THF):** λ_{max} (ϵ) [nm (M⁻¹cm⁻¹)]: 234 (84412), 249 (81432), 283 (59726), 298 (sh, 48807), 380 (4970), 485 (4415), 560 (sh, 1511).

polar-Tris-5-bromopentyl-*eq*-trimethyl-*e,e,e*-trisadduct 98 & *polar-Bis-(5-bromopentyl)-methyl-*eq*-5-bromopentyl-dimethyl-*e,e,e*-trisadduct 99:*

Compounds **98** and **99** were synthesized according to **GP IV** from 40.0 mg (29.2 μmol ; 1 eq.) trisadduct-mixture **81** & **82**, 0.10 mL (0.116 g; 0.758 mmol; 26 eq.) TMSBr and 0.10 mL (0.102 g; 0.669 mmol; 23 eq.) DBU in 20 mL HPLC-grade CHCl_3 . The reaction mixture was refluxed for one hour. The products were purified by column chromatography (silica; toluene : DCM = 1 : 1; $R_f(\mathbf{98}) = 0.15$; $R_f(\mathbf{99}) = 0.09$).

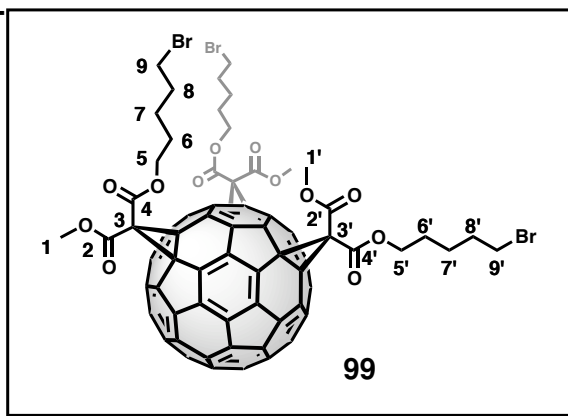
polar-Tris-5-bromopentyl-*eq*-trimethyl-*e,e,e*-trisadduct 98: Red solid; Yield: 19 mg (12.4 μmol), 43 % corresponding to trisadducts **81** & **82**.

- **Empirical Formula:** $\text{C}_{87}\text{H}_{39}\text{O}_{12}\text{Br}_3$
- **Molecular Weight:** M_w [g/mol] = 1515.95.
- **$^1\text{H-NMR}$ (CDCl_3 , 400 MHz):** δ [ppm]= 4.28 (*m*, 6H, **5**), 3.92 (*s*, 9H, **1**), 3.38 (*t*, $^3J = 6.6$ Hz, 6H, **9**), 1.86 (*m*, 6H, **8**), 1.72 (*m*, 6H, **6**), 1.50 (*m*, 6H, **7**).
- **$^{13}\text{C-NMR}$ (CDCl_3 , 100 MHz):** δ [ppm]= 163.8, 163.3 (6C, **2/4**), 147.2, 146.8, 146.7, 146.6, 146.5, 146.4, 146.3, 145.6, 145.5, 145.1, 144.9, 144.3, 143.5, 142.8, 142.3, 141.7, 141.6, 141.0 (54C, $\text{C}_{60}\text{-sp}^2$), 70.8, 70.0 (6C, $\text{C}_{60}\text{-sp}^3$), 66.7 (3C, **5**), 53.8 (3C, **1**), 52.7 (3C, **3**), 33.4 (3C, **9**), 32.1 (3C, **8**), 27.6 (3C, **6**), 24.5 (3C, **7**).
- **MS (MALDI-TOF, DCTB):** $m/z = 1512$ [M] $^+$.
- **HiRes-MS (ESI-TOF):** $m/z = \text{calc. for } \text{C}_{87}\text{H}_{39}\text{O}_{12}\text{Br}_3\text{Na}: 1534.98839$; found: 1534.99277 ($\Delta = 2.9$ ppm).
- **IR (neat):** $\bar{\nu}$ [cm^{-1}]: 2924, 2854, 1741, 1454, 1433, 1390, 1279, 1233, 1213, 1103, 1064, 1013, 985, 890, 817, 730, 703, 666.
- **UV/Vis (DCM):** λ_{max} [nm]: 251, 283, 304 (sh), 379, 483, 562 (sh).



polar-Bis-(5-bromopentyl)-methyl-*eq*-5-bromopentyl-dimethyl-*e,e,e*-trisadduct 99: Red solid; Yield: 11 mg (7.52 μmol), 26 % corresponding to trisadducts **81** & **82**.

- **Empirical Formula:** $\text{C}_{87}\text{H}_{39}\text{O}_{12}\text{Br}_3$
- **Molecular Weight:** M_w [g/mol] = 1515.95.



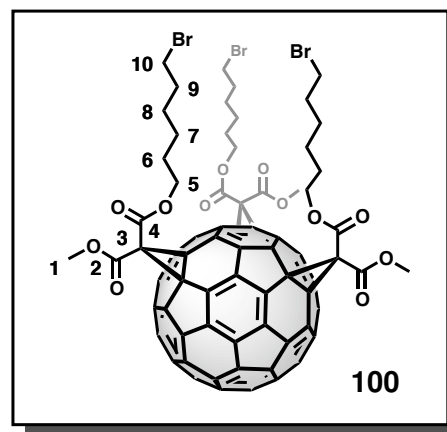
- **¹H-NMR (CDCl₃, 400 MHz):** δ [ppm]= 4.34 (*m*, 2H, 5'), 4.28 (*m*, 4H, 5), 3.93, 3.92 (2 *x s*, 6H, 1), 3.87 (*s*, 3H, 1'), 3.38 (*t*, ³*J* = 6.6 Hz, 6H, 9 + 9'), 1.86 (*m*, 6H, 8 + 8'), 1.73 (*m*, 6H, 6 + 6'), 1.52 (*m*, 6H, 7 + 7').
- **¹³C-NMR (CDCl₃, 100 MHz):** δ [ppm]= 163.9, 163.9, 163.4, 163.4 (6C, 2/2'/4/4'), 147.3, 147.3, 146.9, 146.8, 146.7, 146.7, 146.4, 145.7, 145.7, 145.6, 145.2, 145.0, 144.4, 143.6, 143.5, 142.9, 142.4, 142.4, 141.8, 141.7, 141.7, 141.7, 141.7, 141.0, 141.0 (54C, C₆₀-sp²), 70.8, 70.0 (6C, C₆₀-sp³), 66.7 (3C, 5 + 5'), 53.8 (1C, 1'), 53.8 (2C, 1), 52.7 (3C, 3 + 3'), 33.3 (3C, 9 + 9'), 32.1 (1C, 8'), 32.1 (2C, 8), 27.7 (1C, 6'), 27.6 (2C, 6), 24.6 (1C, 7'), 24.5 (2C, 7).
- **MS (MALDI-TOF, DCTB):** m/z = 1512 [M]⁺.
- **HiRes-MS (ESI-TOF):** m/z = calc. for C₈₇H₃₉O₁₂Br₃Na: 1534.98839; found: 1534.98787 (Δ = - 0.3 ppm).
- **IR (neat):** $\bar{\nu}$ [cm⁻¹]: 2924, 2853, 1741, 1454, 1433, 1391, 1234, 1213, 1103, 1065, 1016, 986, 732, 704, 667.
- **UV/Vis (DCM):** λ_{max} [nm]: 251, 282, 303 (sh), 380, 484, 564 (sh).

***polar*-Tris-6-bromohexyl-*eq*-trimethyl-*e,e,e*-trisadduct 100 & *polar*-Bis-(6-bromohexyl)-methyl-*eq*-6-bromohexyl-dimethyl-*e,e,e*-trisadduct 101:**

Compounds **100** and **101** were synthesized according to **GP IV** from 24.0 mg (17.0 μmol ; 1 eq.) trisadduct-mixture **84** & **85**, 0.10 mL (0.116 g; 0.758 mmol; 45 eq.) TMSBr and 0.10 mL (0.102 g; 0.669 mmol; 39 eq.) DBU in 10 mL HPLC-grade CHCl_3 . The reaction mixture was refluxed for 45 minutes. The products were purified by column chromatography (silica; toluene : DCM = 1 : 1; $R_f(\mathbf{100}) = 0.29$; $R_f(\mathbf{101}) = 0.15$).

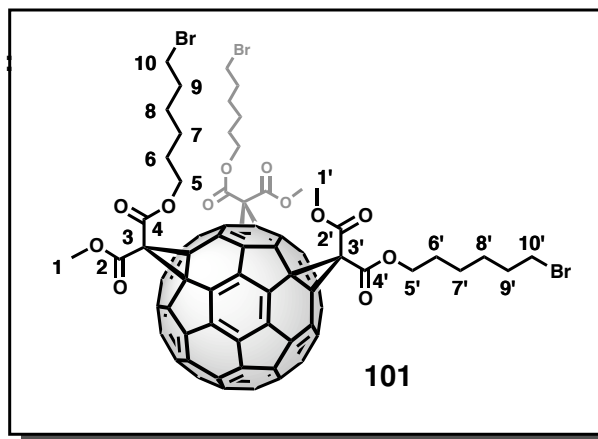
***polar*-Tris-6-bromohexyl-*eq*-trimethyl-*e,e,e*-trisadduct 100:** Red solid; Yield: 8.7 mg (5.58 μmol), 33 % corresponding to trisadducts **84** & **85**.

- **Empirical Formula:** $\text{C}_{90}\text{H}_{45}\text{O}_{12}\text{Br}_3$
- **Molecular Weight:** M_w [g/mol] = 1558.03.
- **^1H -NMR (CDCl_3 , 400 MHz):** δ [ppm]= 4.27 (*m*, 6H, **5**), 3.91 (*s*, 9H, **1**), 3.39 (*t*, $^3J = 6.7$ Hz, 6H, **10**), 1.83 (*m*, 6H, **9**), 1.70 (*m*, 6H, **6**), 1.45 (*m*, 6H, **8**), 1.36 (*m*, 6H, **7**).
- **^{13}C -NMR (CDCl_3 , 100 MHz):** δ [ppm]= 163.8, 163.3 (6C, **2/4**), 147.2, 146.8, 146.7, 146.6, 146.5, 146.5, 146.3, 145.6, 145.5, 145.1, 144.9, 144.3, 143.5, 142.9, 142.3, 141.6, 141.6, 141.0 (54C, $\text{C}_{60}\text{-sp}^2$), 70.8, 70.0 (6C, $\text{C}_{60}\text{-sp}^3$), 66.9 (3C, **5**), 53.7 (3C, **1**), 52.8 (3C, **3**), 33.6 (3C, **10**), 32.5 (3C, **9**), 28.2 (3C, **6**), 27.6 (3C, **8**), 25.0 (3C, **7**).
- **MS (MALDI-TOF, DCTB):** $m/z = 1554$ [M] $^+$.
- **HiRes-MS (ESI-TOF):** $m/z = \text{calc. for } \text{C}_{90}\text{H}_{45}\text{O}_{12}\text{Br}_3\text{Na}: 1577.03534$; found: 1577.05100 ($\Delta = 2.1$ ppm); calc. for $\text{C}_{90}\text{H}_{45}\text{O}_{12}\text{Br}_3\text{K}: 1593.00927$; found: 1593.01051 ($\Delta = 0.8$ ppm).
- **IR (neat):** $\bar{\nu}$ [cm^{-1}]: 2928, 2855, 1740, 1454, 1433, 1390, 1279, 1234, 1213, 1103, 1065, 1013, 986, 908, 728, 666.
- **UV/Vis (DCM):** λ_{max} [nm]: 251, 282, 303 (sh), 380, 483, 564 (sh).



polar-Bis-(6-bromohexyl)-methyl-*eq*-6-bromohexyl-dimethyl-*e,e,e*-trisadduct 101

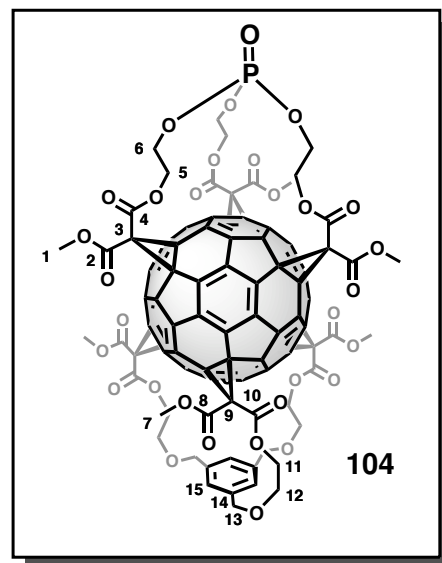
Red solid; Yield: 8.3 mg (5.32 μmol), 31 % corresponding to trisadducts **84** & **85**.



- **Empirical Formula:** $\text{C}_{90}\text{H}_{45}\text{O}_{12}\text{Br}_3$
- **Molecular Weight:** M_w [g/mol] = 1558.03.
- **^1H -NMR (CDCl_3 , 400 MHz):** δ [ppm]= 4.34 (*m*, 2H, **5'**), 4.26 (*m*, 4H, **5**), 3.92, 3.91 (2 x *s*, 6H, **1**), 3.86 (*s*, 3H, **1'**), 3.39 (*t*, $^3J = 6.7$ Hz, 4H, **10**), 3.38 (*t*, $^3J = 6.8$ Hz, 2H, **10'**), 1.83 (*m*, 6H, **9** + **9'**), 1.72 (*m*, 6H, **6** + **6'**), 1.46 (*m*, 6H, **8** + **8'**), 1.38 (*m*, 6H, **7** + **7'**).
- **^{13}C -NMR (CDCl_3 , 100 MHz):** δ [ppm]= 163.8, 163.8, 163.3, 163.3 (6C, **2/2'/4/4'**), 147.3, 147.2, 146.8, 146.7, 146.6, 146.6, 146.5, 146.5, 146.3, 145.6, 145.5, 145.1, 144.9, 144.3, 143.5, 143.4, 142.9, 142.9, 142.3, 141.7, 141.6, 141.0, 140.9 (54C, $\text{C}_{60}\text{-sp}^2$), 70.8, 70.0 (6C, $\text{C}_{60}\text{-sp}^3$), 66.9 (3C, **5** + **5'**), 53.7 (1C, **1'**), 53.7 (2C, **1**), 52.8 (3C, **3** + **3'**), 33.6 (3C, **10** + **10'**), 32.6 (1C, **9'**), 32.5 (2C, **9**), 28.3 (1C, **6'**), 28.2 (2C, **6**), 27.7 (1C, **8'**), 27.6 (2C, **8**), 25.1 (1C, **7'**), 25.0 (2C, **7**).
- **MS (MALDI-TOF, DCTB):** $m/z = 1554$ [M] $^+$.
- **HiRes-MS (ESI-TOF):** $m/z = \text{calc. for } \text{C}_{90}\text{H}_{45}\text{O}_{12}\text{Br}_3\text{Na}: 1577.0353; \text{found: } 1577.0408$ ($\Delta = -3.5$ ppm).
- **IR (neat):** $\bar{\nu}$ [cm^{-1}]: 2930, 2856, 1740, 1454, 1433, 1390, 1345, 1233, 1213, 1103, 1065, 1013, 985, 907, 714, 704, 666.
- **UV/Vis (DCM):** λ_{max} [nm]: 251, 282, 303 (sh), 379, 483, 564 (sh).

***polar*-Tris-(2-ethyl)-phosphate-*polar*'-1',3',5'-tris-(2''-ethoxy)methylbenzene-1',3',5'-triy-*eq,eq'*-hexamethyl-[3:3]-hexakisadduct 104:**

Hexakisadduct **104** was synthesized according to **GP V** from 33.0 mg (26.5 μmol ; 1 eq.) phosphate-trisadduct **59**, 24.0 mg (40.0 μmol ; 1.5 eq.) 1,3,5-tris-(2'-methylmalonyl)ethoxymethylbenzene **45**, 80 mg (0.241 mmol; 9 eq.) CBr_4 and 25.0 μL (25.5 mg; 0.167 mmol; 6.3 eq.) DBU in HPLC-grade DCM (40 + 15 mL). The reaction mixture was stirred overnight. The product was purified by column chromatography on silica, at first with DCM : THF = 10 : 1 and then with DCM : MeOH = 98 : 2 (R_f = 0.15).



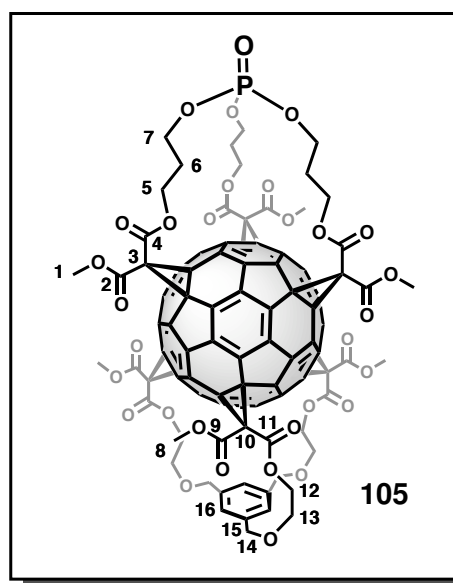
***polar*-Tris-(2-ethyl)-phosphate-*polar*'-1',3',5'-tris-(2''-ethoxy)methylbenzene-1',3',5'-triy-*eq,eq'*-hexamethyl-[3:3]-hexakisadduct 104:** Yellow-orange solid; Yield: 11 mg (5.98 μmol), 23 % corresponding to trisadduct **59**.

- **Empirical Formula:** $\text{C}_{105}\text{H}_{51}\text{O}_{31}\text{P}$
- **Molecular Weight:** M_w [g/mol] = 1839.48.
- **^1H -NMR (CDCl_3 , 400 MHz):** δ [ppm]= 7.09 (s, 3H, **15**), 4.80 (m, 3H, **5**), 4.66 (m, 3H, **11**), 4.46 (m, 6H, **13**), 4.25 (m, 3H, **11'**), 4.19 (m, 6H, **6**), 4.07 (m, 3H, **5'**), 3.86 (s, 18H, **1 + 7**), 3.65 (m, 6H, **12**).
- **^{13}C -NMR (CDCl_3 , 100 MHz):** δ [ppm]= 164.3, 164.2, 163.6, 163.3 (12C, **2/4/8/10**), 147.5, 147.2, 146.0, 145.7, 145.6, 145.5, 144.6, 143.4, 142.4, 142.2, 141.5, 141.1, 140.8, 140.8, 139.5, 139.4 (48C, $\text{C}_{60}\text{-sp}^2$), 137.8 (3C, **14**), 126.1 (3C, **15**), 72.4 (3C, **13**), 69.3, 69.2, 68.9, 68.8 (12C, $\text{C}_{60}\text{-sp}^3$), 67.3 (3C, **12**), 65.1 (3C, **11**), 64.8 (d, $^2J_{\text{C-P}}$ = 3.4 Hz, 3C, **6**), 64.6 (d, $^3J_{\text{C-P}}$ = 11.9 Hz, 3C, **5**), 53.7, 53.7 (6C, **1/7**), 45.3 (6C, **3 + 9**).
- **^{31}P -NMR (CDCl_3 , 162 MHz):** δ [ppm]= - 1.61.
- **MS (MALDI-TOF, DCTB):** m/z = 1839 [M + H] $^+$.

- **HiRes-MS (ESI-TOF):** m/z = calc. for $C_{105}H_{51}O_{31}PNa$: 1861.20441; found: 1861.20167 (Δ = - 1.5 ppm).
- **IR (neat):** $\bar{\nu}$ [cm^{-1}]: 2952, 1741, 1435, 1370, 1251, 1215, 1047, 985, 851, 823, 714, 669.
- **UV/Vis (DCM):** λ_{max} [nm]: 244, 271, 281, 315, 333.

***polar*-Tris-(3-propyl)-phosphate-*polar*'-1',3',5'-tris-(2''-ethoxy)methylbenzene-1',3',5'-triyl-*eq,eq*'-hexamethyl-[3:3]-hexakisadduct 105:**

Hexakisadduct **105** was synthesized according to **GP V** from 57.0 mg (44.3 μ mol; 1 eq.) phosphate-trisadduct **73**, 40.0 mg (66.4 μ mol; 1.5 eq.) 1,3,5-tris-(2'-methylmalonyl)ethoxymethylbenzene **45**, 130 mg (0.392 mmol; 8.9 eq.) CBr_4 and 60.0 μ L (61.0 mg; 0.402 mmol; 9.1 eq.) DBU in HPLC-grade DCM (70 + 25 mL). The reaction mixture was stirred overnight. The product was purified by column chromatography on silica, at first with DCM : THF = 10 : 1 and then with DCM : MeOH = 98 : 2 (R_f = 0.17).



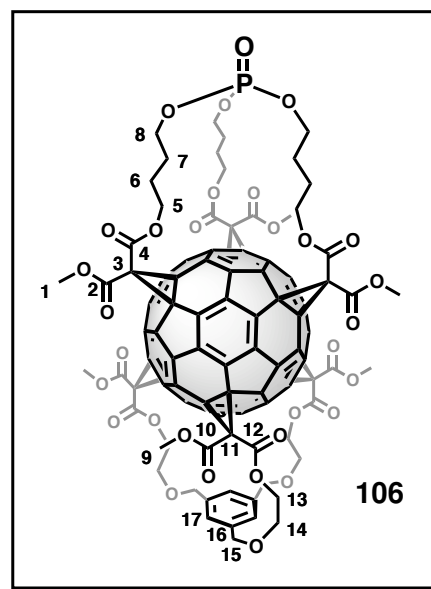
***polar*-Tris-(3-propyl)-phosphate-*polar*'-1',3',5'-tris-(2''-ethoxy)methylbenzene-1',3',5'-triyl-*eq,eq*'-hexamethyl-[3:3]-hexakisadduct 105:** Yellow-orange solid; Yield: 6 mg (3.19 μ mol), 7 % corresponding to trisadduct **73**.

- **Empirical Formula:** $C_{108}H_{57}O_{31}P$
- **Molecular Weight:** M_w [g/mol] = 1881.56.
- **1H -NMR ($CDCl_3$, 400 MHz):** δ [ppm]= 7.09 (s, 3H, **16**), 4.65 (m, 3H, **12**), 4.46 (m, 6H, **14**), 4.28 (m, 9H, **5** + **12'**), 4.09 (m, 3H, **7**), 3.87, 3.86 (2 x s, 18H, **1/8**), 3.84 (m, 3H, **7'**), 3.65 (m, 6H, **13**), 2.05 (m, 6H, **6**).

- **^{13}C -NMR (CDCl_3 , 100 MHz):** δ [ppm]= 164.1, 164.0, 163.6, 163.1 (12C, **2/4/9/11**), 146.8 (2x), 146.0, 145.7, 145.6, 145.4, 144.3, 144.2, 142.5, 142.0, 141.5, 141.1, 141.1, 140.9, 139.8, 139.6 (48C, C_{60} - sp^2), 137.7 (3C, **15**), 126.2 (3C, **16**), 72.4 (3C, **14**), 69.1, 69.1 (2x), 68.9 (12C, C_{60} - sp^3), 67.3 (3C, **13**), 65.2 (3C, **12**), 63.5 (d , $^2J_{\text{C-P}} = 5.8$ Hz, 3C, **7**), 62.2 (3C, **5**), 53.8, 53.7 (6C, **1/8**), 45.3, 45.3 (6C, **3/10**), 29.0 (d , $^3J_{\text{C-P}} = 5.9$ Hz, 3C, **6**).
- **^{31}P -NMR (CDCl_3 , 162 MHz):** δ [ppm]= - 1.20.
- **MS (MALDI-TOF, DCTB):** $m/z = 1880$ $[\text{M}]^+$.
- **HiRes-MS (ESI-TOF):** $m/z = \text{calc. for } \text{C}_{108}\text{H}_{57}\text{O}_{31}\text{PNa}: 1903.2514$; found: 1903.2449 ($\Delta = - 3.4$ ppm).
- **IR (neat):** $\bar{\nu}$ [cm^{-1}]: 2955, 2853, 1743, 1435, 1355, 1260, 1214, 1078, 1036, 1014, 863, 803, 713, 668.
- **UV/Vis (DCM):** λ_{max} [nm]: 244, 273, 281, 315, 334.

***polar*-Tris-(4-butyl)-phosphate-*polar'*-1',3',5'-tris-(2''-ethoxy)methylbenzene-1',3',5'-triyl-*eq,eq'*-hexamethyl-[3:3]-hexakisadduct **106**:**

Hexakisadduct **106** was synthesized according to **GP V** from 76.0 mg (57.2 μmol ; 1 eq.) phosphate-trisadduct **78**, 52.0 mg (58.8 μmol ; 1.5 eq.) 1,3,5-tris-(2'-methylmalonyl)ethoxymethylbenzene **45**, 350 mg (1.06 mmol; 18 eq.) CBr_4 and 120 μL (122 mg; 0.803 mmol; 14 eq.) DBU in HPLC-grade DCM (100 + 40 mL). The reaction mixture was stirred overnight. The product was purified by column chromatography on silica, at first with DCM : THF = 10 : 1 and then with DCM : MeOH = 98 : 2 ($R_f = 0.16$).

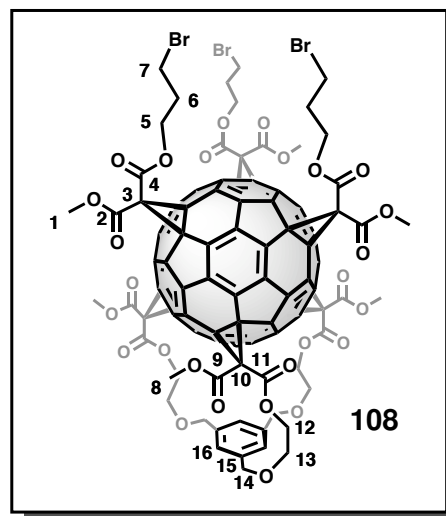


polar-Tris-(4-butoxy)-phosphate-polar'-1,3,5-tris-(2'-ethoxy)benzene-1,3,5-triyl-eq,eq'-hexamethyl-[3:3]-hexakisadduct 106: Yellow-orange solid; Yield: 10 mg (5.20 μmol), 9 % corresponding to trisadduct **78**.

- **Empirical Formula:** $\text{C}_{111}\text{H}_{63}\text{O}_{31}\text{P}$
- **Molecular Weight:** M_w [g/mol] = 1923.64.
- **^1H -NMR (CDCl_3 , 400 MHz):** δ [ppm]= 7.09 (s, 3H, **17**), 4.64 (m, 3H, **13**), 4.51 (m, 3H, **5**), 4.46 (m, 6H, **15**), 4.25 (m, 3H, **13'**), 4.05 (m, 3H, **5'**), 3.96 (m, 3H, **8**), 3.90 (m, 3H, **8'**), 3.86, 3.86 (2 x s, 18H, **1/9**), 3.65 (m, 6H, **14**), 1.70 (m, 6H, **6**), 1.63 (m, 6H, **7**).
- **^{13}C -NMR (CDCl_3 , 100 MHz):** δ [ppm]= 164.2, 164.1, 163.6, 163.5 (12C, **2/4/10/12**), 146.1, 145.9, 145.9, 145.7, 145.6, 145.4, 145.3, 144.9, 141.9, 141.5, 141.1 (2x), 141.0, 140.8, 140.6, 140.3 (48C, $\text{C}_{60}\text{-sp}^2$), 137.7 (3C, **16**), 126.2 (3C, **17**), 72.4 (3C, **15**), 69.1, 69.1, 68.9, 68.9 (12C, $\text{C}_{60}\text{-sp}^3$), 67.3 (3C, **14**), 67.0 (d, $^2J_{\text{C-P}} = 6.2$ Hz, 3C, **8**), 65.7 (3C, **5**), 65.2 (3C, **13**), 53.7, 53.7 (6C, **1/9**), 45.3, 45.3 (6C, **3/11**), 25.9 (d, $^3J_{\text{C-P}} = 7.3$ Hz, 3C, **7**), 25.0 (3C, **6**).
- **^{31}P -NMR (CDCl_3 , 162 MHz):** δ [ppm]= - 1.62.
- **MS (MALDI-TOF, DCTB):** $m/z = 1923$ [M + H] $^+$.
- **HiRes-MS (ESI-TOF):** $m/z = \text{calc. for } \text{C}_{111}\text{H}_{63}\text{O}_{31}\text{PNa}: 1945.2983$; found: 1945.3007 ($\Delta = 1.2$ ppm).
- **IR (neat):** $\bar{\nu}$ [cm^{-1}]: 2954, 1741, 1435, 1397, 1354, 1260, 1210, 1078, 997, 856, 753, 712, 667.
- **UV/Vis (DCM):** λ_{max} [nm]: 244, 273, 281, 315, 334.

***polar*-Tris-3-bromopropyl-*polar'*-1',3',5'-tris-(2''-ethoxy)methylbenzene-1',3',5'-triyl-*eq,eq'*-hexamethyl-[3:3]-hexakisadduct 108:**

Hexakisadduct **108** was synthesized according to **GP V** from 25.0 mg (17.5 μmol ; 1 eq.) bromoalkyl-trisadduct **96**, 17.0 mg (28.3 μmol ; 1.5 eq.) 1,3,5-tris-(2'-methylmalonyl)ethoxymethylbenzene **45**, 41.0 mg (0.124 mmol; 7.1 eq.) CBr_4 and 25.0 μL (25.5 mg; 0.167 mmol; 9.6 eq.) DBU in HPLC-grade DCM (40 + 15 mL). The reaction mixture was stirred for two days. The product was purified by column chromatography (silica; DCM : THF = 98 : 2; R_f = 0.36).



***polar*-Tris-3-bromopropyl-*polar'*-1',3',5'-tris-(2''-ethoxy)methylbenzene-1',3',5'-triyl-*eq,eq'*-hexamethyl-[3:3]-hexakisadduct 108:** Yellow-orange solid; Yield: 3.8 mg (1.88 μmol), 11 % corresponding to trisadduct **96**.

- **Empirical Formula:** $\text{C}_{108}\text{H}_{57}\text{O}_{27}\text{Br}_3$
- **Molecular Weight:** M_w [g/mol] = 2026.30.
- **^1H -NMR (CDCl_3 , 500 MHz):** δ [ppm]= 7.09 (s, 3H, **16**), 4.66 (m, 3H, **12**), 4.46 (m, 6H, **14**), 4.40 (t, $^3J = 5.9$ Hz, 6H, **5**), 4.26 (m, 3H, **12'**), 3.86, 3.86 (2 x s, 18H, **1/8**), 3.65 (m, 6H, **13**), 3.42 (t, $^3J = 6.4$ Hz, 6H, **7**), 2.21 (m, 6H, **6**).
- **^{13}C -NMR (CDCl_3 , 125 MHz):** δ [ppm]= 164.2, 164.1, 163.6, 163.5 (12C, **2/4/9/11**), 146.0, 145.9, 145.7 (2x), 145.6, 145.6, 145.5, 145.5, 141.4, 141.1, 141.0 (2x), 141.0, 140.8, 140.8, 140.7 (48C, $\text{C}_{60}\text{-sp}^2$), 137.8 (3C, **15**), 126.1 (3C, **16**), 72.4 (3C, **14**), 69.0, 69.0, 68.9, 68.9 (12C, $\text{C}_{60}\text{-sp}^3$), 67.3 (3C, **13**), 65.2 (3C, **12**), 64.5 (3C, **5**), 53.7 (6C, **1 + 8**), 45.2, 45.1 (6C, **3/10**), 31.3 (3C, **6**), 29.0 (3C, **7**).
- **MS (MALDI-TOF, DCTB):** $m/z = 2022$ $[\text{M}]^+$.
- **HiRes-MS (ESI-TOF):** $m/z = \text{calc. for } \text{C}_{108}\text{H}_{57}\text{O}_{27}\text{Br}_3\text{Na}: 2045.05296; \text{found}: 2045.04520$ ($\Delta = -3.8$ ppm).

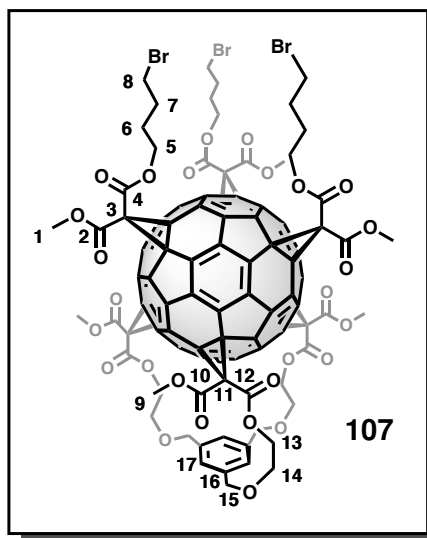
- **IR (neat):** $\bar{\nu}$ [cm^{-1}]: 2952, 2853, 1742, 1434, 1354, 1261, 1214, 1077, 998, 758, 713, 669.
- **UV/Vis (DCM):** λ_{max} [nm]: 245, 273, 281, 315, 333.

***polar*-Tris-4-bromobutyl-*polar*'-1',3',5'-tris-(2''-ethoxy)methylbenzene-1',3',5'-triyl-*eq,eq*'-hexamethyl-[3:3]-hexakisadduct 107:**

Hexakisadduct **107** was synthesized by two different methods.

Method 1:

107 can be synthesized according to **GP V** from 43.0 mg (29.2 μmol ; 1 eq.) bromoalkyl-trisadduct **97**, 26.0 mg (43.3 μmol ; 1.5 eq.) 1,3,5-tris-(2'-methylmalonyl)ethoxymethylbenzene **45**, 90.0 mg (0.271 mmol; 9.3 eq.) CBr_4 and 40.0 μL (40.8 mg; 0.264 mmol; 9.2 eq.) DBU in HPLC-grade DCM (45 + 20 mL). The reaction mixture was stirred for two days. The product was purified by column chromatography (silica; DCM : THF = 98 : 2; R_f = 0.35).



Method 2:

107 can also be synthesized according to **GP IV** from 10.0 mg (5.20 μmol ; 1 eq.) hexakisadduct **106**, 0.05 mL (58.0 mg; 0.379 mmol; 73 eq.) TMSBr and 0.05 mL (51.0 mg; 0.335 mmol; 64 eq.) DBU in 10 mL HPLC-grade CHCl_3 . The reaction mixture was refluxed for 2 hours. The product was purified by column chromatography (silica; DCM : THF = 98 : 2; R_f = 0.35).

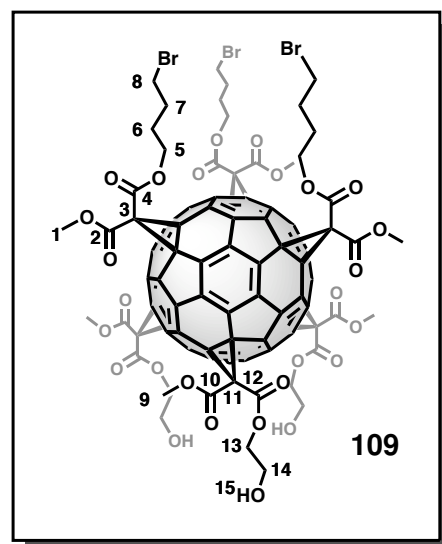
***polar*-Tris-4-bromobutyl-*polar*'-1',3',5'-tris-(2''-ethoxy)methylbenzene-1',3',5'-triyl-*eq,eq*'-hexamethyl-[3:3]-hexakisadduct 107:** Yellow-orange solid; Yield: Method 1: 7.5 mg (3.63 μmol), 12 % corresponding to trisadduct **97**; Method 2: 5.0 mg (2.41 μmol), 47 % corresponding to hexakisadduct **106**.

- **Empirical Formula:** $\text{C}_{111}\text{H}_{63}\text{O}_{27}\text{Br}_3$
- **Molecular Weight:** M_w [g/mol] = 2068.38.

- **^1H -NMR (CDCl_3 , 400 MHz):** δ [ppm]= 7.09 (s, 3H, **17**), 4.66 (m, 3H, **13**), 4.46 (m, 6H, **15**), 4.29 (t, $^3J = 5.9$ Hz, 6H, **5**), 4.25 (m, 3H, **13'**), 3.86, 3.85 (2 x s, 18H, **1/9**), 3.65 (m, 6H, **14**), 3.39 (t, $^3J = 6.4$ Hz, 6H, **8**), 1.92 (m, 6H, **7**), 1.83 (m, 6H, **6**).
- **^{13}C -NMR (CDCl_3 , 100 MHz):** δ [ppm]= 164.3, 164.3, 163.8, 163.8 (12C, **2/4/10/12**), 146.0, 146.0, 145.8, 145.8, 145.7, 145.6, 145.6, 145.5, 141.5, 141.1, 141.1, 141.1, 141.1, 141.0 (2x), 140.7, (48C, $\text{C}_{60}\text{-sp}^2$), 137.8 (3C, **16**), 126.2 (3C, **17**), 72.4 (3C, **15**), 69.0, 69.0, 69.0, 68.9 (12C, $\text{C}_{60}\text{-sp}^3$), 67.3 (3C, **14**), 65.9 (3C, **5**), 64.2 (3C, **13**), 53.7, 53.7 (6C, **1/9**), 45.2 (6C, **3 + 11**), 32.8 (3C, **8**), 29.0 (3C, **7**), 27.1 (3C, **6**).
- **MS (MALDI-TOF, DCTB):** $m/z = 2065$ $[\text{M} + \text{H}]^+$.
- **HiRes-MS (ESI-TOF):** $m/z = \text{calc. for } \text{C}_{111}\text{H}_{63}\text{O}_{27}\text{Br}_3\text{Na}: 2087.0999$; found: 2088.1006 ($\Delta = 0.0$ ppm).
- **IR (neat):** $\bar{\nu}$ [cm^{-1}]: 2951, 1741, 1434, 1397, 1353, 1261, 1213, 1077, 1041, 996, 758, 713, 669.
- **UV/Vis (DCM):** λ_{max} [nm]: 245, 273, 281, 315, 334.

***polar*-Tris-4-bromobutyl-*polar'*-tris-2'-hydroxyethyl-*eq,eq'*-hexamethyl-[3:3]-hexakisadduct **109**:**

A 50-mL two-necked round-bottom Schlenk flask equipped with a dropping-funnel was heat-dried and filled with nitrogen. 11 mg (5.32 μmol ; 1 eq.) hexakis-adduct **109** were dissolved in 8 mL dry DCM and cooled with an ice-bath. 0.05 mL (50 μmol ; 9 eq.) of a 1 M solution of BCl_3 in DCM was diluted with 6 mL dry DCM in the dropping funnel and added dropwise to the stirred solution. A saturated solution of sodium hydrogen carbonate was added after 3 hours to hydrolyze the reaction and the mixture was stirred for another 30 minutes. The phases were separated, the organic phase was washed with water and dried over magnesium sulfate. The raw product was purified by column chromatography (silica; DCM :



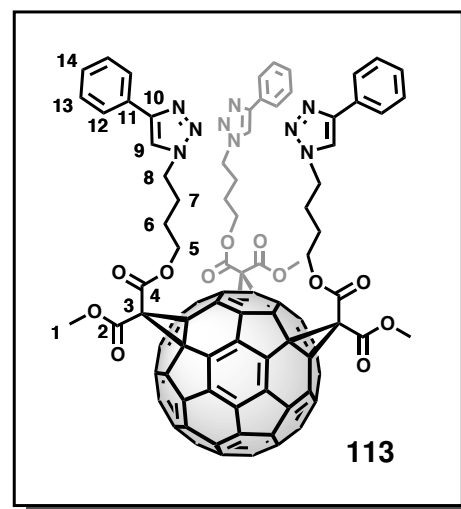
MeOH = 95 : 5; R_f = 0.27) and reprecipitated from CHCl_3 /pentane.

polar-Tris-4-bromobutyl-polar'-tris-2'-hydroxyethyl-eq,eq'-hexamethyl-[3:3]-hexakis-adduct 109: Yellow-orange solid; Yield: 5.8 mg (2.97 μmol), 56 % corresponding to hexakis-adduct **107**.

- **Empirical Formula:** $\text{C}_{102}\text{H}_{57}\text{O}_{27}\text{Br}_3$
- **Molecular Weight:** M_w [g/mol] = 1954.24.
- **^1H -NMR (CDCl_3 , 400 MHz):** δ [ppm]= 4.51 (*m*, 3H, **13**), 4.31 (*m*, 6H, **5**), 4.26 (*m*, 3H, **13'**), 3.87, 3.87 (2 x *s*, 18H, **1/9**), 3.81 (*m*, 6H, **14**), 3.41 (*t*, 3J = 6.3 Hz, 6H, **8**), 2.41 (*s br*, 3H, **15**), 1.93 (*m*, 6H, **7**), 1.85 (*m*, 6H, **6**).
- **^{13}C -NMR (CDCl_3 , 100 MHz):** δ [ppm]= 164.3, 164.1, 163.8, 163.7 (12C, **2/4/10/12**), 146.3, 146.3, 145.8 (3x), 145.7, 145.2, 145.0, 141.6, 141.5, 141.3, 141.2, 141.1, 141.1, 140.7, 140.6 (48C, $\text{C}_{60}\text{-sp}^2$), 69.1, 69.1 (2x), 69.0 (12C, $\text{C}_{60}\text{-sp}^3$), 68.2 (3C, **13**), 66.0 (3C, **5**), 60.6 (3C, **14**), 53.8, 53.8 (6C, **1/9**), 45.4, 45.3 (6C, **3/11**), 32.8 (3C, **8**), 29.1 (3C, **7**), 27.2 (3C, **6**).
- **MS (MALDI-TOF, DCTB):** m/z = 1950 $[\text{M}]^+$, 1973 $[\text{M} + \text{Na}]^+$, 1989 $[\text{M} + \text{K}]^+$.
- **HiRes-MS (ESI-TOF):** m/z = calc. for $\text{C}_{102}\text{H}_{57}\text{O}_{27}\text{Br}_3\text{Na}$: 1973.05296; found: 1973.05578 (Δ = 1.4 ppm).
- **IR (neat):** $\bar{\nu}$ [cm^{-1}]: 3566, 2953, 1740, 1434, 1397, 1353, 1263, 1219, 1077, 1041, 998, 913, 759, 713, 669.
- **UV/Vis (DCM):** λ_{max} [nm]: 245, 272, 281, 316, 334.

polar-Tris-(4-(4'-phenyl-1'H-1',2',3'-triazol-1'-yl)butyl)-eq-trimethyl-e,e,e-trisadduct 113:

10.0 mg (6.78 μmol ; 1 eq.) bromobutyl-trisadduct **97** were dissolved in 4 mL DMF in a 25-mL round-bottom Schlenk flask under nitrogen atmosphere. 2.6 mg (40.7 μmol ; 6 eq.) NaN_3 dissolved in 4 mL DMF were added and the reaction mixture was stirred at room temperature for three hours until TLC control (silica; DCM) showed complete conversion. Water was added until a red precipitate formed, the solution was subsequently centrifuged and washed with water. The solid was taken up in 7 mL DCM, transferred to a round-bottom Schlenk flask and 4 mL



EtOH and 10 μL (9.30 mg; 77.4 μmol ; 11.4 eq.) phenylacetylene were added. 0.2 mg (0.68 μmol ; 0.1 eq.) $\text{CuSO}_4 \cdot 5\text{H}_2\text{O}$ and 0.4 mg (2.04 μmol ; 0.3 eq.) sodium ascorbate were separately dissolved in 3 mL water each, then mixed until a yellowish suspension had formed. Subsequently, it was added to the reaction mixture. It was stirred under exclusion of light and monitored by TLC (silica; DCM : THF = 95 : 5). After one night no more reactant could be observed. The phases were separated, the organic phase was washed with water and dried over magnesium sulfate. The raw product was purified by flash column chromatography (silica; DCM : THF = 10 : 1; R_f = 0.42) and finally reprecipitated from CHCl_3 /pentane.

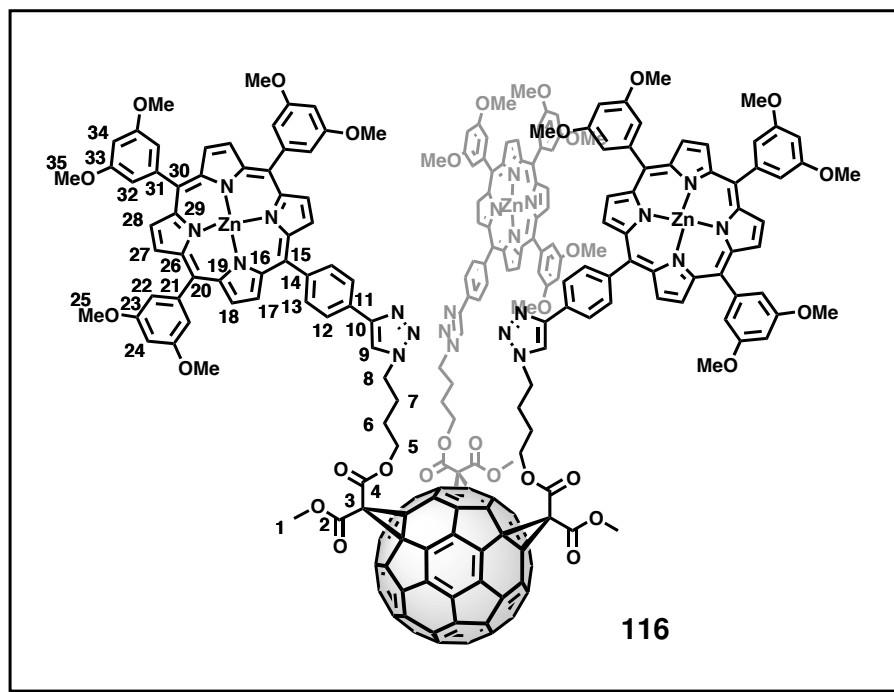
polar-Tris-(4-(4'-phenyl-1'H-1',2',3'-triazol-1'-yl)butyl)-eq-trimethyl-e,e,e-trisadduct 113:
Red solid; Yield: 3.9 mg (2.34 μmol), 36 % corresponding to trisadduct **97**.

- **Empirical Formula:** $\text{C}_{108}\text{H}_{51}\text{O}_{12}\text{N}_9$
- **Molecular Weight:** M_w [g/mol] = 1666.61.
- **^1H -NMR (CDCl_3 , 400 MHz):** δ [ppm]= 7.80 (*m*, 6H, **12**), 7.75 (*s*, 3H, **9**), 7.39 (*m*, 6H, **13**), 7.30 (*m*, 3H, **14**), 4.37 (*t*, 3J = 7.0 Hz, 6H, **8**), 4.26 (*t*, 3J = 6.1 Hz, 6H, **5**), 3.88 (*s*, 9H, **1**), 1.97 (*m*, 6H, **7**), 1.70 (*m*, 6H, **6**).
- **^{13}C -NMR (CDCl_3 , 100 MHz):** δ [ppm]= 163.8, 163.3 (6C, **2/4**), 148.0 (3C, **10**), 147.1, 146.9, 146.8, 146.7, 146.6, 146.5, 146.5, 145.8, 145.7, 145.0, 144.6, 144.5, 143.5,

142.7, 142.6, 141.9, 141.8, 141.2 (54C, C₆₀-sp²), 130.6 (3C, **11**), 128.9 (6C, **13**), 128.2 (3C, **14**), 125.8 (6C, **12**), 119.7 (3C, **9**), 70.6, 70.0 (6C, C₆₀-sp³), 66.0 (3C, **5**), 53.4 (3C, **1**), 52.7 (3C, **3**), 49.6 (3C, **8**), 26.8 (3C, **7**), 25.4 (3C, **6**).

- **MS (MALDI-TOF, DCTB):** $m/z = 1665 [M]^+$, $1688 [M + Na]^+$, $1704 [M + K]^+$.
- **HiRes-MS (ESI-TOF):** $m/z = \text{calc. for } C_{108}H_{51}O_{12}N_9Na: 1688.35494; \text{found: } 1688.35363$
($\Delta = -0.8$ ppm).
- **IR (neat):** $\bar{\nu} [cm^{-1}]$: 3136, 2952, 1737, 1459, 1433, 1279, 1236, 1215, 1104, 1067, 909, 816, 763, 728, 695, 669, 647.
- **UV/Vis (DCM):** $\lambda_{\text{max}} [nm]$: 249, 279, 301 (sh), 378, 480, 564 (sh).

***polar*-Tris-(4-(4'-(4''-(10''',15''',20'''-tris(3''',5'''-dimethoxyphenyl)-porphyrinato-zinc(II))-5'''-yl)phenyl-1'*H*-1',2',3'-triazol-1'-yl)butyl)-*eq*-trimethyl-*e,e,e*-trisadduct 116:**



39.0 mg (26.5 μmol ; 1 eq.) bromobutyl-trisadduct **97** were dissolved in 12 mL DMF in a 50-mL round-bottom Schlenk flask under nitrogen atmosphere. 15.0 mg (231 μmol ; 8.7 eq.) NaN_3 were added and the reaction mixture was stirred at room temperature for three hours until TLC control (silica; DCM) showed complete conversion. The solution was diluted with THF, brine was added and the phases were separated. The organic phase was washed with water and the solvent was removed under reduced pressure. The solid was taken up in DCM, transferred to a round-bottom Schlenk flask, 122 mg (138 μmol ; 5.2 eq.) ZnPor **115** were added and DCM was added to obtain a total volume of 14 mL. 1.5 mg (6.01 μmol ; 0.2 eq.) $\text{CuSO}_4 \cdot 5\text{H}_2\text{O}$ and 3.1 mg (15.9 μmol ; 0.6 eq.) sodium ascorbate were separately dissolved in 7 mL water each, then mixed until a yellowish suspension had formed and subsequently added to the reaction mixture. 2 mL EtOH were added in addition to achieve a better mixing of the phases. After one night, some fullerene reactant could still be detected by TLC (silica; DCM), hence more catalyst was added. After another night, there was still some fullerene reactant left, so 12 mL THF were added to prevent a possible aggregation of

the porphyrins, which would reduce their reactivity. After another four hours, no more fullerene reactant could be detected, the phases were separated, the organic layer was washed with water and the solvent was removed under reduced pressure. The raw product was purified by column chromatography (silica) starting with pure DCM to remove excess ZnPor **115**. Some less polar byproducts were removed by changing the eluent to DCM : THF = 95 : 5 and finally the product was eluted with DCM : THF = 10:1 ($R_f = 0.80$). Residual impurities were removed by a second column chromatography (silica; DCM : THF = 95 : 5). Finally the product was reprecipitated from CHCl_3 /pentane.

polar-Tris-(4-(4'-(4''-(10''',15''',20'''-tris(3''',5'''-dimethoxyphenyl)-porphyrinato-zinc(II))-5'''-yl)phenyl-1'H-1',2',3'-triazol-1'-yl)butyl)-eq-trimethyl-e,e,e-trisadduct **116:** Purple solid; Yield: 8.0 mg (2.0 μmol), 8 % corresponding to trisadduct **97**.

- **Empirical Formula:** $\text{C}_{240}\text{H}_{153}\text{O}_{30}\text{N}_{21}\text{Zn}_3$
- **Molecular Weight:** M_w [g/mol] = 4007.05.
- **^1H -NMR (CDCl_3 , 400 MHz):** δ [ppm]= 8.92 (*m*, 18H, **17/18/27/28**), 8.80 (*m*, 6H, **17/18/27/28**), 7.91 (*d*, 6H, $^3J = 8.1$ Hz, **12/13**), 7.52 (*d*, 6H, $^3J = 8.1$ Hz, **12/13**), 7.35 (*s*, 3H, **9**), 7.20 (*d*, $^4J = 2.2$ Hz, 12H, **22**), 7.16 (*d*, $^4J = 2.3$ Hz, 6H, **32**), 6.60 (*t*, $^4J = 2.2$ Hz, 6H, **24**), 6.50 (*t*, $^4J = 2.1$ Hz, 3H, **34**), 4.30 (*m*, 6H, **8**), 4.20 (*m*, 6H, **5**), 3.72 (*m*, 63H, **1 + 25 + 35**), 1.88 (*m*, 6H, **6**), 1.69 (*m*, 6H, **7**).
- **^{13}C -NMR (CDCl_3 , 100 MHz):** δ [ppm]= 163.8, 163.3 (6C, **2/4**), 158.6 (12C, **23**), 158.5 (6C, **33**), 150.1, 150.1, 150.0, 149.9 (24C, **16/19/26/29**), 147.4 (3C, **10**), 147.1, 147.0, 146.6, 146.5 (2x), 146.3, 146.1, 145.6, 145.5, 145.2, 144.8 (33C, $\text{C}_{60}\text{-sp}^2$), 144.7 (6C, **21**), 144.6 (3C, **31**), 144.3, 143.3, 142.6 (2x) 142.6, 141.7 (2x) (21C, $\text{C}_{60}\text{-sp}^2$), 135.0 (3C, **14**), 134.8 (6C, **12/13**), 132.1, 131.8 (24C, **17/18/27/28**), 129.2 (3C, **11**), 123.6 (6C, **12/13**), 120.8 (6C, **20**), 120.7, 120.5 (6C, **15/30**), 119.7 (3C, **9**), 113.8 (18C, **22 + 32**), 99.9 (9C, **24 + 34**), 70.7, 70.0 (6C, $\text{C}_{60}\text{-sp}^3$), 66.1 (3C, **5**), 55.5 (18C, **25 + 35**), 53.8 (3C, **1**), 52.7 (3C, **3**), 49.5 (3C, **8**), 26.8 (3C, **7**), 25.5 (3C, **6**).
- **MS (MALDI-TOF, DCTB):** $m/z = 4000$ [M] $^+$.
- **HiRes-MS (ESI-TOF):** $m/z = \text{calc. for } [\text{C}_{240}\text{H}_{153}\text{O}_{30}\text{N}_{21}\text{Zn}_3\text{Na}_2]^{2+}$: 2022.93755; found: 2022.93639 ($\Delta = -0.6$ ppm).

- **IR (neat):** $\bar{\nu}$ [cm^{-1}]: 2926, 2851, 1743, 1588, 1451, 1419, 1345, 1235, 1202, 1151, 1061, 1025, 998, 936, 795, 761, 719, 694.
- **UV/Vis (toluene):** λ_{max} (ϵ) [nm ($\text{M}^{-1}\text{cm}^{-1}$)]: 303 (81488), 349 (41548), 426 (684967), 514 (7926), 552 (40372), 592 (6442).
- **Emission (toluene, $\lambda_{\text{ex}} = 431 \text{ nm}$):** λ_{max} [nm]: 602, 648.

References

- [1] D. N. Marshall, *Proceedings of the Society of Antiquaries of Scotland* **1976/77**, 180, 40.
- [2] W. Grahn, *Chem. Unserer Zeit* **1981**, 15, 52.
- [3] E. Haeckel, *Kunstformen der Natur*. Prestel Verlag, München, New York **1998**.
- [4] w:en>User:cyp, <http://en.wikipedia.org/wiki/User:Cyp>. New Polyhedra.
- [5] Euclid, *The Thirteen Books of Euclid's Elements*. Dover Publications, New York **1956**.
- [6] P. E. Eaton, T. W. Cole Jr., *J. Am. Chem. Soc.* **1964**, 86, 962.
- [7] P. E. Eaton, T. W. Cole Jr., *J. Am. Chem. Soc.* **1964**, 86, 3157.
- [8] G. Maier, S. Pfriem, U. Schäfer, R. Matusch, *Angew. Chem. Int. Ed. Engl.* **1978**, 17, 520; *Angew. Chem.* **1978**, 90, 552.
- [9] R. J. Ternansky, D. W. Balogh, L. A. Paquette, *J. Am. Chem. Soc.* **1982**, 104, 4503.
- [10] H. W. Kroto, J. R. Heath, S. C. O'Brien, R. F. Curl, R. E. Smalley, *Nature* **1985**, 318, 162.
- [11] E. Osawa, *Kagaku* **1970**, 25, 854.
- [12] Z. Yoshida, Z. Osawa, *Kagakudojin: Kyoto* **1971**, 174.
- [13] E. A. Jackson, B. D. Steinberg, M. Bancu, A. Wakamiya, L. T. Scott, *J. Am. Chem. Soc.* **2007**, 129, 484.
- [14] K. Y. Amsharov, M. A. Kabdulov, M. Jansen, *Angew. Chem. Int. Ed.* **2012**, 51, 4594; *Angew. Chem.* **2012**, 124, 4672.
- [15] H. W. Kroto, *Computers Math. Applic.* **1989**, 17, 417.

-
- [16] H. W. Kroto, *Nature* **1987**, *329*, 529.
- [17] R. C. Haddon, *Science* **1993**, *261*, 1545.
- [18] S. Schein, T. Friedrich, *Proc. Natl. Acad. Sci.* **2008**, *105*, 19142.
- [19] T. G. Schmalz, W. A. Seitz, D. J. Klein, G. E. Hite, *Chem. Phys. Lett.* **1986**, *130*, 203.
- [20] T. G. Schmalz, W. A. Seitz, D. J. Klein, G. E. Hite, *J. Am. Chem. Soc.* **1988**, *110*, 1113.
- [21] P. W. Fowler, R. C. Batten, D. E. Manolopoulos, *J. Chem. Soc., Faraday Trans.* **1991**, *87*, 3103.
- [22] L. Dunsch, S. Yang, *Small* **2007**, *3*, 1298.
- [23] Y.-Z. Tan, S.-Y. Xie, R.-B. Huang, L.-S. Zheng, *Nat. Chem.* **2009**, *1*, 450.
- [24] Y.-Z. Tan, Z.-J. Liao, Z.-Z. Qian, R.-T. Chen, X. Wu, H. Liang, X. Han, F. Zhu, S.-J. Zhou, Z. Zheng, X. Lu, S.-Y. Xie, R.-B. Huang, L.-S. Zheng, *Nat. Mater.* **2008**, *7*, 790.
- [25] Q.-H. Weng, Q. He, T. Liu, H.-Y. Huang, J.-H. Chen, Z.-Y. Gao, S.-Y. Xie, X. Lu, R.-B. Huang, L.-S. Zheng, *J. Am. Chem. Soc.* **2010**, *132*, 15093.
- [26] S.-Y. Xie, F. Gao, X. Lu, R.-B. Huang, C.-R. Wang, X. Zhang, M.-L. Liu, S.-L. Deng, L.-S. Zheng, *Science* **2004**, *304*, 699.
- [27] X. Han, S.-J. Zhou, Y.-Z. Tan, X. Wu, F. Gao, Z.-J. Liao, R.-B. Huang, Y.-Q. Feng, X. Lu, S.-Y. Xie, L.-S. Zheng, *Angew. Chem. Int. Ed.* **2008**, *47*, 5340; *Angew. Chem.* **2008**, *120*, 5420.
- [28] G.-J. Shan, Y.-Z. Tan, T. Zhou, X.-M. Zou, B.-W. Li, C. Xue, C.-X. Chu, S.-Y. Xie, R.-B. Huang, L.-S. Zhen, *Chem. Asian J.* **2012**, *7*, 2036.
- [29] W. Krätschmer, L. D. Lamb, K. Fostiropoulos, D. R. Huffman, *Nature* **1990**, *347*, 354.
- [30] J. M. Hawkins, A. Meyer, T. A. Lewis, S. Loren, F. J. Hollander, *Science* **1991**, *252*, 312.
- [31] C. S. Yannoni, P. P. Bernier, D. S. Bethune, G. Meijer, J. R. Salem, *J. Am. Chem. Soc.* **1991**, *113*, 3190.
-

- [32] M. S. Dresselhaus, G. Dresselhaus, P. C. Eklund, *Science of Fullerenes and Carbon Nanotubes*. Academic Press, San Diego **1996**.
- [33] R. E. Smalley, *Acc. Chem. Res.* **1992**, *25*, 98.
- [34] A. J. Stone, D. J. Wales, *Chem. Phys. Lett.* **1986**, *128*, 501.
- [35] H. Ajie, M. M. Alvarez, S. J. Anz, R. D. Beck, F. Diederich, K. Fostiropoulos, D. R. Huffman, W. Krätschmer, Y. Rubin, *J. Phys. Chem.* **1990**, *94*, 8630.
- [36] F. Diederich, R. L. Whetten, *Acc. Chem. Res.* **1992**, *25*, 119.
- [37] D. M. Rivera-Nazario, J. R. Pinzón, S. Stevenson, L. A. Echegoyen, *J. Phys. Org. Chem.* **2013**, *26*, 194. DOI: 10.1002/poc.3009.
- [38] S. Stevenson, G. Rice, T. Glass, K. Harich, F. Cromer, M. R. Jordan, J. Craft, E. Hadju, R. Bible, M. M. Olmstead, K. Maitra, A. J. Fisher, A. L. Balch, H. C. Dorn, *Nature* **1999**, *401*, 55.
- [39] J. Alford, M. Diener, J. Nabity, M. Karpuk, *U.S. Pat. Appl. Publ.* **2003**, 14.
- [40] C. Thilgen, F. Diederich, R. Whetten, *Buckminsterfullerenes* **1993**, 59.
- [41] M. T. Beck, G. Mandi, *Fullerene Sci. Technol.* **1997**, *5*, 291.
- [42] F. Djojo, A. Herzog, I. Lamparth, F. Hampel, A. Hirsch, *Chem. Eur. J.* **1996**, *2*, 1537.
- [43] F. Djojo, A. Hirsch, S. Grimme, *Eur. J. Org. Chem.* **1999**, 3027.
- [44] A. Hirsch, I. Lamparth, H. R. Karfunkel, *Angew. Chem. Int. Ed. Engl.* **1994**, *33*, 437; *Angew. Chem.* **1994**, *106*, 453.
- [45] G. Rapenne, F. Diederich, J. Crassous, A. Collet, L. Echegoyen, *Chem. Commun.* **1999**, 1121.
- [46] U. Reuther, T. Brandmüller, W. Donaubaue, F. Hampel, A. Hirsch, *Chem. Eur. J.* **2002**, *8*, 2261.
- [47] I. Lamparth, C. Maichle-Mössmer, A. Hirsch, *Angew. Chem. Int. Ed. Engl.* **1995**, *34*, 1607; *Angew. Chem.* **1995**, *107*, 1755.
- [48] S. C. O'Brien, J. R. Heath, R. F. Curl, R. E. Smalley, *J. Chem. Phys.* **1988**, *88*, 220.

- [49] R. C. Haddon, L. E. Brus, K. Raghavachari, *Chem. Phys. Lett.* **1986**, *125*, 459.
- [50] M. Bühl, A. Hirsch, *Chem. Rev.* **2001**, *101*, 1153.
- [51] R. Tycko, G. Dabbagh, M. J. Rosseinsky, D. W. Murphy, R. M. Fleming, A. P. Ramirez, J. C. Tully, *Science* **1991**, *253*, 884.
- [52] Q. Xie, E. Perez-Cordero, L. Echegoyen, *J. Am. Chem. Soc.* **1992**, *114*, 3978.
- [53] Q. Xie, F. Arias, L. Echegoyen, *J. Am. Chem. Soc.* **1993**, *115*, 9818.
- [54] C. Boudon, J.-P. Gisselbrecht, M. Gross, L. Isaacs, H. L. Anderson, R. Faust, F. Diederich, *Helv. Chim. Acta* **1995**, *78*, 1334.
- [55] L. E. Echegoyen, F. D. Djojo, A. Hirsch, L. Echegoyen, *J. Org. Chem.* **2000**, *65*, 4994.
- [56] A. Pasquarello, M. Schlüter, R. C. Haddon, *Science* **1992**, *257*, 1660.
- [57] L. Isaacs, A. Wehrsig, F. Diederich, *Helv. Chim. Acta* **1993**, *76*, 1231.
- [58] A. Hirsch, M. Brettreich, *Fullerenes - Chemistry and Reactions*. Wiley-VCH Verlag, Weinheim **2005**.
- [59] R. C. Haddon, A. F. Hebard, M. J. Rosseinsky, D. W. Murphy, S. J. Duclos, K. B. Lyons, B. Miller, J. M. Rosamilia, R. M. Fleming, A. R. Kortan, S. H. Glarum, A. V. Makhija, A. J. Muller, R. H. Eick, S. M. Zahurak, R. Tycko, G. Dabbagh, F. A. Thiel, *Nature* **1991**, *350*, 320.
- [60] A. F. Hebard, M. J. Rosseinsky, R. C. Haddon, D. W. Murphy, S. H. Glarum, T. T. M. Palstra, A. P. Ramirez, A. R. Kortan, *Nature* **1991**, *350*, 600.
- [61] C. A. Reed, R. D. Bolskar, *Chem. Rev.* **2000**, *100*, 1075.
- [62] M. J. Rosseinsky, *Chem. Mater.* **1998**, *10*, 2665.
- [63] K. Tanigaki, T. W. Ebbesen, S. Saito, J. Mizuki, J. S. Tsai, Y. Kubo, S. Kuroshima, *Nature* **1991**, *352*, 222.
- [64] M. Saunders, H. A. Jimenez-Vazquez, R. J. Cross, S. Mroczkowski, M. L. Gross, D. E. Giblin, R. J. Poreda, *J. Am. Chem. Soc.* **1994**, *116*, 2193.

- [65] M. Saunders, R. J. Cross, H. A. Jimenez-Vazquez, R. Shimshi, A. Khong, *Science* **1996**, *271*, 1693.
- [66] H. Mauser, N. J. R. van Eikema Hommes, T. Clark, A. Hirsch, B. Pietzak, A. Weidinger, L. Dunsch, *Angew. Chem. Int. Ed. Engl.* **1997**, *36*, 2835; *Angew. Chem.* **1997**, *109*, 2858.
- [67] F. Hörmann, A. Hirsch, K. Porfyrakis, G. A. D. Briggs, *Eur. J. Org. Chem.* **2011**, *2011*, 117.
- [68] T. Almeida Murphy, T. Pawlik, A. Weidinger, M. Höhne, R. Alcala, J. M. Spaeth, *Phys. Rev. Lett.* **1996**, *77*, 1075.
- [69] M. Murata, Y. Murata, K. Komatsu, *J. Am. Chem. Soc.* **2006**, *128*, 8024.
- [70] J. C. Hummelen, C. Bellavia-Lund, F. Wudl, *Top. Curr. Chem.* **1999**, *199*, 93.
- [71] T. Guo, C. Jin, R. E. Smalley, *J. Phys. Chem.* **1991**, *95*, 4948.
- [72] P. W. Dunk, A. Rodríguez-Forteza, N. K. Kaiser, H. Shinohara, J. M. Poblet, H. W. Kroto, *Angew. Chem. Int. Ed.* **2013**, *52*, 315; *Angew. Chem.* **2013**, *125*, 333.
- [73] J. Averdung, H. Luftmann, I. Schlachter, J. Mattay, *Tetrahedron* **1995**, *51*, 6977.
- [74] I. Lamparth, B. Nuber, G. Schick, A. Skiebe, T. Grösser, A. Hirsch, *Angew. Chem. Int. Ed. Engl.* **1995**, *34*, 2257; *Angew. Chem.* **1995**, *107*, 2473.
- [75] J. F. Christian, Z. Wan, S. L. Anderson, *Chem. Phys. Lett.* **1992**, *199*, 373.
- [76] J. J. Stry, J. F. Garvey, *Chem. Phys. Lett.* **1995**, *243*, 199.
- [77] C. Möschel, M. Z. Jansen, *Z. Anorg. Allg. Chem.* **1999**, *625*, 175.
- [78] T. Kimura, T. Sugai, H. Shinohara, *Chem. Phys. Lett.* **1996**, *256*, 269.
- [79] M. Pellarin, C. Ray, J. Lerme, J. L. Vialle, M. Broyer, X. Blase, P. Keghelian, P. Melinon, A. Perez, *J. Chem. Phys.* **1999**, *110*, 6927.
- [80] T. Ohtsuki, K. Ohno, K. Shiga, Y. Kawazoe, Y. Maruyama, K. Masumoto, *Phys. Rev. B: Condens. Matter* **1999**, *60*, 1531.

- [81] W. Branz, I. M. L. Billas, N. Malinowski, F. Tast, M. Heinebrodt, T. P. Martin, *J. Chem. Phys.* **1998**, *109*, 3425.
- [82] A. Hayashi, Y. Xie, J. M. Poblet, J. M. Campanera, C. B. Lebrilla, A. L. Balch, *J. Phys. Chem. A* **2004**, *108*, 2192.
- [83] J. C. Hummelen, B. Knight, J. Pavlovich, R. Gonzalez, F. Wudl, *Science* **1995**, *269*, 1554.
- [84] B. Nuber, A. Hirsch, *Chem. Commun.* **1996**, 1421.
- [85] U. Reuther, *Evaluation of synthetic pathways for the heterofullerene $C_{58}N_2$ and introduction of the first concept for a completely regioselective control of multiple adduct formation of C_{60}* , Dissertation, Friedrich-Alexander-Universität, Erlangen-Nürnberg (Germany), **2001**.
- [86] M. von Delius, F. Hauke, A. Hirsch, *Eur. J. Org. Chem.* **2008**, 4109.
- [87] A. Gmehling, *Synthesis of $C_{58}N_2$* , Master's thesis, Friedrich-Alexander-Universität, Erlangen-Nürnberg (Germany), **2008**.
- [88] G. Otero, G. Biddau, C. Sanchez-Sanchez, R. Caillard, M. F. Lopez, C. Rogero, F. J. Palomares, N. Cabello, M. A. Basanta, J. Ortega, J. Mendez, A. M. Echavarren, R. Perez, B. Gomez-Lor, J. A. Martin-Gago, *Nature* **2008**, *454*, 865.
- [89] N. Xin, H. Huang, J. Zhang, Z. Dai, L. Gan, *Angew. Chem. Int. Ed.* **2012**, *51*, 6163; *Angew. Chem.* **2012**, *124*, 6267.
- [90] M. Keshavarz-K, R. Gonzalez, R. G. Hicks, G. Srdanov, V. I. Srdanov, T. G. Collins, J. C. Hummelen, C. Bellavia-Lund, J. Pavlovich, F. Wudl, K. Holczer, *Nature* **1996**, *383*, 147.
- [91] M. Prato, Q. C. Li, F. Wudl, V. Lucchini, *J. Am. Chem. Soc.* **1993**, *115*, 1148.
- [92] J. C. Hummelen, M. Prato, F. Wudl, *J. Am. Chem. Soc.* **1995**, *117*, 7003.
- [93] O. Vostrowsky, A. Hirsch, *Chem. Rev.* **2006**, *106*, 5191.
- [94] G. Zhang, S. Huang, Z. Xiao, Q. Chen, L. Gan, Z. Wang, *J. Am. Chem. Soc.* **2008**, *130*, 12614.

- [95] H. R. Karfunkel, T. Dressler, A. Hirsch, *J. Comput.-Aided Mol. Des.* **1992**, *6*, 521.
- [96] A. G. Shipov, I. A. Savost'yanova, Y. I. Baukov, *Zh. Obsh. Khim.* **1989**, *59*, 1204.
- [97] P. J. Krusic, E. Wasserman, P. N. Keizer, J. R. Morton, K. F. Preston, *Science* **1991**, *254*, 1183.
- [98] S. I. Troyanov, E. Kemnitz, *Eur. J. Org. Chem.* **2005**, 4951.
- [99] R. Taylor, *Chem. Eur. J.* **2001**, *7*, 4074.
- [100] S. I. Troyanov, P. A. Troshin, O. V. Boltalina, I. N. Ioffe, L. N. Sidorov, E. Kemnitz, *Angew. Chem. Int. Ed.* **2001**, *40*, 2285; *Angew. Chem.* **2001**, *113*, 2345.
- [101] P. R. Birkett, A. G. Avent, A. D. Darwish, H. W. Kroto, R. Taylor, D. R. M. Walton, *J. Chem. Soc., Chem. Commun.* **1993**, 1230.
- [102] U. Reuther, A. Hirsch, *Chem. Commun.* **1998**, 1401.
- [103] H. Al-Matar, A. K. Abdul-Sada, A. G. Avent, P. W. Fowler, P. B. Hitchcock, K. M. Rogers, R. Taylor, *J. Chem. Soc., Perkin Trans. 2* **2002**, 53.
- [104] G. Schick, K.-D. Kampe, A. Hirsch, *J. Chem. Soc., Chem. Commun.* **1995**, 2023.
- [105] M. Tsuda, T. Ishida, T. Nogami, S. Kurono, M. Ohashi, *Chem. Commun.* **1993**, 1296.
- [106] V. M. Rotello, J. B. Howard, T. Yadav, M. M. Conn, E. Viani, L. M. Giovane, A. L. Lafleur, *Tetrahedron Lett.* **1993**, *34*, 1561.
- [107] P. Belik, A. Gügel, J. Spickermann, K. Müllen, *Angew. Chem. Int. Ed. Engl.* **1993**, *32*, 78; *Angew. Chem.* **1993**, *105*, 95.
- [108] S. H. Hoke, J. Molstad, D. Dilettato, M. J. Jay, D. Carlson, B. Kahr, R. G. Cooks, *J. Org. Chem.* **1992**, *57*, 5069.
- [109] T. Suzuki, Q. Li, K. Khemani, F. Wudl, O. Almarsson, *Science* **1991**, *254*, 1186.
- [110] T. Suzuki, Q. Li, K. C. Khemani, F. Wudl, *J. Am. Chem. Soc.* **1992**, *114*, 7301.
- [111] A. B. Smith, R. M. Strongin, L. Brard, G. T. Furst, W. J. Romanow, K. G. Owens, R. C. King, *J. Am. Chem. Soc.* **1993**, *115*, 5829.

-
- [112] T. Grösser, M. Prato, V. Lucchini, A. Hirsch, F. Wudl, *Angew. Chem. Int. Ed. Engl.* **1995**, *34*, 1343; *Angew. Chem.* **1995**, *107*, 1462.
- [113] J. Brecht, H. Thouet, J. Schmitz, *Justus Liebigs Ann. Chem.* **1924**, 437, 1.
- [114] M. Maggini, G. Scorrano, M. Prato, *J. Am. Chem. Soc.* **1993**, *115*, 9798.
- [115] M. Prato, M. Maggini, *Acc. Chem. Res.* **1998**, *31*, 519.
- [116] C. Bingel, *Chem. Ber.* **1993**, *126*, 1957.
- [117] J.-F. Nierengarten, V. Gramlich, F. Cardullo, F. Diederich, *Angew. Chem. Int. Ed. Engl.* **1996**, *35*, 2101; *Angew. Chem.* **1996**, *108*, 2242.
- [118] X. Camps, A. Hirsch, *J. Chem. Soc., Perkin Trans. 1* **1997**, *11*, 1595.
- [119] A. Hirsch, I. Lamparth, G. Schick, *Liebigs Ann.* **1996**, 1725.
- [120] R. W. Alder, S. P. East, *Chem. Rev.* **1996**, *96*, 2097.
- [121] J. F. Nierengarten, T. Habicher, R. Kessinger, F. Cardullo, F. Diederich, V. Gramlich, J. P. Gisselbrecht, C. Boudon, M. Gross, *Helv. Chim. Acta* **1997**, *80*, 2238.
- [122] A. Herrmann, M. Ruttimann, C. Thilgen, F. Diederich, *Helv. Chim. Acta* **1995**, *78*, 1673.
- [123] A. Hirsch, I. Lamparth, T. Grösser, H. R. Karfunkel, *J. Am. Chem. Soc.* **1994**, *116*, 9385.
- [124] L. Isaacs, R. F. Haldimann, F. Diederich, *Angew. Chem. Int. Ed. Engl.* **1994**, *33*, 2339; *Angew. Chem.* **1994**, *106*, 2434.
- [125] L. Isaacs, F. Diederich, R. F. Haldimann, *Helv. Chim. Acta* **1997**, *80*, 317.
- [126] F. Diederich, R. Kessinger, *Acc. Chem. Res.* **1999**, *32*, 537.
- [127] G. Rapenne, J. Crassous, L. E. Echevoyen, L. Echevoyen, E. Flapan, F. Diederich, *Helv. Chim. Acta* **2000**, *83*, 1209.
- [128] N. Chronakis, A. Hirsch, *Chem. Commun.* **2005**, 3709.
- [129] F. Djojo, A. Hirsch, *Chem. Eur. J.* **1998**, *4*, 344.
-

- [130] L.-L. Shiu, K.-M. Chien, T.-Y. Liu, T.-I. Lin, G.-R. Her, T.-Y. Luh, *J. Chem. Soc., Chem. Commun.* **1995**, 11, 1159.
- [131] C. K. F. Shen, K.-M. Chien, C.-G. Juo, G.-R. Her, T.-Y. Luh, *J. Org. Chem.* **1996**, 61, 9242.
- [132] C. K. F. Shen, H.-H. Yu, C.-G. Juo, K.-M. Chien, G.-R. Her, T.-Y. Luh, *Chem. Eur. J.* **1997**, 3, 744.
- [133] I. Lamparth, A. Hirsch, *Chem. Commun.* **1994**, 1727.
- [134] L. L. Dugan, D. M. Turetsky, C. Du, D. Lobner, M. Wheeler, C. R. Almli, C. K. Shen, T. Y. Luh, D. W. Choi, T. S. Lin, *Proc. Natl. Acad. Sci. U. S. A.* **1997**, 94, 9434.
- [135] J. Lotharius, L. L. Dugan, K. L. O'Malley, *J. Neurosci.* **1999**, 19, 1284.
- [136] A. M. Lin, B. Y. Chyi, S. D. Wang, H. H. Yu, P. P. Kanakamma, T. Y. Luh, C. K. Chou, L. T. Ho, *J. Neurochem.* **1999**, 72, 1634.
- [137] S. Bosi, T. Da Ros, S. Castellano, E. Banfi, M. Prato, *Bioorg. Med. Chem. Lett.* **2000**, 10, 1043.
- [138] L. L. Dugan, E. G. Lovett, K. L. Quick, J. Lotharius, T. T. Lin, K. L. O'Malley, *Parkinsonism Relat. Disord.* **2001**, 7, 243.
- [139] S. S. Ali, J. I. Hardt, K. L. Quick, J. Sook Kim-Han, B. F. Erlanger, T.-T. Huang, C. J. Epstein, L. L. Dugan, *Free Radical Biol. Med.* **2004**, 37, 1191.
- [140] F. Beuerle, P. Witte, U. Hartnagel, R. Lebovitz, C. Parng, A. Hirsch, *J. Exp. Nanosci.* **2007**, 2, 147.
- [141] F. Beuerle, A. Hirsch, *Chem. Eur. J.* **2009**, 15, 7434.
- [142] F. Beuerle, A. Hirsch, *Chem. Eur. J.* **2009**, 15, 7447.
- [143] M. Braun, U. Hartnagel, E. Ravanelli, B. Schade, C. Böttcher, O. Vostrowsky, A. Hirsch, *Eur. J. Org. Chem.* **2004**, 1983.
- [144] J. lehl, R. Pereira de Freitas, B. Delavaux-Nicot, J.-F. Nierengarten, *Chem. Commun.* **2008**, 2450.

-
- [145] F. Hörmann, A. Hirsch, *Chem. Eur. J.* **2013**, *19*, published online; DOI: 10.1002/chem.201203881.
- [146] L. Dunsch, P. Rapta, A. Gromov, A. Stasko, *J. Electroanal. Chem.* **2003**, *547*, 35.
- [147] J. Dannhäuser, W. Donaubaue, F. Hampel, M. Reiher, B. Le Guennic, B. Corzilius, K.-P. Dinse, A. Hirsch, *Angew. Chem. Int. Ed.* **2006**, *45*, 3368; *Angew. Chem.* **2006**, *118*, 3446.
- [148] M. Sawamura, Y. Kuninobu, M. Toganoh, Y. Matsuo, M. Yamanaka, E. Nakamura, *J. Am. Chem. Soc.* **2002**, *124*, 9354.
- [149] K. N. Raymond, E. A. Dertz, S. S. Kim, *Proc. Natl. Acad. Sci.* **2003**, *100*, 3584.
- [150] E. J. Corey, S. Bhattacharyya, *Tetrahedron Lett.* **1977**, *18*, 3919.
- [151] L. F. Jones, D. M. Low, M. Helliwell, J. Raftery, D. Collison, G. Aromi, J. Cano, T. Mallah, W. Wernsdorfer, E. K. Brechin, E. J. L. McInnes, *Polyhedron* **2006**, *25*, 325.
- [152] F. Beuerle, *Synthesis of Spherically Well Defined [60]Fullerene Multiple Adducts with up to Four Independently Addressable Addend Zones*, Dissertation, Friedrich-Alexander-Universität, Erlangen-Nürnberg (Germany), **2008**.
- [153] M. Yasuda, S. Yoshioka, S. Yamasaki, T. Somyo, K. Chiba, A. Baba, *Org. Lett.* **2006**, *8*, 761.
- [154] D. Shanmukaraj, S. Grugeon, G. Gachot, S. Laruelle, D. Mathiron, J.-M. Tarascon, M. Armand, *J. Am. Chem. Soc.* **2010**, *132*, 3055.
- [155] M. F. Lappert, *J. Chem. Soc.* **1953**, 667.
- [156] R. Colorado-Peralta, A. Xotlanhua-Flores, J. C. Gálvez-Ruíz, S. A. Sánchez-Ruíz, R. Contreras, A. Flores-Parra, *J. Mol. Struct.* **2010**, *981*, 21.
- [157] L. Anh, A. Soldatenkov, Z. Mamyrbekova, S. Soldatova, K. Polyanskiy, T. Tung, V. Khrustalev, *Chem. Heterocycl. Comp* **2008**, *44*, 1404.
- [158] L. D'Accolti, M. Fiorentino, C. Fusco, F. Capitelli, R. Curci, *Tetrahedron Lett.* **2007**, *48*, 3575.

- [159] M. Hesse, H. Meier, B. Zeeh, *Spektroskopische Methoden in der Organischen Chemie*. Thieme, Stuttgart, 7th. Ed. **2005**.
- [160] E. Adams, M. Hiegemann, H. Duddeck, P. Welzel, *Tetrahedron* **1990**, *46*, 5975.
- [161] F. Beuerle, N. Chronakis, A. Hirsch, *Chem. Commun.* **2005**, 3676.
- [162] T. Nishiguchi, M. Kuroda, M. Saitoh, A. Nishida, S. Fujisaki, *J. Chem. Soc., Chem. Commun.* **1995**, 2491.
- [163] I. Bauer, O. Rademacher, M. Gruner, W. D. Habicher, *Chem. Eur. J.* **2000**, *6*, 3043.
- [164] B. P. Friedrichsen, D. R. Powell, H. W. Whitlock, *J. Am. Chem. Soc.* **1990**, *112*, 8931.
- [165] M. Stollenz, M. Barbasiewicz, A. J. Nawara-Hultsch, T. Fiedler, R. M. Laddusaw, N. Bhuvanesh, J. A. Gladysz, *Angew. Chem. Int. Ed.* **2011**, *50*, 6647; *Angew. Chem.* **2011**, *123*, 6777.
- [166] S. Hauptmann, G. Mann, *Stereochemie*. Spektrum, Akademischer Verlag, Heidelberg, Berlin, Oxford **1996**.
- [167] I. Bauer, W. D. Habicher, *Phosphorus, Sulfur, and Silicon and the Related Elements* **1997**, *130*, 89.
- [168] I. Bauer, R. Fröhlich, A. Y. Ziganshina, A. V. Prosvirkin, M. Gruner, E. K. Kazakova, W. D. Habicher, *Chem. Eur. J.* **2002**, *8*, 5622.
- [169] H. Ohta, M. Tokunaga, Y. Obora, T. Iwai, T. Iwasawa, T. Fujihara, Y. Tsuji, *Org. Lett.* **2006**, *9*, 89.
- [170] I. Bauer, M. Gruner, S. Goutal, W. D. Habicher, *Chem. Eur. J.* **2004**, *10*, 4011.
- [171] S. Berger, S. Braun, H.-O. Kalinowski, *NMR Spectroscopy of the Non-Metallic Elements*. John Wiley & Sons, Chichester **1997**.
- [172] F. Hörmann, W. Donaubaue, F. Hampel, A. Hirsch, *Chem. Eur. J.* **2012**, *18*, 3329.
- [173] F. Hörmann, M. Brettreich, W. Donaubaue, F. Hampel, A. Hirsch, *Chem. Eur. J.* **2013**, *19*, published online; DOI:10.1002/chem.201203863.

-
- [174] M. Riala, M. S. Markoulides, E. E. Moushi, N. Chronakis, *Chem. Commun.* **2011**, 47, 11948.
- [175] A. Duarte-Ruiz, K. Wurst, B. Kräutler, *Helv. Chim. Acta* **2008**, 91, 1401.
- [176] R. Kessinger, J. Crassous, A. Hermann, M. Rüttimann, L. Echevoyen, F. Diederich, *Angew. Chem. Int. Ed.* **1998**, 37, 1919; *Angew. Chem.* **1998**, 110, 2022.
- [177] R. Kessinger, M. Gómez-López, C. Boudon, J.-P. Gisselbrecht, M. Gross, L. Echevoyen, F. Diederich, *J. Am. Chem. Soc.* **1998**, 120, 8545.
- [178] C. Malanga, N. Spassky, R. Menicagli, E. Chiellini, *Synth. Commun.* **1982**, 12, 67.
- [179] T. W. Greene, P. G. M. Wuts, *Protective Groups in Organic Synthesis*. Wiley, New York, 2nd. Ed. **2006**.
- [180] N. Yoshikawa, F. Xu, J. D. Arredondo, T. Itoh, *Org. Process Res. Dev.* **2011**, 15, 824.
- [181] K. K. Ogilvie, S. L. Beaucage, D. W. Entwistle, *Tetrahedron Lett.* **1976**, 17, 1255.
- [182] P. Huszthy, M. Oue, J. S. Bradshaw, C. Y. Zhu, T. Wang, N. K. Dalley, J. C. Curtis, R. M. Izatt, *J. Org. Chem.* **1992**, 57, 5383.
- [183] A. Naim, P. B. Shevlin, *Tetrahedron Lett.* **1992**, 33, 7097.
- [184] M. Burkhardt, A. Jedaa, M. Novak, A. Ebel, K. Voitchovsky, F. Stellacci, A. Hirsch, M. Halik, *Adv. Mater.* **2010**, 22, 2525.
- [185] M. Voigt, M. Klaumünzer, A. Ebel, F. Werner, G. Yang, R. Marczak, E. Spiecker, D. M. Guldi, A. Hirsch, W. Peukert, *J. Phys. Chem. C* **2011**, 115, 5561.
- [186] J. J. P. Stewart, *J. Mol. Model.* **2007**, 13, 1173.
- [187] J. J. P. Stewart, MOPAC2009, *Stewart Computational Chemistry, Colorado Springs, CO, USA* **2008**.
- [188] S. Burghardt, A. Hirsch, B. Schade, K. Ludwig, C. Böttcher, *Angew. Chem. Int. Ed.* **2005**, 44, 2976; *Angew. Chem.* **2005**, 117, 3036.
- [189] M. Meldal, C. W. Tornøe, *Chem. Rev.* **2008**, 108, 2952.
- [190] J. Iehl, J.-F. Nierengarten, *Chem. Eur. J.* **2009**, 15, 7306.
-

- [191] Y. Hua, A. H. Flood, *Chem. Soc. Rev.* **2010**, *39*, 1262.
- [192] H. Struthers, T. L. Mindt, R. Schibli, *Dalton Trans.* **2010**, *39*, 675.
- [193] B. Colasson, N. Le Poul, Y. Le Mest, O. Reinaud, *Inorg. Chem.* **2011**, *50*, 10985.
- [194] K. E. Djernes, O. Moshe, M. Mettry, D. D. Richards, R. J. Hooley, *Org. Lett.* **2012**, *14*, 788.
- [195] B. M. J. M. Suijkerbuijk, B. N. H. Aerts, H. P. Dijkstra, M. Lutz, A. L. Spek, G. van Koten, R. J. M. Klein Gebbink, *Dalton Trans.* **2007**, 1273.
- [196] M. Ostermeier, M.-A. Berlin, R. Meudtner, S. Demeshko, F. Meyer, C. Limberg, S. Hecht, *Chem. Eur. J.* **2010**, *16*, 10202.
- [197] D. M. Guldi, *Chem. Soc. Rev.* **2002**, *31*, 22.
- [198] D. M. Guldi, G. M. A. Rahman, V. Sgobba, C. Ehli, *Chem. Soc. Rev.* **2006**, *35*, 471.
- [199] F. Wessendorf, A. Hirsch, *Tetrahedron* **2008**, *64*, 11480.
- [200] E. Dietel, A. Hirsch, E. Eichhorn, A. Rieker, S. Hackbarth, B. Röder, *Chem. Commun.* **1998**, 1981.
- [201] D. M. Guldi, C. Luo, A. Swartz, M. Scheloske, A. Hirsch, *Chem. Commun.* **2001**, 1066.
- [202] D. M. Guldi, C. Luo, T. Da Ros, M. Prato, E. Dietel, A. Hirsch, *Chem. Commun.* **2000**, 375.
- [203] T. Da Ros, M. Prato, D. Guldi, E. Alessio, M. Ruzzi, L. Pasimeni, *Chem. Commun.* **1999**, 635.
- [204] L. Isaacs, F. Diederich, *Helv. Chim. Acta* **1993**, *76*, 2454.
- [205] W. A. Scrivens, A. M. Cassell, B. L. North, J. M. Tour, *J. Am. Chem. Soc.* **1994**, *116*, 6939.
- [206] C. Thilgen, *Angew. Chem.* **2005**, *117*, 5065.
- [207] O. V. Dolomanov, L. J. Bourhis, R. J. Gildea, J. A. K. Howard, H. Puschmann, *J. Appl. Cryst.* **2009**, *42*, 339.
- [208] G. Sheldrick, *Acta Cryst. A* **2008**, *64*, 112.

7 Appendix

Refereed Publications

A. Gmehling, W. Donaubaue, F. Hampel, F. W. Heinemann, & A. Hirsch. Invertomers of Fullerenophosphates. *Angew. Chem. Int. Ed.* **2013**, *52*, 3521; *Angew. Chem.* **2013**, *125*, 3606.

A. Gmehling & A. Hirsch. Facile Access to Functional Building Blocks of C₆₀ Involving C₃-Symmetrical Addition Patterns. *in preparation*.

Poster Contributions

A. Gmehling & A. Hirsch. "Exploring the Bulk Preparation of C₅₈N₂".
3rd EuCheMS Chemistry Congress, Nürnberg, Germany. 08/31/2010.

A. Gmehling & A. Hirsch. "Exploring the Bulk Preparation of C₅₈N₂".
BASF 119th International Summer Course, Ludwigshafen, Germany. 07/29/2010.

A. Gmehling & A. Hirsch. "Exploring the Bulk Preparation of C₅₈N₂ & Synthesis of Tripodal Fullerene Adducts for Metal Complexation."
Stipendiatentreffen des Fonds der Chemischen Industrie, München, Germany. 02/08/2010.

Oral Presentations

A. Gmehling. "Heterofullerenes - An Overview".
Graduate School MolecularScience Winter School 2009, Kirchberg, Austria. 03/17/2009.